Molecular characterization of *Tobacco streak virus* infecting okra (*Abelmoschus esculentus*)

Thesis submitted for the degree of

DOCTOR OF PHILOSOPHY

Mahesh Kumar

Department of Plant Sciences
School of Life Sciences
University of Hyderabad
Hyderabad, 500046
India

August 2014

Molecular characterization of *Tobacco streak virus* infecting okra (*Abelmoschus esculentus*)

Thesis submitted to the
University of Hyderabad for the award of

DOCTOR OF PHILOSOPHY

By

Mahesh Kumar
(Enrolment No. 08LPPH29)

Department of Plant Sciences
School of Life Sciences
University of Hyderabad
Hyderabad, 500046
India

August 2014

UNIVERSITY OF HYDERABAD
हैदराबाद विश्वविद्यालय

(A Central University established in 1974 by act of parliament)
HYDERABAD – 500046, INDIA

"DECLARATION"

I, **Mahesh Kumar** hereby declare that this thesis entitled **"Molecular characterization of *Tobacco streak virus* infecting okra (*Abelmoschus esculentus*)"** submitted by me under the guidance and supervision of **Dr. Gopinath Kodetham** is an original and independent research work. I also declare that it has not been submitted previously in part or in full to this University or any other University or Institution for the award of any degree or diploma.

Mahesh Kumar
08LPPH29

Dr. Gopinath Kodetham
(Research Supervisor)

UNIVERSITY OF HYDERABAD
हैदराबाद विश्वविद्यालय

(A Central University established in 1974 by act of parliament)
HYDERABAD – 500046, INDIA

"CERTIFICATE"

This is to certify that this thesis entitled **"Molecular characterization of *Tobacco streak virus* infecting okra (*Abelmoschus esculentus*)"** is a record of bonafide work done by **Mr. Mahesh Kumar,** a research scholar for Ph.D. programme in the Department of Plant Sciences, School of Life Sciences, University of Hyderabad, under my guidance and supervision. The work presented in this thesis is original and plagiarism free, no part has been submitted for any degree or diploma of any other University.

Dr. Gopinath Kodetham
(Research Supervisor)

HEAD

Department of Plant Sciences

DEAN

School of Life Sciences

Acknowledgements

I feel extremely privileged to express my respect for my supervisor ***Dr. Kodetham Gopinath,*** *Associate Professor, Department of Plant Sciences, School of Life Sciences, University of Hyderabad, Hyderabad. It is a great honor for me to be his first Ph.D. student. I am extremely lucky to prosecute this investigation under his exceptional guidance. Working under him gave me a true sense of freedom, broadened my scientific outlook and inculcated a spirit of positive attitude in me. Without his constant support and active guidance, the research work presented in the thesis would not have been possible. As I wrap up this work, I really do not know how far I have met his expectations but I can't forget his care and help showed on me, especially when the time was becoming difficult.*

The members of doctoral committee Prof. Appa Rao Podile and Dr.Y.Sree lakshmi, Dept. of Plant Sciences, have contributed immensely; I express my deepest sense of gratitude to them. Their timely support, suggestions and inspiring words are simply unforgettable. I also express my loyal thanks and heartfelt gratitude to Prof. Appa Rao Podile for allowing me to use their facility with full freedom.

I take this opportunity to acknowledge Prof. A.S. Raghavendra (Dean) and Prof. Aparna Dutta Gupta, Prof. M .Ramanadham (former Deans) of the school of Life Sciences for all the help and necessary infrastructure.

I am equally grateful to Prof. Ch. Venkatramana (Head), Prof. A.R. Reddy Prof. A.R. Podile (Former Head), Department of Plant Sciences, School of Life Sciences, University of Hyderabad for providing high impact common infrastructure facilities to the department.

I give my sincere thanks to all lab members of Prof. P.B. Kirti, Prof. A.K. Bhuyan, Prof. A.R. Podile, Dr. Naresh Sepuri and his lab members for their timely help.

I express my deepest sense of gratitude to all faculties in the school of Life Sciences for inspiring me and supporting me in one or the other aspect.

I appreciate the help of technicians Miss. Nalini and Durga Prasad in CLSM and electron microscopic experiments.

I am appreciative of my fellow graduate students of my laboratory Nagateja, Afsar, Soumya, Sankar, Surendra, Anil, Shilpa, Madhavi and Venkatesh.

I gratefully acknowledge the funding sources that made my Ph.D. work possible. I was funded from UGC project as JRF and SRF. The financial support given to the Department of Plant Science from the DST, UoH DBT-CREBB, DST-FIST, UGC-SAP- CAS and UGC-XI plan are gratefully acknowledged. IPM-CRSP and DBT are duly acknowledged for providing generous grant to our lab.

PhD students often talk about loneliness during the course of their study but this is something which I never experienced at University of Hyderabad. A heartfelt thanks to the really supportive and active student community of the School and all my friends who made me experience something special, in particular Das, Staya, Latha, Kalyan, Anirudh, Pawan, Ramakrishna, Babu, Sashi, Yasin Naveen, Dileep, Sumit, Asif, Deepankar, Abhay Kumar, Abhay Pratap, Suresh, Malathi, and many more…….

I would like to thank Dr. Krishna reddy, IIHR, Blr for providing me the TSV infected okra sample and TMV antibody which are important for my thesis and heartfelt thanks to him for his fruitful discussion during my visit to his laboratory.

I would like to thank Mr. Mahender, lab assistant for carrying out the lab and field works and maintaining the plants required at the appropriate time for my work.

I am obliged to non-teaching staff members of the Department, School and Administration for the valuable information provided by them time to time. I am grateful for their cooperation during the complete period of my assignment.

I would like to extend my deepest gratitude to my family members, my parents and my brothers. They always have provided steady affection and encouragement.

I thank the almighty for the great opportunity he has given me to be, and to be in this beautiful world with all those loving and encouraging people around, for crafting my strength with patience, tolerance and hard work to face and overcome the difficulties.

Mahesh Kumar

I dedicate this dissertation to my family and friends, whose love and patience has encouraged me during my struggle with this research

Table of contents

Abbreviations

µg	:	Microgram
µM	:	Micromolar
°C	:	Degree celcius
APS	:	Ammonium persulfate
ATP	:	Adenosine Tri Phosphate
bp	:	Base pair
BCIP	:	5-Bromo-4-Chloro-Indolyl-Phosphatase
BME	:	β-Mercaptoethanol
cDNA	:	Complementary DNA
CPB	:	Coat protein binding motif
Da	:	Dalton
DAC	:	Direct antigen coating
DMSO	:	Dimethyl Sulfoxide
DMFO	:	Dimethyl formaldehyde
DNA	:	Deoxy ribonucleic acid
dNTPs	:	Deoxy Nucleotide Triphosphates
DTT	:	Dithiothreitol
EBIA	:	Electroblot Immunoassay
EDTA	:	Ethylene diamine tetra acetic acid
ELISA	:	Enzyme-linked immunosorbant assay
EtBr	:	Ethidium Bromide
ER	:	Endoplasmic reticulum
g	:	Gram
G	:	Guanine
h	:	Hour(s)
IgG	:	Immunoglobulin G
IPTG	:	Isopropyl β-D-thiogalactoside
kb	:	Kilobase
kDa	:	Kilodalton
L	:	Litre
LB	:	Luria-Bertani
M	:	Molar
mg	:	Milligram
min	:	Minute
ml	:	Milliliter
mM	:	Millimolar
MMLV	:	Moloney Murine Leukemia Virus
M_r	:	Molecular mass
NBT	:	Nitro blue tetrazolium chloride
nm	:	Nanometers
NC	:	Nitrocellulose
OD	:	Optical Density
ORF	:	Open Reading Frame
PAGE	:	Polyacrylamide Gel Electrophoresis
PCR	:	Polymerase Chain Reaction

PEG	:	Poly Ethylene Glycol
pH	:	Potential of Hydrogen
PMSF	:	Phenylmethylsulfonylfluoride
PPB	:	Potassium phosphate buffer
PBS	:	Potassium buffer saline
PVDF	:	Polyvinylidene Fluoride
RNA	:	Ribonucleic acid
RNase	:	Ribonuclease
rpm	:	Revolutions Per Minute
RT	:	Room temperature
RT-PCR	:	Reverse Transcriptase-polymerase chain reaction
SDS	:	Sodium dodecyl sulphate
sec	:	Seconds
T	:	Thymine
TAE	:	Tris acetate EDTA
TBS-T	:	Tris buffer saline – Tween
T-DNA	:	Transfer DNA
TE	:	Tris-EDTA
TEMED	:	N,N,N′,N′-Tetramethylethane-1,2-diamine
Tm	:	Melting temperature
V	:	Volts
V/V	:	Volume/Volume
W/V	:	Weight/Volume
X-gal	:	5-bromo-4-chloro-3-indolyl β-D- galactoside

List of figures

List of tables & appendix

Chapter-1

General Introduction

General Introduction

The major constraint for development of a country depends on the increasing health concern and food insecurity, for which major funds are diverted toward the control of diseases caused by different infectious pathogens. The top 10 deadly diseases caused by different group of pathogens in the world are collected from the web and tabulated in table 1.1. After critical review of these diseases we found that firstly, six out of 10 diseases caused by viruses leads millions of population death around the globe. Secondly scarcity of food to feed the human population, also leads to the death of the population in developing countries. Food production faces severe challenges because of various factors either directly or indirectly affecting the farming system of crops. Global warming and urbanization of agricultural lands are the major factors, which decrease the land availability for cultivation. Further problems, which are likely to be worsened by climate change, result from the action of pests and diseases that can cause severe crop losses. Environmental change and globalization of trade promotes the emergence of "new viral" epidemics all over the globe. The increasing number of plant viruses becoming major menace to the farming system.

Table 1.1: Top ten deadly diseases caused by different group of pathogens in the world

S.No.	Disease	Causal organism	Death of human population
1.	The Black Death	*Pasturella pestis* or *Yersinia pestis*	75 million
2.	Polio	Polio virus	10,000 Dead since 1916
3.	Smallpox	Variola major and Variola minor virus	Native Americans population drop from 12 million to 235,000
4.	Cholera	Bacterium *Vibrio cholerae*	12,000 dead since 1991
5.	Ebola	*Ebola virus*	160,000 dead since 2000
6.	Malaria	protozoan parasites	515 million people effected and 1-3 million dead
7.	Bubonic Plague	Bacteria Rodents and fleas	250 million Europeans Dead (1/3 population)
8.	Spanish Flu	Influenza A Subtype H1N1.	Between 1918-19: 50-100 million dead
9.	Influenza	Influenza virus A	36,000 Deaths per year
10.	AIDS	HIV	25 Million Dead since 1981. Currently 38.6 million infected

Viruses are infectious, intracellular, and obligate pathogens that are too small to be seen with a light microscope, in spite of their small size, they infect all type of cellular life including animals, plant, bacteria and fungi and causes threat to human health, livestock, and crop plants.

A simple virus particle (virion) is composed of two principal components; the genome that is made up of nucleic acids (RNA or DNA) and protective shell that is protein. Morphology of virus is determined by its coat protein(s) which surrounds the viral genome. Genome will be either DNA or RNA, never both. Nucleic acid shape is either linear or circular. It may be single stranded or double stranded; positive sense, negative sense and ambience. Genomic information may be present in single genome (monopartite) or segmented genomes (bipartite and multipartite).

1.1 Classification of Viruses

Once a new virus is identified and characterized, it is necessary to classify them based on their genetic material, architecture, serology and evolutionary relationship for easy understanding and identification. Classification of viruses is a method of categorization of viruses reported from different parts of the world and has two faces, systematic and nomenclature. Systematic is the arrangement of biological entities into taxonomic categories (taxa) on the basis of similarities and /or relationships; whereas nomenclature is assigning of names to taxa according to. International Committee on Taxonomy of Viruses (ICTV) rules. The current ICTV report contains six orders; Caudovirales, Herpesvirales, Mononegavirales, Nidovirales, Picornavirales and Tymovirales and additionally seventh order Ligamenvirales proposed. The report does not distinguish between subspecies, strains, and isolates. Total 2284 species distributed among 349 genera, 19 sub-families and six orders (King *et al*., 2012).

The virus that infects a plant is called as plant virus. According to recent report of ICTV; total 900 plant virus species have been reported from different parts of the world and thousands of plant viruses are yet to be discovered (Roossinck, 2013). The recent plant virus classification is mentioned in table 1.2.

Table 1.2: Classification of plant viruses

Genome	Family & sub family	Genus	Type member
(-) ssRNA	Rhabdoviridae	Cytorhabdovirus	*Lettuce necrotic yellows virus*
		Nucleorhabdovirus	*Potato yellow dwarf virus*
	Bunyaviridae	Tospovirus	*Tomato spotted wilt virus*
	Ophioviridae	Ophiovirus	*Citrus psorosis virus*
		Unassigned genus : Tenuivirus	*Rice stripe virus*
(+)ssRNA	Bromoviridae	Alfamovirus	*Alfalfa mosaic virus*
		Anulavirus	*Pelargonium zonate spot virus*
		Bromovirus	*Brome mosaic virus*
		Cucumovirus	*Cucumber mosaic virus*
		Ilarvirus	*Tobacco streak virus*
		Oleavirus	*Olive latent virus 2*
	Closteroviridae	Ampelovirus	*Grape vine leafroll-associated virus 3*
		Closterovirus	*Beet yellows virus*
		Crinivirus	*Lettuce infectious virus*
	Secoviridae	Cheravirus	*Cherry rasp leaf virus*
		Sadwavirus	*Satsuma dwarf virus*
		Sequivirus	*Parsnip yellow fleck virus*
		Torradovirus	*Tomato torrado virus*
		Waikavirus	*Rice tungro spherical virus*
	Sub family: Comovirinae	Comovirus	*Cowpea mosaic virus*
		Fabavirus	*Broad bean wilt virus 1*
		Nepovirus	*Tobacco ringspot virus*
	Alfaflexiviridae	Allexivirus	*Shallot virus X*
		Mandarivirus	*Indian citrus ringspot virus 7*
		Potex virus	*Potato virus X*
	Betaflexiviridae	Capillovirus	*Apple stem grooving virus*
		Carlavirus	*Carnation latent virus*
		Citrivirus	*Citrus leaf blotch virus*
		Foveavirus	*Apple stem pitting virus*
		Tepovirus	*Potato virus T*
		Trichovirus	*Apple chlorotic leaf spot virus*
		Vitivirus	*Grapevine virus A*
	Tymoviridae	Maculavirus	*Grapevine fleck virus*
		Marafivirus	*Maize rayado fino virus*
		Tymovirus	*Turnip yellow mosaic virus*
	Luteoviridae	Enamovirus	*Pea-enation mosaic virus 1*
		Luteovirus	*Barley yellow dwarf virus-PAV*
		Polerovirus	*Potato leafroll virus*
	Potyviridae	Brambvirus	*Blackberry virus Y*
		Bymovirus	*Barley yellow mosaic virus*
		Ipomovirus	*Sweet potato mild mottle virus*
		Macluravirus	*Maclura mosaic virus*
		Poacevirus	*Triticum mosaic virus*
		Potyvirus	*Potato virus Y*
		Rymovirus	*Ryegrass mosaic virus*
		Tritimovirus	*Wheat streak mosaic virus*
	Tombusviridae	Alfanecrovirus	*Tobacco necrosis virus*
		Aureusvirus	*Pothos latent virus*
		Avenavirus	*Oat chlorotic stunt virus*
		Betanecrovirus	*Tobacco necrosis virus D*
		Carmovirus	*Carnation mottle virus*
		Dianthovirus	*Carnation ringspot virus*

		Gallantivirus	*Galinsoga mosaic virus*
		Macanavirus	*Furcraea necrotic streak virus*
		Machlomovirus	*Maize chlorotic mottle virus*
		Panicovirus	*Panicum mosaic virus*
		Tombusvirus	*Tomato bushy stunt virus*
		Zeavirus	*Maize necrotic streak virus*
	Virgaviridae	Furovirus	*Soil born wheat mosaic virus*
		Hordeivirus	*Barley stripe mosaic virus*
		Pecluvirus	*Peanut clump virus*
		Pomovirus	*Potato mop-top virus*
		Tobamovirus	*Tobacco mosaic virus*
		Tobravirus	*Tobacco rattle virus*
	Unassigned family	Benyvirus	*Beet necrotic yellow vein virus*
		Emaravirus	*Rose rosette virus*
		Idaeovirus	*Raspberry bushy dwarf virus*
		Ourmiavirus	*Ourmia melon virus*
		Sobemovirus	*Southern bean mosaic virus*
		Tenuivirus	*Rice Stripe virus*
		Umbravirus	*Carrot mottle virus*
ds RNA	Reoviridae		
	Sub family: Sedoreovirinae	Phytoreovirus	*Wound tumor virus*
	Spinareovirinae	Fijivirus	*Fiji disease virus*
		Oryza virus	*Rice ragged stunt virus*
	Partitiviridae	Alphacryptovirus	*White clover cryptic virus 1*
		Betacryptovirus	*White clover cryptic virus 2*
	Unassigned family	Varicosavirus	*Lettuce big-vein associated virus*
ds DNA	Caulimoviridae	Caulimovirus	*Cauliflower mosaic virus*
		Badnavirus	*Commelina yellow mosaic virus*
		Cavemovirus	*Cassava vein mosaic virus*
		Petuvirus	*Petunia vein clearing virus*
		Soymovirus	*Soybean chlorotic mottle virus*
		Solendovirus	*Tobacco vein clearing virus*
		Tungrovirus	*Rice tungro bacilliform virus*
ss DNA	Geminiviridae	Becurtovirus	*Beet curle top Iran virus*
		Begamovirus	*Bean golden yellow mosaic virus*
		Curtovirus	*Beet curly top virus*
		Eragrovirus	*Eragrostis curvula streak virus*
		Mastrevirus	*Maize streak virus*
		Topocuvirus	*Tomato pseudo-curly top virus*
		Tuncurtovirus	*Turnip curly top virus*
	Nanoviridae	Babuvirus	*Banana bushy top virus*
		Nanovirus	*Subterranean clover stunt virus*

1.2 Stages of viral infection *in planta*

The development of viral infections in plants require several steps such as : the introduction of the virus into the plant through wounds, either mechanically or by vectors; replication in the initially infected cells; the spread through plasmodesmata (PD) of the infectious entity to the surrounding healthy cells within the leaf, known as

cell-to-cell movement; the invasion into and spread through the vascular tissue to other parts of the plant by interaction with host proteins, known as systemic movement; and finally spread of infection from one plant to other plant by means of arthropod insect vectors or pollen grains.

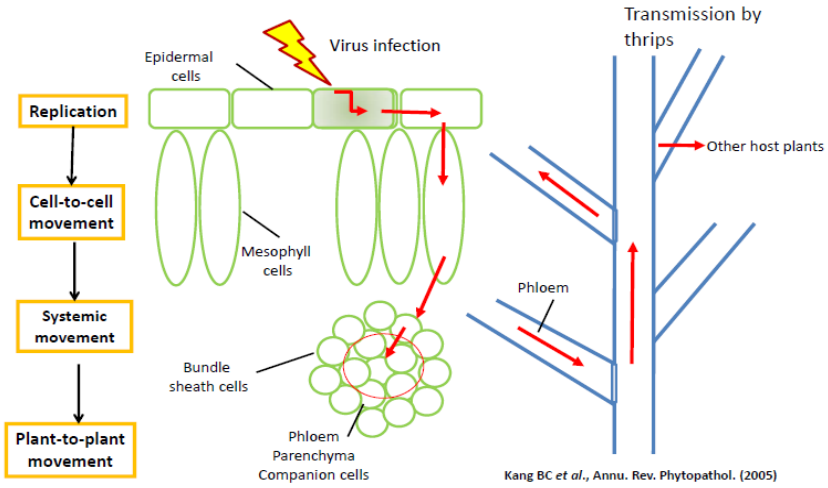

Fig 1.1: Stages of viral infection in plant.

1.3 Disease and economic importance

Development of the symptoms and incidence of the disease depends on the interaction of specific virus and host, and on climatic conditions. The plant's response to infection may range from symptomless condition (latent infection) to severe infection and subsequent plant death. Usually, viruses spread all over the plant and cause systemic infection. In some cases, small necrotic or chlorotic spots called local lesions develop at the site of infection. Typical leaf symptoms of viral diseases include mosaic patterns, chlorotic or necrotic lesions, vein clearing, yellowing, vein banding, stripes or streaks, and leaf rolling and curling. Symptoms on flower include deformation and changes in the color of the flowers including mosaics called color breaking (e.g., tulip flower breaking). In fruit and vegetable crops, the general symptoms produced are mosaic patterns, distortion, stunting, discoloration or malformation, and chlorotic ringspots. Infected stems of plants develop stem pitting and grooving or tumors in response to virus infection.

The symptoms induced by plant viruses lead to reduction of yield, crop failure, increased sensitivity to frost and drought, susceptibility to attack by other pathogen and pests and finally market value due to visual defects such as size, shape and crop quality. The estimated annual losses range from US$ 35-60 billion globally (mention

in table 1.3). This is demonstrated by following the few examples. In Africa, *Cacao swollen shoot virus* (CSSV) occurs severely and causing 50,000 ton loss of cocoa beans annually with an estimated value of US$ 28 million (Bowers *et al*., 2001). In South East Asia, infection of rice with *Rice tungro virus*(es) leads to an estimated annual loss of US$ 1.5 billion (Hull, 2002). *Tomato spotted wilt virus* (TSWV) infects various crops which includes tobacco, peanuts, and tomato (Sherwood *et al*., 2003), the annual estimated losses due to this virus is US$ 1.0 billion across the world (Hull, 2002). An epidemic of *Tobacco streak virus* (TSV) that caused peanut stem necrosis disease (PSND) has recently been reported in peanut crops in the state of Andhra Pradesh, India (Reddy *et al*., 2002). Losses in peanut crops in the Anantapur district of Andhra Pradesh, India, alone were estimated to exceed 42 million pounds. TSV was also shown to cause sunflower (*Helianthus annuus*) necrosis disease (SND) (Prasada Rao *et al*., 2000). The combined losses in these two crops exceed US$ 90 million per year. In the recent past, severe incidence of a disease occurred in okra growing areas of Karnataka and Tamil Nadu and subsequently it spread to other states: Andhra Pradesh, Madhya Pradesh, Haryana, and Maharashtra; caused by *Tobacco streak virus* (Krishna Reddy *et al*., 2003 a). Affected okra plants were showing chlorotic spots, chlorotic leaf blotches, distortion of leaves, chlorotic streaking, distortion of fruits which apparently leads to severe yield losses as much as 63% in the disease growing area.

Table 1.3: Crop loss due to plants viruses

Crop	Virus	Countries	Loss /year	References
Rice	*Rice tungro virus*	SE Asia	$ 1.5 X 10^9	Hull, 2014
	Ragged stunt virus	SE Asia	$ 1.4 X 10^8	
	Hojablanca virus	South & Central America	$ 9.0 X 10^6	
Wheat	*Barley yellow dwarf virus*	UK	£ 5 X 10^6	
Barley	*Barley yellow dwarf virus*	UK	£ 6 X 10^6	
Potato	*Potato leafroll virus*	UK	£ 3-5 X 10^7	
	Potato virus X	Worldwide	10-100%	
	potato virus Y	Worldwide	10-20%	
Sugar beet	*Beet yellows and Beet mild yellows*	UK	£ 5-50 X 10^6	
Citrus	*Citrus tristeza virus*	Worldwide	£ 9-24 X 10^6	
Cassava	*African cassava mosaic virus*	Africa	$ 1.9-2.7 X 10^9	
Bean	*Bean golden yellow mosaic*	San Juan Valley	$ 3X 10^7	Hull, 2002
Many	*Tomato spotted wilt virus*	Worldwide	$ 1 X 10^9	Shewood *et*

crops				*al*., 2003
Pigeon pea	*Sterility mosaic virus*	India , Nepal SE Asia	$ 28 X 10^7	Hull, 2002
Cocao bean	*Cocao swollen shoot virus*	Africa	$ 28 X 10^6	Bowers *et al*., 2001
Peanut	*Tobacco streak virus*	India	$ 65 X 10^6	Reddy *et al*., 2002
	Peanut clump virus	India , Africa	$ 38 X 10^6	
Sunflower	*Tobacco streak virus*	India	$ 25 X 10^6	Prasada Rao *et al*., 2002
Cotton	*Cotton leaf curl virus*	Pakistan (92-95)	$ 5 X 10^9	Briddon and Markham, 2001
Grain Legumes	*Yellow mosaic virus*	India	$ 3 X 10^8	Hull, 2002
Tomato	*Tomato leaf curl virus*	Florida	$ 14 X 10^7	Hull, 2002
Maize	*Maize streak virus*	Africa	$ 120-480 X 10^6	Shepherd *et al*., 2010

1.4 Management of plant viral disease

Practically, there are no antiviral compounds available to control the plant viral diseases. However, use of different cultural practices, reduce the maximum incidence of the disease. Integrated management of viruses can prevent the occurring of viral disease. The first step involved in the management of the viruses is virus identification, which is mandatory. The subsequent strategy depends on, how virus entering in to host plant, how virus is transmitted to other plant within a crop and finally, how virus is surviving in the absence of suitable host plants (Haddidi *et al*., 1998). Integrated management of the viruses include use of the certified virus free seed or vegetative stocks, removing of the wild species from surroundings which act as alternate reservoir host in the absence of crops in field. Modification of planting pattern and harvesting schedule, burning of the virus infected plant to avoid horizontal and vertical transfer from one plant to another plant. Use of insecticides, nematicides, or fungicides to control of insects, nematodes or fungus respectively will work to a greater extent.

An alternative approach for the control of a viral disease is utilization of conventional breeding and genetic engineering practices, which helps in the introduction of natural virus resistance genes and silencing cassettes into crop cultivars respectively. The availability of the natural resistance gene(s) is a constraint for most of the crops and this technique take lots of manpower and time. However, the introduction of resistance gene, silencing cassette have been quicken by using genetic engineering and recombinant DNA technology practices and it leads to the

development of various viral resistant plants, but its large scale cultivation has met major constraints like biosafety, socio and political issues. So, it is very essential to develop an alternative approach which can help in understanding the life cycle of a plant virus at the molecular level. Specifically, the life cycle of RNA virus(es) include phases of genome replication, virion assembly, cell-to-cell movement, systemic movement and plant to plant transmission. Understanding the life cycle of the virus will help in the identification of cellular factors that are responsible for the spread of viruses from the initial site of infection to the whole plant system. Towards this, we plan to use multipartite *Tobacco streak virus* (TSV) as a model system in the laboratory.

TSV is a fast emerging and devastating plant virus transmitted by the Arthropod vector thrips, belongs to the family Bromoviridae and genus *Ilarvirus.* TSV was first discovered on tobacco (*Nicotiana tabacum*) in 1936 by Johnson (Johnson, 1936). Later, it has been reported from more than 26 countries worldwide. TSV has a wide host range infecting more than 200 plant species belonging to 30 dicotyledonous and monocotyledonous plant species (Fulton, 1985). In the present study we have collected field sample infected with viruses from different vegetable crops like tomato, sunflower, okra and peanut and identified four different TSV strains from sunflower, tomato, okra and peanut through serodiagnosis. Major parameters of the thesis are dealt with okra strain of TSV since it replicates efficiently in *Nicotiana benthamiana*, our model plant in the laboratory. Detail about okra and TSV was discussed in the chapter 2 (review of literature). So, based on the above literature we have framed following objectives to pursue in the present study

1. Field surveys and partial characterization of *Tobacco streak virus* infecting different vegetable crops.

2. Complete nucleotide sequence and diversity analysis of three RNAs (RNA1, RNA2 and RNA3) of TSV-Okra strain.

3. Construction and characterization of full-length infectious clones for TSV-Okra strain.

4. *In planta* analysis of TSV movement protein (MP) as a GFP chimera and functional analysis of MP-GFP chimeric mutants through confocal laser scanning microscopy (CLSM).

Chapter-2

Review of literatures

Review of literature

2.1 Introduction

The present thesis is focused on the molecular characterization for okra strain of the TSV since it replicates efficiently in the *Nicotiana benthamiana*, our model plant in the laboratory. A brief review on the importance of okra is thereby discussed.

Okra *Abelmoschus esculentus* L. (Moench), is an economically important vegetable crop grown in tropical and sub-tropical and warm temperate regions around the world. It is grown as kitchen garden crop as well as on large commercial farms. It has been cultivated commercially in India, Pakistan, Bangladesh, Burma, Afghanistan, Iran, Turkey, Western Africa, Yugoslavia, Japan, Malaysia, Brazil, Ghana, Ethiopia, Cyprus and the Southern United States.

In India; it is cultivated in summer season in north India and also as a winter crop in Maharashtra, Gujarat, Andhra Pradesh, Karnataka and Tamil Nadu. It fails to grow in the high hills and areas which experience very low temperatures.

According to FAO statistics, it has been observed that in the world okra grown in about 1.06 million hectares with a production of 8.06 million tonnes during 2011. India is the largest producer of okra occupying 46.87% area with 71.76% of production globally. The other major okra producing countries are Nigeria, Sudan, Iraq Coted'lvore and Pakistan with share of production is 13.15%, 3.18%, 1.96%, 1.6% and 1.27% respectively. In India the major okra producing states are West Bengal, Bihar, Orissa, Andhra Pradesh, Gujarat, Jharkhand and Karnataka.

Okra is known by many vernacular names in different regions of the world. It contains an important source of vitamins C, calcium, potassium (IBPGR, 1990), proteins, carbohydrates (Lamont, 1999; Owolarafe and Shotonde 2004; Gopalan *et al*., 2007; Dilruba *et al*., 2009), and plays a vital role in human diet (Kahlon *et al*., 2007; Saifullah and Rabbani 2009). Every part of okra has a commercial value. 100 g edible portion of okra pods and leaf contains different constituent mentioned in table 2.1. Carbohydrates are mainly present in the form of mucilage (Liu *et al*., 2005). The mucilage is highly soluble in water. Okra seeds contain about 20% protein and 40% oil (Charrier, 1984).

Table 2.1 Different constituents present in 100 g pod and leaf of okra

Constituent	Pod (100 g)	Leaf (100g)
Water	88.6 g	81.50 g
Energy	144.00 kJ (36 kcal)	235.00 kJ (56.00 kcal)
Carbohydrate	8.20 g	11.3 g
Fat (g)	0.20 g	0.60 g
Protein	2.10 g	4.40 g
Fibre	1.70	2.10 g
Calcium	84 mg	532.00 mg
Potassium	90 mg	70.00 mg
Iron	1.20 mg	0.70 mg
Ascorbic acid	47 mg	59.00 mg
Riboflavin	0.08 mg	2.80 mg
Thiamine	0.04 mg	0.25 mg
Niacin	0.60 mg	0.20 mg
B-carotene	185.00 µg	385.00 µg

(Source: Gopalan *et al*., 2007; Varmudy, 2011.)

The roots and stems of okra are used for cleaning the cane juice from which gur or brown sugar is prepared (Chauhan, 1972). Stem bark is used for fibre extraction. The fruits also serve as soup thickeners. Okra seeds are roasted, ground and used as coffee additive or substitute (Moekchantuk and Kumar, 2004). Mature fruits and stems having fibre are used in paper industry. Okra leaves are considered good cattle feed, and the leaf buds and flowers are also edible (Doijode, 2001). Okra seed oil is viewed as alternative source for edible oil; rich in unsaturated fatty acids such as oleic acid and linoleic acid. The oil content of the seed is quite high at about 40%. Moreover, okra mucilage is suitable for industrial and medicinal applications (Akinyele and Temikotan, 2007). Industrially, okra mucilage is usually used for glace paper production and also has a confectionery use. Okra has found medical application as a plasma replacement or blood volume expander (Markose and Peter 1990; Lengsfeld *et al*., 2004; Adetuyi *et al*., 2008; Kumar *et al*., 2010).

There are many reports on the occurrence of several pests and diseases on okra. Insect pest infestation is one of the most limiting factors for accelerating yield potential of okra. The crop is susceptible to damage by various insects, fungi, nematodes and viruses at various growth stages of crops. Some of the important insects are fruit and shoot borer, aphids, white flies, ants, etc. The list of commonly occurring disease on okra in mentioned in table 2.2. The common viruses which infect okra are *Yellow vein mosaic virus* (YVMV), *Okra mosaic virus* (OkMV) and *Okra leaf curl virus* (OkLCV). The most serious viral disease of okra is caused by

yellow vein mosaic virus (YVMV) universally faced by all okra growers (Ndunguru and Rajabu, 2004; Alegbejo *et al*., 2008; Benchasri, 2012).

Table 2.2 List of commonly occurring diseases on okra

Common disease	Scientific name	Susceptible crop stage	References
Powdery mildew	*Erysiphe cichoracearum*	Vegetative	Kumar *et al*., 2010
Damping-off	*Pythium vexans*	Seedling– early vegetative	Ek-amnuay, 2007
Pod spot	*Alternaria* sp	Fruit setting	Kumar *et al*., 2010
Anthracnose	*Colletotrichum* spp	Flowering/Fruiting	Charrier,1984; Lamont, 1999
Leaf Spot	*Pseudocercospora abelmoschi*	Vegetative stage	Charrier, 1984; Moekchantuk and Kumar 2000
Virus			
Yellow Vein Mosaic	*Yellow vein mosaic virus*	Early vegetative-harvest	Sastry and Singh 1975; Givord and Denboer 1980; Rashid *et al*., 2002
Okra Leaf Curl	*Okra leaf Curl virus*	Vegetative- harvest	Ghanem, 2003
Okra mosaic	*Okra mosaic virus*	Vegetative -harvest	Fauquet and Thouvenel 1987

Okra mosaic virus (OkMV)) is another important virus that infects okra; belongs to Tymovirus genus. It was first reported from *Abelmochous esculentus* (okra) in Côted'Ivoire (Fauquet and Thouvenel 1987). It is a persistent virus; infects all stages of the crop and transmitted by the whitefly. Okra leaf curl disease of the okra is caused by *Okra leaf curl virus* (OkLCV) and it belongs to *Begomovirus* genus. *Okra leaf curl virus* infects okra plant from vegetative stage to the harvesting stage. Recently, Krishna Reddy *et al*., (2003a) showed fruit distortion mosaic disease of okra caused by *Tobacco streak virus*. This virus causes characteristic symptoms as chlorotic spots, chlorotic leaf blotches, distortion of leaves, chlorotic streaking, and distortion of fruits. Yield losses due to this virus were reported up to 63% in okra growing area of India.

2.2 *Tobacco streak virus*

2.2.1 History

The first species of Ilarvirus genus was reported by Stewart (1910) is *Apple mosaic virus* (ApMV) associated with the apple, causing variegation of fruit. Subsequently, second species *Prunus necrotic ringspot virus* (PNRSV) was reported

by Valleau in 1932 which infects peach plant. *Tobacco streak virus* was first reported on tobacco (*Nicotiana tabacum*) in 1936 by Johnson and subsequently reported in Brazil in 1940 on *Nicotiana tabacum*.

2.2.2 Taxonomy

According to recent ICTV classification, TSV is placed under the family *Bromoviridae* which comes under an unassigned order. The bromoviridae family includes six genus: *Alfamovirus*, *Anulavirus*, *Bromovirus*, *Cucumovirus*, *Oleavirus* and *Ilarvirus*. Among them, Ilarvirus is the largest genus that contains 19 definitive species, of which *Tobacco streak virus* is the representing type species. Ilarvirus genus is subdivided into six sub groups based on the serological relationship and available sequence (Table 2.3).

Table 2.3 List of genus and species of the bromoviridae family

Genus	Virus	Ilarvirus subgroup
Ilarvirus	***Tobacco streak virus* (TSV)**	Subgroup1
	Blackberry chlorotic ringspot virus (BCRV)	
	Parietaria mottle virus (PMoV)	
	Strawberry necrotic shock virus (SNSV)	
	Citrus leaf rugose virus (CiLRV)	Subgroup 2
	Tulare apple mosaic virus (TAMV)	
	Spinach latent virus (SpLV)	
	Elm mottle virus (EMoV)	
	***Asparagus virus 2* (AV-2)**	
	Citrus variegation virus (CVV)	
	Hydrangea mosaic virus (HdMV)	
	***Prunus necrotic ringspot virus* (PNRSV)**	Subgroup 3
	Humulus japonicus latent virus (HJLV)	
	Apple mosaic virus (ApMV)	
	Blueberry shock virus	
	Prune dwarf virus (PDV)	Subgroup 4
	American plum line pattern virus (APLPV)	Subgroup 5
	Lilac ring mottle virus	Subgroup 6
	Lilac leaf chlorosis virus	
Bromovirus	***Brome mosaic virus***	
	Cassia yellow blotch virus	
	Cowpea chlorotic mottle virus	
	Melandrium yellow fleck virus	
Cucumovirus	***Cucumber mosaic virus* (CMV)**	
	Tomato aspermy virus (TAV)	
	Peanut stunt virus (PSV)	
	Gayfeather mild mottle virus	
Alfamovirus	***Alfalfa mosaic virus* (AMV)**	
Oleavirus	***Olive latent virus-2* (OLV-2)**	
Anulavirus	***Pelargonium zonate spot virus* (PZSV)**	

2.2.3 Morphology

In general, viruses are much smaller than the bacteria, and their diameter varies from 15 nm to 300 nm. Small plant viruses such as the isometric nano- and comoviruses, have a diameter between 17 and 30 nm. Larger viruses can be rod-shaped particles varying in length between 65-350 nm and width between 15-25 nm. Bacilliform particles have a range of 30-500 nm in length and width of 3-8 nm. The largest filamentous plant viruses are known to have a virus particle which measures up to 1000 nm (*Citrus tristeza clasterovirus*) and a width in between 3-20 nm. The naked viral RNA has coiled structure with a diameter of around 10 nm (Citovsky *et al*., 1992). Mimivirus was largest characterized virus, with a capsid diameter of 400 nm. *Megavirus chilensis* was known to be largest virus (Arslan *et al*., 2011) before the discovery of pandoravirus (Nadège *et al*., 2013) and *Pithovirus sibericum* (Matthieu *et al*., 2014). The icosasedral capsid diameter of the *Megavirus chilensis* in native condition was measured 520 nm (Arslan *et al*., 2011). Recently, *Pithovirus sibericum* virus was discovered from Siberian region (Matthieu *et al*., 2014). This virus infects amoeba and its size approximately 1500 nm in length and 500 nm in diameter, making it the largest virus yet found. The size of this virus is 50% larger than the previous largest known viruses i.e. pandoraviruses (Nadège *et al*., 2013).

Viruses display a wide range of sizes and shapes. In general there are four main morphological virus types: Helical, Icosahedral or near spherical, prolate and enveloped. TSV falls under icosahedral group with iscosaheral. The virions are characterized as rigid, non-enveloped, icosahedral particles measuring about 27-35 nm in diameter.

2.2.4 Genome, genome organization and replication mechanism

2.2.4.1 Genome

TSV belongs to single stranded RNA genome of positive polarity. Apart from TSV, about 80% of viruses possess single stranded RNA genome of positive polarity which affects both plants and animals (Mandahar, 2006). These viral genomes play multiple roles during the infection cycle: they act as mRNAs and direct specific viral protein synthesis from their genes, they also act as templates for transcription into negative sense RNA copies which are starting point of all the subsequent stages of virus genome replication. This is followed by encapsidation of progeny positive sense

RNA molecules ultimately leading to formation of progeny virions. They also serve as templates for subgenomic RNA synthesis along with regulators of gene expression. Viral genomic RNA, functions as cis-acting element and recruits the required factors like translation factors, RNA replicase components, and structural proteins (Buck, 1996; Dreher, 1999).

The size of positive sense RNA viral genome ranges from about 3.5 to 30 kb (Koonin and Dolja, 1993). The largest genome size was reported from the *Pandoravirus* and its size varies from 1.9 to 2.5 mega base pair (Nadège *et al*., 2013) The other largest viruses are *Mimivirus*, *Pithovirus* and *Megavirus*, and its genome size varies from 1.0 to 2.3 mega base pair (Matthieu *et al*., 2014).

2.2.4.2 Genome organization

The viral genome contains both coding and noncoding regions. The noncoding region contains information in the form of the *cis*-acting regulatory sequence that control synthesis of full-length positive (+) and negative (-) strand RNAs, translation of the viral protein, transcription of subgenomic RNA. Viral genome may be monopartite- when all the genetic information is contained in a single RNA, or multipartite when genetic information contains more than two RNAs. Each nucleic acid has two ends; 3'end/terminus/untranslated region or (3'UTR) and 5'end/terminus/untranslated region or (5'UTR). These two ends are maintained properly by viruses for their fitness. The coding region is called open reading frame (ORF) and it codes for the protein. Generally, plant viruses have compressed genome to bear extensively overlapping ORF's. For example, grapevine virus has monopartite RNA genome of 8000 nt, which contains five ORFs, out of which 3 ORFs are overlapping and cover 1000 nt.

The total size of TSV genome varies from 8.5 to 9.0 kb. The whole genome is segmented, tripartite in nature (each segment is encapsulated individually) and consist of linear, positive-sense, single stranded RNA (Fig 2.1).

RNA1 contains a single ORF that encodes a polypeptide (1a protein) of 123 kDa. The polypeptide contains two domains with characteristics of methyltransferase and NTP-binding activities. RNA2 contains 2 ORFs. The product of the larger ORF (2a protein) is 94 kDa and contains a domain with sequence characteristics of an RNA dependent RNA polymerase. It is required to perform replication, transcription,

cap- snatching and genomic strand selection. The smaller 2b ORF begins within the larger ORF and extends towards the 3' terminus of the molecule. The product (2b protein) is 22 kDa and appears to be expressed via a subgenomic RNA4a. RNA3 is bi-cistronic and codes for a movement (3a) protein of 31 kDa and the coat (3b) protein of 28 kDa. The coat protein gene is expressed via subgenomic RNA4 (fig 2.1). Cap structure present at the 5' end of each RNA helps in the translation and protect from its degradation.

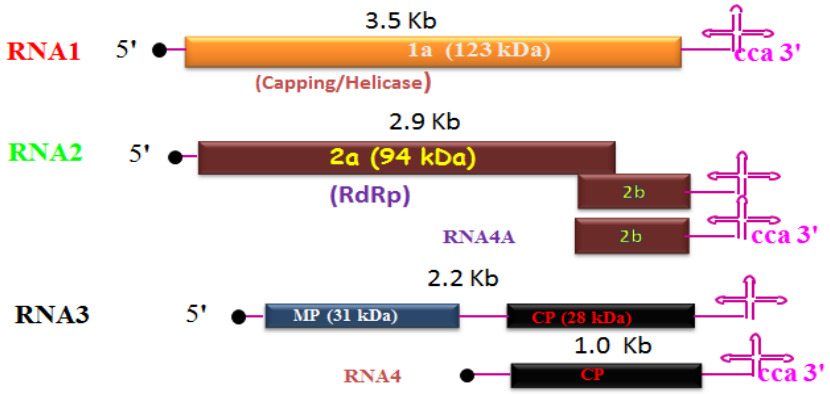

Fig 2.1: Genome organization of TSV. RNAs 1-3 are genomic and act as mRNAs. Black round circle indicate cap structure. Free line indicates the non-coding region of the RNAs. Rectangular box indicate the ORF of the gene. t-RNA like structure is present at the end of each RNA molecule. The ORFs 2b and 3b (CP) are expressed from subgenomic RNA4 and RNA4A respectively.

2.2.4.3 Replication mechanism

A unique feature of ilarviruses that distinguishes them from other viruses in the family of *Bromoviridae* is that the genomic RNAs alone are not infectious; rather, infection is dependent upon a combination of genomic RNAs plus a few molecules of coat protein to initiate the early stages of viral replication (Bol *et al*., 1974)

Generally, viral coat protein does not have any role in replication of majority of plant viruses but has a definite role during the replication of *Alfalfa mosaic virus* (AMV) and species of ilarvirus genus. Probably, capsid protein of AMV and ilarviruses confer a competitive advantage to viral RNAs over polyadenylated cellular mRNAs. The role of coat protein in AMV is the best investigated and reviewed (Jaspars, 1999; Bol, 1999; Bol, 2005). Replication mechanism of the positive stranded (TSV and AMV) virus divided into ten steps which are mentioned below. The figure of the life cycle or natural infection is adopted from the Bol, 2005.

Step 1: Uncoating of virus:

Once the virus comes in contact with the plant cell, it has to enter into the cell to develop infection. For this, the first step is the uncoating of the viral RNA from its coat protein. In most cases, CP was completely uncoated but in case of ilarviruses, few molecules of CP remain bound to 3' end of the viral RNA known as E-CPB (hairpin E plus 3' 112 nt in CPB confirmation). This supports in efficient translation of AMV or ilarvirus RNAs *in vivo*.

Step-2: Translation initiation:

All the four RNA molecules enters in to single cell and viral RNA-CP complex acting as a functional analogue of a poly(A)-bound protein (PABP), by promoting recruitment of 40S ribosomal subunits and /or by enhancing stability of the viral RNA. It interacts with the host translation factor, eIF4F (contains three subunits eIF4A, eIF4G and eIF4E) bound to 5' cap structure. The CP molecules will interact with 4G sub unit of initiation factor and the 5' cap structure of viral RNA binds to 4E subunit.

Step-3: Translation of P1 and P2:

The interaction of 5' cap with 4G initiation factor stimulates translation of the RNAs 1 and 2 leading to formation of the replicase proteins P1 and P2 (Neeleman *et al*., 2001; Bol, 2003). Recently, Krab *et al*., (2005) elucidate that AMV coat protein specially interacts with the eIF4G and eIFiso4G subunits from wheat eIF4F and eIFiso4G, respectively. So that their findings support the hypothesis that the role of CP in translation of viral RNAs into closed loop structure.

Step-4: Formation of replication complex:

Protein, P1 is proposed to recruit viral RNAs from translation machinery and also targets a complex of P1, P2 and viral RNAs to membrane structures where repilication complexes are formed similar to the mechanism employed by the BMV (den Boon *et al*., 2001). The BMV replication complexes are located within endoplasmic reticulum derived vesicles while AMV replication complexes are located within vesicles derived from tonoplast (Bol, 2003).

Step-5: Initiation of Replication:

Replication has to be initiated from the negative strand RNA involved with the dissociation of CP from the viral RNA. Once the CP is dissociated, the viral RNA forms TLS conformation (TLS) (Olsthoorn *et al*., 1999). This is accomplished by the

proteolytic cleavage of the N-terminus of CP and as well as by binding of replicase proteins to hairpin-E. The P1 and P2 proteins will bind to the E-TLS region of viral RNA (Bol, 2005). Presence of TLS at the 3'end permits initiation of AMV negative strand RNA synthesis, and essential for the viral replication *in vivo* and *in vitro* (Neeleman *et al*., 2004). Thus, CP has no role in formation of AMV negative strand RNA.

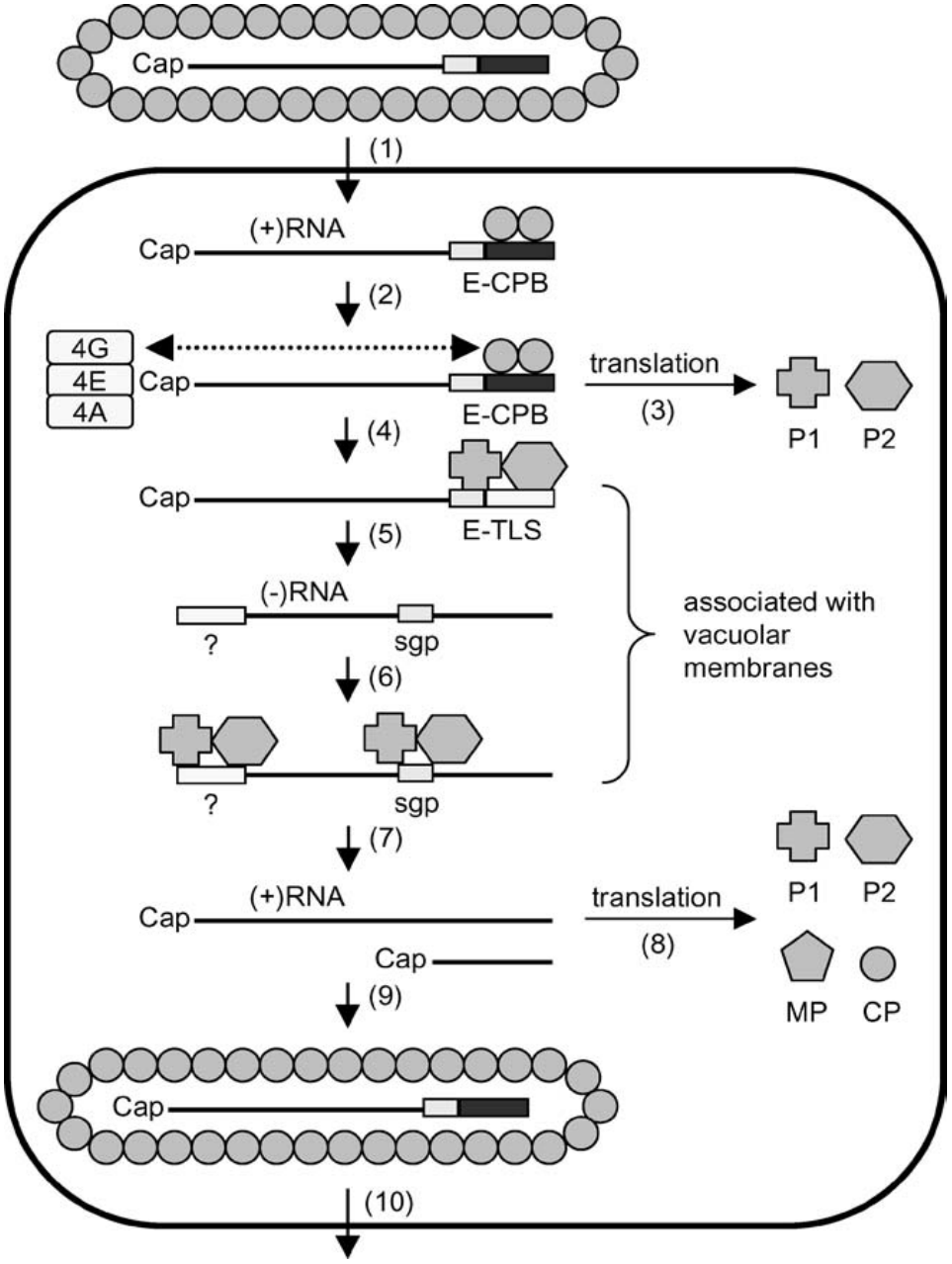

Fig 2.2: Replication mechanism of positive stranded RNA viruses. There are 10 major steps involved in the natural infection and replication of the positive stranded RNA viruses are described in text. (Source: Bol, 2005). Here, E-CPB boxes indicate the 3' end homologous 145 nts sequence of the AMV RNAs (hairpin E plus 3' end 112 nts in CPB conformation) or E-TLS (hairpin E plus 3' end 112 nts in CPB conformation).

Step-6: Replication of negative strand:

Replication steps involved in the negative strand were completely unknown. However, switch off translation, clearance of ribosomes and replications were carried out by the CP dissociation associated with formation of replicase proteins was reported (Bol, 2005).

Step-7: Initiation of positive strands formation:

The sub-genomic promoters on the negative strand of RNA were identified by replicase proteins, P1 and P2 and form the sub-genomic RNA molecules RNA4 and RNA4a (TSV, CMV).

Step-8: Formation of sub-genomic RNAs:

The positive strands of progeny RNA molecules were synthesized. The sequences, in 5'-UTR of RNAs, which are required for RNA replication *in vivo* or for synthesis of positive- strand RNA in vitro, have been identified. The natural negative-strand RNA acts as template for positive- strand RNA synthesis in vivo (Houwing *et al*., 2001). At present no proof exists about the role of CP in synthesis of positive strand RNA. The circular templates are compulsory for RNA replication (Bol, 2005).

Step-9: Translation:

All the viral proteins are translated from the synthesized RNA molecules. The proteins forms will be P1, P2, CP, and MP.

Step-10: Formation of virion particles:

The final step is the assembly of complete virus particle. All the progeny RNA assemble into functional virion particles and capable to move from one cell to another cell with the help of MP.

2.2.5 Transmission of the virus

Plant virus diseases occur because of the spread of the virus in nature. It is a triple interaction between the plant, the virus and a means of virus spread. It can be transmitted from one host to another during every season or year and from field to field or region to region. It can be either through mechanical means due to rubbing manually, wind, animals and implements or by various other biological means like insects, nematodes, fungi, grafting and through seed. Transmission is classified into two broad categories, 'vertical transmission' wherein the virus is passed through the plant seed to the next generation or through the vector egg to its progeny and

"horizontal transmission" in which the virus spreads to neighboring plant or across region by movement through other agents like insects, wind, man and the water. About 88% of plant virus species uses an arthropod vector for their maintenance and survival (Andret-Link and Fuchs, 2005). The remaining 12% vector-transmitted plant viruses use fungi, plasmodiophorids and nematodes.

2.2.5.1 Transmission by seed

TSV transmission through seed was reported for bean, *Datura stramonium*, *Chenopodium quinoa* (Brunt *et al*., 1996), *Melilotus alba, Glycine max, Gomphrena globosa, Nicotiana clevelandii, Vigna unguiculata* (Kaiser *et al.,* 1982), black raspberry (Converse and Lister, 1969) strawberry (Johnson *et al*., 1984) and *Nicandra physalodes* (Salazar *et al.*, 1982). Reported frequencies of transmission range from 90% in *Glycine max* to less than 1% in *Vigna unguiculata* (Kaiser *et al.*, 1982). The black raspberry latent strain is transmitted by pollen not only to seed but also to the plant pollinated (Converse and Lister, 1969).

2.2.5.2 Transmission by thrips

A *Frankliniella* sp. is reported as a vector in Brazil (Costa and Lima Neto, 1976). A mixture of *Thrips tabaci* and *Frankliniella occidentalis* was reported to transmit the virus in USA (Kaiser *et al.*, 1982). *Thrips tabaci* transmitted the virus to *Chenopodium quinoa* (Sdoodee and Teakle, 1987) apparently by mechanical inoculation rather than involving ingestion of the virus by the vector (Sdoodee and Teakle, 1993). A combination of thrips (*Microcephalothrips abdominalis*) and wind-blown pollen is reported to spread the virus from *Ageratum houstonianum* to adjacent crops of tobacco (Greber *et al.*, 1991).

2.2.6 Diseases and geographical distribution

2.2.6.1 Symptomatology

Symptoms may be classified into either local or systemic. When symptoms are confined only to a particular part that develops near the site of entry on leaves, they are called as local infections. On the other hand, when the virus causes disease in the whole plant, it is called systemic infection. In contrast, many viruses can also cause

infection without showing any visible symptoms. These hosts are called asymptomatic and the viruses are called latent viruses.

Usually, local symptoms appear on the inoculated leaves only. They can be discrete isometric lesions. Infected cells lose chlorophyll and other pigments which results in symptoms such as chlorotic spots and chlorotic rings. Necrotic spots and necrotic lesions are observed when the infected cells die. In contrast to local infection, systemic symptoms appear on the uninoculated leaves also. They are the most important symptoms because they can affect any part of the plant such as flower, fruit and petiole. The most important symptom in a systemic infection is mosaic, appearance of irregular and unfixed pattern of green and chlorotic areas of leaf. Yellowing and necrosis are other patterns of systemic infection. (Hull, 2002).

Infected lettuce plants with TSV show symptoms such as: mosaic, vein clearing, vein necrosis, yellowing and leaf distortion. The symptoms of TSV on sunflowers include: black streak on the stem and leaf stalks stunted growth shortened internodes, deformed growing tip, yellow blotches on leaves and apparent plant death, especially in plants that become infected in early stages of development (Bhat *et al*., 2002).

In tomato TSV causes stem necrosis, bud necrosis, yellowing and mosaic pattern in the tomato leaves as well as chlorotic rings in fruits. It also causes various symptoms on groundnut such as chlorotic lesions on terminal leaflets, ring spots and often necrosis of terminal bud, axillary shoot proliferation with small and deformed leaflets. Infected plants remain stunted and seldom die. PBNV and TSV combined together cause severe bud necrosis in the groundnut and it include mosaic, mottling symptoms on leaves, and drooping of the petioles followed by terminal bud necrosis. (Reddy *et al*., 2002).

2.2.6.2 Geographical Distribution

TSV has been reported from more than 26 countries worldwide. It has a wide host range, infecting more than 200 plant species belonging to 30 dicotyledonous and monocotyledonous plant families (Fulton, 1985). TSV is reported from horticultural, agricultural and various weed species (Almeida *et al*., 2005). Horticultural crops include; Black raspberry (*Rubus occidentalis*) [Converse, 1972; Kaiser *et al*., 1991], crane berry (*Vaccinium macrocarpon*) [Jones *et al*., 2001], dahlia (*Dahlia variabilis*)

[Pappu *et al*., 2008]; agricultural crops: Solanaceous crops: pepper (*Capsicum spp*.) [Gracia and Feldman, 1974], tobacco (*Nicotiana tabacum*) [Finlay, 1974], tomato (*S. lycopersicum*) [Cupertino *et al*., 1984], Legume crops: soybean (*Gycine max*) [Ghanekar and Schwenk , 1974], cowpea (*Vinga unguiculata*), white clover (*Melilotus alba*) [Kaiser *et al*., 1982], groundnut (*Arachis hypogaea*) [Cook *et al*., 1999], other crops: sunflower (*Helianthus annuus*) [Sharman *et al*., 2008], cotton (*Gossypium hirsutum*) [Waqar *et al*., 2003]. Kaiser *et al*., (1991) reported TSV naturally infecting chickpea in the United States.

In Australian continent, TSV was first reported in 1971 and has subsequently been reported from tobacco, strawberry, dahlia and various weed species, mostly from south-eastern Queensland (Greber *et al*., 1991). Sharman *et al*., (2008) reported TSV naturally infecting sunflower, cotton, mung bean and chickpea in Australia. TSV has become one of the most damaging virus in Australian oilseed and pulse crops (Sharman, and Thomas, 2013).

In India, TSV was first reported from sunflower (*Helianthus annuus*) field of Karnataka in the year 1997 (Annual progress report of AICRP on oilseeds 1997). On the basis of serological relatedness and sequence identity, it has been proposed that the sunflower ilarvirus from India should be considered as a strain of TSV belonging to subgroup I and designated as TSV-SF. This is the first report of the molecular characterization of TSV on sunflower from the Indian subcontinent (Bhat *et al*, 2002). Epidemic form of TSV was reported on peanut crop from Ananthpur district of Andhra Pradesh during 1999-2000 (Prasada Rao *et al*., 2000; Reddy *et al*., 2002). Later on it was reported from various crops by different groups of scientists with characteristic symptoms and levels of disease incidence that are mentioned in table 2.4.

Table 2.4: Natural occurrence of *Tobacco streak virus* in Indian sub-continent

S.No	Crops	Symptoms	Incidence of disease	References
1.	Sunflower (*Helianthus annuus*)	Extensive necrosis of leaf lamina, petiole, stem and floral calyx.	AP, KA, MH, and TN. Disease incidence 10 to 80 %	Prasada Rao *et al*., 2000; Ramaiah *et al*., 2001; Bhat *et al*., 2002
2.	Cotton (*Gossypium hirsutum*)	Cholotic and necrotic spots of leaf and boll	AP, MH, KA; disease incidence 30-40%	Bhat *et al*., 2002
3.	Sunn-hemp (*Crotalaria juncea*)	Cholotic and necrotic spots of leaf	AP, MH, KA	
4.	Mungbean (*Vigna radiata*)	Chlorotic and necrotic spots of leaves	AP, KA	Bhat *et al*., 2002
5.	Peanut (*Arachis hypogaea)*	Stem necrosis, bud necrosis, leaf mottling	AP	Reddy *et al*., 2002
6.	Okra (*Abelmoschus esculentus*)	Chlorotic spots, leaf blotch, chlorotic streak and distortion of fruit	KA, TN, AP, MP, HA, and MH; disease incidence up to 63%	Krishna Reddy *et al*., 2003a
7.	Cucumber (*Cucumis sativa*)	Symptoms of necrotic leaf lesions on leaves and stems resulting in dieback of vines	Yield losses of 31 to 75% in Bangalore, Bellary, Davanagiree, and Tumkur districts of KA, infected cucumber and gherkin.	Krishna Reddy *et al*., 2003b
8.	Gherkin (*Cucumis anguria*)			
9.	Safflower (*Carthamus tinctorious*)	Necrosis of vein, leaf and terminal buds, Necrotic streak on the stem	Aurangabad, MH	Chander Rao *et al*., 2003
10.	Chilli (*Capsicum annuum*)	Necrosis of leaves and buds	Faizabad, UP	Jain *et al*., 2005
11.	Urdbean (*Vigna mungo*)	Necrosis of plants	AP, MH, KA	Ladhalakshmi *et al*., 2006
12.	Nizer (*Guizotia abyssinica*)	Petiole necrosis	KA	Arun kumar *et al*., 2007
13.	Soybean (*Glycine max*)	Chlorosis, Necrosis of leaves, stem and buds	MH Incidence of disease up to 40%	Arun kumar *et al*., 2008
14.	Onion (*Allium cepa*)	Necrosis of bulbs and reduced size	Kurnool, AP	Sivaprasad *et al*., 2010
15.	Guar (*Cyamopsis tetragonoloba*)	Foliar mosaic, necrotic spotting and streak on buds and stems	Chittoor, AP	Sivaprasad *et al*., 2012
16.	Kenaf (*Hibiscus cannabinus*)	Mosaic and necrotic spots on buds and leaves	Chittoor, AP Incidence of disease up to 10-15 %	Bhaskara Reddy *et al*., 2012
17.	Jasmine (*Jasminum sambac*)	Wilting of jasmine branch and necrosis of leaves & petiole	Cheruvu Belagal and Kadiri madala of Kurnool, AP	Seshadri goud *et al*., 2013
18.	Horse gram *Macrotyloma uniflorum*	Necrotic spots with wrinkle margin	Anantapur, AP	
19.	Lablab bean (*Lablab purpureus*)	Veinal necrosis and wilting of plant	Chittoor, AP	Bhaskara Reddy *et al*., 2013
20.	Pigeon pea (*Cajanus cajan*)	Leaf necrosis with wrinkled margin	Anantapur, kadapa, Kurnool and mahbubnagar, AP	Vemana *et al*., 2014

2.3 Construction of the infectious clone for plant viruses and their introduction into plant

In the last decade, the expression and production of the heterologous protein using transgenic plant as a bioreactor; has been greatly flourished. The generation of the transgenic plant is a time-consuming and tedious process. Transient expression is an alternative approach over stable transformation. Transient expression through viral vector is a very fast robust and efficient over stable transformation. Generation of an infectious clone of the virus is the first step towards the development of a plant viral vector (Nagyova and Subr, 2007).

2.3.1 The construction of infectious clones for plant RNA viruses

An infectious clone is an imperative molecular tool to study the gene expression and replication aspect of plant RNA viruses using mutation and functional genome approaches. This can aid in the study of pathogen host interactions, induced or natural RNA recombination and mechanisms of plant-virus movement. Now a days, generation of infectious clones has become a common laboratory protocol worldwide. However, there are several difficulties and limitations come across during the assembly of such clones. Generally, it is a long and tedious process. The infectivity of a clone is strongly influenced by cDNA synthesis and the cloning strategy used (Boyer and Haenni, 1994). Several steps are involved in the generation of infectious cDNA clones which include purification of virus, extraction of RNA, reverse transcription, PCR amplification of genomic cDNA fragments and adding a promoter to the full length cDNA clone.

2.3.1.1 Types of Infectious clones

Based on the promoter and place of transcription, infectious clones of RNA viruses are divided into two types: infectious RNA (*in vitro* transcripts) and infectious cDNA (based on the transcription *in vivo*).

2.3.1.1a Infectious transcripts

A strong bacteriophage promoter has been driven *in vitro* transcription. The promoters of phages γ (Pm), SP6, T3, and mainly T7 have been used (Melton *et al.*, 1984; Dunn and Studier, 1983). The preparation of good quality of transcript is very difficult because of fragile nature of RNA.

2.3.1.1b. Infectious cDNA

The cDNA clones are transcribed from the CaMV 35S double promoter (Vives *et al.*, 2008) directly in the nucleus of host plants using RNA polymerase II. Full length infectious cDNA containing vector has several advantages over the infectious transcript. The expression of the infectious viral RNA by *in vivo* is less sensitive to RNA degradation because it does not require the *in vitro* transcription and is independent on the viral replication process as well (Van Bokhoven *et al.*, 1993).

The cDNA clones are stable for a long time *in vitro* in the form of isolated plasmid DNA. Apart from advantage it has some disadvantage too as the construct has to be introduced into the nucleus to allow the transcription, that decreases the efficiency of some transfection methods.

2.3.2 Introduction of infectious clones into plants

Many technologies are available to transfer gene product into plant cells and are categorized into two main classes, direct gene transfer and indirect gene transfer methods. The direct gene transfer involves use of physical equipment to transfer the gene product. These include biolistic or particle bombardment or microprojectile bombardment, protoplast transformation, electroporation, etc. The indirect gene transfer method uses the microorganism *Agrobacterium tumefaciens* as the vehicle of DNA delivery, which transfers part of its DNA (T-DNA) into the genomes of host plants (Friedberg, 1998).

2.3.2.1 Mechanical inoculation

Mechanical inoculation is usually used for the *in vitro* RNA transcripts. In this method, leaf exterior is damaged with an abrasive either celite or carborundum, which permits direct introduction of nucleic acid into the injured cells (Ding *et al.*, 2006; Hull, 2002).

2.3.2.2 Agroinfection

Agroinfection is a very efficient method to introduce the gene of insert into the plants. Agrobacterium genus is known to infect plants and launch transfer DNA (T-DNA) into host cell nucleus. This T-DNA is integrated unpredictably into the plant genome. When the T-DNA is substituted with a cDNA clone of a virus, the virus will

be transcribed, transported from the nucleus to the cytoplasm through nuclear pores, where it will get transcribed and replicate and induce infection in the plant. Initially, this method is developed for the transfer of phloem-restricted viruses to allow functional genomics studies in the viral host plants (Grimsley *et al*., 1987; Leiser *et al*., 1992) however it is used for other viruses also (Annamalai and Rao, 2005; Gopinath *et al*., 2005 and other references from there). Agroinfection can be also used in transient expression such as infiltration with a syringe, vacuum or agrodrenching (Liu and Lomonossoff, 2002). This method has a number of advantages over stable transformation procedures: very high amounts of foreign protein expression are obtained in a very short time and the transgene is not passed on to the progeny, because no stable transformation of the plant occurs. Since 1980's foreign genes have been introduced into plants using plant viral vectors. Many improvements have been made to expression systems through recent advances in the field of plant virology and molecular biology. Advantages include extremely fast, high yield of protein expression and enhanced transgene containment.

2.3.2.2.1 Agrobacterium

Agrobacterium tumefaciens, belongs to family *Rhizobiaceae*; genus: *Agrobacterium*, is a gram negative soil resident pathogenic bacterium that causes crown gall disease on many dicotyledonous plants (Braun, 1943; Friedberg, 1998). The crown gall disease is caused because of the expression of the foreign genes known as T-DNA released from Ti (tumour inducing) plasmid. The tumour inducing plasmid is a large double stranded circular DNA of approximately 200 kb, consisting of a specific region (T-DNA, approximately 20 kb), which can be transferred from bacteria into plant cells. The Ti plasmid requires another plasmid that contains virulence genes (*Vir*) which helps in the transfer process of T-DNA (Stewart, 2008). There are at least six essential operons (*Vir*A, *Vir*B, *Vir*C, *Vir*D, *Vir*E, *Vir*G) and two non-essential operons (*Vir*F, *Vir*H) and each has its own number of genes.

The mechanism of gene transfer from *A. tumefaciens* to plant cells is shown in fig 2.3. Viral cDNA of interest is cloned between the left and right borders of the T-DNA region, located on the modified Ti plasmid and subsequently mobilized into *A. tumefaciens*. After inoculation of *Agrobacterium* on to plant tissue, the bacterium recognizes and migrates to attach to the wounded tissue through sensing of chemicals

released from the injured tissue (Friedberg, 1998, Tzfira and Citovsky, 2008). As soon as the bacterium binds itself to the plant cell, *Vir*A and *Vir*G are activated by the phenolic compounds (such as acetosyringone and some monosaccharides) released from the wounded plant (Tzfira and Citovsky, 2008). *Vir*A phosphorylates *Vir*G, which subsequently triggers the transcription of other *Vir* genes.

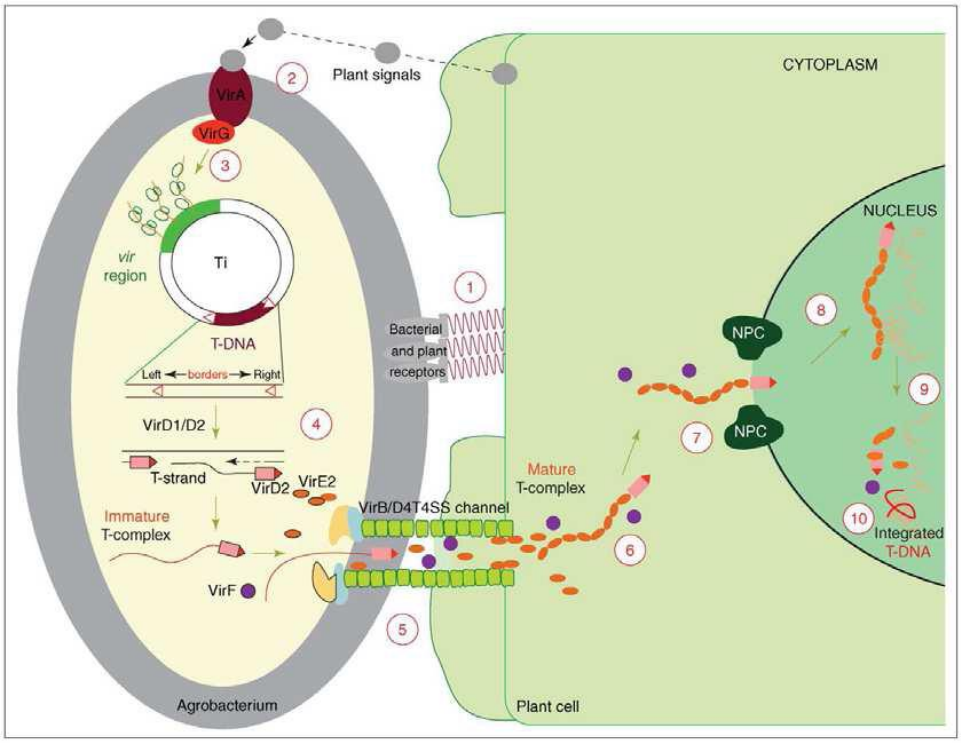

Fig 2.3: Mechanism of T-DNA gene transfer during the *Agrobacterium* mediated transformation process. There are 10 major steps involved in the transformation process, and are described above (Source: Tzfira and Citovsky, 2006).

The activation of the *Vir* system generates a new copy of single stranded (ss) molecules from the bottom DNA fragment located between the T-DNA borders (Tzfira and Citovsky, 2008). Two Vir genes (*Vir*D1 and *Vir*D2) nick the T-DNA border sequences at end of the T-DNA ends and excise the T-region from the Ti plasmid. After excising the ssDNA strand, *Vir*D2 binds covalently to the 5' end of the nicked DNA strand (Stewart, 2008). Once the ssT-DNA-*Vir*D2 complex is formed, then it is coated by *Vir*E2 to prevent degradation and along with other *Vir* proteins transported through the plant cell wall and cellular spaces to the nuclear genome by a system called *Vir*B/D4 type IV secretion (Tzfira and Citovsky, 2006; 2008). The last step in the transformation process is the integration of T-DNA to the plant nucleus, where the attachment of *Vir*D2 and the coat of *Vir*E2 are removed prior to the

integration of T-DNA into the plant genome. During the integration process, T-complex interacts with the VIP1, CAK2M (plant ortholog of cyclin dependent kinase-activating kinases) and TATA-box binding protein (TBP) and other host machinery necessary for transcription to guide it to the site of integration (Tzfira and Citovsky, 2006). However in the transient expression of the gene, T-DNA cassette is transcribed by RNA polymerase II without integration into plant genome.

2.4. Overview of the plant virus movement and movement protein

The present thesis is concerned with the molecular characterization of the movement protein of TSV. A brief review on the various strategies employed by plant viruses for cell-to-cell movements is thereby discussed.

Animal viruses can negotiate their entry into the host cell by manipulation of the host's array of receptor systems. But unlikely to the animal viruses, the plant viruses have to face the impervious barrier of the cell wall. For this reason, the primary infection of plant viruses sometimes remains confined to a single cell or a few cells only. This occurs after mechanical damage to the plant cell wall and plasma membrane by the vectors transmitting the virus, or by mechanical inoculation. The infection can be passed onto the adjacent cells with the help of specialized virus-encoded proteins called movement proteins (MPs). An interesting fact about viruses is that the specificity of a plant virus infection does not occur at the level of replication and plant viruses have the ability to replicate within non-host cells. However, the susceptibility is linked to the ability of the virus to gain access to the phloem tissues of the plant for long distance transport, and thereby spread a systemic infection.

In systemic infection, the virus moves from the source leaves to sink leaves in a passive mode along with the flow of photoassimilates (Leisner and Howell, 1993). But in disparity, the cell-to-cell movement is an active process that involves the contact of virus and PD. In the past, it was widely accepted that the cell-to-cell movement of the plant viruses occurs through a passive diffusion process. The first report opposing this idea came from the works of Nishiguchi *et al*., 1978; 1980). He used temperature-sensitive Ls1 mutants of *Tobacco mosaic virus* (TMV). At restrictive temperatures, these mutants could replicate efficiently at the single cell level and form virus particles, but it was incapable of moving out of the primary infected cells and cause systemic infection. The Ls1 defect was mapped to the gene

encoding 30 kDa protein in TMV (Doem *et al*., 1987). This 30 kDa protein was later named as movement protein (MP). In the past decades, it has been repeatedly proved that not only in TMV, but the MPs are present in most plant virus families and perform the function of intercellular viral transport.

The MPs encoded by different virus families may complement each other or are functionally interchangeable (De jong and Ahlquist, 1992; Giesman-Cookmeyer *et al*., 1995; Fajardo *et al*., 2013). The movement defect of a virus strain in a particular host plant can be complimented by co-infection with another unrelated plant virus which is movement competent (Atabekov and Tilianisky, 1990). One such example is *Brome mosaic irus* (BMV) gains the ability to move through tomato plants when coinfected with TMV (Atabekov and Tilianisky, 1990). Sometimes cell type restriction can be overcome by movement function of heterologous viruses. For example, the blockage to the movement of *Potato leaf roll lutiovirus* into the mesophyll cells from phloem could be overcome by co infection with *Potato virus Y* (Barker, 1987). This exchangeability and complementation of movement function from unrelated virus families suggest that virus can move through common intercellular movement pathways or all movement proteins may have some common ancestors and some common mechanisms of transport within the host.

2.4.1 Classification of movement protein

The genetic constituent of viruses has a particular coding sequence for movement protein which is necessary for their cell- to -cell as well as systemic movements. Movement proteins from plant viruses are classified under two super families (Carrington *et al*., 1996). First was exemplified by TMV movement protein, the MP aids the movement of the virus as a nucleoprotein complex through the plasmodesmata. Second was represented by *Cowpea Mosaic Virus* (CPMV) encoded MP, the MP forms tubular structures through which intact virions move from cell-to-cell. These gross differences in the mechanism by which a virus would transport from cell-to-cell depends on whether the virus requires complete functional capsid protein for its intercellular translocation or not. Based on the requirement of the MP and CP for the movement of virion particle or infectious molecule from one cell to another cell, viruses are grouped under three categories (Scholthof, 2005 and Niehl and Heinlein, 2011) which are mentioned in table 2.5.

Table 2.5: Classification of the viruses based on the requirement of the MP and CP for cell to cell movement

Group I	Only MP required for cell-to-cell movement of their RNA	Example Tobamovirus, Dianthovirus, and Umbravirus
Group II	Multiple MPs and the CP required for both cell-to-cell and systemic trafficking of the viral RNA	Potyviruses, Hordeiviruses, and Potexviruses
Group III	MP and CP required for cell-to-cell and long distance movement	Comovirus and Closteroviruses,

For the Systemic movement of *Tobacco mosaic virus*, it also requires the CP and a component of the replication complex (Liu *et al*., 2005). The role of the CP is to facilitate MP activity or to protect the genome. *Red clover necrotic mosaic virus* (RCNMV) capsid protein deletion mutants could move from inoculated cells to the neighboring cells, but were not capable of spreading to uninoculated leaves and were restricted only to the inoculated leaves (Xiong *et al.*, 1993). On the other hand, some viruses do not require capsid protein for long distance movement. For example, when the capsid protein of *Tomato bushy stunt virus* (TBSV) was replaced with GUS (β-glucoronidase) gene, the genetically modified virus could still systemically infect the host (Scholthof *et al*., 1993). It has been established that viruses for which capsid proteins are necessary for their systemic spread in the host tend to follow the microtubule mediated intracellular transport pathway, since complete viruses are incapable of negotiating the plasmodesmal size exclusion limit (SEL). On the other hand, viruses which can dispense their capsid for the intercellular spread tend to move as nucleoprotein complexes through the plasmodesmata following the TMV strategy. TMV MP increases the SEL of PD by microfilament severing activity (Su *et al*., 2010).

2.4.2 Characteristics of movement proteins

Irrespective of the superfamily to which the MPs belong, they have some basic underlying similarities in their functional domains. Three domains are identified in most of the MP of RNA viruses. These are the domain for RNA binding, the domain for cooperative RNA binding and the domain for interaction with plasmodesmata. The plasmodesmata interacting domain may also be necessary for targeting the MP to the cell wall (Barna *et al*., 1991). Several groups of viruses which replicate in the

cytoplasm encode MPs with structural and functional differences from those encoded by TMV like viruses. But the gross nucleic acid binding property remains a common and highly conserved feature. At least four groups of viruses have a triple gene block, which encodes a set of three MPs (Petty *et al*., 1990, Glimer *et al*., 1992). The largest of the three protein products of the triple block gene block (open reading frame 2 proteins) and *Barley stripe mosaic* Hordivirus βb protein bind ssRNA cooperatively, have ATPase activity and a highly conserved helicase-like sequence motif (Donald *et al.*, 1995). The phosphorylation activities on replication and movement of viruses are still unclear (Tyulkina *et al*., 2010). Although function of helicase and the nature of interaction among the three MPs are not very clear, the RNA binding activity would be required for the formation of nucleoprotein complex, analogous to those formed by the TMV like MPs.

The MP (P1 protein) of *Cauliflower mosaic virus* (CaMV), a dsDNA-containing pararetrovirus also possesses ssRNA binding activity (Citovsky, *et al*., 1992: Thomas and Maule, 1995). Citovsky *et al*., (1992) hypothesized that the 35S RNA reverse transcription template is the entity that moves from cell-to-cell. Although the binding domain of P1 clearly overlaps with a large region required for intercellular movement of the virus (Thomas and Maule, 1995), it remains an open question as to whether or not the RNA-binding function is involved directly in transport, because other evidences indicate that CaMV moves from cell-to-cell as icosahedral virions in which dsDNA is packaged (Maule, 1991). Furthermore, P1 protein induces cell wall spanning tubules through which virions are proposed to pass (Parbal *et al*., 1993). It is possible that CaMV may actually use two distinct movement strategies at different stages of its multiplication cycle or the strategies may be different among tissues it is infecting (Thomas and Maule, 1995; Citovsky and Zambryski, 1991).

2.4.3 Structure of Plasmodesmata

Plasmodesmata serve as intercellular channels that maintain a plant wide simplistic domain and enable the entry and exit of viruses in different parts of the plant. Plasmodesmata have been studied for several decades to delineate their mechanism and molecular organization. Some proteins have been described that seem to be characteristic of PD protein (Blackman *et al*., 1999). According to the ultra-

structural analysis of plant tissues, there are several forms of plasmodesmata including primary plasmodesmata, which are formed during cytokinesis (Lucas *et al*., 1993; Ding, 1997; Crawford and Zambryski, 1999). The secondary plasmodesmata that are formed later during development through existing cell walls and are involved in the expansion of the cytoplasmic continuum (Van der Schoot and Rinne, 1999). Combined cytoplasm of all cells is interconnected by plasmodesmata, which enables communication throughout the plant.

Generally, plasmodesmata are narrow channel with a diameter of 20-30 nm, which cross the plant cell wall (Itaya *et al*., 1998). Plasmodesmata may consist of only one channel, linear or simple plasmodesmata or network of channels which are branched (Itaya *et al*., 1998). Desmotubule is a stretch of appressed endoplasmic reticulum present in the centre of the channel. It links the endomembrane systems of the neighboring cells. Some plasmodesmata contain a central cavity between the plasma membrane and desmotubule. Both the plasma membrane and the desmotubule are associated with protein globules called bridging proteins (Ding *et al*., 1992). These bridging proteins form the linkages between the plasma membrane and desmotubule globules across the central cavity. It is the space between the plasma membrane and desmotubule the cytoplasmic sleeves, through which the virus and other macromolecules are proposed to pass. The cytoplasmic sleeve, the space between the plasma membrane and desmotubule is subdivided into smaller microchannels, each with a diameter of 1.5-2.0 nm. Actin (White *et al*., 1994) and myosin (Reichelt *et al*., 1999; Radford and White, 1998) might be structural components of these microchannels.

Plasmodesmata are influenced by environmental (Cleland *et al*., 1994; Schulz, 1995) and developmental signals (Duckett *et al*., 1994; Oparka *et al*., 1999) and tissue specific features (Kempers and Van Bel, 1997). In general, with respect to metabolism, sink-source transition has been noticed. The source tissues produce excessive photo-assimilates which are transported through the phloem to the different sink tissues which are utilized subsequently for their growth and development. The transition of sink to source results in structural changes in PD's from linear to branched plasmodesmata (Oparka *et al*., 1999). Plasmodesmata act as gateways to local and systemic virus infection (Benitez-Alfonso *et al*., 2010). The structure of PD and the contribution of viral MPs to intercellular movement was explained in several

recent reviews (Ueki and Citovsky, 2011; Benitez-Alfonso *et al*., 2010; Tilsner *et al*., 2011; Niehl and Heinlein, 2011).

2.4.4 Role of movement protein in inter- and intra-cellular transport of viruses

Viruses move throughout the plant via plant intercellular conduits the plasmodesmata (Esau 1948). Viral spread through these connections occurs in two distinct steps, local and systemic. In the initial phase of infection by mechanical or insect mediated inoculation, many plant viruses spread cell to cell through PD until they reach the vascular system. Later, the viruses are transported systemically through the vasculature. Virus particles and naked viral RNAs and viroids are too large to pass through PD by diffusion.

The movement protein of *Cucumber mosaic virus* forms tubular structure on the protoplasts surface (Canto and Palukaitis, 2005). The interactions of the MP with tubular structure were not determined. However, unlike all of the other tubule-forming viruses, these tubules are not necessary for CMV intercellular movement. The MP of TMV, CMV and AMV, members of the alpha virus super group localizes to ER (Huang and Zhang, 1999). Later it was proved that mutant MP did not localize to PD even after fractionation (Huang *et al*., 2001). Recently, the MP of *Prunus necrotic ringspot virus*, an ilarvirus who's MP can complement the function of the related AMV MP, was shown to contain a hydrophobic region that associated with a membrane, but did not span it (Martı´nez-Gil *et al*., 2009). The need of hydrophobic region for the cell-to-cell movement of the virus AMV RNA3 was proved through mutational analysis (Martinez-Gil *et al*., 2009).

In the case of Ilarvirus proteins accumulate early in virus infection, bind RNA co-operatively, associate with the cell wall fraction, locate the plasmodesmatal region, and increase the plasmodesmatal size exclusion limit (SEL) (Zheng *et al*., 1997; Canto and Palukaitis, 1999). Cell-to-cell movement of Bromoviridae requires the viral coat protein in most situations (Rao and Grantham, 1996; kalpan *et al*., 1998) and is associated with the formation of tubules (Zheng *et al*., 1997; Canto and Palukaitis, 1999; Sanchez-Navarro and Herranz, 2006). However, although cell-to-cell movement of *Cucumber mosaic virus* needs coat protein, the virus does not need to be encapsidated as virions (Kalpan *et al*., 1998) whereas *Brome mosaic virus* requires an encapsidation competent coat protein (Schmitz and Rao, 1996).

The one of the well-studied movement protein is *Tobacco mosaic virus* (TMV) p30 with molecular weight of 30 kDa (Deom *et al*., 1987).

TMV MP; Most of the research on this type of MPs was done using TMV and RCNMV. The biochemical nature of the virus encoded MP is well-characterized 30 kDa (Melcher, 2000). Based on the decade-long research, a model has been proposed. By experiments performed in late 1980s, Wolf *et al*., (1989) has demonstrated that fluoresceins-isothiocyanate-labelled dextran with an average molecular mass of 9400 Da and an approximate stockes radius of 2.4 nm was able to move between cells of transgenic plants expressing the movement protein of TMV, whereas the size exclusion limit of normal plasmodesmata is 700-800 Da. They were also unable to visualize MP complex with ssDNA or ssRNA. These complexes were long, unfolded and very thin (1.5-2 nm) in diameter. Unlike TMV virions (diameter 18 nm), the complexes were thus compatible in size with the MP induced increase in plasmodesmatal permeability (2.4-3.1 nm), making them likely candidates for the structures involved in cell-to-cell movement of TMV. Thus after the MP is expressed, it performs two functions. First, it binds to viral RNA and unfolds the viral RNA from a random coil to a linear rod shaped structure so as to reduce its diameter. The RNA-MP complex is then translocated and targeted to the plasmodesmata, where the complex interacts with components of the plasmodesmata to increase its pore size or SEL (Wolf *et al.*, 1989). The increased pore size combined with the reduced molecular diameter of the viral RNA allows the ribonucleoprotein to move through the plasmodesmata to the next cell.

TMV MP binds ssRNA and ssDNA in a strong, highly cooperative and sequence non-specific manner. With the help of in-frame and double deletion mutation strategies, two independent nucleic acid binding domains were identified (amino acid 112-185 and amino acid 185-268). Another region spanning from amino acid 65 to 86 is required for correct folding of the MP (Citovsky and Zambryske, 1991; Citovsky *et al*., 1992).

RCNMV was also shown to follow the same strategy of cell-to-cell transport *in vitro* and *in vivo* as that of TMV. However, cooperative RNA binding was not necessary for cell-to-cell movement in vivo and only a fraction of the wild type RNA binding was shown to be required.

The association of TMV like MP with the interior of the plasmodesmata was shown by immunochemical electron microscopy (Atkins *et al*., 1991) and the central and C-terminal sequence of MP is shown to be necessary for plasmodesmal localization (Giesman- Cookmeyer and Lomel, 1993; McLean *et al*., 1995; Fujiwara *et al*., 1993). It was shown that the MP of various viruses interacts with the plasmodesmal proteins to increase the SEL (Amari *et al.*, 2010). It has been proposed that MP is sequentially transported on microtubules and then on microfilaments towards the cell wall enroot to plasmodesmata. This is consistent with detection of actin in and around plasmodesmata (White *et al*., 1994). The cytoskeleton is not is not responsible for the movement of MP was also proved by treating with inhibitoe Brefeldin A (Huang *et al*., 2000).

It has also been shown that certain mutants of MP, that are defective in cell-to-cell transport of virus are unable to traffic through the plasmodesmata, but the exact point in the trafficking pathway where these altered proteins are arrested are not yet known. The fusion proteins consisting of TMV MP with β-glucoronidase (GUS) also traffic between cells, implying the presence of plasmodesmal transport signal in the movement proteins have shown Waigmann and Zembryski, 1995.

Thus, the three main steps for the passage of MP genome complex through the plasmodesmata are: binding at the plasmodesmatal surface, transit through the channel and release into the adjacent cells. Binding of the MP genome complex at and internalization into plasmodesmata may occur via a default pathway, which is used by cytoskeleton-associated elements involved in intracellular trafficking. Transit of MP-genome complex may be driven by an active mechanism in which both MP and genome components move via interconnections with a plasmodesmal transport apparatus. It is assumed that the apparatus comprises of resident escort proteins, chaperons and molecular motors. Whether genomes are transported as stable nucleoprotein complex or as a dynamic complex in which MP subunits cycle on and off the genome is not known. The mechanism governing the release of the transported complex into the adjacent cell is also not very clear. It can be assumed that like other cellular transport mechanisms, the plasmodesmal transport system is also energy dependent. It has been reported that both TMV and CMV MPs bind to GTP, which may be transferred to and hydrolyzed by plasmodesmata associated GTPase during

transport (Li and Palukaitis, 1996). A conserved aspartate in the D motif is shown to be essential for GTP binding (Carvalho *et al*., 2004).

Tobacco mosaic tobamovirus (TMV) has been used as model system to study the intra and inter cellular movement. For movement TMV, it uses endoplasmic reticulum (ER) network for replication and spread through plasmodesmata (PD), symplastic communication channels through cell walls between neighboring cells (Laliberté and Sanfaçon, 2010; Niehl and Heinlein, 2011; Liu and Nelson, 2013; Niehl *et al*., 2013b). The movement protein of the TMV is present in the viral replication complexes (VRC) (Asurmendi *et al*., 2004) associates with RNA (Brill *et al*., 2000: Sambade *et al*., 2008) and acts as a microtubule associated protein (Ashby *et al*., 2006; Boyko *et al*., 2000; Boyko *et al*., 2007; Ferralli *et al*., 2006; Niehl *et al*., 2012). The interaction of the protein with MTs plays a role during early infection when ER membrane-associated VRCs localize to local inter sections of MTs with the ER (Boyko *et al*., 2007), reviewed in (Niehl *et al*., 2013b; Peña and Heinlein, 2013). These sites, recently termed "cortical MT-associated ER sites" (C-MERs), are proposed to function as specific platforms for the recruitment of host factors and membranes in order to facilitate the maturation of the VRCs into movement competent VRCs and, later, into virus factories (Peña and Heinlein, 2013).

To summarize in last decade there is an explosion in the complete genome sequencing of diverse viral genomes have been reported and efforts to construct infectious clone for representative member of the genus was done. But, among them, very few species were reported as biologically active. Apart from that advancement in the field of cellular and molecular mechanisms of the plant viruses were widen. Molecular biology of movement proteins for different viruses was greatly exploited. Now several viral proteins are discovered in the recent studies that interact with the cytoskeleton even though the importance of these interactions were unclear (Niehl and Heinlein, 2011; Harries *et al*., 2010; Peña and Heinlein, 2013).

Chapter-3

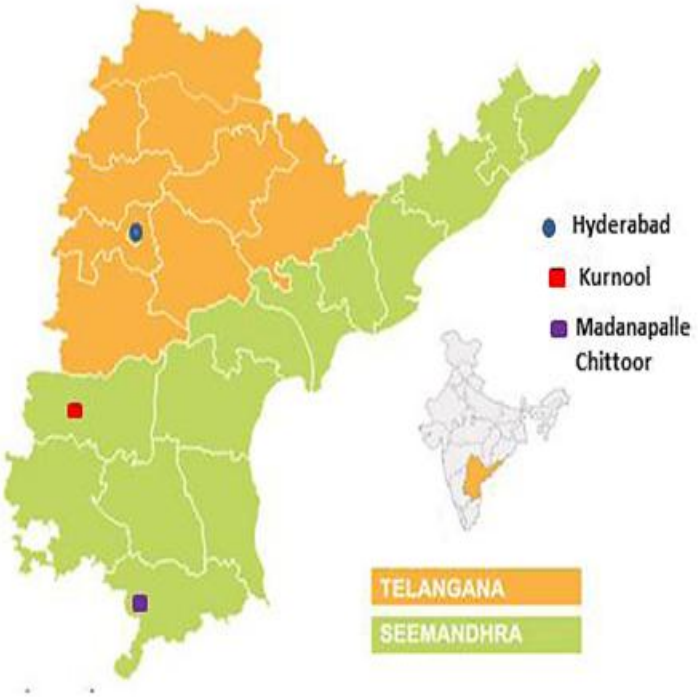

Identification and biological characterization of *Tobacco streak virus*

Identification and biological characterization of *Tobacco streak virus*

3.1 Introduction

The severe impact of the diseases caused by the plant viruses have been one of the major driving forces for the detailed study. To control the viral disease at early stage of infection, it is important for us to know the nature of the virus and its pathogenicity.

In the field, identification of viral infection, based on symptoms is possible but it may be deceiving as they induce variety of symptoms due to the influence of environmental cues like various type of physical and physiological stress as mixed infections. So it is important to characterize the virus, understand the viral side of the story in host-pathogen interaction and devise strategies to avoid infection at an earlier stage of infection. The characterization of viruses includes two major phases; diagnostic and descriptive phases. A diagnostic step based on the symptomatology which is centred on the biological methods includes single lesion assay, host range study, virus purification and serodiagonsis through ELISA, DIBA and Western blots analysis. Descriptive phase rely on physic-chemical properties of the viruses through electron microscopy and pattern of nucleic acid.

Bioassays involving sap inoculation of suspected plant material in the diagnostic hosts such as *Nicotiana* (Tobacco), V*igna unguiculata, Phaseolus vulgaris* and *Chenopodium* etc. The diagnostic host plants show consistent and distinctive viral infection under greenhouse condition (Walkey 1991). There are two major type of responses that occurs; local lesions which are confined to inoculated leaves (local lesion hosts) and systemic infections which produce symptoms on leaves distant from the inoculation site (systemic hosts). By the mechanical transmission or grafting, viruses move from indicator plant to another plant. Selection of the host plant is an important step in purification of plant virus because some plants contain phenols and tannins which form complexes with the viruses and causes yield losses at purification step. Apart from that, protein, organic acids, mucilage, gum and enzyme such as ribonucleases can inhibit, precipitate or destroy the virus. Purified virus was used in various biological characterization steps.

Electron microscopy is one of the fastest way to assign a particular virus to a taxonomic group based on their particle morphology and size for example; round

and knobbly (tymo, tombus); round and smooth (bromo, cucumo); ovoid or imperfectly spherical (ilar); angular (tobacco necrosis, nepoviruses, comoviruses, broad bean wilt) (Brandes and Bercks, 1965). On the other hand, viruses sharing the same size and shape are difficult to distinguish by their appearance. For instance, small spherical viruses may be difficult to distinguish from each other and from plant ribosomes.

The virus-specific structures in infected cells give clue for identification of the virus. The family *Potyviridae* produce 'pinwheel' inclusions that are characteristic of that virus in this family and are not found in healthy cells. Virus-specific inclusions have been characterized for a number of plant virus families and genera, and the detection of these inclusions indicates the presence of a virus within that group (Hull, 2002).

Clarke, *et al*., (1977) developed a method known as Enzyme-Linked Immunosorbent Assay (ELISA) to detect the plant viruses by adopting the use of antigen-antibody interaction. This assay has wide importance throughout the world due to its accuracy, simplicity and low cost. Antibodies arising from animals for the respective antigens are utilized in this technique. The sap extract of samples collected from the field which show symptoms related to our interest is directly coated in the polystyrene microtitre plate and detected with primary antibody and secondary antibody which usually carries a reporter molecules such as an enzymes like Alkaline phosphatase / Horse reddish peroxidase. The intensity of colour is detected / scored visually or quantitated by ELISA reader. This technique can be quantitative as well as qualitative.

o'Donell *et al*., (1982) developed the tissue blotting synonym of DIBA. It also utilizes antibodies raised against viruses. The proteins are immobilized on to the Nitrocellulose (NC) or PVDF membrane instead of wells as in ELISA. It is less labour intensive, rapid, sensitive and suitable for assays of 1,000 to 2,000 samples per day. Hence, the use of antibodies raised against the viral protein is advantageous in detecting the respective viruses.

As regards to molecular biology, much success has been achieved to characterize the viral pathogens. Considerable work has been carried out including whole genome sequencing.

The pattern of nucleic acid of virus gives ample scope for classification of a virus. Either genetic material of virus is DNA or RNA. Genome is monopartite nature, bipartite or multipartite. The molecular weight of the DNA / RNA gives the genome size of the virus. By revealing the complete sequence we can deduce the pathogenic nature of the virus which can be used in the control of viral disease.

Polymerase Chain Reaction (PCR) and Reverse transcriptase enzymes; revolutionized the field of molecular biology of RNA viruses. PCR is a very specific and sensitive method for virus identification that is based on the presence of unique nucleic acid sequence in the genome of a virus (Bartlett, 2003). During the PCR reaction, the number of molecules of the target sequence doubles with each cycle, and after 30 cycles over 10 billion copies of the target sequence are produced. The PCR product can be detected using agarose gel electrophoresis, a process in which an electrical current is used to separate molecules in a gel based on their size.

Genome sequencing is producing huge amounts of DNA sequencing data from various groups of plant viruses. Gene sequence databases are growing rapidly day by day. To analyse data efficiently, Sudhir kumar *et al*., 1994; developed Molecular Evolutionay Genetics Analysis (MEGA) software. It is an integrated tool for conducting sequence alignment, estimating divergence times, reconstructing phylogenetic tree, mining online databases, testing evolutionary hypothesis, inferring ancestral sequences and estimating rates of molecular evolution. MEGA is widely used software by various biologists for reconstructing the phylogenetic tree to unravel the evolutionary histories of species

3.2 Materials and methods

3.2.1 Field survey

Virus infected tomato and sunflower plant samples were collected by my supervisor Dr. K. Gopinath in 2009, during the field trip to Madanapalle town of Chittoor district, Andhra Pradesh and sunflower experimental field of Vibha seed, Hyderabad respectively. The number of the samples collected from each village is mentioned in table no 3.1. The sample collected from the Vibha seed (VS) named as

VS1 to VS20. Apart from that virus infected materials were also collected from other vegetable crops like okra and oilseed crops peanut and sunflower. Sunflower and peanut samples were collected from ICRISAT experimental plots and okra distorted fruits were from vegetable market of Lingampally and Mehdipatnam, Hyderabad, Telangana state. All virus infected samples were subjected to ELISA using different antibody.

Table 3.1a: Virus infected samples collected from sunflower and peanut fields

S. No.	Field visited	Number of samples collected
	Sunflower	
1.	Vibha seed	20
2.	ICRISAT Experimental plot	10
	Peanut	
1.	Nandyal, kurnool	25
2.	ICRISAT Experimental plot	20

Table 3.1b: Virus infected tomato samples collected from field

S.No.	Field visited in	No. of samples collected
1.	Kotavaripalle	72
2.	Valasapalle	49
3.	Ramasamudram	52
4.	Edigapalle	44
5.	Kotur	74
6.	Danduvaripalle	43
7.	Sugalmitta area	53
	Total	387

Table 3.1c: Virus infected okra fruit samples were collected from vegetable market

S.No.	Vegetable Market visited	Number of samples collected
1.	Lingampally	20
2.	Mehdipatnam	10

3.2.2 Virus identification

DAC-ELISA was used to screen the virus infected sample by directly coating the antigen (plant sap) in the microtitre plate wells (Hobbs *et al*., 1987 &

Mowat and Dawson, 1987). Approximately, 200 mg of infected plant leaf was macerated with 500 µl of 0.05 M carbonate buffer (pH 9.6) using pestle and acid washed sand and 200 µl was added to each well of ELISA plate. Plate was incubated for 2 h at room temperature (RT) and this was washed with PBS-T (0.15 M NaCl in 0.1 M phosphate buffer, 0.05% Tween 20 thrice at 5 min interval. The traces of solution were removed by tapping ELISA plate on four fold of tissue paper. The antisera were diluted to required volume in PBS-TPO buffer (0.15 M NaCl, 0.1 M phosphate buffer, 0.05% Tween-20, 2% polyvinyl pyrrolidine, 0.2% ovalbumin). Then 200 µl of respective antisera (1: 20,000 dilution) was added into the well and incubated for 2 h at room temperature. After incubation, the solution was decanted and washing steps were repeated as above to remove the unbound antibody. After that 200 µl of secondary antibody (1:10,000 dilution)-alkaline phosphatase conjugate was added to the wells, incubated and washing steps repeated with PBS-T thrice at 5 min interval. The reaction was developed by adding 200 µl of the substrate solution (9.7% diethanolamine, 50 mg p-nitrophenyl phosphate pH 9.8) and kept for incubation at room temperature for 10 min in the dark. The reaction was terminated by adding 50 µl of 3 M NaOH solution to each well. The positive samples were screened either visually (yellow colour intensity) or by measuring the absorbance at 405 nm wavelength where ever it is necessary.

3.2.3 Dot Immunobinding Assay (DIBA)

DIBA was performed using the total soluble proteins of healthy and infected leaf samples. Approximately 500 mg of leaf samples were macerated with 2 ml of TB Buffer (50 mM Tris Acetate pH 7.4, 10 mM $MgCl_2$, 250 mM KCl and 20% gycerol) at 4°C, then 1 mM PMSF and 1 mM DTT were added and centrifuged at 15,000 rpm for 10 min. The supernatant was collected and used for further study. The PVDF (polyvinylidine diflouride) membrane of required size was cut and soaked in methanol. 5 µl total soluble proteins from healthy and infected tomato, okra, sunflower and peanut leaves, positive for ELISA, were placed as dots on the PVDF membrane. After the dots were dried, the membrane was kept in blocking buffer (5% milk Nestle every day, 0.02 M Tris, 0.5 M NaCl, 0.05% tween-20, pH 7.5) for 40 min at the room temperature on the rocker. After incubation respective primary antibody (1:10,000 dilutions) was added and kept for two hours at room

temperature on the rocker. The solution was discarded and membrane was washed with TBS-T 3 times at 5 min interval. It was incubated again in the antibody buffer (0.02 M Tris, 0.5 M NaCl, 0.05% tween-20, pH 7.5 and 5% milk Nestle every day) containing secondary antibody-enzyme conjugate for a period of 2 h at RT on the rocker. It was washed with TBS-T thrice followed by TBS. Membrane was incubated with 300 µl of BCIP/NBT substrate till colour developed. The reaction was stopped by adding distilled water and membrane was dried on tissue paper.

3.2.4 Mechanical Inoculation

As plant viruses cannot invade plant cells through natural opening like leaf stomata or stem lenticel unlike bacteria or fungi. They can only enter into the cell through wound caused by mechanical damage. This mechanical damage was created by celite or caborundam 600 mesh. The ELISA and DIBA positive samples were taken for further study. 200 mg of positive sample was ground in inoculation buffer (20 mM phosphate buffer pH 8, 0.01% β- Mercaptoethanol) using mortar and pestle. Healthy plant(s) are dusted with carborundum 600 mesh as an abrasive then muslin cloth was wetted in solution and gently applied on the leaf. Leaf was washed with the tap water then kept in growth chamber.

3.2.5 Single Lesion assay

Since the field collected sample might be having a mixed population of viruses transmitted by insect vectors it is important to culture and maintain the viruses in suitable hosts by single lesion assay. The virus which was isolated from the infected leaves was inoculated onto the suitable host by mechanical inoculation method using 20 mM phosphate buffer pH 8 containing 0.01% β-Mercaptoethanol. Isolated single lesion was passaged five times in order to obtain pure virus.

3.2.6 Host range studies of TSV

After performing single lesion assay test pure virus culture was inoculated on to different herbaceous plants for host range study. The laboratory plants viz. *Nicotiana benthamiana, Chenopodium quinoa, Phaseolus vulgaris, Gompherena globosa, Datura stramonium* and *Vigna unguiculata* (strain C-152) were tested for the host range study of virus.

Leaves (500 mg) were macerated with 1 ml of 50 mM Phosphate buffer containing 0.01% 2-Mercaptoethanol. This macerated sample was taken as the inoculum for the laboratory host plants. *Nicotiana benthamiana*, cowpea C-152 and French bean plants were dusted with celite or carborundum in order to carry out the mechanical inoculation and the macerated sap was applied gently on the plant leaf by using a cheese cloth. The plants were maintained at 24ºC in the photoperiod of 16 h light and 8 h dark. The inoculated plants were observed daily / periodically for the appearance of symptoms.

3.2.7 Virus purification

Purified virus preparations are essential to study bio-phisico-chemical properties of viruses. Plant viruses are smaller in size when compared to host constituents. The art of virus purification aims at the separation of virus from the host constituents without affecting its structure and infectivity. Procedures vary from virus to virus and with different strains of the same virus. To purify the virus to finest purity, following protocol (Stenger *et al*., 1987) has been used:

TSV was purified from the *Phaseolus vulgaris* infected leaves showing necrotic lesions (100 g) harvested after 4-5 days post inoculation. The leaves were homogenized in 200 ml 0.1M PPB (Potassium Phosphate Buffer) pH 8.0 with 0.01% Mercaptoethanol. The homogenate was filtered through two layers of cheese cloth. To the filtrate, chloroform (up to 10% v/v) was added and emulsified by stirring for about 30 min at 4°C. The cell debris are removed upon centrifugation at 12,000 rpm for 10 min at 4°C. The supernatant was collected and mixed with 0.2 M NaCl and 8% v/w PEG 8000 final concentration. This solution was stirred at 4°C until both components dissolved properly and was incubated at 4°C for 90 min. The supernatant was discarded after centrifugation at 12,000 rpm for 15 min and pellets were resuspended in 50 ml of 50 mM PPB containing 0.2% Triton X 100. It was clarified at 10,000 rpm for 10 min at 4°C and 20 ml of virus suspension was layered on 5 ml of 20% sucrose cushion solution and subjected to ultracentrifugation at 24,000 rpm for 3 h. The supernatant was discarded; pellets were dissolved in 5 ml of 50 mM PPB (pH 8.0) and kept for overnight in 4°C. This partial purified virus was further purified by sucrose density gradient centrifugation to remove last traces of plant proteins and other remaining contaminants.

A sucrose density gradient regularly used to purify enveloped viruses (with densities 1.1-1.2 g/cm^3), membranes, ribosomes, and other cellular fraction. In 1966 Lister first time used sucrose density gradient to separate bipartite genome of *Tobacco rattle virus* (TRV).

Initially, 40% sucrose was prepared using 50 mM potassium phosphate buffer pH 8.0. Gradient tube was cleaned properly with tissue paper using 70% alcohol and kept in beaker with proper support. First 6 ml of 40% sucrose was placed in 32 ml of gradient tube subsequently; 9 ml of 30%, 9 ml of 20% and finally 4 ml of 10% was layered carefully by using Pasteur pipette without disturbing the bottom layer. The prepared gradient was kept in 4°C overnight to become linear gradient.

Four mL of partially purified preparation of the virus suspension was loaded on overnight linearized sucrose gradient and centrifuged for 3 h at 24,000 rpm in Beckman SW 28 rotor. After centrifugation, the tubes were observed in a dark room by projecting a narrow beam of light from top of the tubes. The light scattering viral zones were collected carefully using long needle. The collected viral zone was diluted with 50 mM potassium phosphate buffer pH 8.0 and mixed gently. The mixed viral zones were pelleted down at 40,000 rpm for 3 h using angular rotor (TI28, Beckman). Resultant pellet was suspended in 20 mM PPB (pH 8.0) and kept for overnight at 4°C. Overnight suspension was centrifuged at 5,000 rpm for 10 min and collected the supernatant into a fresh tube. The purified virus used as source material for checking infectivity, RNA isolation, polyclonal antibody production, DIBA assay, western blot analysis and SDS-PAGE. The purity of virus was checked through SDS-PAGE.

3.2.8 SDS-PAGE analysis

When SDS treated proteins are subjected to electrophoresis in polyacrylamide gels having 0.1% SDS, there is a linear relationship between the logarithm of the molecular weight, and the relative distance of migration of SDS-polypeptide micelle. Therefore, protein is fractionated on the basis of their molecular weights. The SDS-PAGE (12%) was carried out in a slab gel electrophoresis apparatus using a discontinuous buffer system. The polyacrylamide gels (acrylamide to bisacrylamide ratio was 29:0.8) containing 0.1% SDS, 0.1%

APS and 0.05% of TEMED was used for electrophoretic separation of protein. The protein samples were mixed with 2X Laemmlli sample buffer (100 mM Tris-HCl pH 6.8 containing 2% SDS, 0.02% bromophenol blue, 10% BME and 20% glycerol) was added, then boiled up to 5 min in order to denature the protein, spun the sample to remove debris and loaded in to the well using loading tip. Electrophoresis was performed at a constant voltage of 120 V using 1 X SDS running buffer (0.025 M Tris and 0.2 M glycine buffer pH 8.3 containing 0.1% SDS). Once electrophoresis is completed, the gel was removed from glass plate using plastic scalpel and placed in the plastic box contains staining solution (0.1% Commassie blue R250, 50% Methanol (v/v), 10% glacial acetic acid (v/v)). Gel was stained by heating in micro oven for 20 sec and placed in ice for 2 min and it was repeated for three times. The gel was de-stained with 20% Methanol (v/v), 7% glacial acetic acid (v/v) until protein bands were clearly visible with colorless background and molecular weight of the protein analysed by prestained protein marker from Fermentas.

3.2.9 Western Blotting analysis

The proteins separated on SDS-PAGE gel and Whatman No. 3 filter paper strips were kept in transfer buffer (0.025 M Tris, pH 7.4, 0.192 M glycine and 20% methanol). Three layers of Whatman No. 3 filter paper strips (wetted with transfer buffer) were kept on the anode plate assembly, on which, PVDF membrane (soaked in methanol and wetted with transfer buffer) was placed. Air bubbles were removed with the help of a glass rod by gentle pressing and rolling of the membrane. Gel was placed on the membrane and three layers of Whatman No. 3 filter paper strips (wetted with transfer buffer) were placed over the gel. The Trans-blot SD (semi-dry transfer cell, BIO-RAD, USA) was assembled and run at 10 Volts for 20-30 min using Powerpac® 200 (Bio-Rad laboratories). The blot was blocked in 5% milk solution made in 1XTBST buffer (0.02 M Tris, 0.5 M NaCl, 0.05% tween-20, pH 7.5) for 40 min at room temperature and it was incubated with respective primary antisera in an appropriate dilution in 5% milk (Nestle, Everyday dairy whitener) solution for 2 h at room temp (RT) with gentle shaking. The blots were washed thrice with TBS-T at 5 min interval. Then blot was incubated with goat anti-rabbit IgG conjugated with alkaline phosphatase secondary antibody in 1:10,000 dilutions for 2 h at RT. The blots were washed twice with TBS-T and one time TBS for 5

min interval. Substrate (BCIP/NBT) was added on the membrane and incubated in dark for the color development with continuous agitation/shaking.

3.2.10 Electron microscopy

Ernst Ruska and Max Knoll invented the electron microscope in 1931. *Tobacco mosaic virus* was first time examined under electron microscope in 1935 by Wendell Meredith Stanley. The sample was observed by either negative staining (uranyl acetate) or positive staining. The staining of the biological material with the staining dye as uranyl acetate pH 5.0 for the acidic nature of the protein and potassium phosphotungstic acid (PTA, pH 7.0) for basic nature of the protein gives better resolution and nature of the particle. The purified virus diluted to 10-25 µg / ml. Placed 10 µl of diluted sample on a glow discharged carbon coated copper grid. The sample was removed from the grid after 1 min; added 10 µl of 1% uranyl acetate and incubated for 1 min. Uranyl acetate was removed and washed with sterile distil water and allow it to dry for 2 min and subjected to electron microscopy at 200 kev.

3.2.11 Isolation of RNA from Purified virus

RNA was extracted from 40 µl of TSV purified virus diluted up to 300 µl with milliQ water in the microfuge tube and 300 µl lysis buffer (0.1 M glycine pH 9.2, 40 mM EDTA, 100 mM NaCl, 2% SDS and 0.05% bentonite) (Gopinath *et al*., 2005) was added to it. Tube was incubated in a water bath at 42ºC for 15 min and equal volume of phenol and chloroform in 1:1 ratio was added and mixed vigorously. The supernatant was collected after centrifugation at 15,000 rpm for 15 min. To precipitate the RNA, equal volume of isopropanol was added to the supernatant and it was freeze thawed 3 times using liquid nitrogen. It was again centrifuged at 15,000 rpm for 15 min at 4ºC. The pellet was washed with 1 ml of 70% ethanol by centrifuging at 15,000 rpm for 10 min and then air dried and dissolved in 50 µl of milliQ water. 2 µl of TSV RNA was mixed with 1 µl of 6 M urea, 4 µl milliQ and 1 µl of 6X DNA loading dye and heated at 65ºC for 5 min and loaded along with SeMV, PhMV, CMV and TMV RNAs as internal controls and agarose gel electrophoresis was performed.

3.2.12 Agarose gel electrophoresis

1% (W/V) of agarose was prepared in 0.5X TAE buffer (20 mM Tris-acetate and 0.5 mM of EDTA of pH 8.0). Ethidium bromide is added to a final concentration of 0.5 µg/ml of gel. After cooling to 50ºC, the mixture is poured onto a preset template with an appropriate comb. The comb is removed after solidification and the gel with template was placed in an electrophoresis chamber containing the running buffer (0.5X TAE). DNA/RNA to be analysed is mixed with the gel loading buffer (6X buffer contains 0.25% bromophenol Blue, 30% glycerol in 0.5 X TAE buffer) at 5:1 ratio and loaded into the well. Electrophoresis was carried out at 120V (Sambrook *et al.*, 1989).

3.2.13 Raising polyclonal antibodies to purified virus and to recombinant TSV coat protein

The purified virus was emulsified with Freund's complete adjuvant and injected into rabbits subcutaneously for raising polyclonal antibodies. In the case of recombinant TSV-CP, SDS-PAGE was performed and the gel was stained and destained thoroughly. The recombinant protein band was excised with the help of the scalpel, washed 3-4 times with PBS-T and was kept overnight on rocker. Later, the pieces of gel were ground in mortar and pestle along with Freund's complete adjuvant and injected into rabbits subcutaneously for raising of polyclonal antibodies. Subsequent booster (same or half of the initial injection) injections were given at 21 days interval. 10 days after each booster, blood was collected from the ear vein of rabbits. The antiserum obtained from the blood sample was checked for the presence of antibodies by ELISA and western blot analysis.

3.2.13.1 Quantification of polyclonal antibody

DAC-ELISA was performed to check the quantification of antisera. In this, we are diluting the antigen as well as antisera. The dilution of antigen varies from 5 ng to 20 ng (5 ng, 10 ng, 15 ng and 20 ng) and dilution of antibody varies from 1,250 to 80,000 (1,250; 2,500; 5,000; 10,000; 20,000; 40,000 and 80,000). Remaining steps are similar as mentioned in section 3.2.2.

3.2.14 Designing of primers

Complete nucleotide sequences of TSV was retrieved from the NCBI data bank and aligned by the Bio-Edit software. Conserved regions were selected for designing of primers. The forward primer was designed manually; taking 18-24 bases from the conserved region of the sequence. Reverse primer was designed by taking 3′ conserved nucleotide (18-24 bases) sequences of target gene. The selected sequence was placed in complementary software from just bio. Both primers were checked for melting temperature using IDT oligocal online tool.

3.2.15 Reverse transcription and 1st strand cDNA synthesis or TSV RNAs

The RNA isolated from purified TSV virus was used as a template for 1st strand cDNA synthesis by using EPICENTRE Biotechnologies Kit. The cDNA was synthesized; according to manufacturer's protocol. Briefly, 2 µl (100 ng) of RNA was mixed with 8.5 µl nuclease free water and 10.0 µM gene specific reverse primer and it was incubated at 65ºC for 2 min in a water bath and it was cooled down to RT. To this mixture, 7.5 µl cocktail (2.0 µl 10X reaction buffer, 2.0 µl of 100 mM DTT, 2.0 µl of 5 mM dNTP, 0.5 µl of ScriptGuard RNAse inhibitor and 1.0 µl MMLV Reverse Transcriptase) was added and incubated at 37ºC for 90 min. After incubation, the reaction was terminated by heating at 85ºC for 5 min. This mixture was kept on ice for 1 min and used directly to amplify the gene by PCR with the specific sets of primers.

3.2.16 Polymerase Chain Reaction (PCR)

PCR is performed as described by Sambrook *et al*., (1989). Template was added to the cocktail of 25 µl reaction containing 2.5 µl of 10X buffer (50 mM Tris-HCL pH 8.8 and 50 mM KCL, 1.5 mM $MgCl_2$) 50 µM dNTP's, 0.5 µM of each specific forward and reverse primers and 1unit of *pfu* DNA polymerase. Initial denaturation step was carried out at 94ºC for 4 min, then 30 cycles of denaturation at 94ºC for 50 sec, different annealing temp (depending on GC% of oligonucleotides) and extension time (depending on the amplicon size) generally 1 min+1 min/ 1 kb of template @ 68ºC followed by final extension at 68ºC for 10 min. The amplified PCR product is subjected to electrophoresis on 1% agarose gel and was documented by UV-platinum gel documentation instrument.

3.2.17 Gel Elution

The desired bands were excised from the gel and dissolved in gel solubilisation buffer at 1:3 ratio (w/v) and kept at 55ºC until it was dissolved completely, then one volume of isopropanol was added. The solution was passed through the column and spun down at 6,000 rpm for 1 min; this step was repeated twice by passing the eluent then discarded. 750 µl of wash buffer was added to the column and spun down at 12,000 rpm for 2 min followed by blank spin for 1 min at 12,000 rpm. The column was transferred to fresh 1.5 eppendorf tube and 20 µl elution buffer (10 mM Tris pH 8.0) was added carefully onto the filter, incubated at room temperature for 5 min and spun down at 15,000 rpm for 2 min twice.

3.2.18 Generation of 3′ 'A'-overhangs

In the amplification process by PCR, Taq DNA polymerase normally adds a single non-templated nucleotide (nearly always A) to the 3′ end of all duplex DNA strands. Pfu enzyme was used to prevent any mismatched incorporation of nucleotide during amplification. However, pfu enzyme unlike Taq DNA polymerase, lacks the property of adding an A nucleotide at the 3′ end in a template independent manner. Hence, A- addition was performed by using the 4 µl (200 ng) of gel eluted PCR product adding 6 µl of cocktail (1.0 µl 10X PCR, 0.5 µl 5 mM dNTPs, 25 mM MgCl2, 0.5 unit Taq DNA polymerase and 3.5 µl milliQ). "A"– addition program was with initial denaturation period at 94ºC for 3 min then 20 cycles of denaturation at 94ºC for 50 sec , extension 72ºC for 4 min followed by final extension at 72ºC for 10 min.

3.2.19 Competent cell preparation

The well isolated single colony of DH5α from freshly streaked plate was taken and initiated overnight culture in LB medium of pH 7.4. From the overnight culture 1% inoculum was added to 200 ml of LB broth and was kept in shaker at 37ºC until it reaches 0.4-0.6 OD. The culture was incubated in ice for 30 min and the culture was harvested at 4,000 rpm for 15 min at 4ºC. The pellet was dissolved in 200 ml of filter sterilized buffer A (100 mM $CaCl_2$, 70 mM $MnCl_2$ and 70 mM sodium acetate, pH 5.5) and was centrifuged at 3,700 rpm for 30 min. The resulting pellet was dissolved in buffer B (buffer A with 20% glycerol) in appropriate

quantity (3-5 ml) and 100 µl was aliquot in each eppendorf. The eppendorf's were frozen in liquid nitrogen and stored in -80ºC for future use.

3.2.20 Ligation

Ligation is one of most important laboratory procedure used in molecular cloning of DNA. The two fragments of DNA ends are joined together by the formation of phosphodiester bonds between the 3'-hyroxyl of one DNA termini with the 5'-phosphoryl of another ends in the presence of ligase and ATP or NAD^+ as a cofactor.

Mostly ligations were performed according to manufactures protocol. The ligations were carried out for desired DNA inserts into respective vector molar ratio of 3:1. We calculated the molar ratios of vector and insert from mass ratios by following formula.

$$\frac{\text{ng of vector} \times \text{kb size of insert}}{\text{kb size of vector}} \times \text{molar ratio of insert/vector} = \text{ng of insert}$$

Ligation mixture was incubated 4°C for 6 h.

3.2.21 Transformation and screening of recombinant or positive clones

3.2.21.1 Transformation

The whole ligated mixture (15 µl) was added to 100 µl of DH5α competent cell suspension. The mixture was incubated on ice for 30 min. It was subjected to heat shock at 42°C for 90 seconds and immediately kept in ice for 30 min. Transformed bacterial cell suspension was grown in 1 ml of LB broth for 1 hour at 37°C in a rotary shaker at 200 rpm. After incubation, the culture was centrifuged at 10,000 rpm for 1 min and the pellet was resuspended in 100 µl of LB broth. The resuspended culture was spread using sterile spreader on appropriate antibiotic containing LB agar plate and incubated at 37°C for overnight.

3.2.21.2 Screening of recombinant or positive clones

The positive colonies were screened through blue white selection (α-complementation) and colony PCR.

3.2.21.2a Blue white selection (α-complementation)

The ligated mixture was transformed into DH5α competent and spread on the LB agar containing ampicillin 100 µg/ml, 50 µl of X-gal (20 mg/ml dissolved in DMFO) and 40 µl of IPTG (24 mg/ml dissolved in milliQ). The plate was incubated at 37°C for 12-16 h. Prolonged incubation might result into the appearance of satellite colonies. The plate was transferred to 4°C for 2-3 h for blue colour development. The white colonies were selected for colony PCR.

3.2.21.2b Colony PCR and Master plating

Colony PCR is molecular technique which helps in fastest way to screen large number of positive colonies within a short time span. It is more useful when insert size is shorter than 3.0 kb. It was performed; streaking half white colony on LB agar plate containing appropriate antibiotics (called master plate) and another half colony used for PCR. PCR master mix was prepared for the number of colonies screened plus two extra. For each 15 µl reaction, mixed the following reagents: 1.5 µl (10X *Taq* Buffer), 1.0 µl (2 mM dNTP mix), 0.4 µl (25 mM MgCl2), 0.1 µl (*Taq* polymerase 5 u/µl), 1.0 µl (forward primer 10 pg/ µl) , 1.0 µl (reverse primer 10 pg/ µl), 10 µl sterile milliQ and mix well. 15 µl of master mix aliquot PCR tubes on ice and individual half white colony was resuspended. The thermo profile used : 94°C, 2 min; 94°C, 30 s, 55°C, 30 s, 72°C 1 min/kb; 30 cycles. Positives from PCR were selected for plasmid isolation.

3.2.22 Plasmid isolation

Alkaline lysis method was used for isolation of plasmid from the colonies. Single colonies were picked and grown in 3 ml of LB broth containing ampicilin (100 mg/l) for 16 h at 37°C and centrifuged at 10,000 rpm for 2 min at 4°C. The supernatant was discarded and the cells were resuspended in 100 µl TES (25 mM Tris-HCl pH 8.0, 10 mM EDTA pH 8.0, 0.9% Sucrose) and kept on ice for 5 min. To the resuspended cells, 200 µl of lysis solution (0.2 N NaOH + 1.0% SDS) was added, mixed well and kept on ice for 5-10 min. After lysis, 150 µl of neutralization solution (1.32 M sodium acetate pH 4.8-5.2) was added, mixed well by gentle inversion and kept on ice for 5 min. The supernatant was taken by centrifugation at 12,000 rpm for 10 min and 300 µl of cold isopropanol was added to precipitate the

plasmid DNA. Centrifugation was done for 5 min at 12,000 rpm and the supernatant was discarded. The pellet was washed with 500 µl of 70% ethanol and air-dried. It was then dissolved in a 40 µl of 10 mM Tris-HCl and was stored at -20°C for further use.

3.2.23 Purification of plasmid by commercial column

The plasmid purification was carried out according to manufacturer's protocol with slight modification. The overnight grown 5 ml of culture in case of high copy and 10 ml for low copy number plasmid spun down in 1.5 of eppendorf tube at 10,000 rpm. Pellets are resuspended in 250 µl of P1 buffer and incubated at room temperature for 2 min. 300 µl of lysis buffer (P2) was added in to the tube and swirling gently; incubated for 2 min. 350 µl of neutralizing (P3) solution was added in the tube and incubated for 5 min at room temperature. Supernatant was collected after centrifugation at 12,000 rpm for 10 min. supernatant was passed through the column at 6,000 rpm for 1 min, repeated the process until the complete supernatant was passed through column twice then eluent discarded and 750 µl of wash buffer was added to the column and spun down at 12,000 rpm for 2 min followed by blank spin for 1 min. The column was transferred to fresh 1.5 eppendorf tubes and 20 µl elution buffer (10 mM Tris pH 8.0) was added carefully onto the filter, incubated at room temperature for 5 min and centrifuged at 15,000 rpm for 2 min twice.

3.2.25 Restriction Digestion

Restriction digestion is an enzymatic technique that can be used for cleaving DNA molecules at specific sites using specific restriction endonucleases. The restriction digestion of plasmids and PCR products were performed according to standard procedures (Sambrook *et al*., 1989) using restriction endonuclease in appropriate buffer at their respective optimum temperature. The digested product was analysed in the 1% agarose gel electrophoresis.

3.2.26 Sequencing of plasmids

The confirmed positive plasmids through restriction digestion; were purified through column and send for sequencing to the Scigenom Pvt Ltd and Ocimum Biosolution Pvt Ltd. Plasmids were sequenced either through universal primer (T7, SP6 and M13 and) or gene specific primer. Nucleotide sequence and dendogram

obtained after sequencing used as raw material for further analysis of sequencing result.

3.2.27 Analysis of sequencing result

The FASTA format nucleotide sequence obtained from the Scigenom and Ocimum respectively are used for BLASTn analysis. FASTA of nucleotide sequence was pasted in the dialog box indicating "enter accession number (s), or FASTA sequences" and non reductant data base selected for the analysis. Results were predicted based on the following parameter; maximum score, total score, query coverage, E value and indent. Overlapping clones were analysed with BioEdit (version 5.0.9) (Hall, 1999) and restriction sites within the overlap clones were determined with neb cutter

3.2.28 Phylogenetic analysis

Desired nucleotide sequences of the virus strain compared with the same species, genus, and family of virus using MEGA (version 6) offline software. Primary, nucleotide and amino acid sequences of different species of a genus or family collected in FASTA format in notepad from the National Centre for Biotechnology Information (NCBI) database. Multiple sequence alignment was carried out using the MUSCLE in MEGA (version 6) and an aligned sequence file was saved in mega format. Secondly, aligned sequence in mega format was taken for construction of phylogenetic tree using Neighbor-Joining method with bootstrap test (1000 replicates). The identity of the sequences was confirmed by BLAST search analysis.

3.3 Results

3.3.1 Serodiagnosis of field collected samples by ELISA

Serodiagnosis was performed by Direct Antigen Coating -ELISA (DAC-ELISA) using *Peanut bud necrosis virus* (PBNV),) *Tobacco streak virus* (TSV), *Cucumber mosaic virus* (CMV), potyvirus antisera (kindly provided by Dr. Varsha Wesley, ICRISAT, Hyderabad) and *Tobacco mosaic virus* (TMV) antisera (kindly provided by Dr. Krishna Reddy, IIHR Bangaluru). Results were identified by visual scoring on ELISA plates. ELISA results of tomato infected samples from seven villages indicate that maximum infection occurred with that of TMV which account

for 29%. The disease incidence due to TSV, PBNV, CMV, and potyvirus showed 20%, 28%, 14% and 8% (mentioned in table no.3.2) respectively. 25% of the samples were found to be mixed infections of TSV and PBNV, as both viruses were transmitted by thrips vectors (Fig 3.2B). We have also observed CMV-TMV, TMV-poty and other mixed infections (data not shown). However we are confined to TSV-PBNV mixed infection for further characterization. Remaining samples; sunflower, peanut, and okra that assume to be infected with the TSV were subjected to TSV antisera only. In case of sunflower; we screened 30 samples (20 from Vibha seed and 10 from ICRISAT experimental plots). Sample no VS-4, VS-6, VS-7, VS-8, VS-13, VS-16, VS-17, VS-18 and VS-20 samples showed more intense yellow colour in ELISA from Vibha seed and sample no 5 and 6 from ICRISAT. The Vibha seed sample VS-6 and VS-17 selected for further characterization. 45 samples from Peanut (mentioned in table no 3.1B) were screened for TSV; 10 samples showed positive toward the ELISA. Apart from that okra fruit sample collected from vegetable market (mentioned in table no 3.1C) showing characteristic symptom of TSV as fruit distortion (Krishna Reddy *et al*., 2003a) was also screened. Four out of 27 samples; showed positives towards the TSV antisera. As, we are interested on TSV only, so further ELISA positive samples were subjected to DIBA assay for further analysis.

Table 3.2: ELISA results of tomato infected sample from seven villages of Chittoor district of Andhra Pradesh. All villages are located in 10 mile radius of Madanapalli Town

S. No.	Field visited in	No. of samples collected	PBNV	TSV	PBNV/ TSV mixed	CMV	TMV	Potyvirus
1	Kotavaripalle	72	28	13	9	11	15	5
2.	Valasapalle	49	16	11	8	5	10	7
3.	Ramasamudram	52	4	2	-	6	37	3
4.	Edigapalle	44	6	9	5	6	21	2
5.	Kotur	74	24	19	11	12	16	3
6.	Danduvaripalle	43	13	9	8	7	8	6
7.	Sugalmitta area	53	17	15	7	9	7	5
	Total	387	108	78	48	56	114	31
	Percentage		28%	20%	12%	14%	29%	8%

3.3.2 Confirmation by Dot Immuno Binding Assay (DIBA)

To confirm the ELISA results, total seventeen symptomatic field samples were selected randomly. Total soluble proteins were extracted and spotted onto PVDF membrane as mentioned in section 3.2.3. Out of 17 samples tested for PBNV, TSV antisera; eight samples reacted towards PBNV, seven samples reacted towards TSV. Among these five samples which reacted towards both antisera. Remaining seven samples were negative to TSV and PBNV antisera indicating that they might have got infected with other viruses like CMV, Potyvirus, and TMV.

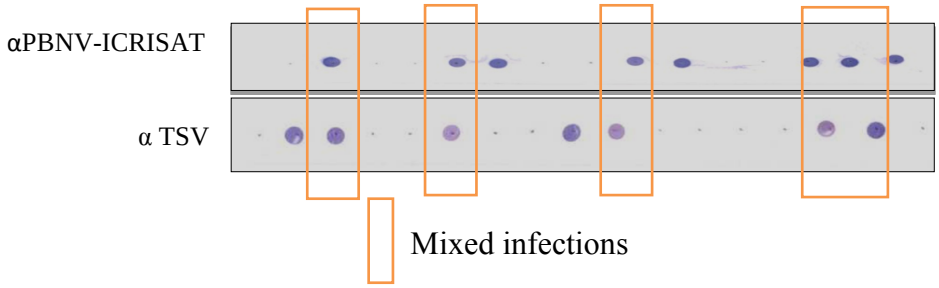

Fig 3.1: DIBA assay of field samples on PVDF membrane. Upper panel-samples reacted positive for PBNV antisera. Lower panel-samples reacted positive for TSV antisera. The Orange colour rectangular box indicates mixed infection.

3.3.3 Single lesion assay

Field infected samples positive for PBNV and TSV were inoculated on diagnostic host plants such as, french bean and cowpea cv c-152. For PBNV cowpea cv c-152 showed characteristic type of symptom as chlorotic concentric rings indicating typical symptoms of PBNV (fig 3.2 C) and for TSV cowpea cv152 showed chlorotic patch along the veins (fig 3.2 A). As both the viruses are transmitted by thrips vector may be the reason for mixed infections in natural field conditions.

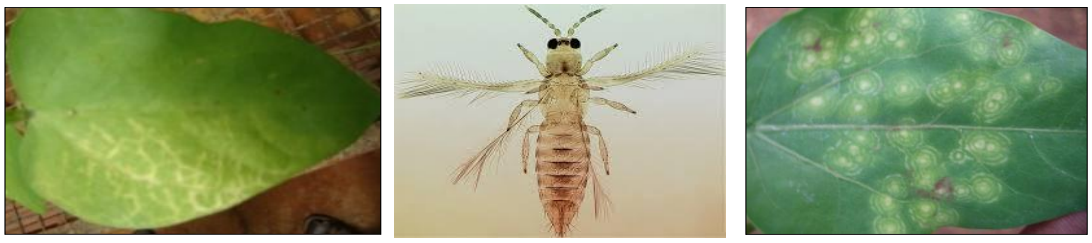

A.TSV B. Thrips C. PBNV

Fig 3.2: Inoculation of the field sample on the indicator plant or diagnostic host plant. In panel A. cowpea cv 152, showed chlorotic patch and inter-veinal chlorosis on the inoculated leaves as characteristic symptoms of TSV. In panel B. Image of Thrips, an arthropod's vector which is responsible for mixed infection in several viruses including that of TSV and PBNV (http://anic.ento.csiro.au/thrips/identifying_thrips/Thripinae.htm) panel C. The characteristic symptom of the PBNV concentric chlorotic symptoms showed on cowpea plant

To isolate TSV from mixed infection further, both viruses were separated on french bean. cowpea cv-152 infected leaf material was used as a source material for single lesion assay. The small chlorotic lesion (in panel 3.3 A) was excised using sharp surgical blade and macerated with pestle in eppendorf tube as mentioned in section 3.2.5 and inoculated on to the primary leaves of french bean. The periodical inoculations were done for about 4-5 passages (fig 3.3 panel A, B, C and D) and finally well differentiated single lesions (panel E) were obtained. Each passage single lesion was confirmed with DIBA assay after inoculation. DIBA positive well separated necrotic spot was used for further study.

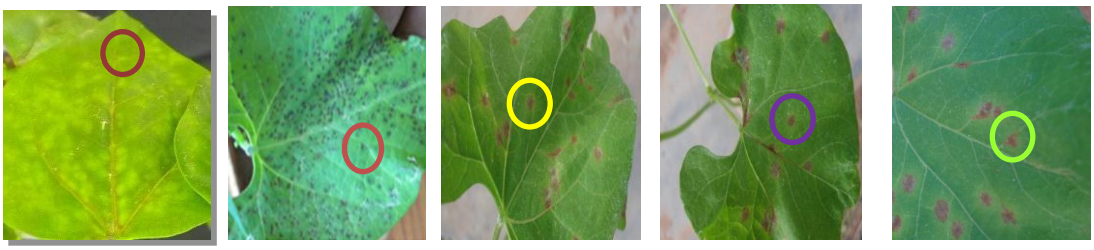

A.Cowpea c-152 B. Passage I C. Passage II D. Passage III E. Passage IV

Fig 3.3: Single lesion assay for TSV infected sample. The local lesion selected for each inoculation was indicated by different colour of ring.

3.3.4 Host range studies of the TSV

The DIBA positive local necrotic spot of okra isolate on the French bean was selected for the host range study and inoculated mechanically onto experimental plants viz. *Vigna unguiculata* cv. C-152, *Phaseolus vulgaris*, *Chenopodium quinoa*, *Datura stramonium*, *Gompherena globosa*, *Nicotiana benthamiana*, *Nicotina rustica*, *Nicotiana plumbigifolia* plants and the results were documented (fig 3.4). The TSV established red bordered local lesions in *Gompherena globosa* within 10 days of post inoculation (DPI) (fig 3.4 B). In contrast, *Datura* plant exhibited characteristic systemic spread of virus on the 7 DPI (fig 3.4 D). The inoculated *Chenopodium* leaves showed characteristic chlorotic spots expanding thorough out the leaf as concentric rings (fig 3.4 F). Inoculated leaves of French bean showed necrotic local lesions within 4 DPI (fig 3.4 H). A characteristic chlorotic spot (fig 3.4 J) observed on *Nicotiana plumbigifolia* after 4 DPI. Necrotic spot was observed on *Nicotina rustica*, after 5 DPI (data not shown). *Nicotiana benthamiana* plant showed chorotic patch (data not shown) after 7 DPI. The following species were not infected: *Cucumis sativus*, *Nicotiana cocker*,

Nicotiana glutinosa, petunia, *Nicotiana clevelandi*, *Chenopodium amaranticolor*, *Vicia faba, Cicer arietinum,* and *Pisum sativum.* The virus was maintained in French bean and cowpea c-152 plants with periodical re-inoculations in the green house at weekly interval.

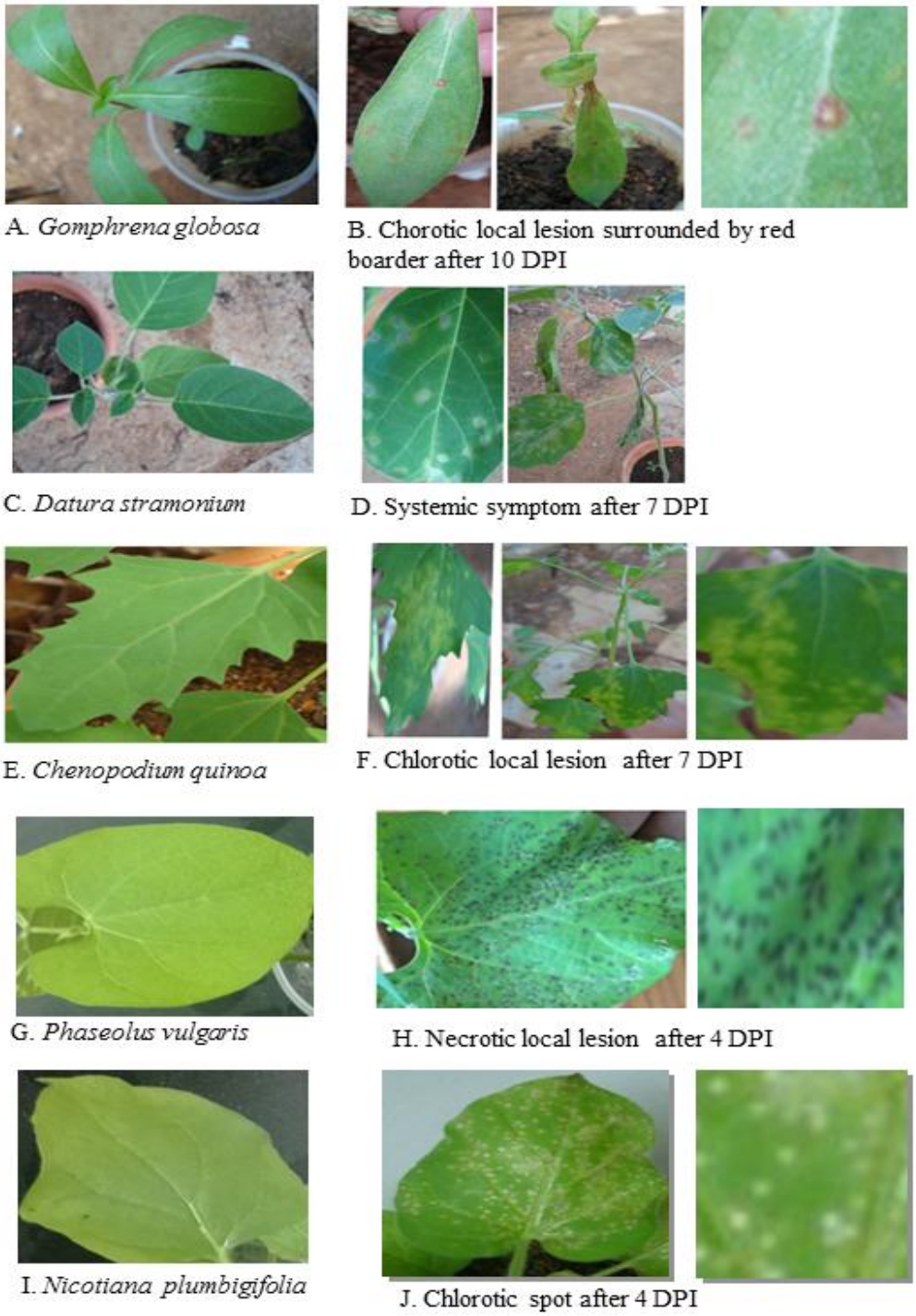

Fig 3.4: Host range study of TSV okra strain: left panel A, C, E, G and I showing healthy plant and middle panel (B, D, F, H and J) showing inoculated plant with symptoms and right panel enlarged version of symptom.

3.3.5 Virus purification

Four identified strains of the TSV in the present study were bulk purified from the french bean. In sucrose gradient two light scattering zones were observed at 20-30% interface for the all the strains of the TSV. Here, I am showing one of the representing picture (fig 3.5) of the TSV strain. Lower and upper viral zone from the bottom of the tube may contain RNA1 & RNA2 and RNA3 & RNA4.

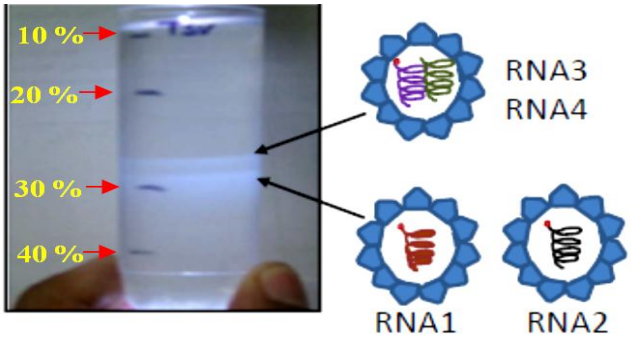

Fig 3.5: Light scattering zone(s) of TSV in 10-40% linearized sucrose density gradient

3.3.6 SDS-PAGE and western blot analysis of purified virus

After purification of virus, SDS-PAGE was performed in order to check the purity and size of coat protein. Sunflower strain of purified virus showed 28 kDa monomer along with non-specific band at 56 kDa (fig 3.6, panel A). To confirm non- specific bands in SDS-PAGE, western blot was carried, as described in section 3.2.10 using coat protein antisera. The antisera reacted positively with 28 kDa monomer along with the 56 kDa (fig 3.6, panel B) place in western blot. This result indicates homogeneity level of purified virus.

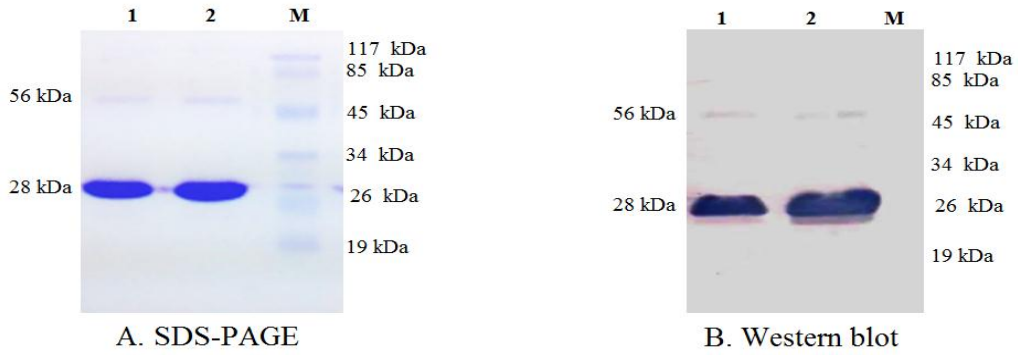

Fig 3.6: SDS-PAGE and western blots analysis of TSV (Sunflower strain) purified virus. In Panel A, Lane 1 and 2: TSV purified virus, M: protein ladder. Left side of the SDS-PAGE gel indicates purified virus molecular weight as 28 kDa and 56 kDa. Right side of the gel indicates molecular weight of marker. In panel B, Lane 1 and 2: TSV purified protein, M: protein ladder. Left side of the western blot indicates antisera reacted with the purified virus at 28 kDa and 56 kDa. Right side of the blot indicates molecular weight of marker

The purified virus obtained from peanut strain of TSV showed multiple bands in SDS-PAGE as monomer, dimer, trimmer, tetramer (fig 3.7, Panel A). Apart from the multiple of monomer sub units, nonspecific bands were also observed. To confirm multiple bands in SDS-PAGE western blot was performed. Antisera reacted to monomer (28 kDa), dimer (56 kDa), trimers (84 kDa) and tetramer (112 kDa). The nonspecific band (*) apart from the multiple of monomer also reacted with the TSV antisera which indicates degradation product of purified virus (fig 3.7 panel B).

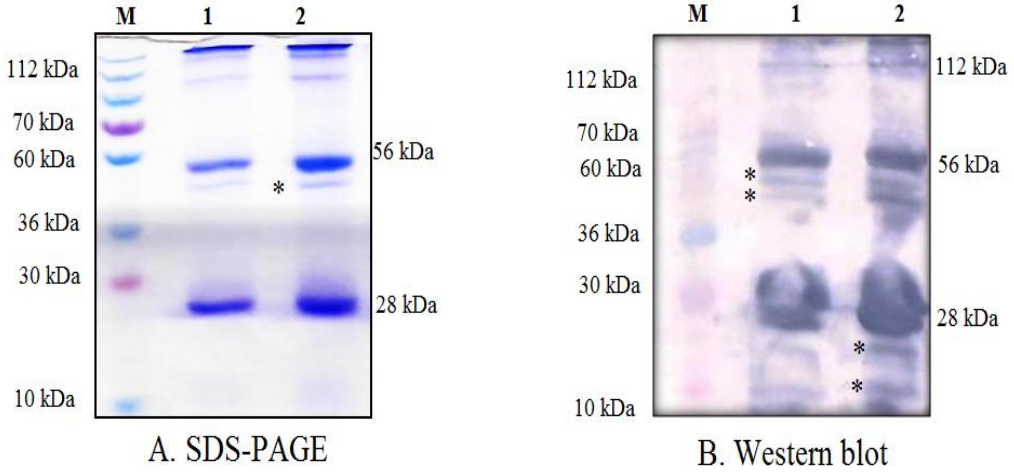

Fig 3.7: SDS-PAGE and western blots analysis of TSV (Peanut strain) purified viruses. In Panel A, Lane 1 and 2: TSV purified virus, M: Prestained protein marker. Right side of the SDS-PAGE gel indicates purified virus molecular weight as 28 kDa and 56 kDa. Left side of the gel indicates molecular weight of marker. In panel B, Lane 1 and 2: TSV purified protein, M: Prestained protein ladder. Right side of the western blot indicates antisera reacted with the purified virus at 28 kDa, 56 kDa, 112 kDa and extra degradation product. Asterisks (*) mark in panel A and B indicate the non-specific bands. Left side of blot indicates molecular weight of marker

Okra strain of TSV was purified and its purity was checked through SDS-PAGE. Monomer, dimer and tetramer were observed in SDS-PAGE (Fig 3.8 A) and it was confirmed through western blot (Fig 3.8 B). Apart from multiple of monomer, nonspecific band also observed in the SDS-PAGE as well as western blot that are represented by the asterisks (*) mark.

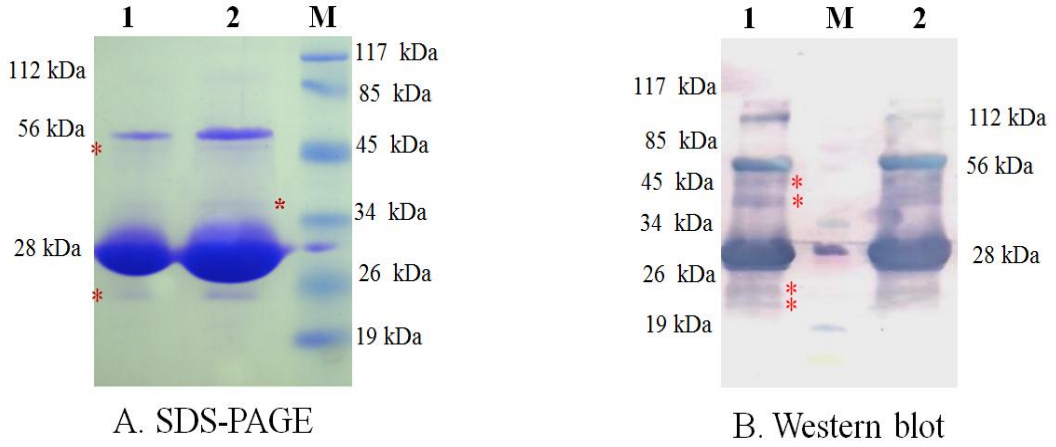

Fig 3.8: SDS-PAGE and western blots analysis of TSV (Okra strain) purified virus. In Panel A, Lane 1 and 2: TSV purified virus, M: protein ladder. Left side of the SDS-PAGE gel indicates purified virus molecular weight as 28 kDa and 56 kDa. Right side of the gel indicates molecular weight of marker. In panel B, Lane 1 and 2: TSV purified protein, M: protein ladder. Left side of the western blot indicates antisera reacted with the purified virus at 28 kDa, 56 kDa and 112 kDa. Right side of the blot indicates molecular weight of prestained protein marker.

3.3.7 Electron microscopy

Electron microscopy was performed according to method described in material and method section 3.2.9. The size of the virion particle was measured 28 nm and shape was found all most spherical (fig 3.9).

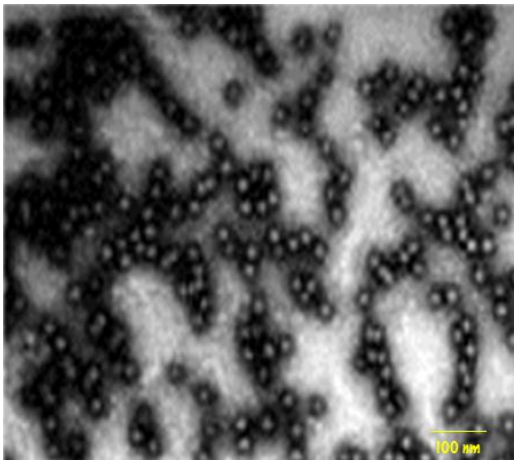

Fig 3.9: Transmission Electron Microscopy view of *Tobacco streak virus* (Okra isolate). TSV virion stained with the negative stain as uranyl acetate and visualized at 200 kev of electron density. Here, size of virion measured as 28 nm diameters.

3.3.8 Raising of polyclonal antibody

Pre immune blood collected was treated as control with respect to those antisera against antigen. 100 µg of purified virus was emulsified with Freund's

complete adjuvant and injected into rabbits subcutaneously. After each booster dose, antiserum was collected to check sensitivity.

3.3.8.1 Quantification of polyclonal antibody

ELISA was performed to check the sensitivity of antisera toward the antigen taking 5 ng, 10 ng, 15 ng and 20 ng antigen dilution and 10k, 20k, 40k and 80k for antisera dilution (fig 3.10, panel A). This showed the sensitivity up to 1:40,000 dilutions for 10 ng antigen. Optical density was recorded at 405 nm using ELISA reader. Antibody titre curve was plotted using antibody dilution (5k to 80k) on X-axis and optical density on the Y-axis (fig 3.10, panel B). The maximum optical density was observed as 1.2 for 5k dilution of antibody against 10 ng antigen and minimum was observed as 0.1 for 1:80k dilution of antibody against 40 ng antigen.

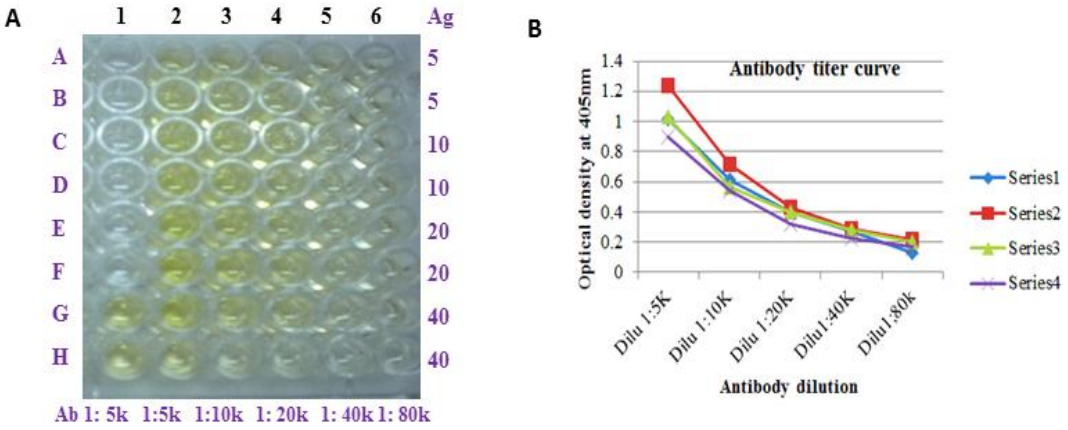

Fig 3.10: DAC-ELISA for quantification of the antibody In panel A: Antigen concentration: A1-A6, B1-B6-5 ng, C1-C6, D1-D6-10 ng, E1-E6, F1-F6-20 ng, G1-G6, H1-H6-40 ng. Antibody concentration: A1-H1, A2-H2-5k dilution, A3-H3-10K dilution, A4-H4-20k dilution, A5-H5-40k dilution, A6-H6-80k dilution. A1, B1- Buffer control, C1, D1 -Healthy control, E1, F1-Uninduced, G1, H1-Positive. In panel B: Antibody titre curve; Y-axis indicates optical density at 405 nm at different dilution. Antibody dilution on represented on X-axis. Series 1, 2, 3 and 4 indicate dilution of antigen.as 5 ng, 10 ng, 15 ng and 20 ng respectively.

3.3.9 RNA characterization by agarose gel analysis

RNA was isolated from the purified virus according to the standardized protocol as mentioned in 3.2.11. TSV RNA along with different internal controls viz; PhMV (molecular weight 6.2 kb) CMV RNAs [RNA-1, RNA-2, RNA-3 and RNA-4 having their molecular weight 3.3 kb, 3.0 kb, 2.1 kb and 1.2 kb respectively] were loaded in 1% agarose gel and its characteristic gel pattern was observed (Fig 3.11). Okra strain of TSV showed expected RNA1, RNA2, RNA3,

RNA4 and RNA4A in gel. In the okra strain of TSV the bands of TSV RNAs were approximately of same size as CMV RNAs, indicating that the virus has tripartite genome. Similar pattern of RNA agarose gels characteristic were observed in case of sunflower and peanut strain of TSV (data not shown). In case of tomato strain of TSV, total RNAs were isolated from the infected French bean leaves. All these RNA materials were used for the First strand c DNA synthesis and Polymerase chain reaction (PCR).

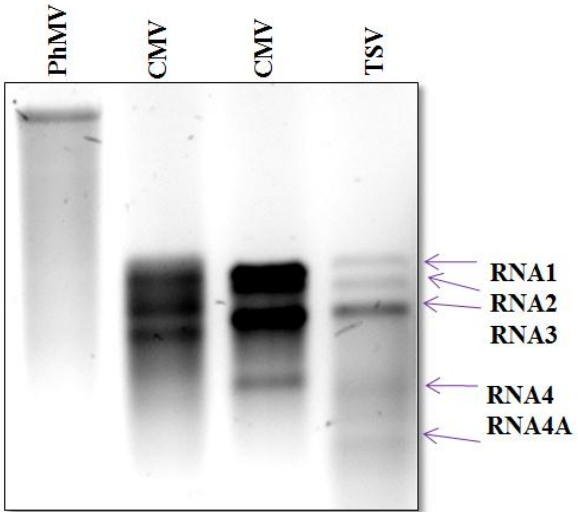

Fig 3.11: Characteristic pattern of TSV RNA along with internal control in 1% agarose gel. *Physalis mottle virus* (PhMV), *Cucumber mosaic virus* (CMV) used as RNA marker for *Tobacco streak virus*. Arrow mark indicates position of the RNA1, 2, 3, 4 and 4A.

3.3.10 First strand c DNA synthesis and PCR

The genomic RNA isolated from purified virus and total nucleic acids isolated from TSV infected leaf were used as a template for cDNA synthesis. PCR was performed with coat protein specific primer [(forward primer: 5'GCCATGGACAATACTTTGATCCAAGTCCAGAC3') and reverse primer: 5' GCTCGAGATCTTGATTCACCAGGAAATCTTCTGG3')], 10X buffer, dNTP's, and *Pfu* DNA polymerase as mentioned in section 3.1.16. Thermo profile was optimized with the help of gradient PCR. The best annealing temperature for amplification of the coat protein of TSV was found @ 57ºC for 30 sec. Amplified PCR product was loaded on 1% agarose gel along with 1.0 kb ladder. The PCR product showed sharp band near the 717 bp (fig 3.12) in all strains (sunflower, peanut, tomato and okra) of TSV used in the present study.

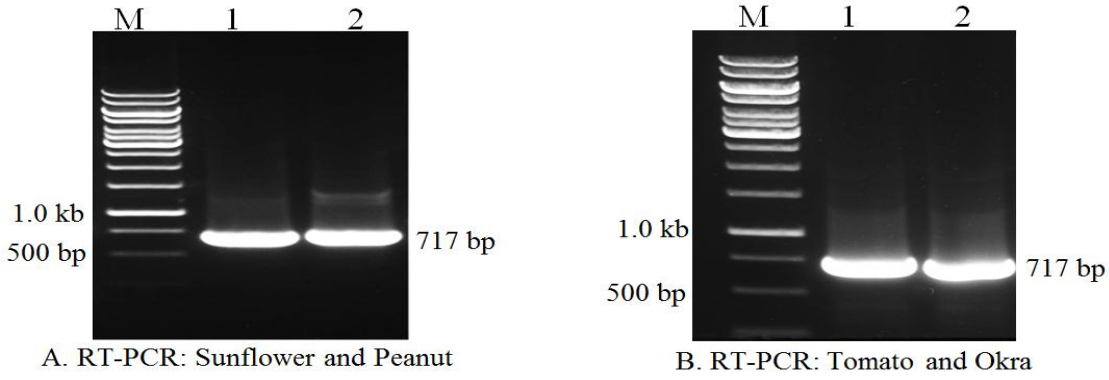

Fig 3.12: Reverse transcription -polymerase chain reaction (RT-PCR) for coat protein gene of TSV in 1% agarose gel. In panel A, Lane 1 and 2; PCR amplified product for coat protein gene sunflower and peanut strain of TSV respectively. In Panel B, Lane 1 and 2; PCR amplified product for coat protein gene tomato and okra strain of TSV respectively. M; 1 kb ladder, right side of the gel indicate 717 bp for PCR amplified product. M; 1 kb ladder and left side of the gel showed size of 1.0 kb DNA ladder.

3.3.11 Cloning of PCR products

PCR amplified products were purified from the gel as mentioned in section 3.2.17. The concentration of the eluted PCR products was checked through Nano drop and ligated into pTZ57R/T TA cloning vector (Fermentas). The 5.0 µl of ligated product was transformed in to DH5α competence cell and spraded on LB agar plate contains IPTZ and X-gal as protocol mentioned in section 3.2.21. After overnight incubation plate was again incubated 2 h at 4°C for development of blue colonies. From each plate five white colonies were selected for colony PCR as described in section 3.2.21.2b. Colony PCR results were observed in 1% agarose gel and it showed 717 bp (data not shown). The two PCR positive samples subjected for plasmid isolation.

3.3.12 Confirmation of the plasmid by restriction digestion

Column purified plasmid was taken for restriction digestion. The total 10 µl of reaction contains; 4.0 µl plasmid, 1.0 µl 10X 'R buffer', 0.3 µl *Eco*RI , 0.3 µl *Hin*dIII restriction enzyme and 4.4 µl of nuclease free milli Q water. After 2 h of incubation at 37°C, reaction was heat inactivated at 65°C for 20 min. Restriction digested product loaded onto 1% agarose gel. The restriction digested products were showed 792 bp (717 bp of CP + 75 bp of multiple cloning sites of TA vector) of insert size (fig 3.13, panel A and B). This indicates the presence of coat protein

gene sequence in the plasmid. Further the presence of insert was confirmed by both directions sequencing of plasmid.

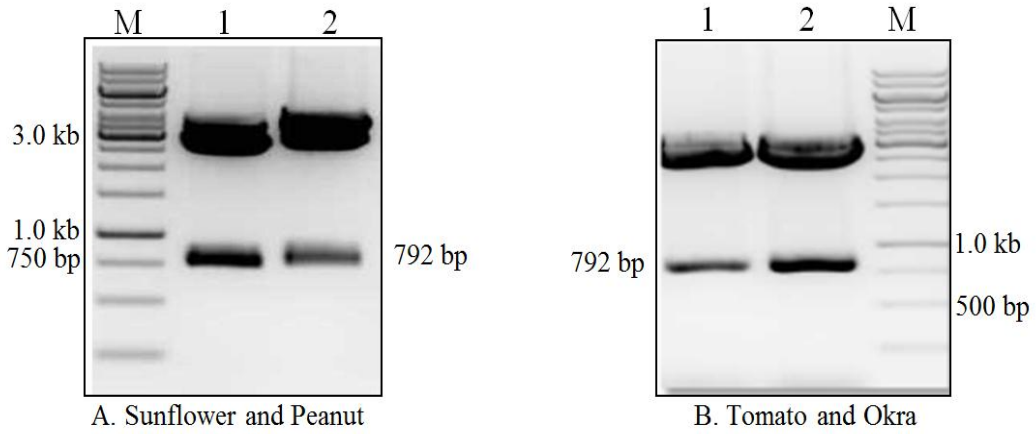

Fig 3.13: Restriction digestion pattern of recombinant pTZ57R/T plasmid harbouring TSV CP gene in 1% agarose gel. In panel A, Lane 1 and 2; restriction digestion pattern for coat protein gene of TSV- sunflower and peanut present in pTZ57R/T vector. In Panel B, Lane 1 and 2; restriction digestion pattern for coat protein gene of TSV-tomato and okra present in pTZ57R/T vector. Right side of the gel indicate 792 bp released CP gene as an insert left side of the gel showed molecular weight of 1.0 kb DNA ladder.

3.3.13 Sequencing of plasmid

Column purified plasmid was quantified by Nano drop as well as in gel before sending for sequencing. 10 µl of restriction digestion confirmed plasmid having 200 ng / µl along with M13 forward and reverse primer was send for sequencing. The plasmid was sequenced from both direction to avoid the mismatches and gaps. The quality of result was checked through the dendogram that showed very sharp and non-overlapping peaks and very less background noise.

3.3.14 Analysis of the sequencing results

FASTA format nucleotide and amino acid sequence were used for multiple alignment, nucleotide- nucleotide blast (blastn) and protein- protein blast (blastp). Multiple alignment nucleotide sequence of identified four strains of TSV showed twelve mismatches compare to the peanut strain of the TSV (Table 3.3). Similarly, multiple alignment of the amino acid showed three mismatches compared to the peanut strain of the TSV that is indicated by asterisk mark (fig 3.14).

Table 3.3: Variation of nucleotide sequence after the multiple alignment of identify four strains of TSV

Nucleotide Position of CP	15	19	51	175	204	678	684	690	691	692	702	711
Peanut	C	A	C	A	C	C	G	A	G	A	G	A
Tomato	A	A	C	A	C	T	G	A	G	A	G	A
Okra	C	G	T	G	C	C	G	A	G	A	G	A
Sunflower	C	A	C	A	T	C	A	G	A	G	A	T

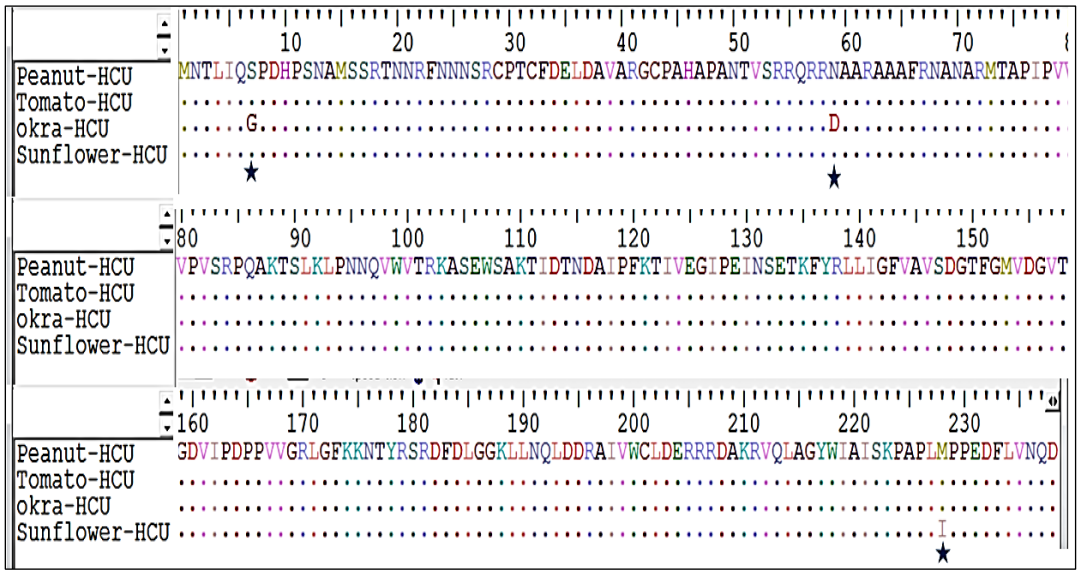

Fig 3.14: Multiple alignment of amino acids sequence for identified four strain of TSV
Here, Peanut-HCU, Tomato-HCU, Okra-HCU and Sunflower-HCU indicate the identified strains of TSV in the present study. Position of the amino acid indicated as number above the amino acid sequence. Asterisk mark indicate the mismatch position of amino acid.

NCBI blatn was performed for the identified four strains of TSV as mentioned in the methods section 3.2.27. Sunflower strain of TSV blast search result showed 99.72% homology with the cotton strain of TSV (Accession no AY505082), 99.58% homology to sunflower strain (Accession no AY501479). Similarly, Okra strain of TSV showed 99.98% homology with okra strain of Tamil Nadu (Accession DQ864456) and 98 to 99% homology to other strain of TSV. Peanut strain of TSV showed 99.78% homology to the Kurnool peanut strain of TSV (Accession no AY505081). Tomato strain of TSV showed 99.78% homology to peanut strain of TSV (Accession no AY505081).

3.4 Discussion

The identification of the viruses based on the symptom in the field condition is very difficult and undistinguishable. While collection of the field sample assuming a particular virus infection was in most cases gave contradictory results in laboratory. As our mentor is establishing a new laboratory at University of Hyderabad (UoH), we have conducted field surveys for new viral infections which can be used in the laboratory as model viruses. For my thesis work we have decided to work on molecular characterization of TSV and use it in the laboratory as a model virus to delineate diverse viral processes in the whole plant scenario. Serodiagonstic of field collected samples were performed basically for the identification of TSV strains/ isolates which infects *Nicotiana benthamiana* our model plant in the laboratory. During the field survey, we come across a TSV strain from okra source which infects *Nicotiana benthamiana*. We have also identified mixed infections with PBNV as both the infections were transmitted by arthropods vector, thrips. And we have found few new viruses also on *Cucumis melo* (Mrs. Naga Teja Natra unpublished data). It was surprising to note that TMV and PBNV are major constraints with 29% and 28% infections respectively in tomato. It will be noteworthy to perform an application orientated research to check the yield losses and commercial implications due to these two viruses as these are predominant infections in the field and tomato is a cash crop to the small time farmers in Indian scenario. TSV infection is fast growing to epidemics in peanut (Reddy *et al*., 2002), sunflower (Parasada Rao *et al*., 2000; Ramaiah *et al*., 2001), okra (Krishna Reddy *et al*., 2003 a) and other crops (mentioned in chapter 2, table 2.4) in Rayalaseema region prompted us to pick up this virus to molecularly characterize in the laboratory.

The identified four strains of TSV were found to be mechanically transmissible by sap inoculation to the experimental host plant. It is similar with various investigations for TSV (Costa & Carvalho, 1961; Salazar *et al.*, 1982; Kaiser *et al.*, 1982). However we have also noticed decline in infectivity with different seasons (data not shown).

A host range study is not a reliable method for the identification of the viruses. It requires more space, labour intensive and time consuming and sometimes ends up with puzzling results. Though there are so many problems, it is very

important for maintenance of viral culture for virus purification purposes and to work with single virus rather than two or more viruses. Very wide host range was observed for the present virus. It infects plants of Solanaceae, Chenopodiaceae, Cucurbitaceae, Leguminosae, Malvaceae and Amaranthaceae. The host range data of the identified TSV is same as that of the reported TSV strains (Vemana and Jain 2010; Salazar *et al.*, 1982; Krishna Reddy *et al.*, 2003a; and Kaiser *et al.*, 1982, 1991). We have identified *Nicotiana plumbigifolia* as a new experimental host for the TSV strain of okra. This host is very amenable for TSV infection and showing the characteristic symptom (chlorotic spots) within 4 days of the post inoculation.

Phaseolus vulgaris was routinely used for purification of okra, sunflower and peanut strain of the TSV. Particles in sucrose density gradient separated as two components with okra, sunflower and peanut strain of TSV; however, various reports showed that TSV separates out into three components (Salazar *et al.*, 1982; Kaiser *et al.*, 1982). This result might indicate the empty capsid is absent as third component in the sucrose gradient at the 10% of sucrose after the centrifugation.

The yield of virus varied among the purification throughout the year even though one cultivar of *Phaseolus vulgaris* and one method were used. Lister and Bancroft (1970) described that yield of the viruses depends on the hosts and extraction procedure. In our case, host and extraction procedure were same throughout the year, therefore, we thought that other factors such as the effect of environmental conditions on plants are be responsible for the differences. For example, temperatures in the greenhouse ranged from 20 °C in the winter up to 42 °C in the summer.

Molecular mass and molecular weight of the coat protein of the TSV depends on the composition of the amino acids, strain, isolate and methods used for purification and electrophoresis (Almeida *et al.*, 2005, Cornelissen *et al.*, 1984). Amino acids analysis of the coat protein of TSV showed molecular mass of the maximum strain and isolate between 26.34 to 28 kDa, and WC isolate of the TSV showed 30.5 kDa (Cornelissen *et al.*, 1984). However, molecular weight of the coat protein reported from various group varies from 28 to 34 kDa [30.9 kDa (Hosseini *et al.*, 2012), 30.5 kDa (Cornelissen *et al.*, 1984), 29.0 kDa (Reddy *et al.*, 2002), 29.0 (Ali *et al.*, 2009, Almeida *et al.*, 2005), 34.0 kDa (Mathur *et al.*, 2014)]. In the present study we have observed that all the identify strains of TSV showed 28-29

kDa. Recently, Mathur *et al*., 2014 reported that recombinant coat protein of TSV strain showed 34 kDa in bacterial expression system however its molecular mass is only 26.71 kDa. Theses variation is mainly because of basic amino acid present at the N-terminal of CP and side chain of basic amino acid used for glycosylation (addition of the glucose molecules) which leads to increase in molecular weight of the protein.

The identified strains of TSV showed multiples of 28 kDa this might be dimer, trimer and tetramer molecules. Occurrence of the dimmer was also reported from the peanut strain of the TSV (Reddy *et al*., 2002). Level of oligomerization of the coat protein varies from the strain to strain. In the Present study we have observed maximum dimerization in the case of peanut strain of TSV (approximately 50:50, fig 3.7) compare to the okra strain of the TSV (approximately 90:10, fig 3.8) and sunflower strain of the TSV (approximately, 95:5, fig 3.6). This variation might be due to differences in the methods of the protein preparation and electrophoresis that was used. Peanut and okra strain of the TSV showed nonspecific band apart from the multiple of the monomer. However, in western blot it reacted very strongly with coat protein antisera (fig 3.7 and 3.8). This result indicates "the presence of nonspecific band is the degradation product of monomer and multiples of it". Based on the results we presume that, peanut and okra strain of the TSV susceptible towards the degradation compare to sunflower strain of TSV (fig 3.6) in the present study.

Electron microscopic studies of purified virus revealed the presence of isometric virus particles measuring about 28 nm in diameter. Morphologically the present virus shows resemblance to the virus reported by Salazar *et al*., 1982; and Almeida *et al*., 2005 Even though *Tobacco streak virus* has sharing similar coat protein and many common biophysical properties with *alfalfa mosaic virus* showing distinct morphologically. The *alfalfa mosaic virus* formed bacillus like particles (Rafiq *et al*., 2008), however, TSV formed icosahedral like particles.

In comparative analysis of coat protein gene at nucleotide and amino acid level, we have observed twelve mismatches at nucleotide level (table 3.3) and three mismatches at amino level (fig 3.14). The maximum mismatches were observed at the C-terminal region of the coat protein i.e. 684 nt to 711 nt. However, we have found that 100% conserved amino acid between peanut and tomato strain of the

TSV at protein level. But, In case of okra strain of TSV we have observed two amino acid changes; one at 7 nt position (Serine to Glycine) and another at 59 nt position of CP (Asparagine to Aspartic acid) (fig 3.14) in comparison with the peanut strain of the TSV. Sunflower strain of TSV showed one amino acid change at 228 nt position of CP (Methionine to Isoleucine) in comparison to the peanut strain of the TSV.

NCBI blastn search result of the sunflower strain of the TSV showed maximum homology (99.98%) with the cotton strain of TSV and 99.58% homology to sunflower strain with coverage of 100% sequence even though TSV was isolated from the sunflower. Peanut strain of TSV showed 99.78 % homology to the Kurnool peanut strain of TSV. Okra strain of TSV showed 99.98% homology with okra strain of Tamil Nadu. Tomato strain of the TSV was found to be closer to the peanut strain of the TSV at nucleotide and protein level with 99.68% and 100% homology respectively. Natural occurrence of TSV on the tomato was reported from Brazil (Costa *et al*., 1961) and USA (Cupertino *et al*., 1984). To our knowledge, this is the first report of TSV infecting tomato from Indian subcontinent

Chapter-4

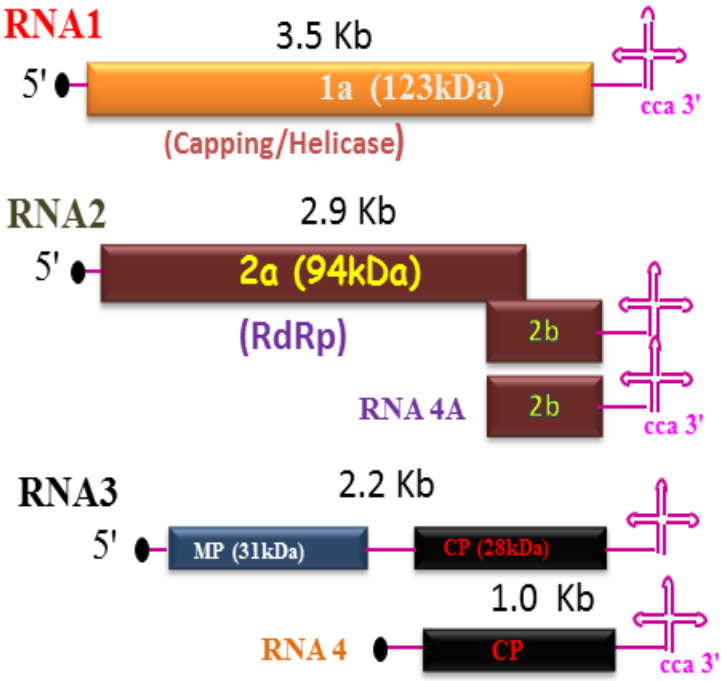

Complete genome sequencing and molecular diversity analysis of *Tobacco streak virus*

Complete genome sequencing and molecular diversity analysis of *Tobacco streak virus*

4.1 Introduction

RNA viruses are basically diverse in nature, mainly because of the error-prone nature in their replication (Domingo and Holland. 1994; Holland *et al*., 1982) and their short life cycle. In addition, genetic exchange either by recombination or reassortment can be another major evolutionary driving force, which is able to rapidly increase variations (Chao, 1997). However, most of the RNA virus populations analysed so far are genetically stable with relatively low diversity (Garcia-Arenal *et al*., 2001) in spite of the high potential for variability of RNA viruses.

Recently, Schneider *et al*., (2001) and Roossinck, (2003) reported that the strong correlation between host range of the virus and mutation frequency in the viral genome. During the replication of the RNA genome, change in single nucleotide or amino acid within the specific motives; leads to change in pathogenicity, specificity toward the host, symptom expression and systemic infection of viruses in their hosts. So, viral genome is playing pivotal role to counteract the most complex host system and causing pathogenicity. There are several reports in support of "the changing the single nucleotide or amino acid may alter the specificity of the host range". Serra *et al*., (2008), showed that a single nucleotide change in the "cachexia expression motif" of *Hop stunt viroid* (HSVd), modulates cachexia symptoms in citrus trees. A single nucleotide change i.e. Adenine to Guanine at 627th position of the HC-Pro cistron of the *Potato virus Y* leads to the loss of vein necrosis phenotype in tobacco (Hu *et al*., 2009). Haviv *et al*., (2006), reported that ORF 5 of *Grapevine virus A* was not essential for replication in protoplasts, but was necessary for efficient infection in plants and showed that 8th amino acid residue (Thr) affect the pathogenicity and symptom development in *N. benthamiana*.

Day-by-day, TSV is fast emerging and becoming more problematic for agriculture sector and medicinal plants across the globe. As for as India is concerned, it has been reported more than 20 field crops (described in section 2.2.6.2, table 2.4) and its host ranges extending to other field crops after breaching the host barrier. The genome of the virus is segmented and multipartite in nature; segregated in to three RNA molecules RNA1, RNA2, and RNA3 respectively and packaged in separate

particles. Virus particles also contain two subgenomic RNAs. Altogether, it encodes five major proteins 1a, 2a (replication associated enzymes), 2b (silencing suppression?), 3a (movement protein [MP]), 3b (coat protein [CP]) that are essential for viral replication, packaging and cell-to-cell movement.

Phylogenetic analysis is widely used software by various biologists for reconstructing the phylogenetic tree to unravel the evolutionary histories of species.

The comparative analysis of complete genome sequence of different strains of viruses might help in identification of specific region of the genome or amino acid responsible for causing the disease, host specificity and systemic nature of virus. This could pave the way for the unravelling of the aetiology of TSV.

After completion of the first objective we are successful in obtaining a TSV (Okra) strain which infects *Nicotiana benthamiana* model plant. Since we would like to use this strain in the laboratory as a model virus, we set the objective of achieving the complete genome sequence of the three RNA molecules using reverse transcribing (RT-PCR) approaches as the second objective.

Based on the above background this chapter was divided into two sub objectives;

i). Obtaining complete genome sequencing for okra strain of *Tobacco streak virus*.

ii). Diversity analysis of okra strain of TSV with reported strains of TSV.

4.2 Materials and methods

4.2.1 Virus culture

Okra strain of *Tobacco streak virus*.

4.2.2 RNA isolation, RT-PCR and cloning

RNA isolation, RT-PCR and molecular cloning was performed as described in chapter 3, section 3.2.

4.2.3 Primer designing

Five sets of forward ($R_1$1+, 1aNcoI+, 1a874+, 1a776+ and 1a2386+) and reverse (1a924-, 1a1836-, 1a2440-, 1aXhbaI- and $R_1$3523-) primers were designed taking okra strain as a template (FJ561302.1) for RNA1. The list of primers was mentioned in table 4.1 and overview for designing of primer in fig 4.3. Similarly, four sets forward ($R_2$1+, 2aNcoI+, 2a1180+, 2a1881+) and reverse primers (2a1255-,

2a1960-, 2a2379XhbaI- and $R_2$2903-) were designed to amplified full length molecule of RNA2, taking okra strain as a template (FJ561303.1). For RNA3; four sets of primers forward (R31+, MP584+, CPNcoI+ and MPNcoI+) and reverse primers (R32203-, CP332-, CPXhbaI-, MPXhbaI-) were designed to amplify the full length, taking okra strain as a template (FJ561304.1) from NCBI (Table 4.1).

To clone RNA encoded genes of *Tobacco streak virus* into pET28a expression and pCB302 binary vector, we introduced restriction enzyme *Nco*I at 5' end of forward and *Xho*I & *Xba*I at 3' reverse primers.

Table 4.1: Primers used in this study for RT-PCR amplification and sequencing of RNA1, 2 and 3

TSV RNA	Primer pairs	**Oligonucleotide sequence (5′----------3′)**
RNA3	R31+	GTATTCTCCG AGCTTAAGAT ACC
	MPNco1+	GCCATG GACGCGTTAGTACCAACGATGAAAGCT
	MPXhoI-	G GAG CTC GGC TGAAAGCAGGTTCCTACCTGC
	MPXbahoI -	GTCTAGACTCGAG TCAGAATTC GGCTGAAAG CAGGTTCCTACCTGC
	CPNco1+	GCCATG GACAATACT TTGATCCAAGTCCAGAC C
	CPXhoI-	GCTCGAGATCTTGATTCACCAGGAAATCTTCTGG
	CPXbahoI-	GTCTAGACTCGAGTCGAATTCATTTATCACCAG GAAATCTTTGG
	R32203-	GCATCTCCTATAAAGGAGGCATCAG
RNA2	R21+	GTGTATTACTGACACATATCTG
	2aNcoI+	GCCATGGATTCCGTTATAAAGAACCTC
	2a1255-	GGGGATGTCATCATGACAACCCC
	2a974+	GTGTTACTAGATTCATAACACATGTCG
	2a1960-	GACATACGTCGGCATCATTAAAAAC
	2a1881+	CTTCAAGTCACCGTGTTGGATG
	2aXhbaI-	GTCTAGACTCGAGTCAGAATTCATGCAATTTGACCC TGCCTTTCCGGGTGGGC
	R22209-	GCATCTCCATTTGGAGGCATAG
RNA1	R11+	GTATTACTGTTTTGTATCCGAAA
	1aNcoI+	GGCCATGGATTCTCGTTCATTACCCACCGT
	1a874+	AGGGTAGAGAGGACAGCCTGTTTATCA
	1a1776+	ACACGTCAACAAGCTTTCAAAGAT
	1a2386+	CCAACCTTTAAGATCACGATTGTT
	1a924-	AGTCATCTCCACGATATATACACC
	1a1836-	AGCTTTCGCTATCGTCATCAGAGC
	1a1836-	AGCTTTCGCTATCGTCATCAGAGC
	1a2440-	GTG TAG TCTTACCACAACCTGCGA
	1aXhbaI-	GGTCTAGACTCGAGAGTTAAAATTCGGACCCATCC
	R13523-	GCATCTCCTTTAAAGGAGGCATTG

4.2.4 Strategies for full length cloning and sequencing of RNA3

Here and in the following sections we are giving a simplified form of presentation for the easy understanding of the steps involved as an overview. To clone and sequence full length molecule of RNA3, we used reverse transcription-polymerase chain reaction (RT-PCR) and cloning approaches. RT-PCR was used for converting RNA molecule into cDNA molecule and cloning was used to clone the amplified cDNA molecule into appropriate vector. Complete genome of RNA3 was divided into three fragments namely, fragment I (that contained complete sequence of MP), fragment II (contained complete sequence of CP) and finally 2.2 kb fragment (contained complete nucleotide sequence of RNA3) as mentioned in fig 4.1. First strand cDNA was synthesized according to the manufacture protocol using MPXhbaI-, CPXhbaI- and $R_3$2203- as a reverse primers. RT-PCR was performed with respective cDNA and forward and reverse primer to amplify the fragment I as MP, fragment II as CP and fragment III as full length sequence of RNA3. PCR amplified products were get purified and cloned into pGEMT-Easy T/A cloning vector.

4.2.5 Strategies for full length cloning and sequencing of RNA2

In similar manner we have divided full length RNA2 molecule into four fragments viz; fragment A, B, C and E as mentioned in fig 4.2. The size of the fragments A, B, C and E has been indicated as 1255 bp, 780 bp, 495 bp and 1022 bp respectively. First strand cDNA was synthesized with gene specific reverse primers (2a1255-, 2a1960-, 2a2379XhbaI- and $R_2$2903-). Taking it as the resultant cDNAs templates, different PCRs were performed to amplify the fragment A, B, C and E with respective sets of specific primers $R_2$1+ & 1255-; 2a1180+ & 2a1960- ; 2a1881+ & 2a2379XhbaI-, 2a1881+ & $R_2$2903- and Pfu polymerase. These PCR products were gel eluted and adenylated at 3′end by Taq polymerase and cloned into pTZ57R/T (Fermentas) cloning vectors.

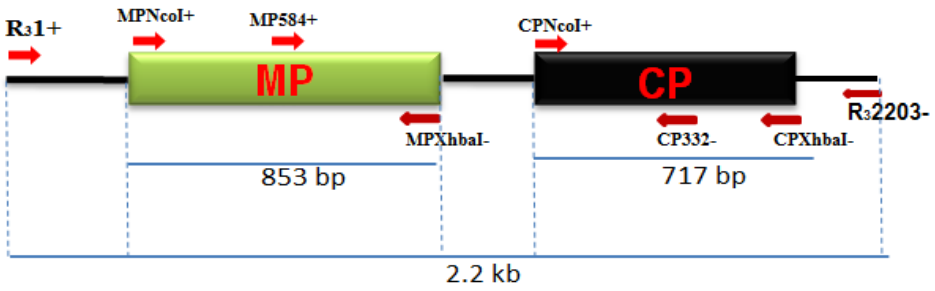

Fig 4.1: Overview for full-length cloning and sequencing of RNA3. Green and black color rectangular box represent the MP and CP respectively. Solid thick black color line at the left and right side indicate untranslated region of the RNA. Black color line between the MP and CP represent inter cistronic region of RNA3. Red color arrows indicate the forward primers as R31+ MPNcoI+, MP584+ and CPNcoI+. The brown color arrows indicate reverse primer as MPXhbaI-, CP332-, CPXhbaI- and R32203. Vertical discontinuous lines represent the demarcation of fragments as MP, CP and full length RNA3. Solid horizontal line represent the size of the fragment as 853 bp, 717 bp and 2.2 kb for fragment MP, CP and full length RNA3 respectively.

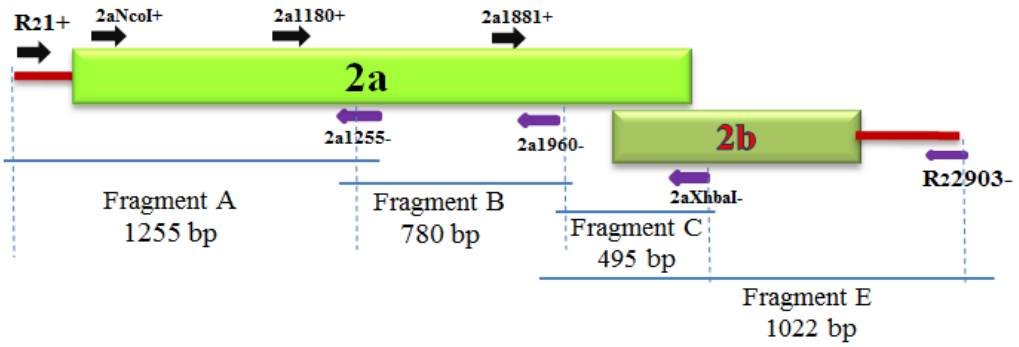

Fig 4.2: Overview for full-length cloning and sequencing of RNA2. Pink color line at the left and right side of rectangular box indicate untranslated region of the RNA. Big and small rectangular box represent 2a and 2b gene respectively. Black color arrow indicate the forward primers as R21+, 2aNcoI, 2a1180+ and 2a 1881+. The violet color arrows indicate reverse primer as 2a1255-, 2a1960-, 2aXhbaI- and R22903. Vertical discontinuous line represent the demarcation of fragments as fragment A, B, C and E. Solid horizontal line represent the size of the fragment as 1255 bp, 780 bp, 495bp and 1022 bp for fragment A, B, C and E respectively.

4.2.6 Strategies for full length cloning and sequencing of RNA1

In similar manner we have divided full length RNA1 molecule into four overlapping fragments viz; fragment I (924 bp), II (962 bp), III (664 bp) and IV (1137 bp) as mentioned in fig 4.3. First strand cDNA was synthesized with gene specific reverse primers (1a924-, 1a1836-, 1a2440- 1aXhbaI- and $R_2$3523-). Taking it as the resultant templates, different PCRs were performed to amplify the fragment I, II, III and IV with respective sets of specific primers R11+ & 1a924-; 1a874+ & 1a1836- ; 1a1776+ & 1a2440- , 1a1776+ & R13523- and Pfu polymerase. These PCR products

were used as a template for the overlap extension PCR. Fragments I & II was fused into single fragment A and fragments III and IV was fused into single fragment D. These PCR products were gel eluted and used for adenylation at 3′end by Taq polymerase and cloned into pTZ57R/T (Fermentas) cloning vectors.

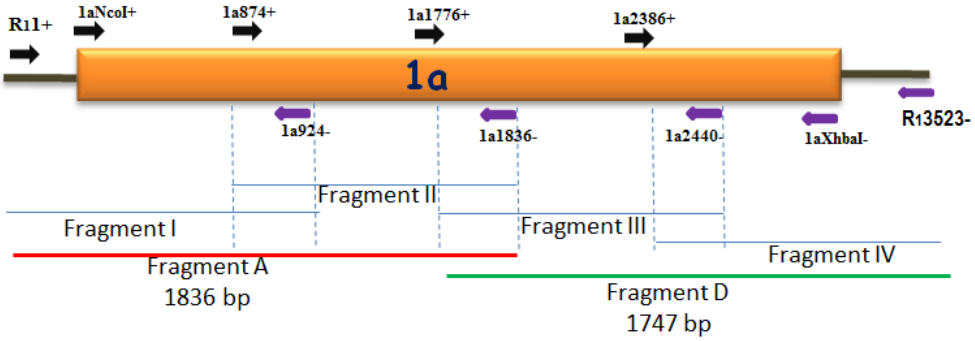

Fig 4.3: Overview for full-length cloning and sequencing of RNA1. Black color line at the left and right side of rectangular box indicate untranslated region of the RNA1. Solid rectangular orange color box represent 1a. Black color arrows indicate the forward primers as R11+, 1aNcoI+, 1a874+, 1a1776+ and 1a2386+. The violet color arrows indicate reverse primer as R13523-, 1aXhbaI-, 1a2440-, 1a1836- and 1a924-. Vertical discontinuous line represent overlapping region between two fragments. Solid horizontal line represent the size of the fragment as 924 bp, 962 bp, 664 bp and 1137 bp for fragment I, II, III and IV respectively. Red color solid line indicate that fusion product of fragment I and II and that represented by the fragment A. Green color solid line represent fragment D that is fusion product of fragment III and IV and its size is 1747 bp.

4.2.7 Sequencing result analysis

BLAST algorithm was used for sequence analysis (Altschul *et al*., 1990) against the NCBI GenBank database (www.ncbi.nlm.nih.gov). BioEdit Version 5.0.9 (Hall, 1999) was used for analysis of the overlapping clones and generation of full-length sequence.

4.2.8 Molecular diversity analysis

Phylogenetic analysis of aligned TSV nucleotide and amino acid sequences were performed using Molecular Evolutionary Genetics Analysis (MEGA 6) offline software. Primarily, multiple sequence alignment was carried out using the MUSCLE embedded in MEGA (version 6) and an aligned sequence file was saved in mega format. Secondly, aligned sequence in mega format taken for construction of phylogenetic tree using Neighbor-Joining method with bootstrap test (1000 replicates).

4.3 Results

4.3.1 Complete genome sequencing for okra strain of *Tobacco streak virus*

The complete genome sequence of okra strain of TSV was performed using reverse transcription-polymerase chain reaction and molecular cloning. The three RNAs of TSV complete genome was deduced in the following steps.

4.3.1.1 RT-PCR amplification, cloning and sequencing of full length molecule of RNA3

Initially, we started cloning and sequencing of RNA3, because it is smallest RNA among three main RNAs.

4.3.1.1.1 RT-PCR amplification of RNA3 fragment as MP, CP and full length RNA3

The complete genome of RNA3 was amplified into three fragments as described in section 4.2.4 and fig 4.1. RT-PCR amplified product showed 873 bp (fig 4.4, lane 1), 2203 bp (fig 4.4, lane 2) and 717 bp (fig 4.4, lane 3) for MP, 2203 fragment and CP respectively.

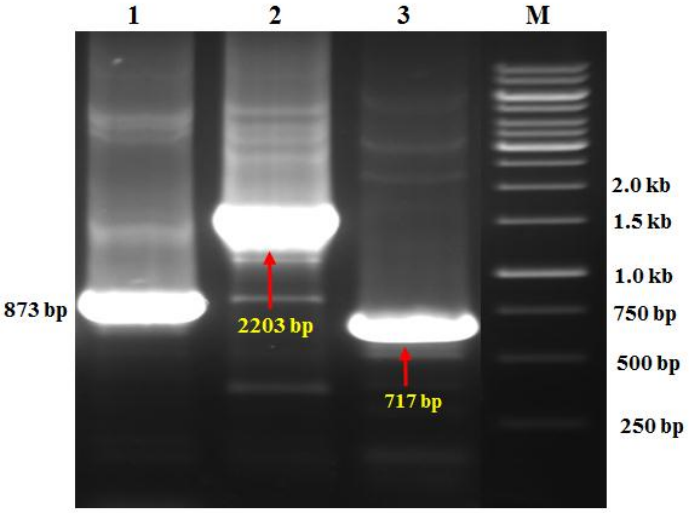

Fig 4.4: Reverse transcription-polymerase chain reaction (RT-PCR) for MP, 2203 bp and CP of RNA3 in 1% agarose gel. Lane 1: RT-PCR amplified product of MP with MPNcoI+ forward and MPXhbaI- reverse primer. Lane 2: RT-PCR amplified product for 2203 bp fragment with R31+ and R32303-. Lane 3: RT-PCR amplified product of MP with CPNcoI+ forward and CPXhbaI- reverse primer. 873 bp, 2203 bp and 717 bp indicate the desired amplified product of MP, 2203 fragment and CP respectively. M: 1 kb ladder.

4.3.1.1.2 Cloning and confirmation of fragments MP, CP and full length RNA3 into pTZ57R/T vector

MP, CP and full length PCR amplified product was cloned into pGEMT-Easy vector. Restriction digestion analysis of recombinant clone harbouring MP and CP gene showed expected band 873 bp and 717 bp (data not shown).

Two independent pGEMT recombinant clones harbouring full length cDNA molecule of RNA3 was digested with *Kpn*I and *Eco*RI. The digested clones were released three fragments with size of 1047 bp, 649 and 450 bp (fig 4.5, lane 1 and 2). This result indicates that presence of the RNA3 sequence in recombinant pGEMT vector. Positive clone was sequenced from the both ends; it was named as pGEMRNA3. This clone was used for the construction of full length infectious molecule of RNA3 in the chapter 5.

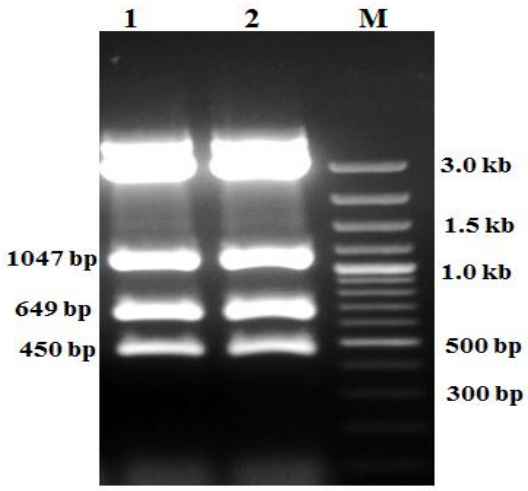

Fig 4.5: Restriction digestion profile of recombinant pGEMT-Easy plasmids harboring fragment 2203 (full length RNA3) in 1% agarose gel. Lane 1 to 2: two independent recombinant pGEMT-Easy plasmids harboring full length RNA3 digested with *Kpn*I and *Eco*RI restriction enzyme. Left side of the gel 1047 bp, 649 bp and 450 bp indicate released insert of RNA3 in three pieces and right side of the gel indicate molecular weight of 1.0 kb ladder.

4.3.1.1.3 Sequence analysis and compilation of overlapping fragments of RNA3

Two plasmids from each clone were sequenced using sequencing primer from both directions. Full length compiled sequence of RNA3 was deduced and mentioned in appendix 1. RNA3 complete genome map was deduced and it showed 211nt of 5' UTR, MP ORF's 873 nt, ICR 123 nt, CP ORF's 717 nt and 289 nt of 3' UTR RNA3.

NCBI blast was performed with full length RNA3 and its encoded gene of TSV okra strain of HCU at nucleotide and amino acid level. More than 100 accession number of coat protein and movement protein gene of TSV matched. TSV-Okra strain

of HCU showed homology 99.8-100% with Indian strain, 85-87% with Australian strain and 90-95% USA strain of TSV at nucleotide level and amino acids level.

4.3.1.2 RT-PCR amplification, cloning and sequencing of full length molecule of RNA2

4.3.1.2.1 RT-PCR amplification of RNA2 fragment A, B, C and E

Full length RNA2 molecule was amplified into four overlapping fragments as strategy and methods described in section 4.2.5 and fig 4.2. PCR amplified product of the fragment A showed faint and diffuse band in between 1.0 kb to 1.5 kb of 1.0 kb DNA ladder (fig 4.6, panel A, lane 1and 2). 1255 bp of desired PCR band was eluted for the further experiment. In case of fragment B, more intense band was observed above the 750 bp i.e. 780 bp. Apart from desired band non-specific band (*) was also observed near 2.0 kb region (fig 4.6, panel B, lane 1 and 2). PCR amplified product of fragment C showed very sharp band near 495 bp (fig 4.7, panel A, lane 1 and 2). PCR amplified product of fragment E showed 1020 bp (fig 4.7, panel B, lane 1 and 2). All these PCR fragments were eluted from the 1% agarose gel and adenylated using Taq DNA polymerase.

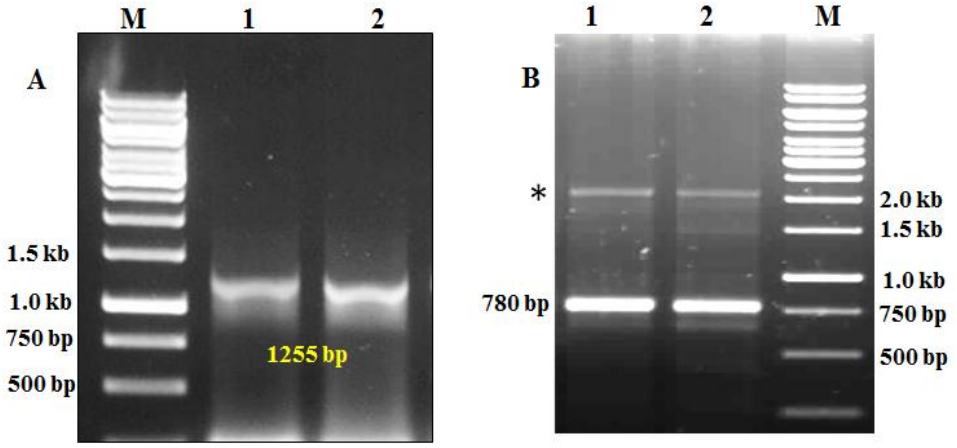

Fig 4.6: Reverse transcription –polymerase chain reaction (RT-PCR) for fragment A and B of RNA2 in 1% agarose gel. In panel A, Lane 1 and 2; PCR amplified product for fragment A, left side of the indicate molecular weight of the marker and below the PCR band 1255 bp indicate molecular weight of PCR amplified product. In panel B, lane 1 and 2 represent PCR amplified product of fragment B. M; 1 kb ladder, left side of the gel indicate 780 bp for PCR amplified product and right side of the gel showed size of 1.0 kb DNA ladder. Asterisk mark (*) indicate the non-specific band

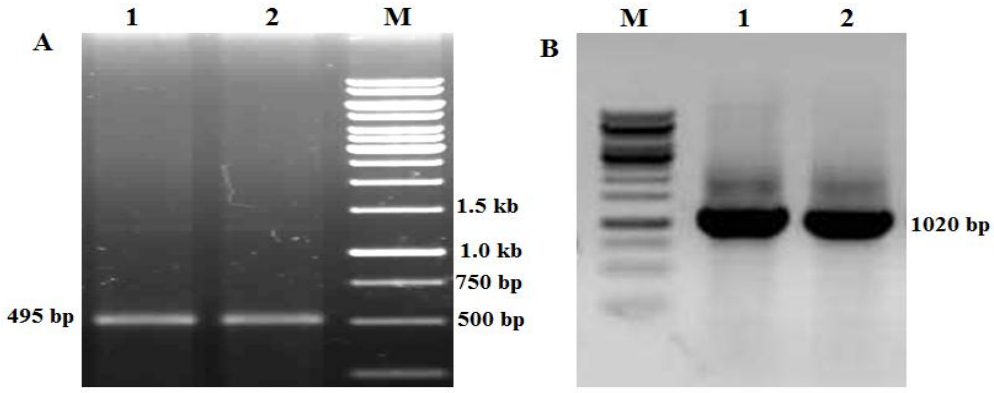

Fig 4.7: Reverse transcription–polymerase chain reaction (RT-PCR) for fragment C and E of RNA2 in 1% agarose gel. In panel A: Lane 1 and 2; PCR amplified product for fragment C, right side of the gel indicate molecular weight of the marker and left side of gel 495 bp indicates molecular weight of PCR amplified product. In panel B: lane 1 and 2 represent PCR amplified product of fragment E. M: 1 kb ladder, 1020 bp indicate molecular weight of PCR amplified product.

The integrity of adenylated PCR product was checked before the ligation in 1% agarose gel. The fragment A, B, and C showed sharped band near 1255 bp, 780 bp and 495 respectively (fig 4.8, panel A, lane 1, 2, 3). Fragment E was also observed at 1022 bp (fig 4.8, panel B, lane 1). All the above fragments were cloned into pTZ57R/T cloning vector.

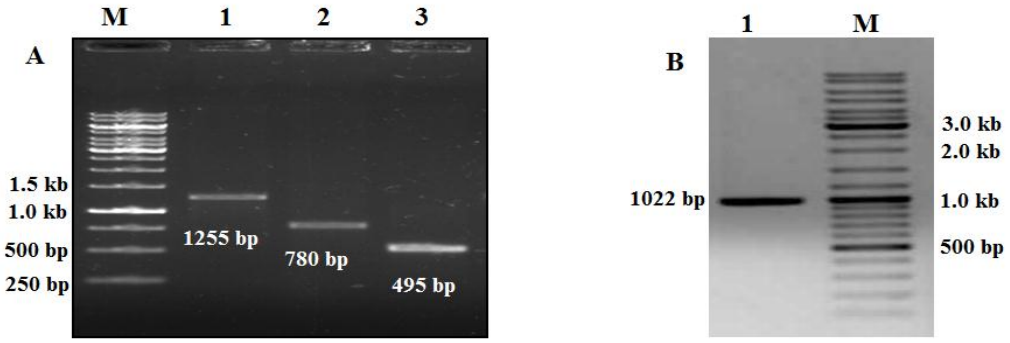

Fig 4.8: Adenylated PCR product of fragment A, B, C and E in 1 % agarose gel. Panel A: Lane 1, 2 and 3 indicate the fragment A (1255 bp), B (780 bp) and C (495 bp) respectively. Panel B. lane 1 indicate fragment E (1022 bp).

4.3.1.2.2 Cloning and confirmation of fragments A, B, C and E of RNA2 into pTZ57R/T vector

Fragments A, B, C and E were cloned into pTZ57R/T vector. Isolated recombinant pTZ57R/T plasmids harbouring fragment A, B, C, and E were confirmed

through restriction digestion using *Eco*RI and *Hin*dIII restriction enzyme. We have selected two PCR positives colonies for plasmid isolation and restriction digestion. 1255 bp of fragment was released after restriction of plasmid with *Eco*RI and *Hin*dIII. The positive plasmids were named as pR2A8 and pR2A12 (fig 4.9, panel A, lane 1 and 2). In a similar way, recombinant plasmids of fragment B, C and E were screened and confirmed through restriction digestion. Two plasmids from each clone were digested with *Eco*RI and *Hin*dIII restriction enzyme and it released 780 bp (fig 4.9, panel B, lane 1 and 2) for fragment B, 495 bp (fig 4.9, panel B, lane 4 and 5) for fragment C and 1022 bp (fig 4.9, panel C, lane 1 and 2) for fragment E. Sequenced confirmed plasmids were named as pR2B2, pR2B4 for clone of B, pR2C1, pR2C2 for clone C and pR2E1, pR2E2 for clone E. All these plasmids were used as for construction of full length infectious clone in chapter 5. The 5' end and 3' end of RNA2 was confirmed through 5'-RACE and 3'-RACE.

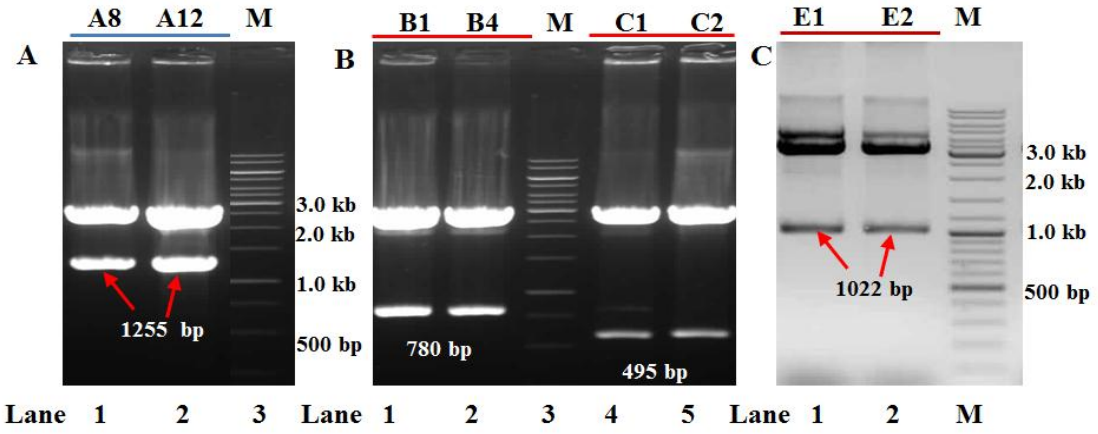

Fig 4.9: Restriction digestion profile of recombinant pTZ57R/T plasmids harboring fragment A, B, C and E in 1% agarose gel. In panel A: lane 1 and 2: restriction digestion pattern of fragment A present in pTZ57R/T vector, arrows indicate 1255 bp released fragment. A8 and A12 represent clone no 8th and 12th for fragment A. Panel B: Lane 1 and 2; restriction digestion pattern of fragment B and lane 3 & 4 for restriction pattern for fragment C present in pTZ57R/T cloning vector. B1 and B4 represent clone no 2 and 4 for fragment B. C1 and C2 represent clone 1st and 2nd respectively. 780 bp and 495 bp indicate released fragment B and C respectively. In panel C: lane 1 and 2 restriction digestion pattern of fragment E present in pTZ57R/T cloning vector. Arrows indicate the 1022 bp released fragment E and right side of the gel indicate molecular weight of 1.0 kb ladder.

4.3.1.2.3 Sequence analysis and compilation of overlapping fragments

Two plasmids from each clone were sequenced from both directions. Sequence obtained after sequencing result used for compilation of full length molecule of RNA2 using overlapping sequence and Bioedit software. Full length compiled sequence of

RNA2 was elucidated into genome map (appendix 2). RNA2 genome map deduced which has 42 nts of 5' UTR, 2a ORF 2379 nt, 2b ORF 600 nt and 140 nt of 3' UTR.

NCBI blast was performed for full length RNA2 and its encoded gene at nucleotide and amino acid level. NCBI blast result showed, 8 accessions (FJ5611303, FJ5611300, JX463335, JX463338, NC003842, U75538, JX073657 and FJ403376) were matching with the different level of homology and coverage of sequence of our RNA2 (TSV-Okra-HCU). All these accessions belong to different region of the world mainly, India, Australia and USA. Total size of the genome is also varied from one region to another region. For example, All Indian strain showed genome size of RNA2 is 2903 nt, Australian strain 2901 to 2922 nt and USA strain 2911 to 2926 nt (table 4.2). Among all analysed strains of TSV, 1973 strain of Australia showed minimum length of 5' UTR i.e. 39 nt compared to 42 nt in maximum reported strain. Similarly, 3' UTR of 1973 strain showed minimum length i.e 117 nt compare to 140 nt (Indian strain) and 139 (USA strain).

The level of TSV okra strain showed homology 99.7-99.8% with Indian strain, 80-82% with Australian strain and 81-86% USA strain of TSV with 93% coverage of sequence at nucleotide level (details mentioned in table 4.2). At amino acid level it showed homology 98-99% Indian strain, 80-86% with Australian strain and 89-93% with USA strain with 95% coverage of sequence (details mentioned in table 4.2). Based on analysis of TSV strain sequences these are divided into three main molecular group; Indian, Australian and USA respectively. The detail analysis of all strains was compiled in table 4.2.

4.3.1.3 RT-PCR amplification, cloning and sequencing of full length molecule of RNA1

4.3.1.3.1 RT-PCR amplification of RNA1 fragment I, II, III and IV

Similar to that of RNA3 and RNA2 we have amplified full length RNA1 molecule into four overlapping fragments viz; fragment I, II, III and IV as mentioned in fig 4.3 and described in section 4.2.6. PCR amplified product showed 924 bp for fragment I (fig 4.10, panel A, lane 1) and 962 bp for fragment II (fig 4.10, panel A, lane 2). Fragment III and IV showed 664 bp (fig 4.10, panel B, lane 1) and 1137 bp (fig 4.10, panel B, lane 1 and 2) respectively.

Table 4.2: Genome sizes, genomic position, amino acid, length of the ORF's, percentage of homology, percentage of query coverage, isolate / host of TSV RNA2 variant compare to our TSV RNA2

Gene bank Accession No	Genome size (nt)	ORF / Amino acids	% Homology / % Query cover	Isolate / Host	Research Group	Molecular group
FJ561303 ACT67448-2a ACT67449-2b	2903 5'UTR-41 2a-2378 2b-599 3'UTR-140 **Overlap-256**	42-2420 **792 aa** 2164-2763 **199 aa**	99.8 /100 99.6/100 99.8 /100 99.6/100	Okra / TN	M. Krishna Reddy, IIHR, Bengaluru, INDIA, 2009	INDIA
FJ561300 ACT67443-2a ACT67444-2b	2903 5'UTR-41 2a-2378 2b-599 3'UTR-140 Overlap-256	42-2420 792 aa 2164-2763 199 aa	99.5/100 98.7/99.54 99.6/100 98.72/99.54	Pumpkin / BLR		
JX463335 AGN29708-2a AGN29709-2b	2922 5'UTR-38 2a-2423 2b-681 3'UTR-117 **Overlap-308**	39-2462 **807 aa** 2154-2805 **217 aa**	79.7/67 80/87.8 78.5/67.8 70.83/77.8	1973 AUS	Thomas, J.E. Queensland Australia	AUSTRALIA
JX463338 AGN29713-2a AGN29714-2b	2901 5'UTR-39 2a-2375 2b-608 3'UTR-117 Overlap-265	40-2415 791 aa 2150-2758 202 aa	87.22/99 86.73/97 82/92 82/92	2334 AUS		
NC003842 NP620768-2a NP620769-2b	2926 5'UTR-41 2a-2402 2b-617 3'UTR-117 Overlap-274	42-2444 800 aa 2170-2787 205 aa	84/100 89.73/93.5 81.4/97 80/87	WC/ Tobacco USA	Scott, S.W. Clemson University, USA	USA
U75538 AAB48409-2a AAB48410-2b	2926 5'UTR-41 2a-2402 2b-617 3'UTR-117 Overlap-274	42-2444 800 aa 2170-2787 205 aa	86.41/97 89.0/94 85.4/97 80/87.8	WC/ Tobacco USA		
JX073657 AFP24897-2a AFP24898-2b	2911 5'UTR-41 2a-2387 2b-617 3'UTR-139 Overlap- 274	42-2429 795 aa 2155-2772 205 aa	87.8/97 93.13/97 85.4/97 80/87.8	Henery / USA	Singh, A.K University of Kentucky ,USA	
FJ403376 ACJ38088-2a ACJ38089-2b	2911 5'UTR-41 2a-2387 2b-617 3'UTR-139 Overlap- 274	42-2429 795 aa 2155-2772 205 aa	84.73/100 92/97 85.4/100 89.73/93.5	Illiinois / Soybean USA	Domier,L. L University of Illinois, USA	

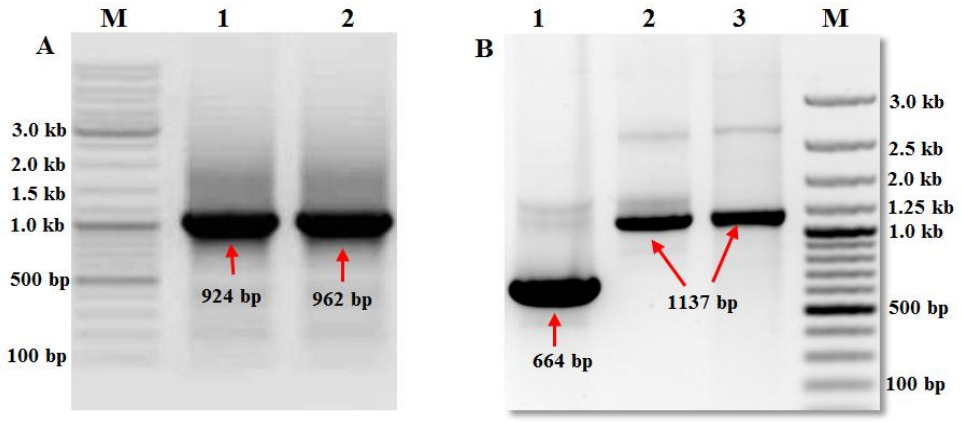

Fig 4.10: Reverse transcription-polymerase chain reaction amplification of fragment I, II, III and IV of RNA1. Panel A, RT-PCR amplification of fragment I and II. Lane 1: PCR amplification of fragment I with R11+ forward and R1924- reverse primer, using cDNA as template, lane 2: PCR amplification of fragment II with R1874+ forward and R11930- reverse primer, using cDNA as a template. M: 1.0 kb ladder. Panel B, RT-PCR amplification of fragment III and IV. Lane 1: PCR amplification of fragment III with R11776+ forward & R12440- reverse primer using cDNA as a template, Lane 2 and 3: PCR amplification of fragment IV with R12384+ forward & R13523- reverse primer, using synthesized cDNA with R13523- primer as a template. M: 100 bp ladder. Arrows indicate the PCR amplified product of fragment I, II, III and IV with amplicon size 924 bp, 962 bp, 664 bp and 1137 bp respectively.

4.3.1.3.2 Overlap extension PCR for fragment A and D

Fragment A was obtained after fusion of fragments I & II and it showed 1836 bp (fig 4.11, panel A, lane 1 and 2). Fragment D was obtained after fusing of fragment III and IV, using overlap extension PCR and amplified product showed 1747 bp (fig 4.11, panel B, lane 1 and 2. Desired PCR bands were eluted and used for the cloning purpose.

4.3.1.3.3 Cloning and confirmation of fragments A and D of RNA1 into pTZ57R/T vector

Fragments A and D were cloned into pTZ57R/T vector. Isolated recombinant pTZ57R/T plasmids harbouring fragment A and D were confirmed through restriction digestion using *Eco*RI and *Hin*dIII restriction enzyme. pTZ57R recombinant plasmids harbouring fragment A was digested with *Eco*RI and *Hin*dIII restriction enzyme and it released 1836 bp (fig 4.12, lane 1). The sequence confirmed plasmid was named as pR1aA2. Two pTZ57R recombinants plasmid harbouring fragment D was confirmed through restriction digestion with *Eco*RI and *Hin*dIII. The digested plasmids were released 1253 bp, 333 bp and 181 bp (fig 4.12, panel B, lane 1 and 2) due to three

internal *Eco*RI sites (at 1776, 1957 and 2290) and one *Hin*dIII (at 1787) restriction sites present in RNA1. The sequence confirmed plasmids were named as pR1aD1, pR1aD2. All these plasmids were used for construction of full length infectious clone in chapter 5. The 5' end and 3' end of RNA1 was confirmed through 5'-RACE and 3'-RACE.

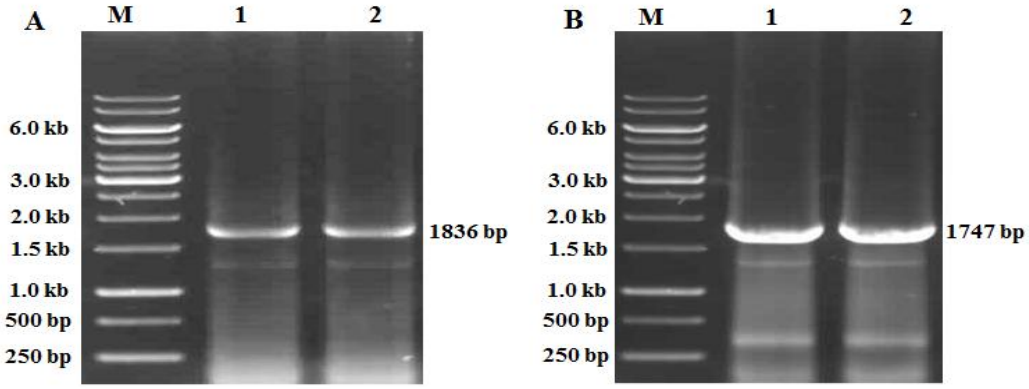

Fig 4.11: PCR amplification of fragment A and D of RNA1 through overlap extension PCR. Panel A, PCR amplification of fragment A using overlap extension PCR. Lane 1 and 2: PCR amplification of fragment A with R11+ forward & R11836- reverse primer, using fragment I and II as a template. 1836 bp indicate PCR amplified product of fragment A. M: 1.0kb ladder. Panel B, PCR amplification of fragment A using overlap extension PCR. Lane 1 and 2: PCR amplification of fragment D with 1776+ forward & R13523- reverse primer using fragment III and IV as template. 1747 bp indicate PCR amplified product of fragment D. M: 1.0kb ladder

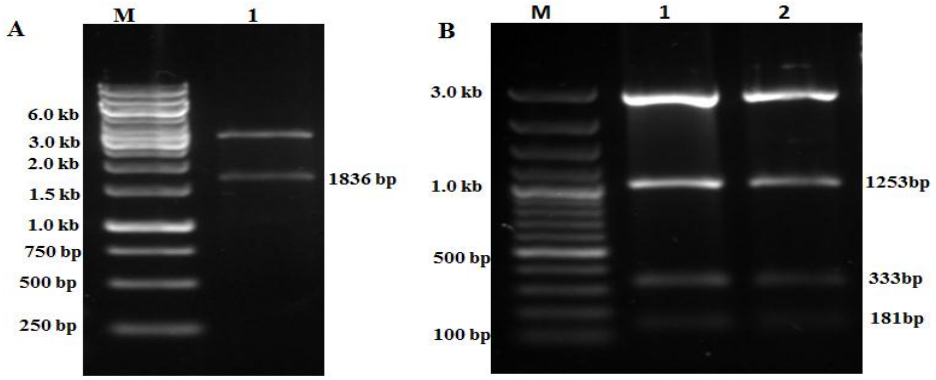

Fig 4.12: Restriction digestion confirmation pTZ57R/T recombinant plasmids p1aA and p1aD plasmid harboring fragment A and D respectively. Panel A: Lane 1 indicates the p1aA plasmid digested with *Eco*R1 and *Hin*dIII restriction enzymes. Right side of gel indicates the molecular weight of the released insert i.e. 1836 bp. M: 1.0 kb DNA ladder. Panel B: Lane 1 and 2 indicate the p1aD plasmid digested with *Eco*R1 and *Hin*dIII restriction enzymes. Right side of gel indicates the molecular weight of the released insert i.e. 1253 bp, 333 bp and 181 bp. M: 100 bp DNA ladder.

4.3.1.3.4 Sequence analysis and compilation of overlapping fragments of RNA1

Two plasmids from each clone were sequenced using sequencing primer from both directions. Overlapped sequence used for compilation of full length molecule of RNA1 using Bioedit software. Full length compiled sequence of RNA1 was elucidated into genome map (appendix 3). RNA1 genome map was deduced as 37 nt of 5' UTR, 1a ORF 3279 nt and 207 nt of 3' UTR.

NCBI blast was performed for full length RNA1 and its encoded gene at nucleotide and amino acid level. NCBI blast result showed, 12 accessions (FJ5611302, FJ5611299, KF264471, KF264472, KF264473, KF264474, JX463335, JX463338, NC003842, U75538, JX073657 and FJ403376) were matching with the different level of homology and coverage of sequence of our RNA1. All these accession belongs to different region of the world mainly, India, Australia and USA. Total size of the genome is also varied from one region to another region. For example, All Indian strain showed genome size of RNA1 is 3523 nt, Australian strain 3481 to 3512 nt and USA strain 3482 to 3491 (table 4.3).

The level of TSV okra strain showed 99.7-99.8% homology with Indian strain, 79-80% with Australian strain and 85-86% USA strain of TSV with 95% coverage of sequence at nucleotide level. At amino acid level it showed 98-99% homology Indian strain, 86-93% with Australian strain and 89-93% with USA strain with 95% coverage of sequence (details mentioned in table 4.3). Based on analysis of TSV strains sequence obtained from NCBI, these are classified into three main molecular group; Indian, Australian and USA. The detail analysis of all strains was compiled in table 4.3.

Table 4.3: Genome sizes, genomic position, amino acid, length of the ORF's, percentage of homology, percenage of query coverage, isolate / host of TSV RNA1 variant compare to our TSV RNA1

Gene bank Accession No	Genome size	ORF / Amino acids	% Homology / % Query cover	Isolate / Host	Research Group	Molecular group
FJ561302 ACT67447	Total 3523 5'UTR- 37 3'UTR- 207	38-3316 1092 aa	99.4 /100 99.6/100	Okra / TN	M. Krishna Reddy, IIHR, Bengaluru, INDIA, 2009	INDIA
FJ561299 ACT67442	Total 3523 5'UTR- 37 3'UTR- 207	38-3316 1092 aa	99.32/100 98.72/99.54	Pumpkin / BLR		
KF264471 AGW7466	3463 5'UTR- 21 3'UTR- 164	21-3299 1085 aa	99.65/98 99.45/100	Okra / CBE /TN		

KF264472 AGW7467	Total 3465 5'UTR- 23 3'UTR- 164	23-3301 1092 aa	99.57/98 99.45/99.7	Sunflower / CBE2/TN	Chandrasekhar, TNAU, Coimbatore INDIA December 2013	
KF264474 AGW7468	Total 3465 5'UTR- 23 3'UTR- 164	23-3301 1092 aa	99.65/98 99.36/99.63	Sunflower DHP/TN		
KF264473 AGW7469	Total 3465 5'UTR- 23 3'UTR- 164	23-3301 1092 aa	99.42/99 99.36/99.73	Sunflower KAR/TN		
JX463337 AGN29707	Total 3512 5'UTR- 37 3'UTR- 190	38-3322 1094 aa	88.1/97 93.42/99.68	1973 / AUS	Thomas, J.E. Queensland Australia	AUSTRALIA
JX463337 AGN29707	Total 3481 5'UTR- 37 3'UTR- 159	38-3322 1094 aa	79.17/99 86.73/93.5	2334 AUS		
NC003844 NP620772	Total 3491 5'UTR- 37 3'UTR- 169	38-3322 1094 aa	85.4/97 89.73/93.5	Tobacco USA	Scott, S.W. Clemson University, USA	USA
U80934 AAB48983	Total 3491 5'UTR- 37 3'UTR- 169	38-3322 1094 aa	86.41/97 89.0/94	Tobacco USA		
JX073656 AFP24896	Total 3482 5'UTR- 38 3'UTR- 169	39-3320 1093 aa	87.8/97 93.13/97	Henery / USA	Singh, A.K University of Kentucky ,USA Domier,L.L University of Illinois, USA	
FJ403375 ACJ38087	Total 3491 5'UTR- 37 3'UTR- 169	38-3322 1092 aa	86.73/97 93/97	Illinois / Soybean USA		

4.3.1.3.5 Comparison analysis of 1a gene using BLAST

The comparative analysis of 1a protein of the TSV and *Alfalfa mosaic virus* (AMV) using BLASTP 2.2.28 software revealed that TSV 1a protein having two conserved domain viz; V-methyltransferase and helicase, whose domains ranges from 70 aa to 412 aa and 785 aa to 1060 aa respectively (fig 4.13). Further, motifs were identified after comparison with *Ilarvirus* 1a protein sequences. There are four motifs in V-methyltransferase domain and six motifs in case of helicase domain. Six motif include; motif I, II, III, IV, V and VI ranges from 801-812, 838-844, 899-908, 953-961, 1006-1021 and 1047-1054 of 1a gene respectively.

According to Jhon F. Bol's reseach group, helicase domain is responsible for negative strand synthesis of RNA. Vlot *et al*., (2003) reported that motifs I, III, and VI of the AMV replicase protein disrupt the putative helicase activity of P1 and are involved in viral RNA replication. Similar type of motifs was also found in *Tobacco streak virus* with slight variation (fig 4.13). Comparative analysis of motif sequence in *Alfalfa mosaic virus* and *Tobacco streak virus* is given in table 4.4.

Table 4.4: Helicase domain motifs

Motifs	*Alfalfa mosaic virus*	*Tobacco streak virus*	Variation at position
I	IVDGVAGCGKT	IVDGVAGCGKT	No change
II	SSADELK	SSSDELK	A to S
III	VIAFADTEQ	VIAFGDTEQ	A to G
IV	K--VKSASV	KPV**KT**NSR	T-S, N-A, R-V
V	IKTTHEAQG**E**TWDHV	IKTTHEAQGKTWDHV	E- K
VI	VALSRHKK	VALSRHKK	No change

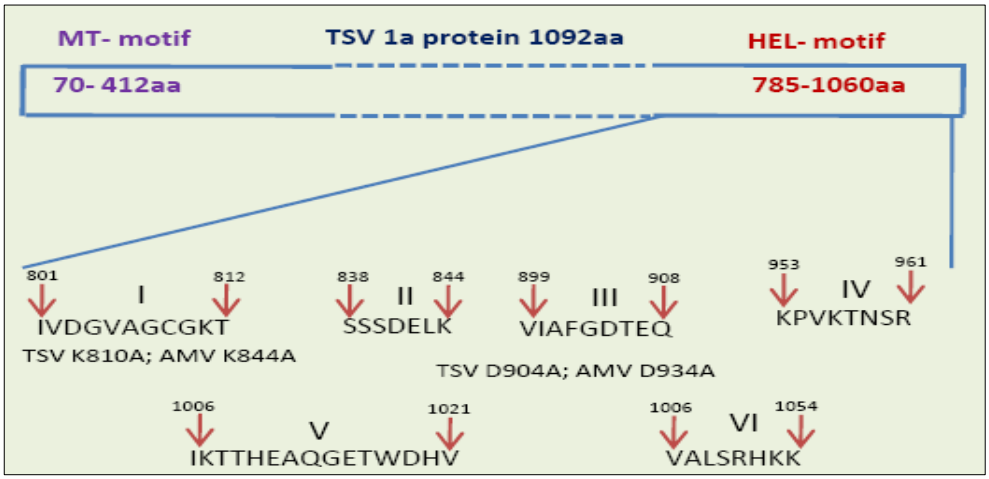

Fig 4.13: Elucidation of Motifs in Helicase domain of 1a protein.
MT and HEL indicate the methyltransferase and Helicase domain respectively. Roman letter I to VI indicate the motif of helicase domain.

Bol group created three mutants of helicase domain viz; K844A, D934A, and R1085A in motifs of I, III and VI respectively and found them responsible for negative strands synthesis of RNA.

4.3.2 Molecular diversity analysis of *tobacco streak virus*

Molecular diversity analysis of individual RNA and its encoded gene was carried out at nucleotide as well as amino acid level using MEGA 6 software.

4.3.2.1 Molecular diversity analysis of RNA1 and its encoded gene

Phylogenetic tree was constructed for nucleotide and amino acid sequence of 1a gene using MEGA 6 software. In both the cases constructed tree showed two clusters and one out group. Here, all Indian strains are clustering together and USA strain are forming another cluster, Australian 1973 strain of TSV showed maximum variation and separated as an out group member (fig 4.14).

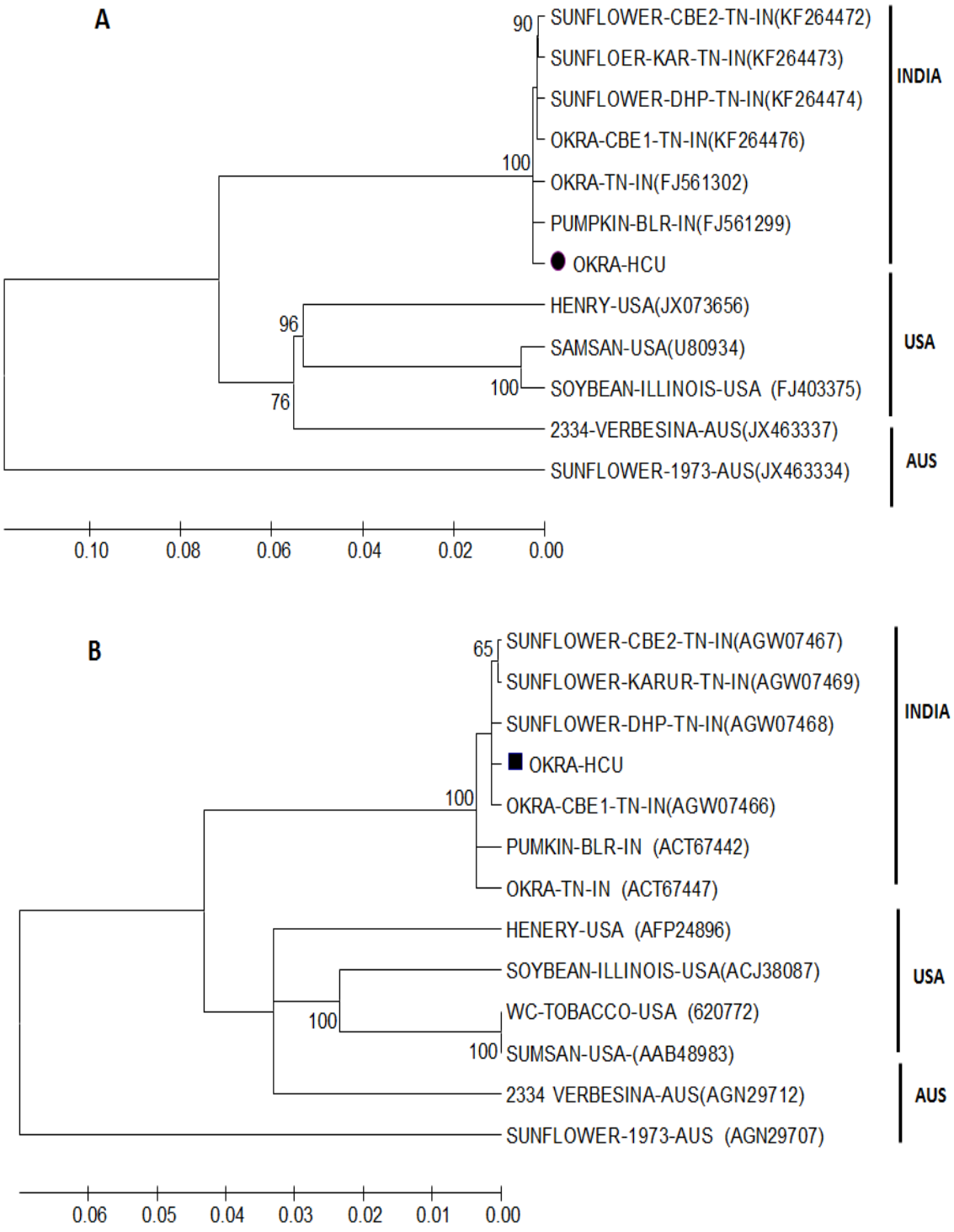

Fig 4.14: Construction of phylogenetic tree for full length RNA1 and 1a protein using MEGA 6.
In panel A and B represent the phylogenetic tree constructed using full length nucleotide sequence of RNA1 and 1a amino acids sequence respectively. Phylogenetic tree analysis was constructed using the Neighbour-Joining method. Bootstrap values (%) are shown at nodes. Right side of the node indicate TSV strain, place of isolation or host and gene bank accession numbers used for the construction of the tree. Vertical line at right side of the gene bank accession number indicates clustering of Indian strain, USA strain and Australian strain. Sunflower 1973-AUS (JX463334) (panel A) and Sunflower 1973-AUS (AGN29707) indicate as out group. Lower side of tree indicate the scale. Solid circle (panel A) and solid square (panel B) represent the okra strain of TSV from HCU.

4.3.2.2 Molecular diversity analysis of RNA2 and its encoded gene

Phylogenetic trees were constructed for nucleotide sequence and amino acid sequence of 2a gene using MEGA 6 software. It showed two clusters; all Indian strains are clustering together and forming one group. Among Indian strain our strain found more close to strain isolated from okra of Tamil Nadu (FJ561303). USA strains were clustered into one group and forming another cluster. Here, 2334 verbesina strain of TSV from Australia was closer to the Indian strain of the TSV (fig 4.15). However, another Australian strain as 1973 strain of TSV showed maximum variation and separated as an out group member.

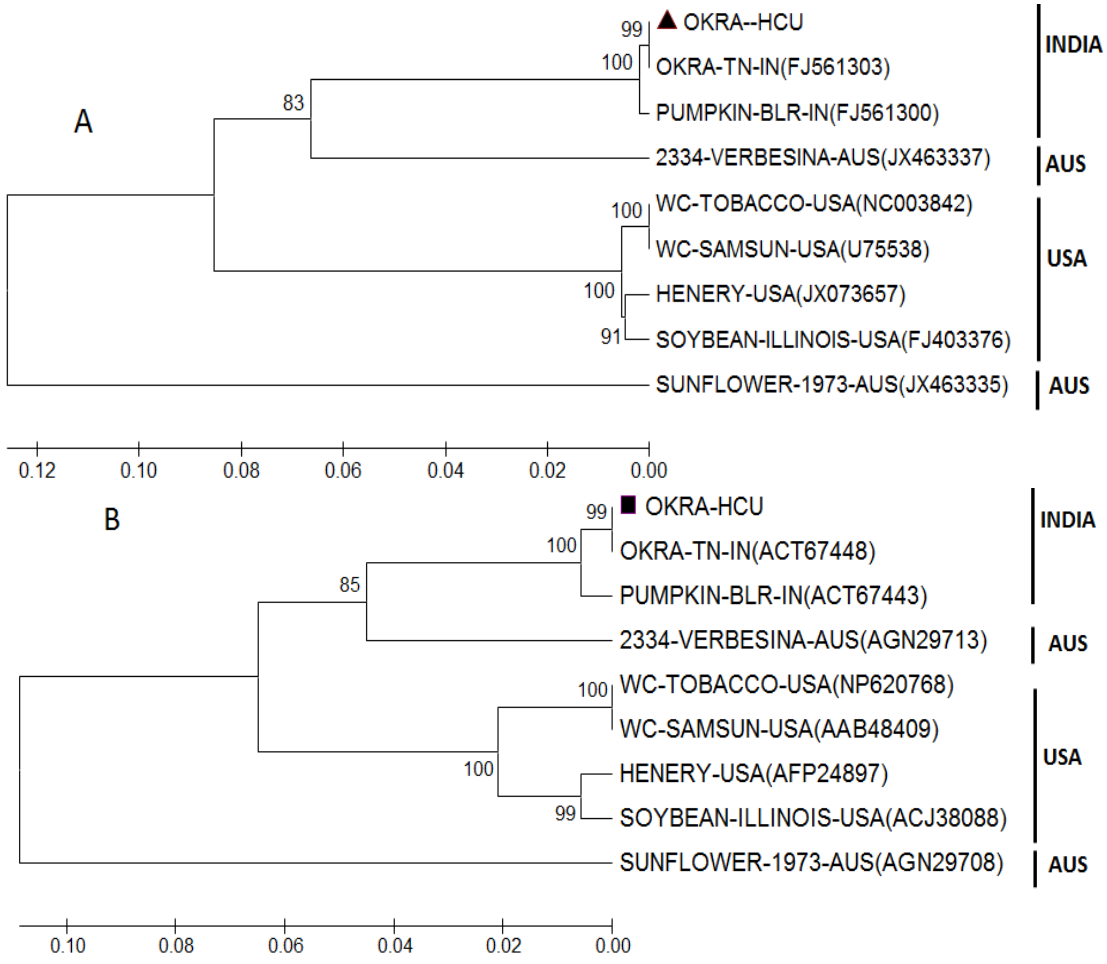

Fig 4.15: Construction of phylogenetic tree for 2a (RDRP) gene using MEGA 6.
In panel A and B represent the phylogenetic tree constructed using full length nucleotide sequence of RNA2 and 2a amino acids sequence respectively. Phylogenetic tree analysis was constructed using the Neighbour-Joining method. Bootstrap values (%) are shown at nodes. Right side of the node indicate TSV strain, place of isolation or host and gene bank accession numbers used for the construction of the tree. Vertical line at right side of the gene bank accession number indicates clustering of Indian strain, USA strain and Australian strain. Sunflower 1973-AUS (JX463335) (panel A) and Sunflower 1973-AUS (AGN29708) indicate as out group. Lower side of tree indicate the scale. Solid triangle (panel A) and solid square (panel B) represent the okra strain of TSV from HCU.

Phylogenetic tree of 2b gene at nucleotide as well as protein level showed; Indian strains are forming one cluster, USA strains are clustering along with the Australian strain (fig 4.16). The TSV isolate named 1973 from Australia showed maximum variation and separated as out group.

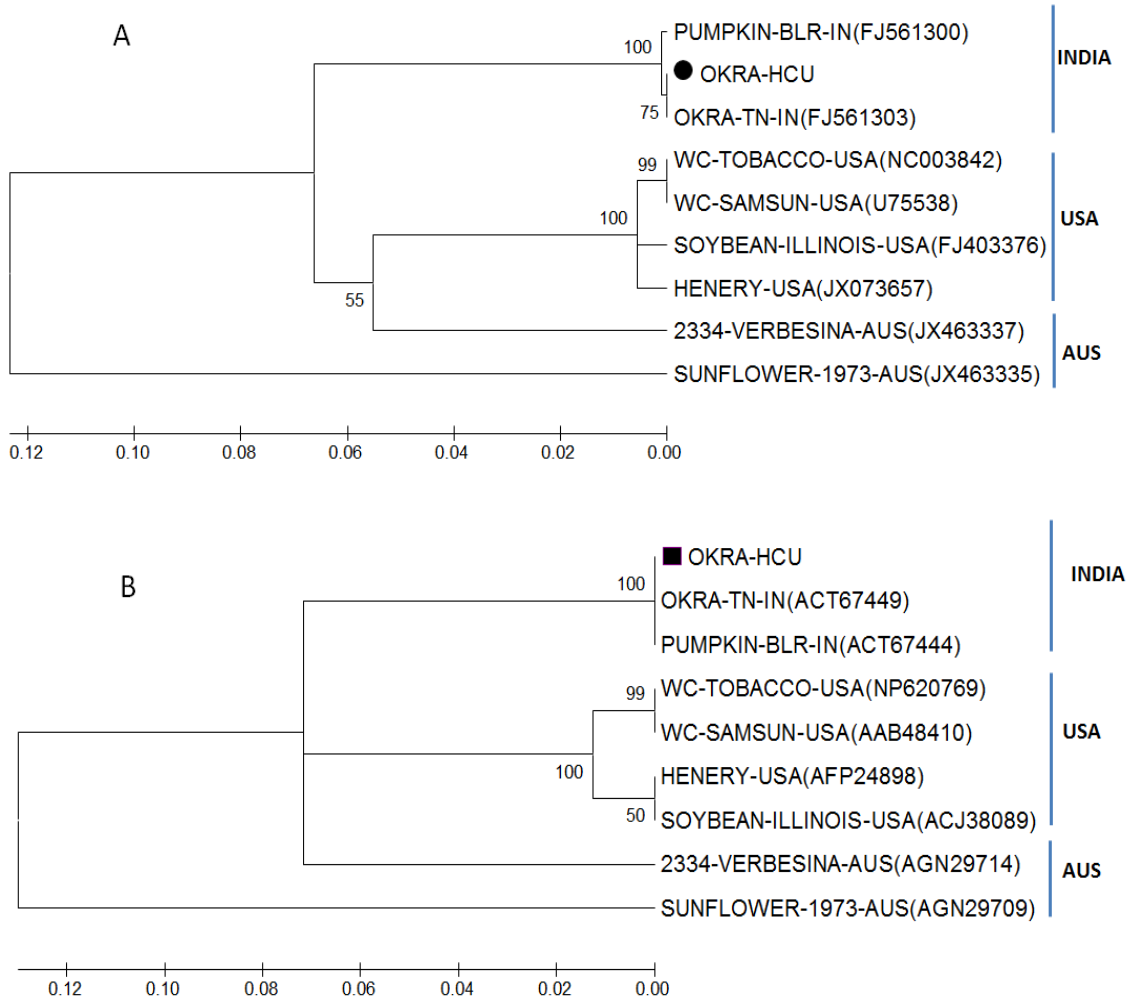

Fig 4.16: Construction of phylogenetic tree for 2b gene and 2b protein using MEGA 6

In panel A and B represent the phylogenetic tree constructed using full length nucleotide sequence of 2b gene and amino acids sequence of 2b protein respectively. Phylogenetic tree analysis was constructed using the Neighbour-Joining method. Bootstrap values (%) are shown at nodes. Right side of the node indicate TSV strain, place of isolation or host and gene bank accession numbers used for the construction of the tree. Vertical line at right side of the gene bank accession number indicates clustering of Indian strain, USA strain and Australian strain. Sunflower 1973-AUS (JX463335 for 2b sequence) (panel A) and Sunflower 1973-AUS (AGN29709) indicate as out group. Lower side of tree indicate the scale. Solid circle (panel A) and solid square (panel B) represent the okra strain of TSV from HCU.

4.3.2.3 Comparative analysis of 2b gene at nucleotide and protein level

Comparative analysis of 2b gene of okra strain was performed with the reported strain of the TSV using clastalw. At nucleotide level okra strain of TSV

showed conserved with Indian strain and variable with the USA and Australian strain of the TSV (fig 4.17). Fifty four nucleotides of 2b gene were removed in the case of the Indian strains (fig 4.17, box I, II and III) and 36 nucleotide in case of USA strain (fig 4.17, box I and III) of the TSV. Each box is stretch of the 18 nucleotide. These variations were observed in the overlapping region of the 2b gene. Apart from these variations many mismatches are also observed in the non-overlapping reason of the 2b gene (fig 4.17).

Fig: 4.17 Comparative analysis of 2b nucleotide sequence of TSV okra strain with the reported strains of the TSV. Black color solid arrow indicates overlapping nucleotide sequence of the 2a and 2b gene. Solid brown color arrow indicates the non-overlapping nucleotide sequence of the 2b gene. Below the arrow number indicate the position of the nucleotide sequence. Left side of the nucleotide sequence indicate the strains of the TSV used for comparison analysis.

Comparative analysis of the 2b gene at protein level showed less variation compare to the nucleotide level. The patch of seven amino acid i.e. GTSRVER (fig 4.18, box A) and twelve amino acid i.e. LETPNIPEDPET (fig 4.18, box B) were absent in the Indian strain and partially in USA strain of the TSV.

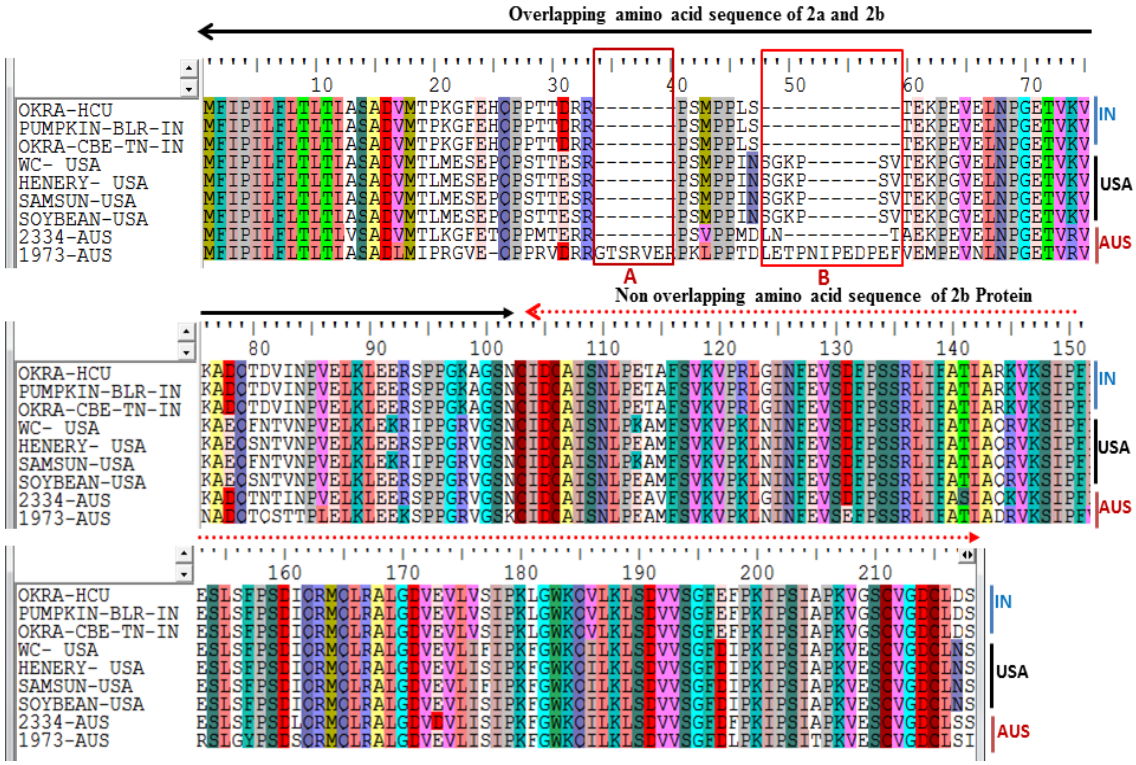

Fig 4.18: comparative analysis of 2b amino acid sequences of TSV okra strain with the reported strains of the TSV. Black color solid arrow indicates overlapping amino acids sequence of 2a and 2b gene. Discontinuous red color arrow indicates the non-overlapping amino acids sequence of the 2b gene. Below the arrow number indicate the position of the amino acid. Left side of the amino acid sequence indicate the strains of the TSV used for comparison analysis. Right side of the amino acid sequence: IN, USA and AUS indicate the India, United States of America and Australia respectively. Box A and B indicate extra amino acids introduced in 2b gene compare to the other amino acid.

4.3.2.3 Molecular diversity analysis of RNA3 and its encoded gene

For the construction of the phylogenetic tree of RNA3, we have selected coat protein gene sequence. In the NCBI data base more than 100 queries were found when we blasted our okra strain of TSV. Among them, 39 diverse strains were selected along with the 4 identified strain of TSV in the present study for the construction of the phylogenetic tree. The constructed phylogenetic tree showed three clusters. Twenty strains of TSV were present in cluster I, eight strains in cluster II and 15 in cluster III. Peanut–HCU, Sunflower–HCU and Tomato-HCU strain of the TSV clustered along the other reported strain of the TSV in cluster III. However, Okra-HCU strain of the TSV was clustered along with the reported strains of II cluster.

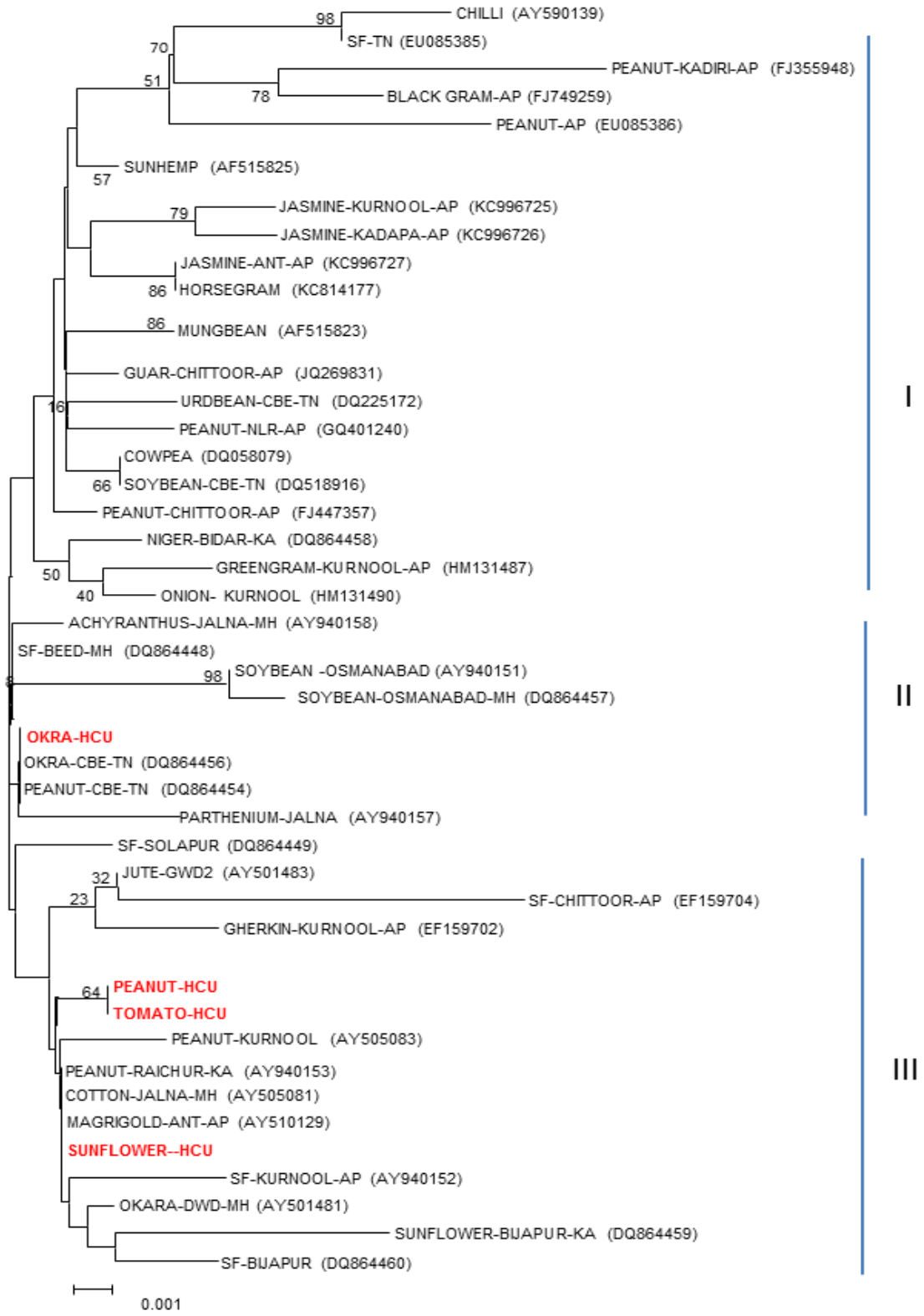

Fig 4.19: Construction of phylogenetic tree for CP gene using MEGA 6.

Phylogenetic tree analysis was constructed using the Neighbour-Joining method. Bootstrap values (%) are shown at nodes. Right side of the node indicate TSV strain, place of isolation or host and gene bank accession numbers used for the construction of the tree. Red coloured text indicate the present strains of TSV from HCU.

4.4 Discussion

Working with the RNA is very tedious and laborious job because of two reasons; its fragile nature and prone to RNase contamination. So, it is important to convert RNA molecule into DNA molecule to work easily. Due to lack of reverse transcriptase enzyme in early nineties of the 20th century, it was difficult to convert into cDNA. After the discovery and commercial availability of enzymes for reverse transcription was opened up gates in the field of basic and applied research of RNA viruses.

Reverse transcriptase was discovered by Howard Temin and David Baltimore in 1970 from two RNA tumour viruses: *Murine leukemia virus* and *Rous sarcoma virus* respectively. Subsequently, PCR was developed by Kary Mullis 1983. These two (reverse transcriptase enzyme and PCR) revolutionized the complete genome sequencing of several organisms including that of viruses.

One of the main features of the last decade has been the great explosion of sequence data on the plant virus genomes. The first viral genome was to be sequenced the DNA of *Cauliflower mosaic virus* (CaMV) (Franck *et al*., 1980) followed by the RNA of *Tobacco mosaic virus* (TMV) (Goelet *et al*., 1982). In the year 2000, the genome of about 250 species had been fully sequenced including representative of most plant virus genera. Complete nucleotide sequence of the three genomic RNAs has been determined for *Tobacco streak virus* (TSV), *Parietaria mottle virus* (PMoV), *Strawberry necrotic shock virus* (SNSV), *Blackberry chlorotic ringspot virus* (BCRV), *Spinach latent virus* (SpLV), *Prunus necrotic ringspot virus* (PNRSV), *Tulare apple mosaic virus* (TAMV), *Citrus leaf rugose virus* (CiLRV), *Humulus japonicus latent virus* (HJLV), *Prune dwarf virus* (PDV) and *American plum line pattern virus* (APLPV) and partial sequences are known for the other ilarviruses. The first complete sequence of *Tobacco streak virus* RNA3 was elucidated by Cornelissen *et al*., 1984. Later on different groups of scientists submitted complete genome sequence of TSV to NCBI database. In case of India, first complete sequence of TSV was deposited by Dr. Krishna Reddy's research group in December 2009 for okra strain, pumpkin and subsequently by Dr. Chandrasekhar,s research group from TNAU in December 2013.

RNA Viruses are able to establish huge molecular diversity. This diversity is mainly because of error-prone replication (Drake & Holland, 1999) and short generation times. A virus having higher mutation frequency is more likely to become adapted to a variety of plant hosts, upon insect transmission and could mean survival in a natural setting (Schneider *et al*., 2001; Roossinck, 2003). Recently, Ingwell *et al*., (2012) reported that plant viruses are able to change the behavioural pattern of the insect directly. For example, aphids that had already acquired *Barley yellow dwarf virus* were attracted to uninfected plants, whereas aphids that had not acquired the virus were attracted to infected plants. This is one of the salient behavioural modifications that can enhance the spread of the virus (Ingwell *et al*., 2012).

In the present study we have obtained the complete nucleotide sequence of RNA1, RNA2 and RNA3 by RT-PCR, cloning and sequencing of the recombinant clones. The 5' and 3' authentic ends of all viral RNAs were confirmed through 5'-RACE and 3'-RACE. The genome map of each RNA molecule was deduced by BioEdit software using different overlapping clone sequences.

The elucidated genome map for okra strain of the TSV RNA1 has a very short 5' UTR (37 nt), 3279 nt of 1a ORF and 207 nt of 3' UTR. The untranslated regions of viruses are very important for their fitness. It acts as *cis*-acting regulatory sequence and control synthesis of full-length positive (+) and negative (-) strand RNAs, translation of the viral protein, transcription of subgenomic RNA. Present strain showed the 5' UTR of the RNA1 was consistent with the strain reported from India by Dr. Krishna Reddy's group at IIHR. However, report from the Dr. Chandrasekhar's group showed inconsistency, indicating that sequence available in NCBI is incomplete at 5' end (Table 4.3). Henery strain of TSV from USA showed 38 nt of 5' UTR instead of the 37 nt.

The 3' UTR of the RNA1 showed 219 nt and that is highest among the reported strains of the TSV across the globe. The present strain showed result similar to the report from the Dr. Krishna Reddy group. However, lowest nucleotides (159 nt) reported from the 2234 strain of TSV from the Australia. These variations of the 3' UTR indicates extent of the selection pressure depends on the geographical region and crops from which it isolated.

The amino acid sequence of the 1a protein showed 1092 aa which is similar to the report from the Dr. Krishna Reddy's group from India. However we found one or two amino acid more in case USA strain of the TSV.

TSV 1a protein contains two conserved domain viz; V-methyltransferase and Helicase, whose domain ranges from 70 aa to 412 aa and 785 aa to 1060 aa respectively. The comparative analysis of the TSV 1a protein with *Alfalfa mosaic virus* (AMV) gave very similar types of four motifs in V-methyltransferase domain and six motifs in case of helicase domain, that are present in AMV.

According to Jhon F. Bol research group, motifs present in helicase domain of the AMV are responsible for the negative strand synthesis of RNA. Similarly, Corina Vlot *et al*., 2003 reported that motifs I, III, and VI of the AMV replicase protein disrupt the putative helicase activity of P1 and are involved in viral RNA replication. Similar type of motifs was also found in *Tobacco streak virus* with slight variation (fig 4.13). The motif I and VI were found conserved among the TSV strain and AMV; however, AMV is very distantly related to the TSV. But, In case of the motif II to V, we observed one or two amino acids change (table 4.4). Overall we have found that 1a gene is very less predisposed toward the evolution pressure even though, largest gene among five encoded gene by TSV.

RNA2 also has short 5' UTR (42 nt) and it is consistence in Indian, Australian and USA strain, except in 1973 strain of the Australia showed more variation. 2a protein was varied from 792 aa to 807 aa. The minimum length of the 2a protein was found in the Indian and USA strain of the TSV and highest number of aa was observed in Australian strain i.e.1973. This result indicates that the Indian strains are more evolved compare to the Australian strain. In a similar way 2b gene of TSV varies from 199 aa to 217 aa (table 4.2). The 2b gene present in all the member of genus cucumovirus and subgroup I and II member of the ilarvirus genus (Ding *et al*., 1995; Xin *et al*., 1998). The role of 2b protein in cucumovirus is well studied in interaction with host protein, long distance virus movement, silencing suppressor, symptom induction and as pathogenicity factor (Ding, *et al*., 1994; Brigneti *et al*., 1998; Diaz-Pendon, *et al*., 2007; Ding, *et al*., 1995 and Lewsey *et al*., 2009). Recently, Shimura *et al*., (2013) first time reported RNA silencing suppressor activity of ilarvirus 2b protein.

Due to multiple role in the pathogenic cycle and development of the symptom to the host; theoretically, 2b gene considered as more flexible to nucleotide and amino acid changes (Lin *et al*., 2004). In the present study we have observed that 2b gene seemed to be most flexible among the coding region of the TSV (fig 4.17 and 4.18). Moreover, a small region in the 2b gene starts from the nucleotide position 2164-2763 (in Indian strain), 2154-2805 (Australian strain) and 2155-2772 (USA strain) [table 4.2.] of RNA2 and seemed to more variable specially in the Australian strain compare to Indian and USA strain of the TSV. Overlapping nature of the 2b gene might be lead to high variability. Approximately, 43% (Indian and USA) to 44% (Australian strain) of the 2b gene sequence are embedded in 2a gene (fig 4.17 and 4.18). However, in case of CMV it was reported that 72% of 2b gene sequence was embedded in the 2a gene (Lin *et al*., 2004). Approximately, 54 nucleotides (fig 4.17, box I, to III) of the 2b gene were removed from the Indian strains or added into Australian strains course of the evolution but in case USA strains 36 nucleotides was removed or added in comparison to the Australian strains of the TSV (fig 4.17, box I and III). These variations were observed in overlapping region of the 2b gene. However, more mismatches were also observed in the non-overlapping region of the TSV. Considering above facts together, it is reasonable to postulate that positive selection might still be apparent in the 2b gene and that this gene is still evolving. Further analysis for positive selection in the 2b gene will require the use of more-sophisticated tools and additional data sets.

RNA3 had 211 nt of 5' UTR, 873 nt of MP ORF, 123 nt of inter cistronic region (ICR), 717 nt of coat protein ORF and 289 nt of 3' UTR respectively. RNA3 was found more conserved among the three RNAs.

Phylogenetic trees were constructed for nucleotide and amino acid sequence of genes using MEGA 6 software; showed two clusters; all Indian strains are clustering together and USA strains are forming another cluster, Australian strain 1973 showed maximum variation and separated as an out group member.

Extensive studies need to be performed in the future to unravel the role of TSV encoded proteins in the aetiology of disease expression in diverse crop plants.

Chapter-5

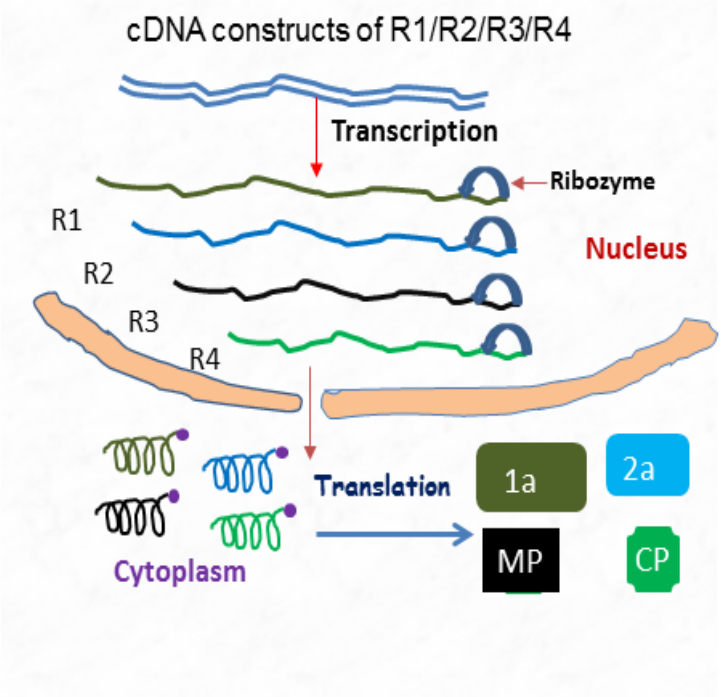

Construction and characterization of full-length infectious cDNA clones for *Tobacco streak virus*

Construction and characterization of full-length infectious cDNA clones for *Tobacco streak virus*

5.1 Introduction

Plants RNA viruses have severe impact on crop production and productivity. Therefore, it is necessary to study viral pathogenesis in depth to acquire knowledge into their role in disease development. The available approaches to control the viral disease are limited which includes cultural practice, by developing transgenic plants using genetic engineering and conventional breeding. Each approach has its own limitations. The mentioned approaches are not suitable for studying of the viral life cycle, identification of host factor and development of the viral vector. So, there is urgent need to develop an alternative method which can enable the study of the diverse viral process at single cell level and or whole plant level.

Infectious clones are very important molecular tools, which are used in several fields of RNA virus research. First, they are used in functional genomics; includes expression study of viral RNA encoded protein and replication, using *in vitro* mutagenesis (substitutions, deletions, insertions) and complementation. They may markedly contribute to the analysis of virus-host interactions (Deom, *et al*., 1987; Knorr, *et al*., 1988; Saito, *et al*., 1987). The infectious clones are also considered as the pools of viral genes for the development of antiviral strategies. Last, but not least, they are an essential source of a material for preparation of the new viral vectors (Boyer and Haenni, 1994).

The generation of infectious clones, *in vitro* or *in vivo*, is routinely the first step for reverse genetic studies of RNA virus. Several infectious clones to different RNA viruses (negative and positive-stranded) like bacteriophage (Qβ), polio, rabies, influenza-A and many plant viruses. The first infectious clone of RNA viruses was active as cDNA in Qβ (Taniguchi *et al.,* 1978). *Brome mosaic virus* was the first RNA plant virus for which full length infectious cDNA clones were produced (Ahlquist *et al*., 1984) and later on it expanded to several other plant viruses, *Tobacco mosaic virus* (Dawson *et al*., 1986 and Meshi *et al*., 1986) *Cucumber mosaic virus* (Hayes and Buck,1990), *Beet necrotic yellow vein virus* RNAs 3 and 4 (Commandeur *et al.*, 1991), *Tomato mosaic virus* (Weber *et al.,* 1992) and *Plum pox virus* (Maiss *et al.*, 1992), *Melon necrotic spot virus* (Diaz *et al*., 2003 and Genoves *et al*., 2006),

Saguaro cactus carmovirus (Weng and Xiong , 1997), *Hibiscus chlorotic ringspot virus* (Huang *et al*., 2000) *Pelargonium flower break virus* (Rico and Hernandez, 2009), *Olive mild mosaic virus* (Cardoso et al. 2012). The first biologically active infectious clones of *Tobacco streak virus* was reported in 2003 (Xin and Ding 2003). After this report, very few literatures are available on the infectious clone of the TSV. In Indian scenario, infectious clone of RNA viruses was reported on the *Sesbania mosaic virus* (Govind *et al*., 2012).

Development of infectious cDNA clones (icDNAs) includes different steps like virus purification; viral RNA extraction, reverse transcription, PCR amplification of genomic cDNA fragments and this full length cDNA clone have its own promoter in the form of CaMV 35S double promoter at 5′ and a ribozyme at the 3′ end for the efficient processing of the unit length molecule of infectious clones. Details about the infectious clone was discussed in chapter 2 section 2.3.

In the present study we report the construction of full-length infectious cDNA clone of *Tobacco streak virus*, from which infectious RNA can be transcribed *in vivo*. The biological activity / infectious nature of icDNA clone and development of the symptoms were analysed.

5.2 Materials and methods

5.2.1 Plant material

Vigna unguiculata and *Nicotiana benthamiana* plants were grown in heat sterilised soil and maintained at 27ºC temperature with 70% humidity and 16/8 hours of light and dark periods in the growth chamber.

5.2.2 Primers synthesis

Primers used in this study were synthesised by Integrated DNA technologies (IDT, Coralville, USA). Primers are listed in table 5.1 also refer to chapter 4, table 4.1 for primers described earlier.

Table 5.1: List of primers used for construction of full-length infectious cDNA clone

S.No.	Primer name	Oligonucleotide sequence (5′----------3′)	Purpose
1	*Bgl*II+	C**AGCGCT**TTACTGAGATCT CCTGTG	Primer 1 used to fuse the 35S promoter to the 5′end of RNA 1, 2, and 3 c DNA and introduced *Bgl*II site (in bold) at 5′ end of 35S promoter.
2	ER31-	CAAGTGGTATCTTAAGCTC GGAGAATACCCTCTCCAAA TGAAATGAACTTCCTTATA TAG	Primer 2, add 31 nt from RNA3 and primer 3, add 32 nt from RNA3 and *Eco*RI internal site at 3′ end. Primer 1, 2 and 3 used to get fragment I of RNA3
3	ER32-	GGAATTCAAAGTTGGAAATCG TCCGATTCGGAATCAAATTGC AAGTGGTATCTTAAGCTCGGA GAATAC	
4	R31166*Xba*I+	CGAGTATTAAGTTGATGAAT TCTAGAG	Primer 4 and 5 add 1166-2213 nt of TSV RNA3 with *Xba*I site at 5′ end ending with ribozyme partially. primer 4 and primer 6 which added 30 nts remaining sequence of Ribozyme (RZ) *Xma*I site (bold) downstream to ribozyme of RNA3. Primer 4, 5 and 6 used to get fragment IV of RNA3
5	R3RZ1-	TCATCAGAAGACATGTGAA TCATGTCTTGAGCATCTCC TATAAAGGAGGCATCAGTAG	
6	R3RZ2-	CGATC**CCCGGG**CCGTTTCG TCCTCACGGACTCATCAGA AGACATGTGAATCATGTCT TGA	
7	35STR2-	GGAGGTTCTGACCCAGATA TGTGTCAGTAATACACCTC TCCAAATGAAATGAACTTC CTTATATAG	Primer 1 and primer 7 used to get fragment IA of RNA2
8	TSVR2+	GTGTATTACTGACACATATCT G	Primer 8 and primer 9 used to get fragment IB of RNA2
9	R2ERV1255-	CCTCTCCAGATATCGGGTTCA G	
10	R21881+	CCTCACGGACTCATCAGAAGA	Primer 10 and 11 used to get fragment IIIA of RNA 2 and ending with ribozyme partially. primer 10 and primer 12 used to get fragment III B, which added 30 nts remaining sequence of Ribozyme (RZ) *Xma*I site (bold underlined) downstream to ribozyme of RNA2.
11	R2RZ1-	TCATCAGAAGACATGTGAATC ATGTCTTGAGCATCTCCATTT GGAGGCATCAGTTATATC	
12	R2RZ2-	CGATC**CCCGGG**CCGTTTCGTC CTCACGGACTCATCAGAAGAC ATGTGAATCATGTCTTGA	
12	R11+	GTATTACTGTTTTGTATCCG	Primer 12 and 13 used to get fragment IB of RNA1.
13	TR1BHI 709-	CATAAGCGGATCCATCATGAC A	
14	35S TR1-	CCATTTCTGGAGGTTCTGTTTC GGATACAAAACAGTAATACCT CTCCAAATGAAATGAACTTCC TTATATAG	Primer 1 and primer 14 used to get fragment IA of RNA1
15	R1 *Kpn*I+	GAAAATAAGTGGTACCCCTCT G	Primer 15 and 16 used to get fragment

16	R1RZ1-	CATCAGAAGACATGTGAATCATGTCTTG GCATCTCCTTTAAAGGAGGCATTGTTTATG	IIIA of RNA1 and ending with ribozyme partially. primer 15 and primer 17 used to get fragment III B, which added 30 nts remaining sequence of Ribozyme (RZ) *Xma*I site (bold underlined) downstream to ribozyme of RNA1.
17	R1RZ2-	CGATC**CCCGGG**CCGTTTCGTCCTCACGGACTCATCAGAAGACATGTGAATCATGTCTTGA	

5.2.3 Virus purification, RNA extraction, cDNA synthesis, PCR, cloning sequencing and sequence analysis

These procedures were performed as described in chapter 3 section 3.2.

5.2.4 Binary vector

5.2.4.1 pCB301 binary vector

In the present study we have used pCB301 binary vector [(Gene Bank accession number AF139061) (Gopinath *et al*., 2005)] for cloning of full-length infectious cDNA (ic-DNA) molecule of TSV RNAs. It is a very low copy number binary plasmid; contain kanamycine as selectable marker and its size is around 3.5 kb.

5.2.4.2 pCB302 binary vector

For cloning of full length genes (1a, 2a, MP and CP), we have used pCB302 binary vector (Gopinath *et al*., 2005), which contains a CaMV 35S double promoter and a 5′ nontranslated leader sequence from *Tobacco etch virus* and a 3′ 35S terminator. This vector has kanamycine as selectable marker and its size is 7.0 kb.

5.2.5 Fusion of overlapping PCR fragments

Overlapping fragments were assembled into single fragment either using restriction digestion or overlap extension PCR (OE-PCR, Higuchi *et al*., 1988).

5.2.5.1. Restriction digestion using unique restriction site

A unique restriction site was identified within the overlap fragment that doesn't cut elsewhere within the two fragments to be fused.

5.2.5.2 Overlap extension-PCR (OE-PCR)

Two cloned overlapping fragments were re-amplified from the existing clone using respective primers. The amplified products were purified and diluted up to 10 ng

/µl. Both the fragments were mixed in equal amount and used as template for the fusion PCR (fig 5.3 panel A, fig 5.4 panel A).

5.2.6 Site directed mutagenesis (SDM)

The mutagenesis was carried out using Phusion®HF DNA polymerase and *Dpn*I restriction enzyme from NEB (England). Supercoiled plasmid was isolated using Qiagen plasmid isolation kit and used for SDM. The mutagenesis reaction mixture contains; 1 µl forward primer (10 ng/µl), 1 µl reverse primer (10 ng/µl), 2.0 µl (5 mM dNTP mix), 4.0 µl 5x Phusion buffer®HF buffer, 1 µl supercoiled plasmid DNA (200 ng / µl), 1 µl Phusion®HF DNA polymerase (5 unit/µl),10 µl sterile H_2O. Initial denaturation step was carried out at 95ºC for 4 min, then 18 cycles of denaturation at 95ºC for 50 sec, different annealing temp (depending on GC % of mutagenic primer) and extension time (depending on the amplicon size) generally 1 min+1 min/ 3 kb of template @ 72ºC followed by final extension at 72ºC for 5 min. The PCR product was visualized on a 1% agarose gel. The amplified products were treated with *Dpn*I enzyme. 5 µl of *Dpn*I treated product was transformed into DH5α cells, positive clones were screened through both end sequencing.

5.2.7 Assembly strategies of RNA3 into pCB301 binary vector

To bring full length cDNA molecule of RNA3 under control of 35S double promoter at 5' and ribozyme at 3' end assemble into pCB301 binary vector between left and right borders, we used overlap extension PCR and restriction digestion approach. Based on the above strategy full-length cDNA molecule of RNA3 along with 35S promoter and ribozyme was divided into four fragments as mentioned in fig 5.1. Fragment I (621 bp) was fused with 35S promoter, and flanked with *Bgl*II and *Eco*RI restriction site, fragment II (649 bp) flanked with *Eco*RI and *Kpn*I, fragment III (454 bp) flanked with *Kpn*I and *Xba*I. Fragment IV (1100 bp) has 3' proximal end of RNA3 fused with Ribozyme, flanked with *Xba*I and *Xma*I. After getting all four fragments, were ligated into pCB301 binary vector (Gopinath *et al*., 2005) into left border and right borders by replacing BMV RNA3 nucleotide sequences.

pGEMT-Easy recombinant clone containing full-length cDNA molecule of RNA3 (pGEMRNA3) discussed in chapter 4, was used as template for getting different fragments.

5.2.7.1 Cloning strategy for fragment I

In order to get fragment I; it was divided into two sub fragments as fragment IA and IB as mentioned in fig 5.1, panel A. Fragment IA was amplified with forward primer (BglII+) and reverse primer (ER31-) (mentioned in table 5.1) and pBR3 plasmid (Gopinath *et al*., 2005) as a template. Taking IA as a template, IB was amplified with BglII+ forward and ER32- reverse primer; cloned into pTZ57R/T cloning vector. Fragment I has been obtained after restriction digestion of the pTZ57R/T recombinant plasmid contains fragment IB with *Bgl*II and *Eco*RI restriction enzyme.

5.2.7.2 Cloning strategy for fragment IV

Fragment IV was obtained in three steps: First; PCR was performed with the R31166XbaI+ forward and R3Rz1- reverse primer and pGEMRNA3 as the template. Secondly, First PCR amplified product was used as template for amplification of fragment IVB with R31166XbaI+ and R3Rz2- primers; cloned into T/A cloning vector. The recombinant T/A vector harboring fragment IVB was used for generation of fragment IV after restriction digestion with appropriate enzyme. All obtained fragments were assembled into pCB301 binary vector (Gopinath *et al*., 2005).

5.2.7.3 Cloning strategy for fragment II and III

Restriction digestion strategy was used to get fragments II and III. The clone was digested with the respective restriction enzyme to get desired fragment as mentioned in fig 5.2. Fragments II and III were released after restriction digestion of pGEMRNA3 clone. RNA3 has two restriction sites of *Eco*RI, one at 63 nt and another 1162 nt from 5' end of RNA3. Apart from this, pGEMT-Easy vector have two *Eco*RI restriction sites in multiple cloning sites. So, total four *Eco*RI restriction (fig 5.2) sites were present in pGEMRNA3 clone. In order to get fragment II, pGEMRNA3 plasmid was digested with *Eco*RI and *Kpn*I restriction enzyme. For fragment III, it was digested with the *Kpn*I and XbaI restriction enzyme.

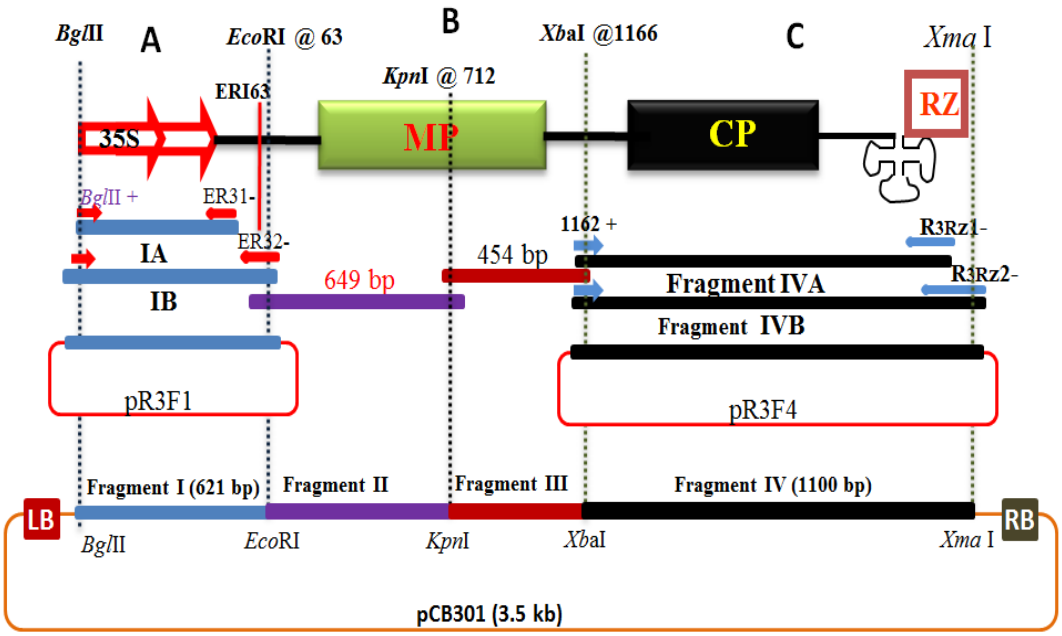

Fig 5.1: Overview for construction of full length infectious clone for RNA3 in pCB301 binary vector. In panel A: Fusions of 35S double promoter at 5' end of RNA3. Small and big blue color rectangular box represent the PCR amplified product of 35S double promoter along with 31 nt (IA) and 70 nt (IB) from 5' UTR of RNA3 respectively. Red color arrows above the box indicate the primer *Bgl*II+, ER31- and ER32-. pR3F1 indicate the pTZ57R/T recombinant plasmid harboring IB. Fragment I (621 bp) released after restriction digestion of plasmids pR3F1 plasmid with *Bgl*II and *Eco*RI. In panel B: Fragment II and III, detail strategy showed fig 5.2. In panel C: Fusion of Ribozyme at 3' ends of RNA3. Upper and middle black color rectangular box indicate fragment IVA and IVB. Blue color arrow above the box indicate the forward (R31166XbaI+) and reverse (R3RZ1-, R3RZ2-) primer. pR3F4 indicates pTZ57R/T vector harboring fragment IVB. Fragment IV (1100 bp) represent the released insert after restriction digestion of plasmid pR3F4 with *Xba*I and *Xma*I restriction enzyme. The vertical discontinuous lines indicate the restriction site (B*gl*II, *Eco*RI, *Xba*I and *Xma*I from left to right) used for assembly of fragment I to III into pCB301 binary vector. Orange color rectangular free box indicate, pCB301 binary vector backbone (3.5 kb) and all three fragments were assemble between left and right boarder.

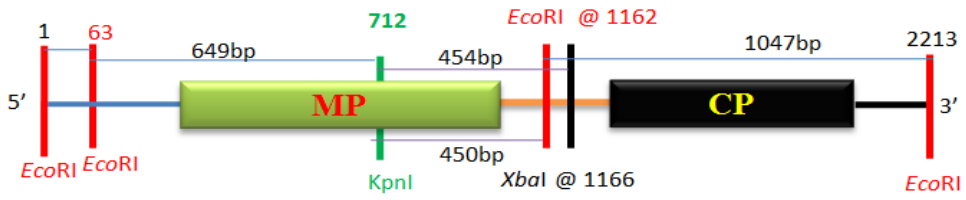

Fig 5.2: Overview for fragment II and III of RNA3.
Fragment II and III of RNA3 was obtained from pGEMRNA3 plasmid. pGEMRNA3 contains four *Eco*R1 (two from vector and two from RNA3 internal sequence) at @ 1, 63, 1162 and 2213 nt. Fragment II was produced with restriction digestion of pGEMRNA3 plasmid with *EcoR*I and *Kpn*I, produced 63 bp, 649 bp, 450 bp and 1047 bp. Out of these insert 649 bp act as fragment II. Fragment III was produced after digestion of pGEMRNA3 with *Kpn*I and *Xba*I restriction enzyme and released into 454 bp.

5.2.8 Cloning strategies of RNA2 into pCB301 binary vector

In order to get full length clone in pCB301 binary vector, we divided complete cDNA of RNA2 molecule along with 35S double promoter at 5' end and ribozyme at 3' end into three fragments (fig 5.3); Fragment I (1414 bp) has fused 35S promoter, and flanked with *Bgl*II and *Sal*I restriction site, fragment II (1,096 bp) flanked with *Sal*I and *Hin*dIII and fragment III (1.0 kb) has 3′ proximal end of RNA2 fused with ribozyme, flanked with *Hin*dIII and *Xma*I.

5.2.8.1 Strategy for fragment I

To get fragment I; it was amplified into two sub fragments, fragment IA and IB then fused to a single fragment using overlap extension PCR as mentioned in fig 5.3, panel A. Fragment IA was amplified with forward primer (BglII+) and reverse primer (2a1255-) (chapter 4 in table 4.1) and pBR3 as a template. Fragment IB was amplified using forward primer ($R_2$1+) and reverse primer ($R_2$1255-) taking pR_2A12 plasmid as a template (mentioned in chapter 4, section 4.3.1.2.2). The PCR amplified product of fragment IA and IB was diluted to 100 ng and used as a template to amplify the fragment IC by the overlap extension PCR. Amplified PCR product of the fragment IC was cloned into the pGEMT-Esay cloning vector and fragment I was excised from the recombinant pGEMT-Esay vector using *Bgl*II and *Sal*I restriction enzyme.

5.2.8.2 Cloning strategy for fragment II

To get fragment II, first PCR was performed with $R_2$600+ forward and $R_2$1960- reverse primers, using cDNA as a template. The PCR amplified product was cloned into pTZ57R/T cloning vector and confirmed through the restriction digestion as well as both end sequencing. Positive plasmids were selected for getting the fragment II after restriction digestion with *Sal*I and *Hin*dIII restriction enzyme (mentioned in fig 5.3, panel B). The eluted product of released insert has been taken for fusion of fragment I and II into pET28a vector.

5.2.8.3 Fusion of fragment I and II into larger fragment (~2.5 kb)

Fragments I and II were fused into single fragment (~2.5 kb) using restriction digestion and cloning approaches. First, pET28a back bone was prepared after

digesting with *Bgl*II and *Hin*dIII restriction enzymes taking wild type pET28a plasmid as a template. Second, fragments I and II were cloned into eluted backbone at same restriction site. Positive clone was confirmed through restriction digestion. This larger fragment was excised from positive clone and used for assembly into pCB301 binary vector.

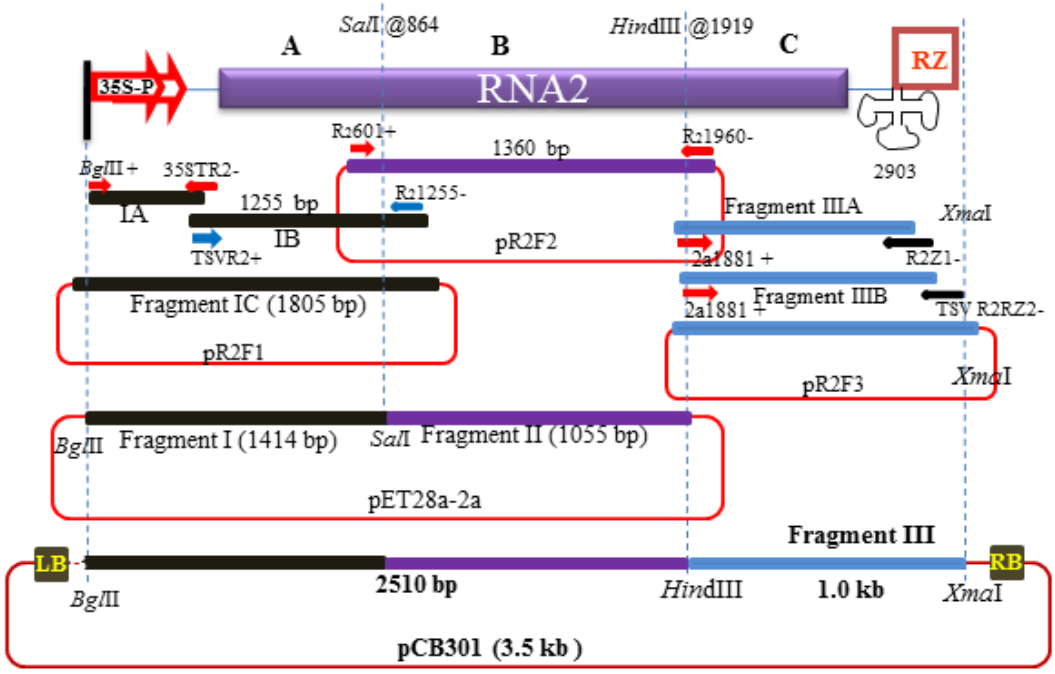

Fig 5.3: Overview for construction of full length clone for RNA2 in pCB301 binary vector. In panel A, fusion of 35S double promoter at 5' end of RNA2. Left side small black color rectangular box (IA) represent the PCR amplified product of 35 S double promoter along with 60 nt from 5' UTR of RNA2 and red color arrow above the box indicate the primer *Bgl*II+ and 35STR2-. Right side black rectangular box (IB) represent the 1009 bp PCR amplified product start with 1st nucleotide and end with 1009 nt of RNA2, contains *Sal*I restriction site at 864 position. Big black color rectangular box (fragment IC) indicate fusion product of IA and IB. pR2F1 indicate pTZ57R/T plasmid contains fragment IC. In panel B, Violet color rectangular box represented by fragment II with *Sal*I restriction site at 5' and *Hin*dIII at 3' end of Fragment II and its size indicate 1360 bp. pR2F2 indicate the pTZ57R/T plasmid contain fragment II. pET28a-2a represent recombinant pET28 plasmid contains fragment I and II at *Bgl*II and *Hin*dIII restriction site. The larger fragment 2469 bp indicate fusion product of fragment I and II in pET 28a vector and it used for assembly into pCB301 binary vector. In panel C, Fusion of ribozyme at 3' end of RNA2. Upper and middle blue color rectangular box indicate fragment III A and IIIB. Lower of the blue color rectangular box red and black color arrow indicate the forward (2a1881+) and reverse primer (R2RZ1-, R2RZ2-). pR2F3 indicate pTZ57R/T vector contain fragment IIB. 1.0 kb size of blue color rectangular box indicate fragment III. The vertical discontinuous lines indicate the restriction site (B*gl*II, *Sal*I, *Hin*dIII and *Xma*I from left to right) used for assembly of fragment I to III into pCB301 binary vector.

5.2.8.4 Strategy for fragment III

Fragment III was obtained in three steps: First; PCR was performed with the forward (2a1881+) and reverse (R_2RZ1-) primers and pR_2E_2 plasmid (described in chapter 4) as the template. Secondly, First PCR amplified product was used as template for amplification of fragment IIIB with 2a1881+ and R_3Rz2- primers (Fig 5.3, panel C); cloned into pTZ57R/T cloning vector. The recombinant pTZ57R/T vector harboring fragment IIIB was used for generation of fragment III after restriction digestion with appropriate enzyme. All the obtained fragments were assembled into pCB301 binary vector by three point ligation at *Bgl*II and *Xma*I restriction sites.

5.2.9 Assembly strategies of RNA1 into pCB301 binary vector

For cloning into binary vector we divided whole RNA into three fragments (fig 5.4) fragment I (1260 bp) has fused 35S promoter, and flanked with *Bgl*II and *Bam*HI site, fragment II (1515 bp) with *Bam*HI and *Kpn*I and fragment III (1376 bp) has 3′ proximal end of RNA1 fused with Ribozyme, flanked with *Kpn*I and *Xma*I. All the three fragments were cloned into pCB301 vector containing TSV RNA3 by replacing it through sequential cloning. Detail strategy for each fragment is described below.

5.2.9.1 Cloning strategy for Fragment I

Fragment I was obtained in three steps of PCR and overlap extension PCR (OE-PCR). First, PCR was performed to obtain 35S double promoter along with 30 nts of 5' UTR of RNA1 using forward (*Bgl*II+) and reverse (35STR1-) primers and pBR3 plasmid as a template. Secondly, fragment IB was amplified with the $R_1$1+ and TR_1BH709- using pR1aA2 plasmid (mentioned in chapter 4, section 4.3.1.3.3) as a template. Fragment IB starts with 1st nucleotide and end with 720 nts of RNA1, containing *Bam*HI restriction site at 709 positions. Finally , both fragments IA and IB were fused by overlap extension PCR; using *Bgl*II+ and TR_1BH709- forward and reverse primer and 100 ng diluted quantity of fragment IA and fragment IB used as a template. Obtained PCR product after OE-PCR, was cloned into the pTZ57R/T cloning vector and fragment I was excised from the recombinant pTZ57R/T vector using *Bgl*II and *Bam*HI restriction enzyme.

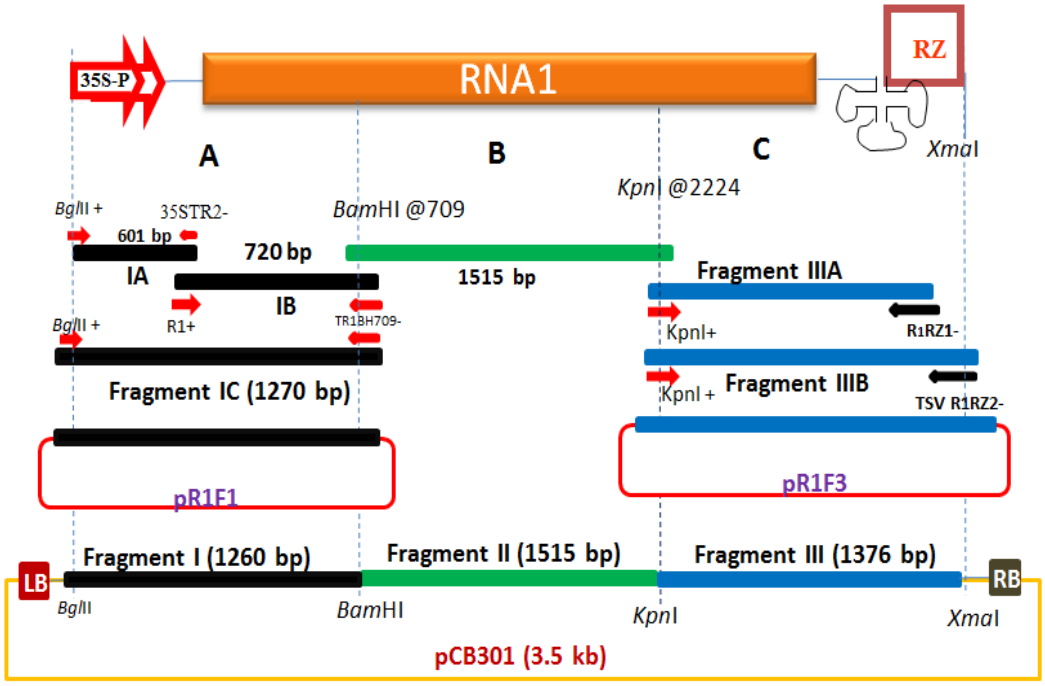

Fig 5.4: Overview for construction of full length clone for RNA1 in pCB 301 binary vector. In panel A: Fusions of 35S double promoter at 5' end of RNA1. Left side small black color rectangular box (IA) represent the PCR amplified product of 35 S double promoter along with 51 nt from 5' UTR of RNA1 and red color arrow above the box indicate the primer *Bgl*II+ and 35STR2-. Above the box 601 bp [(550 bp from 35S promoter) + 51 bp (5' nt of RNA1). Right side black rectangular box (IB) represent the 720 bp PCR amplified product start with 1st nucleotide and end with 720 nt of RNA1,conating *Bam*HI restriction site at 709 position. Big black color rectangular box indicate fusion product of IA and IB; represented by fragment IC and its amplified size 1270 bp. pRIFI represent the recombinant pTZ57R/T plasmid contains fragment IC. Rectangular black color box indicates fragment I (1260 bp); released after restriction digestion of pRIFI plasmid with *Bgl*II and *Bam*HI. Panel B: Green color rectangular box represented by fragment II with *Bam*HI restriction site at 5' and *Kpn*I at 3' end of fragment II and its size indicate 1515 bp. In panel C: Fusion of Ribozyme at 3' ends of RNA1. Upper and middle blue color rectangular box indicate fragment III A and IIIB. Lower of the blue color rectangular box red and black color arrow indicate the forward (KpnI+) and reverse primer (R1RZ1-, R1RZ2-). pR1F3 represent the recombinant pTZ57R/T plasmid contains fragment IIIB. Rectangular blue color box indicates fragment III (1376 bp); released after restriction digestion of pRIF3 plasmid with *Kpn*I and *Xam*I. Fragment III represented by the Lower blue color rectangular box. The vertical discontinuous lines indicate the restriction site (B*gl*II, *Bam*HI, *Kpn*I and *Xma*I from left to right) used for assembly of fragment I to III into pCB301 binary vector. Orange color rectangular free box indicate, pCB301 binary vector backbone (3.5 kb) and all three fragments were assemble between left and right boarder.

5.2.9.2 Strategy for fragment II

In order to get fragment II, we have selected pET clone harboring 1a gene and restriction digestion approach. 1a gene contains two *Bam*HI restriction sites one at 709 nt and another at 3149 nt position and one *Kpn*I restriction sites at 2224 nt position

(fig 5.4, panel B). The pET1a plasmid was digested with the *Bam*HI and *Kpn*I restriction enzyme and desired released insert was used as fragment II.

5.2.9.3 Strategy for fragment III

Fragment III was obtained in three steps: first; PCR was performed with the forward (KpnI+) and reverse (R1RZ1-) primer and p1aD2 plasmid (mentioned in chapter 4, section 4.3) as the template. Secondly, First PCR amplified product was used as template for amplification of fragment IIIB with KpnI+ and R3Rz2- primers (Fig 5.4, panel C); cloned into pTZ57R/T cloning vector. The recombinant pTZ57R/T vector harboring fragment IIIB was used for generation of fragment III after restriction digestion with appropriate enzyme.

All the obtained fragments were assembled into pCB301 binary vector by replacing TSV RNA3 nucleotide sequence present in pCB301 binary vector (strategies explained in fig 5.5).

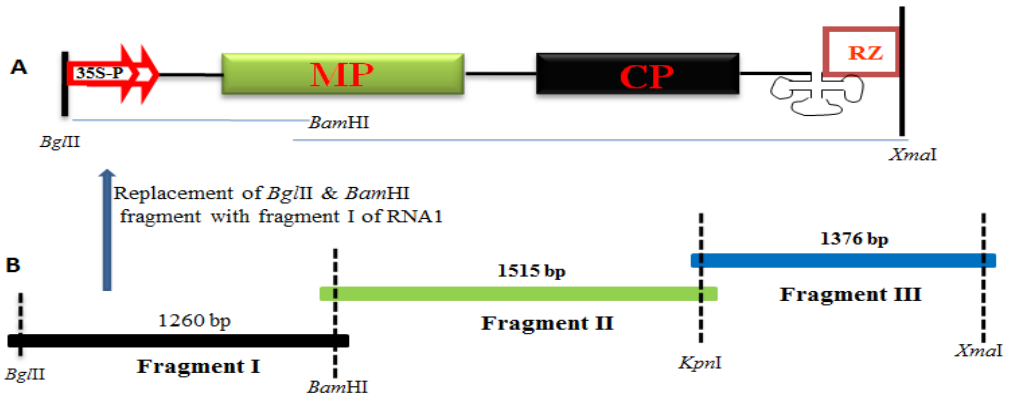

Fig 5.5: Assembly of fragment I, II and III into pCB301 binary vector.
In panel A, Full length clone of TSV RNA3 in pCB301 binary vector. Below the RNA3 restriction sites *Bgl*II, *Bam*HI and *Xma*I. In panel B, black, green and blue color rectangular box represent fragment I, II and III. 1260 bp, 1515 bp and 1376 bp represent the size of the fragment I, II and III respectively. Vertical discontinuous line represent restriction site as *Bgl*II, *Bam*HI, *Kpn*I and *Xma*I from left to right. Vertical arrows represent the replacement of *Bgl*II & *Bam*HI fragment of RNA3 present in pCB301 binary vector with the fragment I of RNA1.

5.2.10 Cloning of full length RNAs encoded genes of TSV into pCB302 binary vector

To express the TSV encoded genes in replication incompetent RNAs, the cDNAs encoding the 1a, 2a, 2b, MP, and CP genes were cloned into the *Nco*I and *Xba*I restriction sites in pCB302 which contained a CaMV 35S double promoter and a

5′nontranslated leader sequence from *Tobacco etch virus* and a 3′ end 35S terminator (fig 5.6). To clone full-length gene of 1a and 2a genes in to pCB 302 binary vector; we performed silent mutation to knock out of restriction site using site directed mutagenesis.

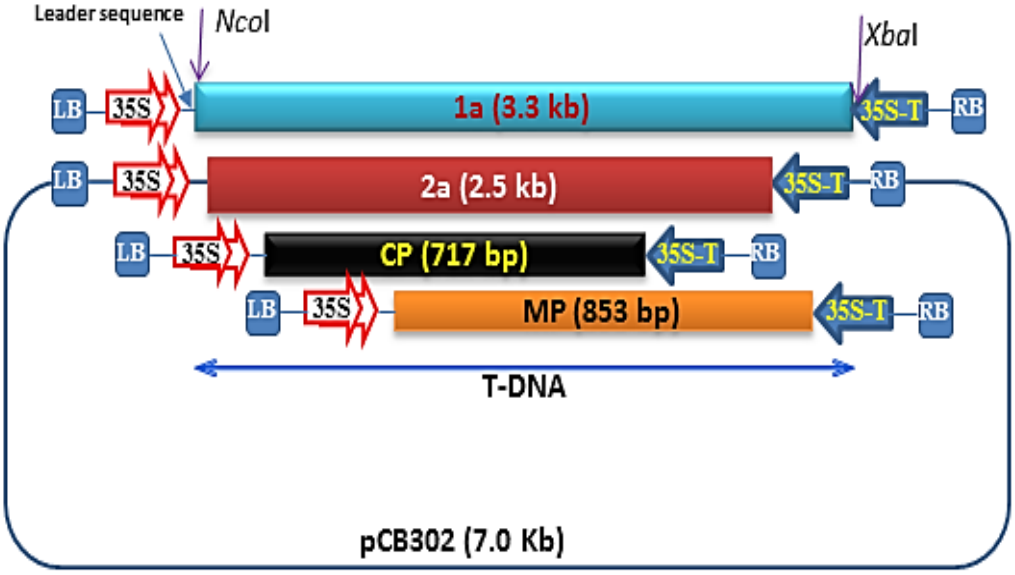

Fig 5.6: Overview for cloning of TSV encoded protein in pCB302 binary vector.
TSV encoded genes 1a, 2a, MP and CP was cloned at *Nco*I and *Xba*I restriction site. Light Blue, crimson red, black and orange solid colored rectangular boxes indicate 1a, 2a, CP and MP with sizes 3.3 kb, 2.5 kb, 717 bp and 853 bp respectively. Left side of the gene indicate untranslated leader sequence from *Tobacco etch virus*. Arrow at left side and right side of the gene represent the 35S double promoter and 35S terminator. LB and RB indicate the border and right border.

5.2.11 Agrobacterium competent cell preparation

A single isolated colony of agrobacterium from freshly streaked plate was taken for overnight culture in LB medium containing rifampicin (20 µg/ml) of pH 7.0. From the overnight culture 1% inoculum was added to 200 ml of LB broth and was kept in shaker at 28ºC until it reached 0.5-0.6 OD. The culture was harvested and kept in ice for 30 min and pelleted at 4,000 rpm for 15 min at 4ºC. The pellet was dissolved in 200 ml of milliQ and was centrifuged at 3,700 rpm for 30 min. This step was carried out once again and the resulting pellet was dissolved in milliQ containing 15% glycerol in appropriate quantity (3-5 ml) and 100 µl was aliquoted in each eppendorf. The eppendorf's were freezed in liquid nitrogen and stored in -80ºC for future use.

5.2.12 Mobilization of binary plasmid by freeze thaw method

Glycerol stocks of competent cells (100 µl) were thawed on ice for 5 min and 1.5 µl of binary construct (1 µg/µl) was added to it, mixed by gently tapping and frozen in liquid Nitrogen for 1 min and then thawed at room temp for 5 min. This procedure was repeated two times. Then 1 ml LB broth was added without antibiotics and incubated for 2 h at 28°C in a rotary shaker at 160 rpm. After incubation, culture was spun down at 6,000 rpm for 2 min, supernatant was discarded and pellet was resuspended in 200 µl of LB broth, plated on LB agar kanamycin plate and incubated at 28°C for 48 h.

5.2.13 Agroinfiltration

Agroinfiltration was followed with modification to the method described in Gopinath *et al*., (2005). Where in the LB medium containing Kanamycin (50 µg/mL) and Rifampicin (20 µg/ml) was used throughout the procedure. The positive agrobacterial clones were grown individually from single colonies. 0.5 ml of overnight grown culture was transferred to 50 ml of medium supplemented freshly with 1 ml of 500 mM filter sterile MES Buffer pH 5.85 and 6.5 µl acetosyrinzone (3,5' Dimethoxy-4'-hydroxyacetophenone, (MW 196.20) dissolved in DMSO and stored in -20ºC) and culture was grown for the period of 36 h. The culture was spun down at 6,000 rpm for 10 min and the supernatant was discarded. The pellet was resuspended in 5 ml of 10 mM $MgCl_2$ and 75 µl of 150 mM acetosyrinzone was added. The suspension was kept on the bench top for overnight. The cultures were diluted with 10 mM $MgCl_2$ up to 0.2, 0.3, 0.4, 0.6, 0.8 OD (OD at 600 nm). With the help of 1 ml blunt syringe by exerting slight pressure, the culture was infiltrated to *Nicotiana benthamiana* leaves.

5.2.14 Symptom development

The development of the symptom was monitored at daily intervals.

5.2.15 RNA isolation from agroinfiltrated leaves

Total RNA extraction was performed according to the method described in chapter 3; section 3.2.11. 200 mg of agroinfiltrated leaf tissue was used as starting material. Total RNA was treated with the 10 units of DNase I for 30 min at 37ºC in 1X DNase buffer. This reaction mixture was precipitated with isopropanol and washed

with the 80% ethanol. Integrity of RNA was checked on 1% (w/v) agarose gel. RNA samples were quantified with the NanoDrop®ND-1000 spectrophotometer (NanoDrop Technologies, Inqaba Biotechnical Industries (Pty) Ltd, SA) according to manufacturer's instruction.

5.2.16 RT-PCR to detect TSV infiltrated plants

First strand cDNA synthesis was performed according to the method described in chapter 3, section 3. 2.15. Two microliter (100 ng) of DNaseI treated total RNA and reverse primer were used for first strand cDNA synthesis. PCR was performed using first strand cDNA as template as described in chapter 3, section 3.2.16.

5.2.17 Isolation of cellular fraction

Cell wall (CW) fractions were obtained by the method of Epel *et al*., (1995) with some modifications. One gram of agroinfiltrated *N. benthamiana* leaf tissue was ground in 4 ml of ice-cold homogenization buffer (20 mM Tris-HCl [pH 8.5], 0.25 M sucrose, 10 mM EDTA, and 10 mM phenylmethylsulfonyl fluoride). The homogenates were then centrifuged at 1,000 g for 10 min at 4°C. The pellets were suspended in 4 ml of ice cold homogenization buffer containing 1% Triton X-100 and pH 7.5. Samples were then centrifuged at 1,000 g for 10 min at 4°C. This washing process was repeated until the supernatants became clear to obtain cell wall fractions. Finally, cell wall fraction was suspended in homogenization buffer pH 8.5. For SDS-PAGE analysis, the CW fractions were suspended in equal volumes of Laemmli sample buffer (Laemmli, 1970), incubated for 5 min at 60°C and centrifuged at 15,000 g for 5 min. Supernatant samples were then stored at -20°C.

5.2.18 Western blot

Western blot was performed using total soluble protein and cell wall fraction as described in chapter 3, section 3.2.10.

5.3 Results

5.3.1 Construction of Full-length infectious clone for RNA3

5.3.1.1 Fusion of 35S promoter upstream to 5' UTR of RNA3 (fragment I)

Fusion of 35S promoter was performed according to the method described in section 5.2.7. The PCR amplified product of fragment IA showed 585 bp (fig 5.7, lane 1). This fragment contains *Bgl*II restriction site at 5' end, 35S double promoter (554 bp) in middle and ending with 31 nt from 5' end of RNA3. The PCR amplified product of Fragment IB showed desired band near 621 bp (fig 5.7, line 2). Fragment IB contains 35S double promoter (554 bp) along with 67 nt from 5' end of RNA3.

5.3.1.2 Fusion of Ribozyme downstream to 3'UTR of RNA3 (fragment IV)

Fusion of the ribozyme to 3' end of RNA 3 was carried according to the method described in section 5.2.8 and fig 5.1, panel C. PCR amplified product of fragment IVA showed desired intense band at 1070 bp (fig 5.7, lane 4). Desired PCR amplified product contains nucleotide from 1166 to 2213 nt of TSV RNA3 with *Xba*I site at 5' end and ended with partial ribozyme sequence. Fragment IVB amplified PCR product showed approximately 1100 bp (fig 5.7, lane 4). This PCR product (fragment IVB) contains nucleotides from 1166 to 2213 nt of TSV RNA3 with *Xba*I site at 5' complete sequence of Ribozyme and *Xma*I site downstream to it.

5.3.1.3 Cloning of PCR product of fragment IB and Fragment IVB

Fusion PCR product was eluted, adenylated and cloned in pTZ57R/T cloning vector. After the restriction digestion of recombinant pTZ57R/T plasmid harboring fragment IB and IV B with *Bgl*II & *Eco*RI and *Xba*I & *Xma*I; it released 617 bp of fragment I (fig 5.8, lane 2) and 1100 bp of fragment IV (fig 5.8, lane 4 & 5) respectively.

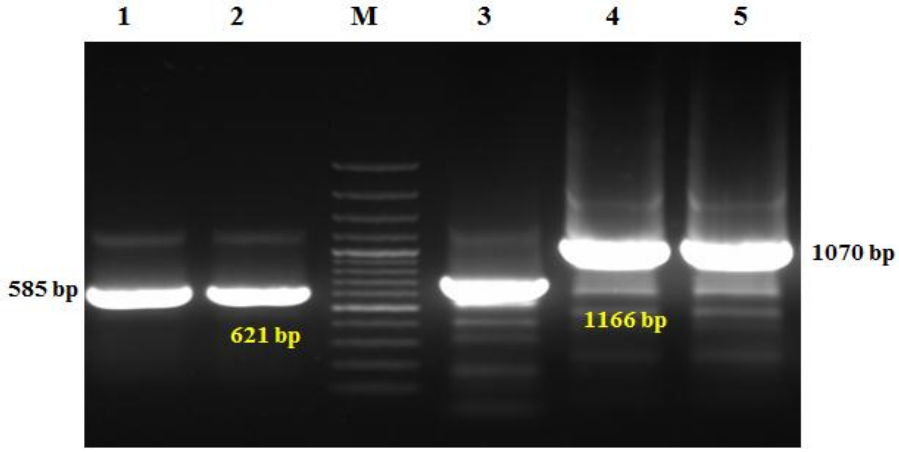

Fig 5.7: Fusion PCR of fragment I and fragment IV of RNA3.
Fragment I and fragment IV was obtained through fusion PCR. Lane1: PCR amplified product of IA, lane 2: PCR amplified product of IB. Lane 3: PCR amplified product for coat protein of TSV as positive control, Lane 4: PCR amplified product of fragment IVB, Lane 5: PCR amplified product of IVA. 585 bp, 1070 bp and 621 bp & 1166 bp indicate desired amplified PCR product present left and right side of the gel and below the PCR band respectively. M: 1 kb ladder

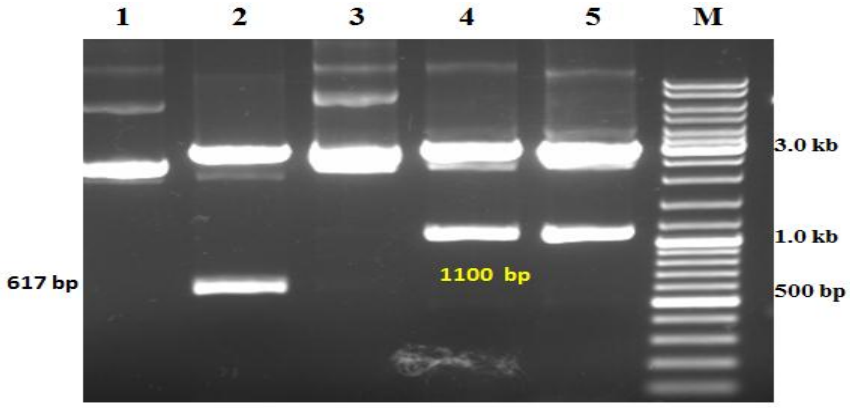

Fig 5.8: Cloning and confirmation of fragment I and Fragment IV of RNA3.
Restriction digestion pattern of the plasmid pR3F1 and pR3F4 in 1% agarose gel. Lane 1: pR3F1uncut plasmid; lane 2: pR3F1 plasmid cut with *Bgl*II and *Eco*R1; lane 3: pR3F4 uncut plasmid; lane 4 and 5: pR3F4 plasmid cut with *Xba*I and *Xma*I. Insert released 617 bp [(554 bp from 35S promoter + 63 bp from 5' end of RNA3) and 1100 bp after digestion indicated by arrow. Left side of the gel indicates molecular weight of 1.0 kb ladder.

5.3.1.4 Strategy for fragment II and III

pGEMRNA3 plasmid released four fragment after restriction digestion with *Eco*RI and *Kpn*I restriction enzyme. Larger fragment and smaller fragment have their molecular weights as 1047 bp and 63 bp (fig 5.9 lane 4 and 5) respectively. Smaller fragment appeared as very faint band as its molecular weight is only 63 bp. Remaining two fragments showed 649 bp and 450 bp. Fragment of 649 bp contains *Eco*RI at 5'

end and *Kpn*I at 3' end but 450 bp fragments contain restriction enzyme reverse of fragment 649 bp, i.e. *Kpn*I at 5' end and *Eco*RI at 3'. Here, fragment 649 bp flanked with *Eco*RI at 5' end and *Kpn*I at 3' act as fragment II. Fragment III was obtained after restriction digestion of pGEMRNA3 plasmid with the *Kpn*I and *Xba*I restriction enzyme. The released fragment showed desired 454 bp of fragment near 500 bp of DNA ladder. These two fragments were eluted from gel and used as inserts for assembly of fragment into pCB301 binary vector.

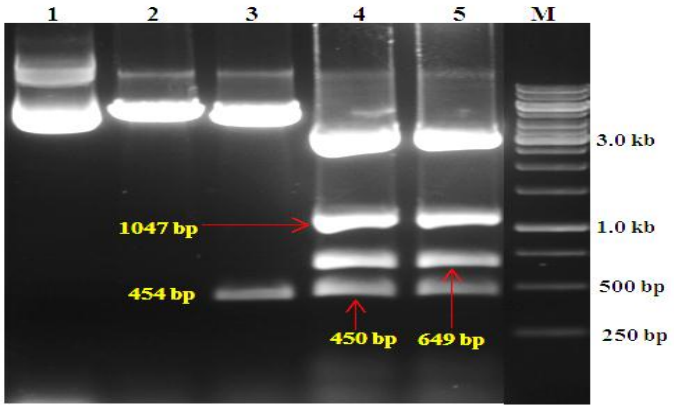

Fig 5.9: Restriction digestion of pGEMRNA3 plasmid to get fragment II and III. Fragment II and III was obtained after restriction digestion of pGEMRNA3 plasmid with respective enzyme. Lane 1: pGEMRNA3 uncut plasmid; lane 2: pGEMRNA3 plasmid cut with *Bgl*II; lane 3: pGEMRNA3 plasmid cut with *Kpn*I & *Xba*I; lane 4 and 5: pGEMRNA3 plasmid cut with *Kpn*I & *Eco*RI. 454 bp and 649 bp of released insert indicate fragment III and fragment II. Arrow head indicate the released insert and below the tail of the arrow indicate size of the insert. M: 1.0 kb DNA ladder.

5.3.1.5 Assembly of fragment I, II, III and IV into pCB301 binary vector

After getting all fragments, we started assembling into pCB301 binary vector replacing BMV RNA3 nucleotide sequences. First, pBR3 plasmid (Gopinath *et al.*, 2005) was digested with *Xba*I & *Xma*I restriction endonucleases and backbone was eluted. Backbone contains partial sequence of BMV RNA3 sequence and complete pCB301 vector sequence and it showed 6.0 kb (Fig 5.11, panel A, lane 2). The Fragment lV (Fig 5.11 panel A, lane 1) was ligated into 6018 bp back bone (Fig 5.11, panel A, lane 2). Cloned product was confirmed through the double digestion as well as sequencing and resultant plasmid was named pBTR3. Second, pBTR3 plasmid that has fragment IV of TSV RNA3 and partial sequence of BMV RNA3; was digested with *Bgl*II & *Xba*I, backbone was eluted and it showed 4.624 kb (fig 5.11 panel B,

lane 1 and 2). Finally, Fragment I, II and III, digested with *Bgl*II-*Eco*RI, *Eco*RI-*Kpn*I and *Kpn*I-*Xba*I respectively (fig 5.10, lane 1, 2 and 3) were ligated into 4624 bp eluted backbone (fig 5.11 panel B). Ligated product was transformed and positive clone was screened through PCR as well as restriction digestion.

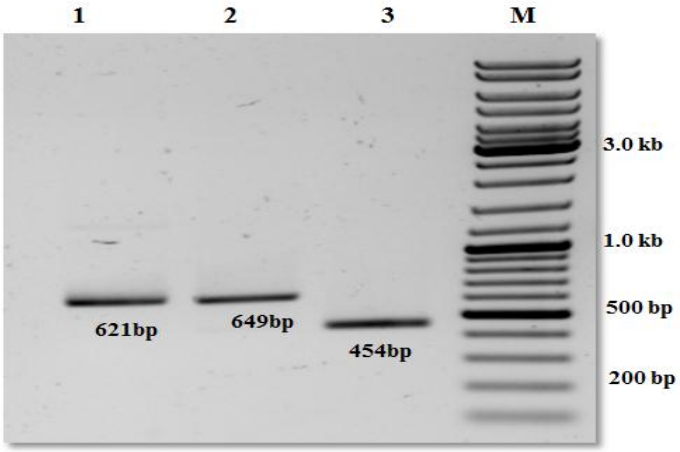

Fig 5.10: Elution pattern of fragments I, II and III in 1 % agarose gel.
Lane 1, 2 and 3 the elution of fragment I flanked with *Bgl*II - *Eco*RI, fragment II flanked with *Eco*RI - *Kpn*I and fragment III of RNA1 with *Kpn*I & *Xba*I respectively. 613 bp, 649 bp and 454 bp indicate the molecular weight of fragment I, II and III. M: 1.0 kb DNA ladder

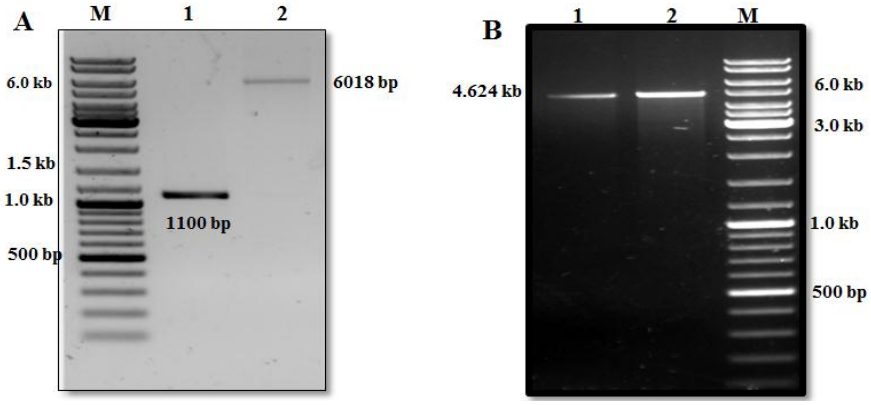

Fig 5.11: Elution of back bone and insert for assembly of fragment I, II and III in pCB301 binary vector. Panel A, Lane1: fragment IV with *Xba*I and *Xma*I, lane 2: pBR3 plasmid backbone flanked with *Xba*I and *Xma*I. In panel B: lane 1 & 2: eluted back bone flanked by *Bgl*II and *Xba*I. M: 1.0 kb ladder.

5.3.1.6 PCR confirmation of positive clone of TSV RNA3 in pCB301 binary vector

PCR was performed with different sets of RNA3 primers. In all combination of primers recombinant clone harboring full length RNA3 in pCB301 binary vector

showed expected PCR amplification. Here, we were shown few combinations as representative picture. PCR amplified product of CP gene and MP gene resulted into 717 bp (fig 5.12, lane 3 and 6) and 853 bp (fig 5.12, lane 2 and 5). PCR amplified product with CPNcoI+ forward and MPXhoI- reverse primer showed 1713 bp. (fig 5.12, lane 1 and 4) These results indicate the presence of RNA3 nucleotide sequences in the pCB301 binary vector. No amplification was observed in case of empty vector (data not shown). The resultant sequence confirmed plasmid was named as pTR3.

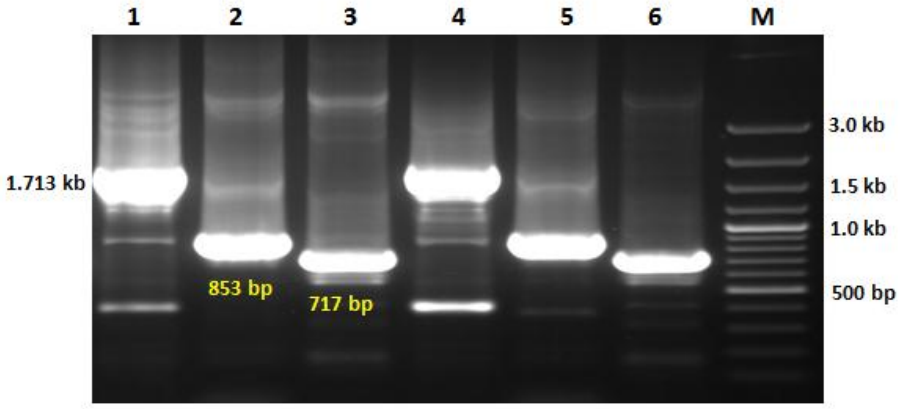

Fig 5.12: PCR confirmation of RNA3 in pCB301 binary vector.
Lane 1 and 4: 1.713 kb of PCR amplified product with MPNcoI+ (forward primer) and reverse primer (CPXhbaI-). Lane 2 and 5: 853 bp of PCR amplified product with MPNcoI+ (forward primer) and reverse primer (MPXhbaI-). Lane 3 and 6: 717 bp of PCR amplified product with CPNcoI+ (forward primer) and reverse primer (CPXhbaI-). M: 100 bp ladder.

5.3.2 Construction of Full-length infectious clone for RNA2

5.3.2.1 Fusion of 35S promoter upstream to 5′ UTR of RNA2 (fragment I)

PCR amplified product of fragment 1A showed 603 bp (fig 5.13, panel A, lane 3 and 4) which conatined 35S double promoter sequence flanked with *Bgl*II restriction site at 5' end and 49 nt sequence of RNA2 at 3' end. This 49 nt of 5' end of RNA2 was added to 35S promoter using fusion PCR. Fragment IB amplified PCR product showed 1255 bp (fig 5.13, panel A, lane 1 and 2), that contained 1255 nt satrting from the first nucleotide of RNA2. These two overlapped fragments were fused into single fragment as fragment IC using overlap extension PCR and resultant PCR product showed 1805 bp amplicon size (fig 5.13, panel B, lane 1 and 2). Apart from the desired fragment size, non specfic band was observed near 600 bp. Desired PCR band (1805 bp) was cloned into pGEMT- Easy cloning vector. Positive plasmids were confirmed through restriction digestion with *Eco*RI restriction enzyme and it released

1805 bp (fig 5.14, panel A, lane 1 and 2) of expected insert. This positive plasmid was named as pR2F1. The fragment I was released 1414 bp (fig 5.14, panel B, lane 1 and 2) upon restiction digestion of pR2F1 plasmid with *Bgl*II and *Sal*I restiction enzyme.

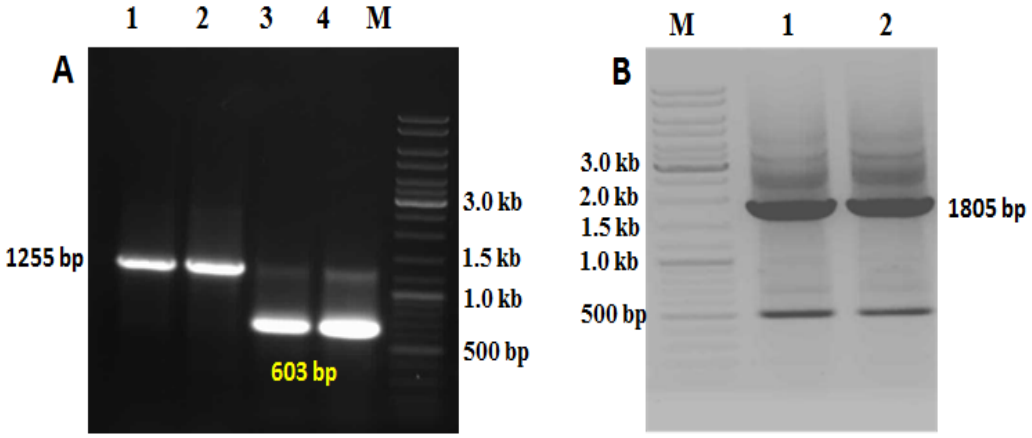

Fig 5.13: PCR amplification of fragment I of RNA2 through overlap extension PCR. Panel A, Lane 1 and 2: PCR amplification of fragment IB with R21+ & 2a 1255- primer, using pR2A12 plasmid as a template. Lane 3 and 4: PCR amplification of fragment IA with BglII + & 35TR2- primer using pBR3 plasmid as template. 1255 bp and 603 bp indicate PCR amplified product of fragment IA and IB respectively. Panel B, Lane 1 and 2: PCR amplification of fragment IC with fusion of fragment IA and fragment IB through overlap extension PCR. M:1.0 kb ladder.

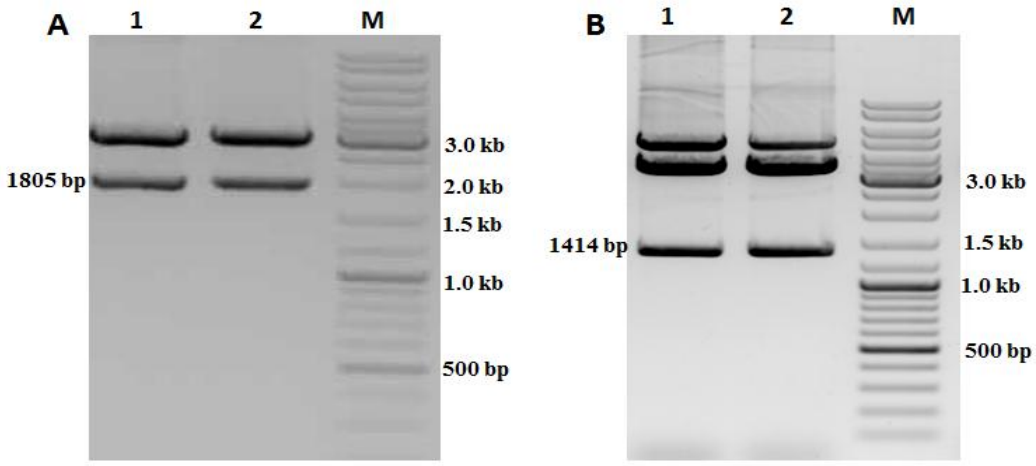

Fig 5.14 Cloning and confirmation of fragment I of RNA2 in pGEMT-Easy vector.
Panel A: restriction digestion confirmation of pR2F1 plasmid with Not I restriction enzyme. Lane 1 and 2 released 1805 bp released insert from recombinant pGEMT plasmid harboring IC fragment. Panel B: Restriction digestion of pR2F1 plasmid with *Bgl*II and *Sal*I restriction enzyme. Lane 1 and 2: restriction digestion of pR2F1 plasmid with *Bgl*II and *Sal*I and released 1414 bp. M: 1.0kb ladder

5.3.2.2 Fragment II

Fragment II was amplified through PCR and cloned into pTZ57R/T cloning vector according to the method decribed in section 5.2.8.2. The restriction digestion of the positives plasmids were performed with *Sal*I and *Hin*dIII restriction enzyme and it resulted into release of 1096 bp insert (fig 5.15, panel A). This insert was eluted from the gel (fig 5.15, panel B, lane 1) and used as insert for fusion of fragment I to II in pET 28a vector. The sequence confirmed plasmid was named as pR2F2.

5.3.2.3 Fusion of fragment I and II into pET28a vector

Fragments I and II were fused into approximately 2.5 kb bigger fragment according to the method described in 5.2.8.3. Fragment I (1414 bp) flanked with *Bgl*II and *Sal*I , fragment II (1055 bp) flanked with *Sal*I and *Hin*dII restriction sites were cloned into pET 28a vector at *Bgl*II and *Hin*dIII retriction site. Two independent clones were confirmed through restriction digestion. Both clones were released, 2469 bp (~2.5 kb) (fig 5.15, lane 1 and 2) of expected insert size was released. The positive plasmid was named as pET28-35S-2a and it contained 35S promoter fused with 5′ UTR region of RNA2 along with partial sequence of 2a gene. 2469 bp of released fragment was purified from the gel and used as insert for cloning into pCB301 binary vector.

5.3.2.4 Fragment III

PCR was performed with M13 forward and reverse primers, taking pR2F3 plasmids as template. Amplified product showed 1.1 kb (data not shown). PCR product was eluted and digested with *Hin*dIII-*Xma*I (fig 5.16, panel A, lane 1 to 2). Here, fragment III showed 1.0 kb expected size and 100 bp extra nucleotide that came from the vector back bone The eluted product of the fragment showed 1.0 kb (fig 5.16, panel B, lane 1 and 2). Eluted fragment was used as insert in the ligation step.

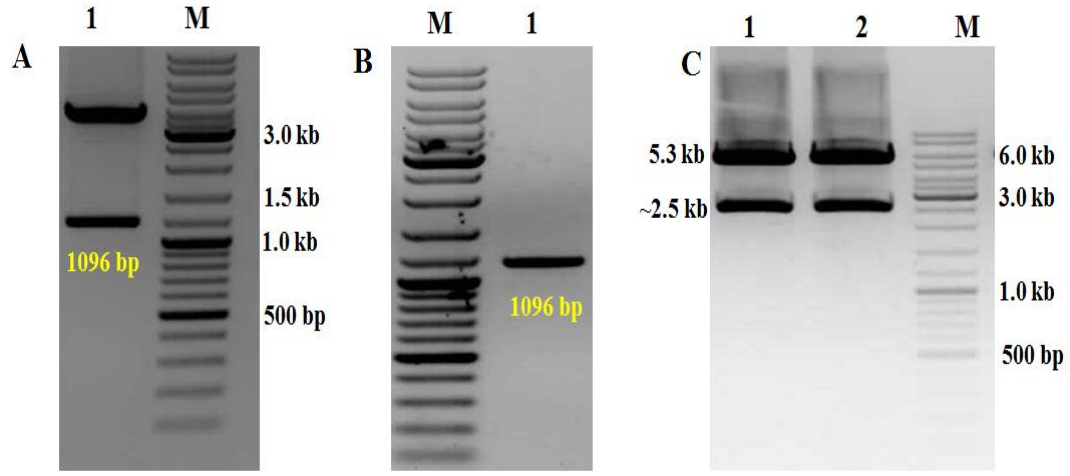

Fig 5.15: Cloning and confirmation of fragment II of RNA2 into pTZ57R/T vector and fragment I and II in pET28a vector.

Fragment II was cloned into pTZ57R/T and confirmed through restriction digestion with *Sal*I and *Hin*dIII restriction enzyme. Panel A: restriction digestion confirmation of pR2F2 plasmid with *Sal*I and *Hin*dIII restriction enzyme. Lane 1 released 1096 bp released insert from recombinant pTZ57R/T plasmid harboring II fragment. Panel B: Elution pattern of fragment II in 1% agarose gel. Lane 1: elution of fragment II. M: 1.0kb ladder. In panel C: Fragment I and II was fused into single fragment (2.5 kb) in pET 28a vector at *Bgl*II and *Hin*dIII restriction sites. Clone was confirmed through restriction digestion. Lane 1 and 2 represents restriction digestion of two independent pET28a-35S-2a plasmid harboring 2.5 kb insert with *Bgl*II and *Hin*dIII. Both plasmids were showed; release of 2.5 kb size of insert. 5.3 kb represent the pET 28a backbone. M: 1.0 kb ladder.

5.3.2.5 Assembly of 2.5 kb fragment and fragment III into pCB301 binary

Three points ligation was performed with two inserts viz; 2.5 kb fragment flanked with *Bgl*II-*Hin*dIII and Fragment III (1.0 kb insert flanked with *Hin*dIII-*Xma*I) at *Bgl*II and *Xma*I restriction sites in pCB301binary vector. Positives clone was confirmed through PCR. PCR was performed using forward (BglII+) and reverse (R2RZ2-) primer and plasmids as template. The PCR amplified products of all the selected plasmids were showed expected amplification 3.5 kb (fig 5.17, lane 1 to 4).

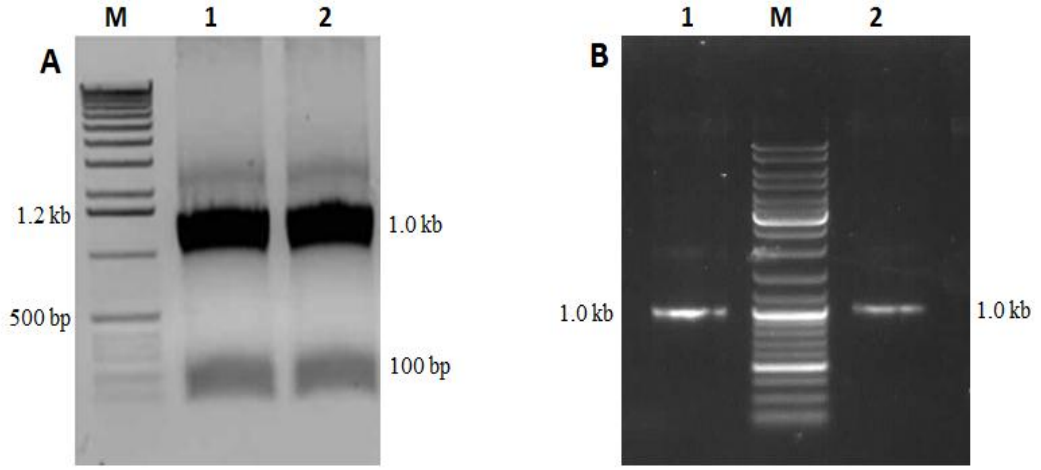

Fig 5.16: PCR amplification and restriction for fragment III of RNA2.
In panel A, lane 1 and 2: restriction digestion of PCR product with *Hin*dIII and *Xma*I restriction enzyme, amplified through M13 forward and reverse primer using pR2F3 plasmid as template. 1.1 kb of amplified product digested into two fragments; 1.0 kb indicate fragment III and 100 bp indicate extra sequence came from vector. Panel B, lane 1 and 2: eluted product of fragment III. M: 1.0 kb ladder.

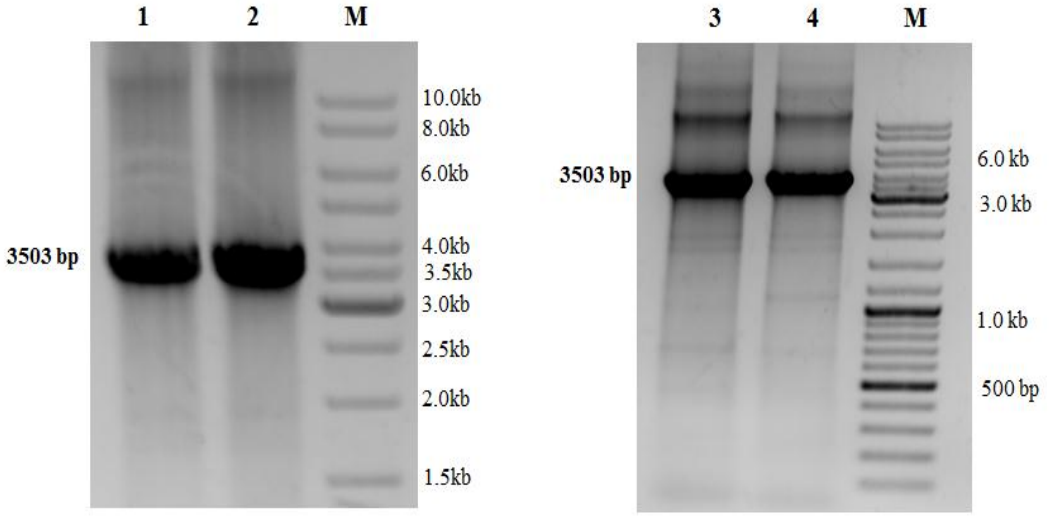

Fig 5.17: PCR confirmation of recombinant pCB301 binary plasmid contains RNA2.
Lane 1 to 4 : four independent clones of RNA2 present in pCB301 vector confirmed through PCR using forward primer (BglII+) and reverse primer (R2Rz2-) Left side of the gel indicate expected size i.e. 3503 bp [(550 bp from 35S promoter) + 2903 bp (RNA2)+ 49 bp (ribozyme sequence)]. Right side of the gel indicates the molecular weight of the 1.0 kb ladder.

5.3.4 Construction of Full-length infectious clone for RNA1

5.3.4.1 Fusion of 35S promoter upstream to 5' UTR of RNA1 (Fragment I)

PCR amplified product of fragment 1A resulted into 601 bp and which conatined 35S double promoter sequence flanked with *Bgl*II restriction site at 5' end and 47 nt sequence of RNA1 at 3' end. This 47 nt of 5' end of RNA1 was added to 35S promoter using fusion PCR. Fragment IB amplified PCR product showed 720 bp (data not shown), that contained 720 nt starting from the first nucleotide of RNA1. These two overlap fragments were fused into single fragment as fragment IC (1270 bp) using overlap extension PCR. Desired PCR band (1270 bp) was cloned into pGEMT- Easy cloning vector. Positive plasmids were confirmed through restriction digestion with *Bgl*II and *Bam*HI restriction enzyme and it released 1260 bp (fig 5.18, panel A, lane 2) of expected insert.

5.3.4.2 Fragment II

Recombinant pET1a plasmid was digested with *Bam*H1 and *Kpn*I restriction enzyme to get fragment II. Three different sizes of inserts were released namely; 2440 bp, 1515 bp and 925 bp (fig 5.18, panel B, lane 1 and 2), because; 1a gene contains two *Bam*H1 restriction sites at 709 nt and 3149 nt positions and one *Kpn*I at 2224 nt position. The desired band of 1515 bp fragment was eluted from the gel (fig 5.19, lane 3) and used for assembling into pCB301 binary vector.

5.3.3.3 Fusion of Ribozyme downstream to 3'UTR of RNA1 (fragment III)

Fusion of the ribozyme to 3' end of RNA1 was carried according to the method described in section 5.2.9.3 and fig 5.4, panel C. PCR was performed to amplify fragment IIIB and it showed expected band 1376 bp (data not shown). This fragment contains, 2224-3523 nt of TSV RNA1 with *Kpn*I site at 5' end and ending with complete ribozyme and *Xma*I restriction site at 3' end. It was cloned into pTZ57R/T vector and fragment III was released 1376 bp (fig 5.18, panel A, lane 1). Released eluted fragment showed 1376 bp size (fig 5.19, lane 3).

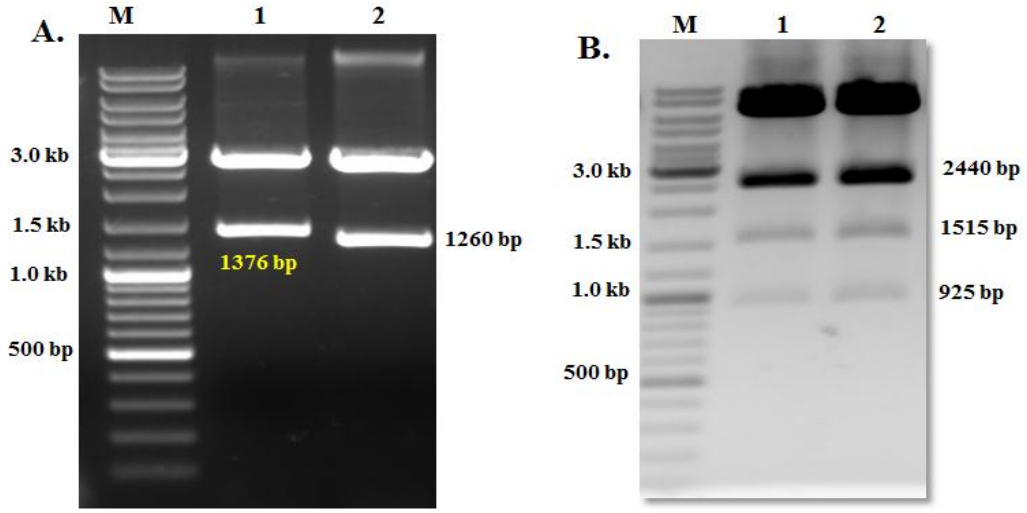

Fig 5.18: Restriction digestion analysis for fragment I, II and III of RNA1 in 1% agarose gel. In panel A: lane 1; recombinant pTZ57R/T plasmid harboring fragment III (pR1F3) released 1376 bp of insert after restriction digestion with *Kpn*I and *Xma*I restriction enzyme, lane 2; recombinant pTZ57R/T plasmid harboring fragment I (pR1F1) released 1260 bp of insert after restriction digestion with *Bgl*II and *Bam*HI. Panel B: Restriction digestion profile of recombinant pET28a vector harboring 1a gene. Lane 1 and 2 indicate restriction digestion of pET28-1a plasmid with *Bam*HI and *Kpn*I restriction enzyme. Left side of the gel indicate molecular weight of the 1.0 kb ladder and right side of the gel indicate 2440 bp, 1515 bp and 925 bp insert.

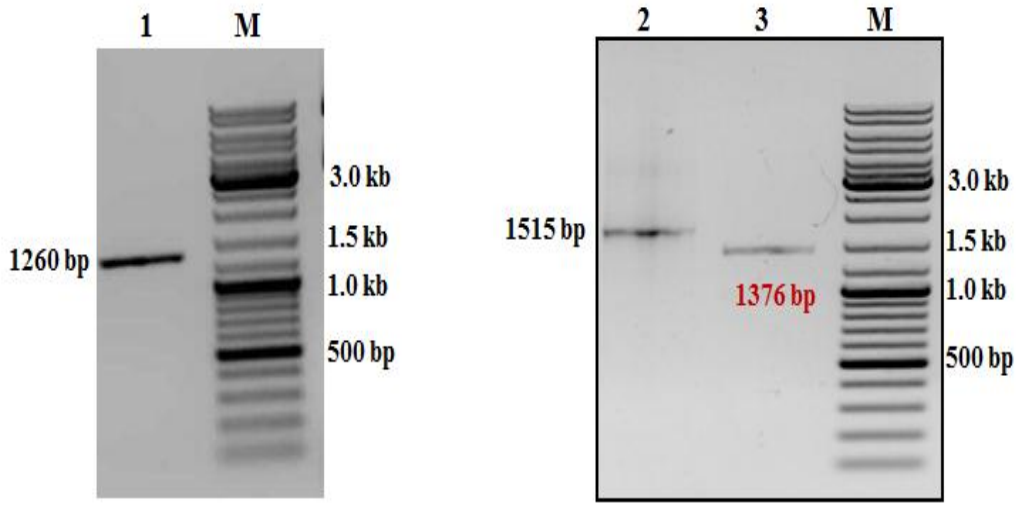

Fig 5.19: Elution profile of fragment I, II and III of RNA1 in 1% agarose gel. Lane 1, 2 and 3 the elution of fragment I flanked with *Bgl*II-*Bam*HI, fragment II flanked with *Bam*HI-*Kpn*I and fragment III of RNA1 with *Kpn*I & *Xma*I respectively. Left side of the gel, 1260 bp and 1515 bp indicate the molecular weight of fragment I and II. 1376 bp indicate molecular weight of the fragment III. M: indicate 1.0 kb ladder.

5.3.3.4 Assembly of fragment I, II and III in pCB301 binary vector

After getting all fragments, we started assembling into pCB301 binary vector replacing TSVRNA3 nucleotide sequences as depicted in fig. 5.5. First, pTR3 plasmid was digested with *Bgl*II & *Bam*H1 restriction endonucleases and backbone was eluted. Backbone contained partial sequence of TSVRNA3 sequence and complete pCB301 vector sequence and it showed 5.2 kb (data not shown). The Fragment l (fig 5.19, lane 1) was ligated into 5.2 kb back bone. Cloned product was confirmed through the double digestion as well as sequencing of resultant plasmid named as pTR3PRI. Second, pTR3PRI plasmid that has fragment I of TSV RNA1 and partial sequence of TSV RNA3; was digested with *Bam*H1 & *Xma*I, it showed 5073 bp of backbone and 2095 of insert (fig 5.20 panel A, lane 1 and 2). 2095 bp of insert indicated remaining sequence of TSV RNA3 and 5073 bp indicated the complete nucleotide sequence of pCB301 backbone along with fragment I of RNA1. Back bone was eluted and it showed 5073 bp (fig 5.20 panel B, lane 1 and 2). Finally, Fragment II and III, digested with *Bam*HI-*Kpn*I and *Kpn*I-*Xma*I respectively (fig 5.19, lane 2 and 3) were ligated into 5073 bp eluted backbone. Ligated product was transformed and positive clone was screened through restriction digestion.

5.3.3.5 Restriction digestion confirmation of TSV RNA1 in pCB301 binary vector

Four pCB301 plasmids harboring RNA1 and three pET1a plasmid (as an internal control) were digested with *Bam*HI restriction enzyme to check the presence of the insert. Full length RNA1 has three *Bam*HI restriction sites at 709 nt, 3149 nt and 3384 nt but 1a gene contains two at 709 nt and 3149 nt. Restriction digestion of plasmid containing RNA1 with *Bam*HI resulted into two fragments; one at 2440 bp and another at 235 bp (fig 5.21, lane 1 to 4), but in case of pET1a plasmid, it resulted into single fragment at 2440 bp (fig 5.21, lane 5 to 7). These results indicate the presence of RNA1 sequence into pCB301 binary vector. Positive full length pCB301 RNA1 plasmid was sequenced from both directions. The resultant plasmid was named as pTR1.

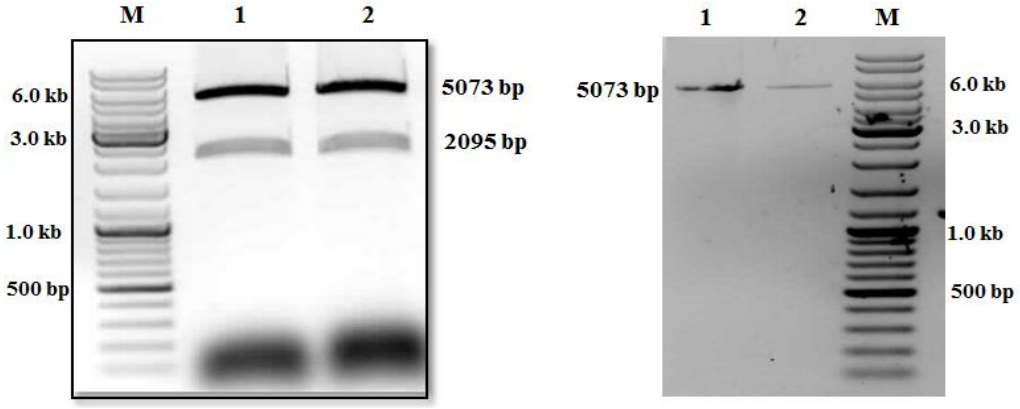

Fig 5.20: Restriction digestion confirmation of pTR1 plasmid, harboring fragment of RNA1 and partial sequence of TSV RNA3.

In panel A: lane 1 and 2; restriction digestion pattern of pTR1 plasmid with *Bam*HI & *Xma*I in 1 % agarose gel. Right side of the gel 5073 bp indicate pCB301 complete nucleotide sequence along with fragment I of RNA1 and 2095 bp indicate remaining nucleotide sequence of RNA3. Panel B: elution profile of back bone (complete sequence of pCB301 + fragment I). 5073 bp indicate backbone size as mentioned in panel A. M: 1.0 kb ladder.

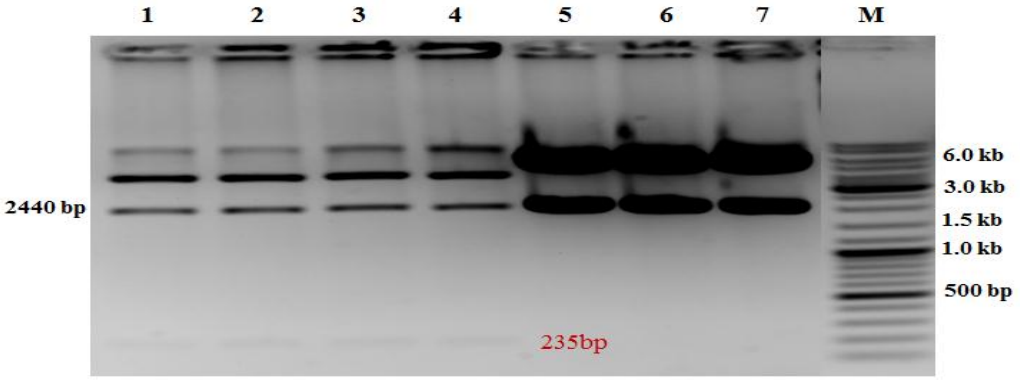

Fig 5.21: Restriction digestion confirmation of pCB301 binary plasmid harboring RNA1 nucleotide sequence and pET1a plasmid.

Lane 1 to 4; four independent clone for RNA1 in pCB301 restricted digested with *Bam*HI. Lane 5 to 7; three independent clone of 1a gene present in pET28a vector, digested with *Bam*HI and this was used as internal control. 2440 bp and 235 bp indicate, released insert after digestion. M: 1.0 kb ladder.

5.3.4 Cloning of full length RNAs encoded genes of TSV into pCB302 binary vector

Full-length of *Tobacco streak virus* encoded genes *1a, 2a, MP* and *CP* were cloned into pCB302 binary vector at *Nco*I and *Xba*I restriction site. The positive clone was confirmed through restriction digestion as well sequencing. Recombinant pCB302 plasmids were digested with *Nco*I and *Xba*I to check the presence of inserts. The 3.3

kb of insert (fig 5.22, panel A, lane 1) was released in case of 1a gene, 2.5 kb (fig 5.22, panel B, lane 2). Recombinant pCB302 plasmids harboring MP and CP gene was released 717 bp (fig 5.22, panel C, lane 1) and 853 bp of insert (fig 5.22, panel C lane 2) after restriction digestion with *Nco*I and *Xba*I restriction enzymes. The resultant positive plasmids were named as pT1a, pT2a, pTMP and pTCP.

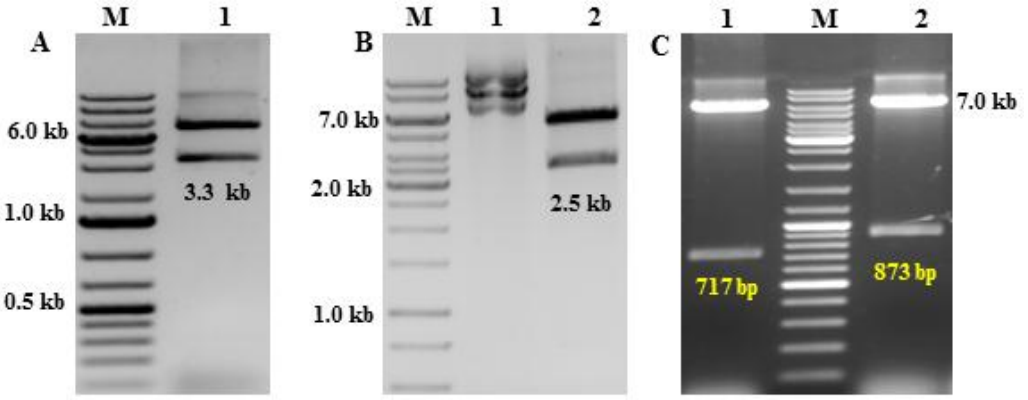

Fig 5.22: Cloning and confirmation of fragment 1a, 2a, MP and CP gene into pCB302 binary vector. In panel A, 1a gene was cloned into pCB302 binary vector at *Nco*I and *Xba*I restriction site. Lane 1: positive clone digested with *Nco*I and *Xba*I enzymes released 3.3 kb of insert size. Panel B, 2a gene was cloned into pCB302 binary vector at *Nco*I and *Xba*I restriction site. Lane 1: uncut plasmid of pCB302 harboring 2a gene, lane 2: recombinant pCB302 plasmid harboring 2a gene digested with *Nco*I and *Xba*I enzymes released 2.5 kb of insert size. Panel C, CP and MP gene was cloned into pCB302 binary vector at *Nco*I and *Xba*I restriction site. Lane 1: recombinant pCB302 plasmid harboring CP gene digested with *Nco*I and *Xba*I restriction enzymes and it was released 717 bp of coat protein gene. Lane 2 recombinant pCB302 plasmid harboring MP gene was digested with *Nco*I and *Xba*I restriction enzymes and it was released 873 bp of movement protein gene.

5.3.5 Agroinfiltartion

All the binary plasmid constructs named as pTR1, pTR2, pTR3 and pTR4 (present in pCB301 binary vector) and pT1a, pT2a, pTMP and pTCP (present in pCB302 binary vector), along with empty vector as negative control and pGFP as positive control were mobilized into agrobacterium strain EHA105. Here after, R1 represent for full-length clone of RNA1 present in agrobacterium expressing wild type RNA1. In similar way, R2, R3, R4, 1a, 2a, MP and CP indicated agrobacterium clone expressing wild type RNA2, RNA3, RNA4, 1a, 2a, MP and CP respectively.

5.3.6 Characterization of full length infectious clone

To check the biological activity and infectious nature of the constructed clones; we have infiltrated empty vector, internal controls, R3, R4, CP, R1+R2+R4,

R3+1a+2a and R1+R2+R3 (three main RNAs) along with the CP and R4 (sub genomic RNA). No visual symptom expression was observed in the icDNA clones infiltrated plants in any of the above said combinations. So, we wanted to check the infectious nature of the infiltrated cDNA molecules. Towards this, after 72 h of infiltration, total soluble proteins were isolated and fractionated in 12 % SDS-PAGE and fractionated proteins are transferred from gel to PVDF membrane.

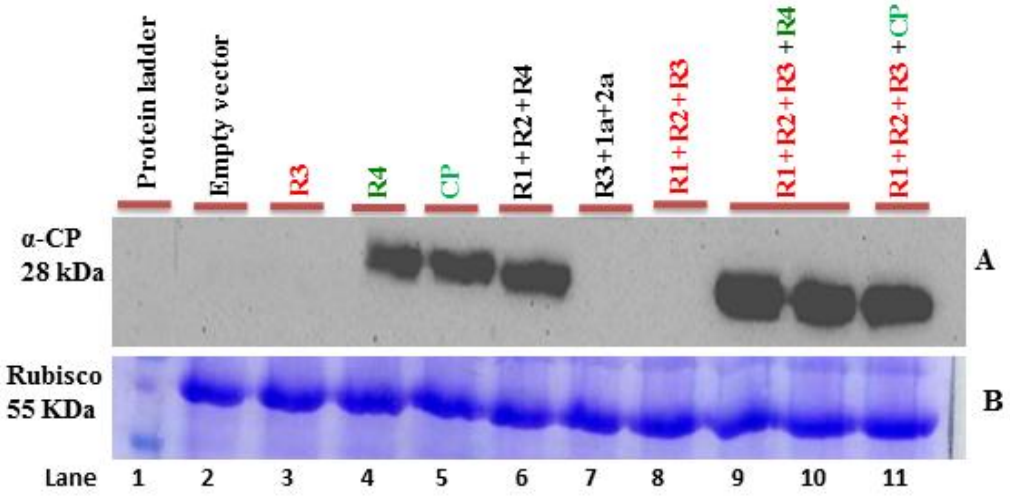

Fig 5.23: Western blot confirmation for infectious nature of constructed clone.
Confirmation for infectious nature of clones by western blot using TSV antisera. Panel A, indicate western blot of isolated total soluble protein from agroinfiltrated leaf. Lane 1: Protein ladder, Lane 2: Empty vector, Lane 3: R3, Lane 4 : R4, Lane 5: CP, Lane 6: R1+R2+R4 , Lane 7 : R3+1a+2a, Lane 8:R1+R2+R3, Lane 9 and 10 : R1+R2+R3+R4, Lane 11: R1+R2+R3+CP. 28 kDa present left side of the western blot indicate molecular weight of reacted protein i.e. coat protein of the TSV. In panel B is represented by SDS-PAGE with 55 kDa of protein. It indicates the larger subunit of Rubisco and used as loading control. Here, empty vector used as negative control and larger subunit of Rubisco used as loading control.

The total proteins were checked in western blot with coat protein antibody according to the protocol mentioned under section 3.2.9. CP was detected in the infiltrated leaves with CP gene and protein individually as well as in combination with replicase genes (fig 5.23; lane 4, 5, 6, 9, 10 and 11). Marginal increase in the CP accumulation was observed in the western blot when main RNAs infiltrated with in combination with subgenomic RNA4 or CP (fig 5.23 lane 9, 10, 11) in comparison to individual CP genes or RNA4 alone (lane 4 and 5). However, no signal was detected in the combination of replicase gene with R3 gene (fig 5.23; lane 7 and 8,) even the CP is encoded by R3 gene.

The R4 translated after transcription and produced the CP that was detected in western blot. In similar manner, CP gene also translated after transcription in the

nucleus of the host cell upon agroinfiltartion. In this experiment RNA4 and coat protein used as internal control for the combination of R1+R2+R3+R4 and R1+R2+R3+CP.

5.3.6.1 Confirmation of transcripts in the infiltrated plants

The efficiency of the transcription processes after the introduction of the genes into plant cell nuclei from agrobacterium was performed. Firstly the accumulation level of individual transcripts was checked; two independent clones from all constructs namely R1, R2, R3 and R4 from pCB301 binary vector along with empty vector were infiltrated into the epidermal tissue of *Nicotiana benthamiana* leaves. Total RNAs were isolated from agroinfiltrated leaves after 36 and 48 h of post infiltration as described in section 5.2.15. 100 ng of total RNA was used as a template for RT-PCR amplification, using primers in 3′ UTR region (mentioned in fig 5.24, panel A, above the each construct in the right side indicated by arrow), designed for 400 bp amplicon size in all RNAs. RT-PCR amplified product showed 400 bp in all cases (fig 5.24, panel C, lane 2, 3, 4 and 5). Apart from this, RT-PCR was also performed with different sets of internal primers for all RNAs and it showed expected results in all cases (data not shown).

In similar way the transcription efficiency was performed through pCB302 construct (1a, 2a, MP and CP). Two independent clones of 1a, 2a, MP and CP along with empty vector were infiltrated into the epidermal tissue of *Nicotiana benthamiana* leaves (fig 5.25, panel B). 100 ng of total RNA was used as template for RT-PCR amplification, using primer in 3′ UTR region (mentioned in fig 5.25, panel A, above the each construct in the right side indicated by arrow), designed for 400 bp amplicon size in all RNAs. RT-PCR amplification was observed in all cases (fig 5.25, panel C, lane 2, 3, 4 and 5). Apart from this, RT-PCR was also performed with different sets of internal primers for all RNAs and it showed expected results in all cases (data not shown). Based on the above results, it was clear that, all binary constructs were able to transcribe efficiently. Further, we have checked the translational efficiency of transcribed RNA.

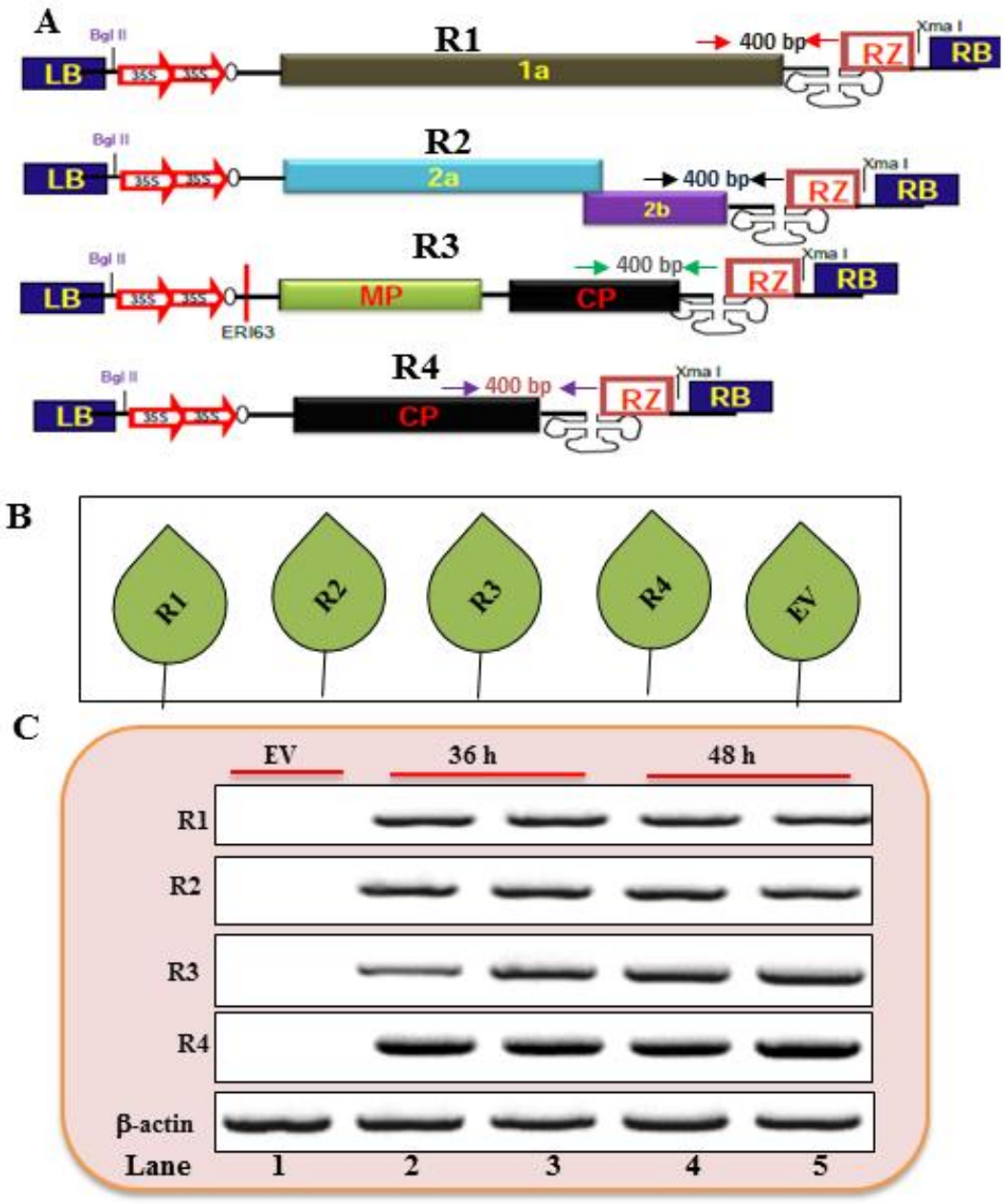

Fig 5.24: Confirmation of transcripts upon agroinfiltraion of full length cDNA molecule of TSV RNAs by RT-PCR.

Panel A: R1, R2, R3 and R4 represent full length infectious cDNA molecule of each RNA of TSV present in between LB and RB. Small arrow color as red, black, green and violet at right side of the each RNA indicate forward and reverse primer. 400 bp indicate the amplicon size of the designed primers. In panel B: R1, R2, R3, R4 and EV represent the *Nicotiana benthamiana* plant agroinfiltrated with individual full length cDNA molecule of RNA1, RNA2, RNA3, RNA4 and empty vector respectively. Panel C: RT-PCR amplified product of R1, R2, R3, R4 and EV from agroinfiltrated leaf in 1% agarose gel. Left side of the each gel indicate infiltrated cDNA molecule of RNA as R1, R2, R3, R4 and β- actin and empty vector used as positive and negative control . Lane 1: RT- PCR amplification of negative and positive control. Lane 2 and 3 RT-PCR amplification of RNA isolated from the agroinfiltrated constructs of R1, R2, R3 and R4 after 36 h of infiltration. Lane 4 and 5; RT-PCR amplification of RNA isolated from the agroinfiltrated constructs of R1, R2, R3 and R4 after 48 h of infiltration.

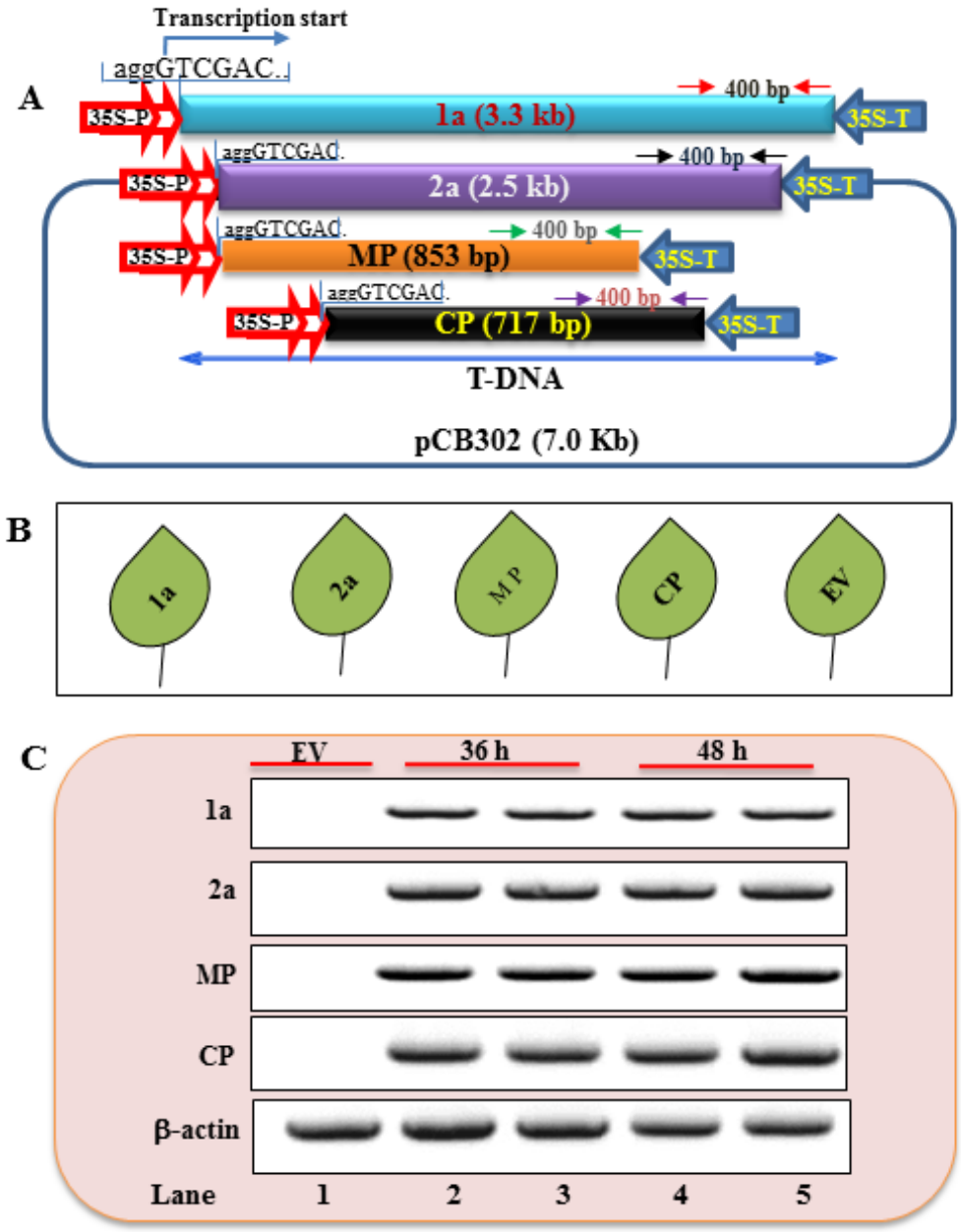

Fig 5.25: Confirmation of individual transcript upon agroinfiltraion of full length cDNA molecule of TSV RNAs encoded genes by RT-PCR.

Panel A: 1a, 2a, MP and CP represent full length cDNA molecule TSV RNAs gene present in between LB and RB. Small arrow color as red, black, green and violet at right side of the each gene indicate forward and reverse primer. 400 bp indicate the amplicon size of the designed primers. In panel B: 1a, 2a, MP, CP and EV represent the *Nicotiana benthamiana* plant agroinfiltrated with individual full length cDNA molecule of 1a, 2a, MP, CP and empty vector respectively. Panel C: RT-PCR amplified product of 1a, 2a, MP, CP and EV from agroinfiltrated leaf in 1% agaroose gel. Left side of the each gel indicate agroinfiltrated cDNA molecule of TSV encoded genes as 1a, 2a, MP, CP; β- actin and empty vector used as positive and negative control . Lane 1: RT- PCR amplification of negative and positive control. Lane 2 and 3 RT-PCR amplification of RNA isolated from the agroinfiltrated constructs of 1a, 2a, MP and CP after 36 h post infiltration. Lane 4 and 5; RT-PCR amplification of RNA isolated from the agroinfiltrated constructs of 1a, 2a, MP and CP after 48 h post infiltration.

5.6.2 Confirmation of translational efficiency in the agroinfiltrated plants

Upon transcription, the translation levels were also analyzed by using R1, R2, R3, R4 and encoded genes. Towards this, we produced antibody against encoded protein 1a, 2a, MP and CP after cloning it into pET 28a over expression vector (strategy and data not shown).

We have infiltrated R1, R3 and encoded gene (1a and MP) into the *Nicotiana benthamiana* plant. After 72 hours of infiltration, cell wall and soluble fraction of proteins were extracted according to the method described in section 5.2.17. Western blot was performed with respective antisera and proper controls. In western blot, we have observed signal in membrane fraction of R1 and 1a at 123 kDa (fig 5.26, lane 2 and 3) whereas soluble fractions showed no detectable signals (fig 5.26, lane 4 and 5).

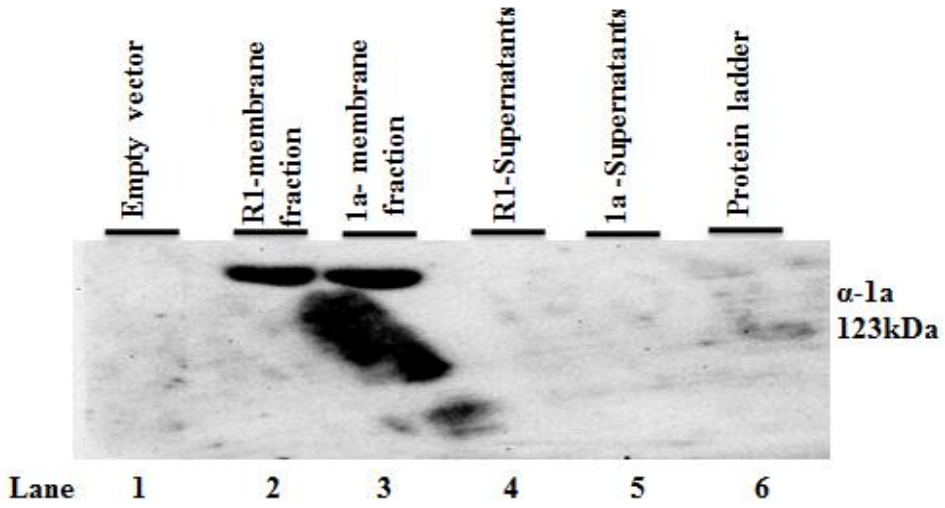

Fig 5.26: Western blot confirmation of the RNA1 and 1a translation upon transcription after agroinfiltration of R1 and 1a construct. Western blot was performed with isolated membrane and soluble fraction of protein after 72 h of agroinfiltartion with 1a raised antisera. Lane 1: empty vector, lane 2; membrane fractions of R1 was reacted with 1a antisera, lane 3; membrane fractions of 1a protein was reacted with 1a antisera. Lane 4: A soluble fraction of R1 was reacted with 1a antisera, lane 5: soluble fractions of 1a protein reacted with 1a antisera and lane 6 indicate protein ladder.

In western blot result of RNA3 and MP, we have observed signal in cell wall fraction of R3 and MP at 33 kDa (fig 5.27, lane 3 and 4) whereas soluble fractions showed no detectable signal (fig 5.27, lane 5 and 6. In similar manner we have checked the RNA4 and CP also; we have observed signal in soluble fraction R4 and CP at 28 kDa (fig 5.23, lane 4 and 5)

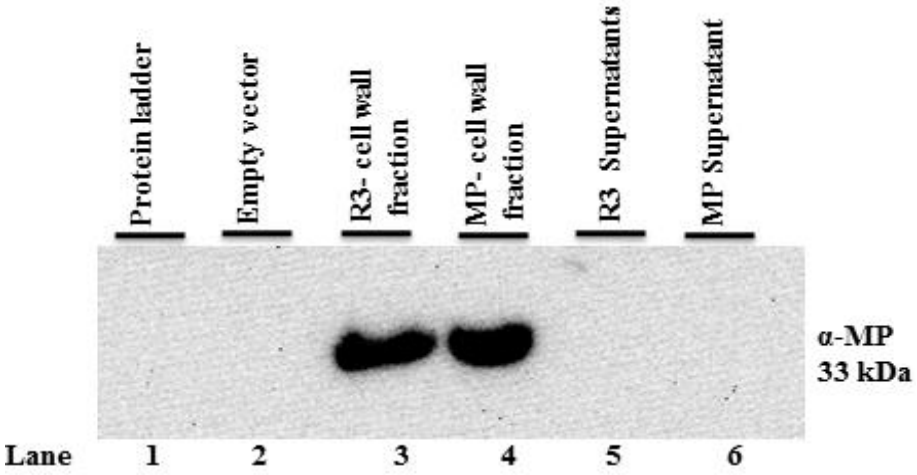

Fig 5.27: Western blot confirmation of the RNA3 and MP translation upon transcription after agroinfiltration of R3 and MP construct.
Western blot was performed with isolated membrane and soluble fraction of protein after 72 h of agroinfiltartion with MP raised antisera. Lane 1: protein ladder, lane 2: empty vector, lane 3; cell wall fraction of R3 was reacted with MP antisera, lane 4; cell wall fraction of MP protein was reacted with MP antisera. Lane 5: A soluble fraction of R3 was reacted with MP antisera, lane 6: a soluble fraction of MP protein was reacted with MP antisera.

We are facing problem to produce antibodies against RNA2 to check the *in planta* translated products of RNA2 even though we are able to express the protein successfully in bacterial system (fig 5.28, lane 4). In the soluble fraction, we did not observe the desired protein (fig 5.28 lane 3).

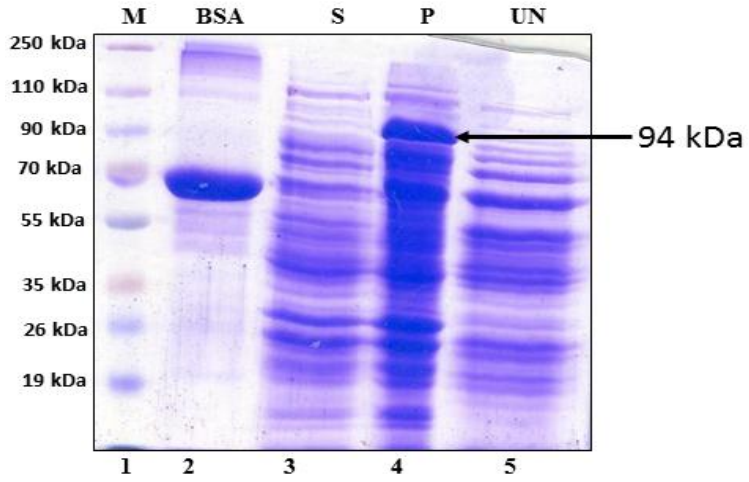

Fig 5.28: SDS-PAGE analysis of over expressed 2a gene in bacterial expression host. Lane 1: Prestained protein ladder (M), lane 2: BSA as internal control for ladder, lane 3: soluble fraction (S) after sonication and lane 4: pellet fraction (P) of the sonication and lane 5: un-induced (UN). Arrow at right side of the gel indicates molecular weight of overexpressed protein.

5.4 Discussion

The huge improvement in the field of molecular virology of RNA viruses were observed after implementing the infectious clones as molecular tool and agroinfiltartion as an approach; to deliver the DNA in the plant cell. Over the years, construction of the infectious clone of the RNA viruses becoming a regular laboratory practice to unravel the host pathogen interaction and various process of the RNA viruses such as packaging, replication, movement and antiviral strategies of plant viruses (Knorr, *et al*., 1988; Saito, *et al*., 1987). However, development of the biological active infectious clones encounters many difficulties. Few factors that affect the construction of an infectious clone includes: heterogeneity of transcript cDNAs caused by the use of low fidelity reverse transcriptase and polymerases and presence of point mutations or single base substitution when dealing with long viral genomes. The presence of non-viral nucleotides at either the 5' terminus or the 3' terminus of viral genome can render cDNA clones non-infectious. It is generally found that nucleotide extension (even only 1 or 2 nucleotides) at 5' terminus strongly reduces infectivity in *in vitro* transcription, although *in vivo* transcripts containing up to 40 additional nucleotides at the 5' end have been able to infect (Commandeur *et al*., 1991). Nucleotide extension at the 3' terminus (1-7 nucleotides) is better tolerated than at the 5' terminus (Boyer and Haenni, 1994). However, in BMV infectious clone, it was also proved that extra non-viral 21 nt at the 3' end of the viral genome were also tolerated and made it infectious (Annamalai and Rao, 2005). Finally, the instability of full-length cDNA in bacteria, particularly (+) sense RNA viruses (like TSV, GVA and many more), influence their infectivity in host plants. Synthesizing a single cDNA of an RNA virus is a tedious task because secondary structures on the RNA template often interfere with full-length cDNA synthesis. In the present chapter we have discussed about our effort in development of an infectious clone for *Tobacco streak virus*.

Once we have achieved all the three genomic RNA sequences by reverse transcribing approaches, (in the form of DNAs), extensive molecular manipulations were performed to clone them into binary vectors under the right and left borders of the *Agrobacterium* T-DNA sequence. As an overview, we have fused *Cauliflower mosaic virus* 35S double promoter to the 5′ end of the genomes individually for efficient transcription of the introduced DNA in the plant cell nuclei. Proper care is

taken that no additional nucleotides are there in between the 35S transcription initiation sequence and the 5′ end of the viral genome. Similarly, we have fused a viroid rhibozyme (Gopinath *et al.,* 2005) sequence at the 3′ end of all the three genomes for the *cis* preferential catalytic cleavage and generation of authentic viral ends similar to that of the wild type viral RNAs. The whole genomes were individually cloned into pCB 301 binary vectors in the *Bgl*II and *Xma*I restriction sites (Gopinath *et al*., 2005) with multistep cloning approaches. The agroinfiltration assay system was used to check the constructed infectious clones of TSV.

Primarily, the plants, *N. benthamiana* and *Phaselous vulgaris* were infiltrated with different combinations of constructs and observed for the expression of wild type symptoms. No symptoms were observed in any of the infiltrated combinations even after 21 dpi. Some reports have shown that absence of visual symptoms is not an indication for the virus free plants (Hull, 2014). In this case, we went ahead to check the virus by isolation of total soluble proteins from the infiltrated plants and analysis through western blot with the antisera against virion particles. The western blot results showed no detectable signal in lane 2, 3, 7 and 8 (fig 5.23) that represented empty vector, R3, R3+1a+2a, R1+R2+R3 combination respectively. cDNA construct of R3 generated wild type RNA3 upon transcription into the nucleus of the plant cells after agroinfiltration. This RNA3 is bi-cistronic in nature and codes for MP and CP. From RNA3, MP ORF was efficiently translated in cytoplasm once it transcribed because, MP ORF located near to the 5' end whereas 3' proximal ORF (CP) is transnationally silent (Miller and Koev, 2000) hence, we did not observe any detectable signal. Unexpectedly, we did not observe detectable signal in western blot against CP in combination of replicase gene along with RNA3 [R3+1a+2a (fig 5.23, lane 7) and R1+R2+R3 (fig 5.23, lane 8)]. However, in case BMV and AMV de Boon *et al*., 2001; Hasnot *et al*., (2000) reported; after the translation of the replicase gene (1a and 2a) efficiently binding to 3' end of conserved t-RNA like structure (TLS) of RNA3 and starts synthesis of negative strand of the subgenomic RNA4 with help of host factor, further this strand converted into positive strand. This result indicates several queries as i) synthesis of the effective transcript from the constructed cDNA clone in the host plant cell nuclei, ii).effectiveness of translational product from transcribed transcript, iii) effective binding of replicase protein at 3' TLS, iv) synthesis of the

functional negative strand of the subgenomic RNA and finally v) effectiveness of translated products from newly synthesized positive strand subgenomic RNA.

In 1999, Bol reported, that TSV and other member of ilarvirus and *Aflalfa mosaic virus*, a mixture of three main genomic RNAs (RNA1, 2 and 3) does not constitute infectious unless coat protein or its mRNA, RNA4, is added. Based on above report we have infiltrated main RNAs along with CP or RNA4. The western analysis result showed that; accumulation levels from the infiltrated leaves were more (fig 5.23, lane 9, 10 and 11), however, we could be able to observe only marginal increase over CP and R4 alone. After critical review of above results, we thought there may be problem with R1, R2, and R3 and its encoded protein either at transcription level or translational level. Towards this, we infiltrated individual construct to check the transcription and translation efficiencies.

The transcription levels in the infiltrated plants was analyzed using RT-PCR approach by amplifying about 400 bp fragment from the 3' end of the transcribed RNA molecules. As we all know that the transcription starts from 5' and goes towards 3', we have amplified only the last 3' fragment for confirmation. Desired PCR fragment was observed in all the infiltrated combinations in RT-PCR when the isolated RNA from the agroinfilatrated leaf was used as template. This result indicates that transcription efficiently occurs from the 5' end of cDNA of R1, R2, R3 and R4. In similar way we have checked the 1a, 2a, MP and CP gene also. This result indicates, all the binary cDNA constructs are efficiently transcribing inside the nucleus of plant cell using RNA polymerase II and reaches up to 3' end of RNAs. Further we have analyzed the productivity of the transcribed transcript from the cDNA constructs for the formation of the respective products after translation.

To check the translational products from these transcripts by western blot analysis using the polyclonal antibodies raised against encoded protein 1a, (truncated version), MP and CP genes. In Western blot results of the all the constructed clones signal at the desired molecular weight was observed in the membrane fraction (RNA1 and 1a) cell wall fraction (RNA3 and MP) and soluble fraction (RNA4 and CP) with the respective antibody. These finding is agreeing with the reports from BMV (de Boon *et al*., 2001) and AMV (Bol, 2003; 2005). Desired size of protein in the western blot against respective antibody indicates that transcribed; transcript from the cDNA construct is efficiently translating without premature termination of translation.

Presence of the protein in membrane fraction might indicate that, upon transcription of cDNA constructs, translation occurring and residing in the membrane fraction. From literature survey, we know that in BMV & AMV 1a and 2a genes; form replicase complex along with the host factors (de Boon *et al*., 2001; Bol, 2005). So, it might be possible that the host factor is membrane bound or 1a is itself associated with the membrane bound structure.

Results pertaining to the translation of individual genes, MP and RNA3 of TSV showed the signal in cell wall fraction in western analysis (fig 5.27, lane 3 and 4). This might indicate that, upon transcription of cDNA constructs, translation is occurring and residing in the cell wall fraction. The CP and RNA4 were observed in soluble fraction (fig 5.23, lane 4 and 5).

We have faced some problem for the production of antisera against RNA2 even though we are successful in the overexpression of the 94 kDa protein in bacterial expression host system (fig 5.28). Expected size of 2a gene overexpression in bacterial system is also indicates that product was translated without premature termination.

Bol, (1999) reported that mutation in the GDD motif greatly influences the replication and formation of the effective replicase complex along with 1a protein and along host factor and subsequently synthesis of the subgenomic RNA. Xin *et al*., (2003) reported that point mutation in the inter-cistronic region; especially in subgenomic promoter region change in single nucleotide i.e. Adenine to guanine at 1193 position RNA3 greatly influences the infectivity of the transcript. In the present study, we did not observe any mismatch in the GDD motif and its vicinity and subgenomic promoter region compare to the reported strain of TSV from different part of the globe. At present we did not check the *in planta* translation product of the RNA2 and its encoded gene and production of the authentic 3' end after the self-cleavage by ribozyme. Based on the above result and discussion we conclude that; the constructed cDNA clones in the present study are not biological active even though all clones are able to transcribe and translate efficiently; but not able to produce visible symptom on *N. benthamiana* and *Phaselous vulgaris.*

Chapter-6

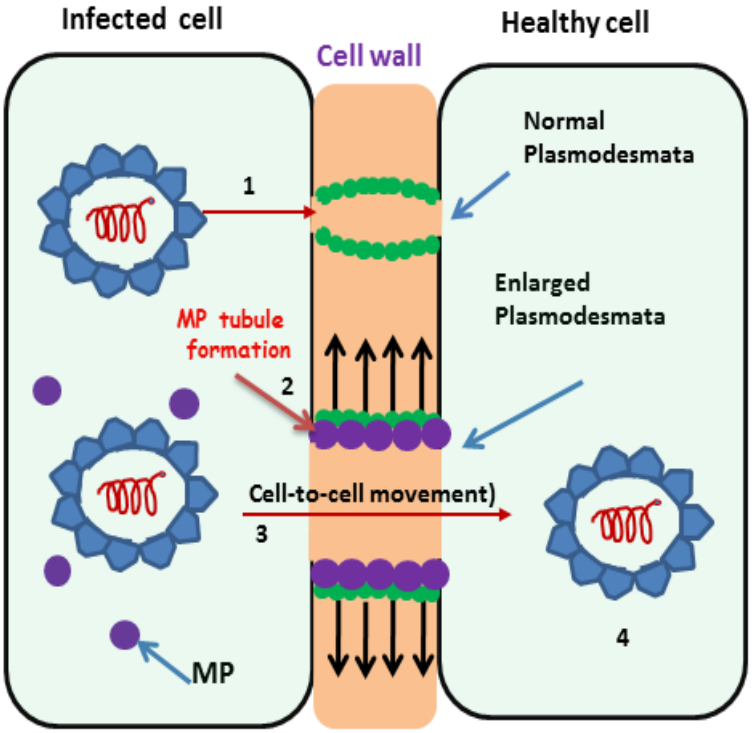

In planta analysis of TSV movement protein (MP) as a GFP chimera and functional analysis of MP-GFP chimeric mutants through confocal laser scanning microscopy (CLSM)

In planta analysis of TSV movement protein (MP) as a GFP chimera and functional analysis of MP-GFP chimeric mutants through confocal laser scanning microscopy (CLSM)

6.1 Introduction

Plant viruses have to face the impermeable cell wall barrier for transfer of the infectious material or virion particles from infected cell to uninfected neighboring cells. The movement of infectious particle is possible only after the mechanical damage to the plant cell wall and plasma membrane by the vectors transmitting the virus, or by mechanical inoculation. To combat this cell wall barrier, during course of evolution viruses have developed specialized proteins called movement proteins (MPs). Different MPs are encoded by different viruses but the interesting fact about movement proteins is that they target to plasmodesmata irrespective of their sizes.

Based on the degree of structural changes in the plasmodesmata, MP can be divided into two broad categories (Carrington *et al.*, 1996). *Tobacco mosaic virus* (TMV) represents the first category. In this category, Viral MP interacts with the PD in the cell and increases the size exclusion limit (SEL) of the PD without causing visual changes to the PD structure and help the movement of MP–RNA complex from infected cell to neighboring cells. In second category represented by the *Cowpea mosaic virus* (CPMV) or *Cauliflower mosaic virus* (CaMV) type, are involved in dramatically restructuring the PD by removing the appressed endoplasmic reticulum (desmotubule) from the PD and increasing pore with diameters up to 50 nm and MP can form the passage tubule and allows the virion particles to move through it to healthy cell.

The cellular distribution pattern of movement protein of different viruses was elucidated based on the deletion of amino acids from the C-terminal end and Alanine based point mutation in acidic, aromatic and hydrophobic amino acid of the movement protein. Deletion of the C-terminal 55 aa of the *Tobacco mosaic virus* (TMV) MP does not affect the cell-to-cell transport of the TMV nor the cell wall localization of the protein (Berna *et al*., 1991). However, The *Alfalfa mosaic virus* (AMV) MP specifically interacts with its cognate CP through its C-terminal region and in the *Cowpea mosaic virus* (CPMV) MP this region is the virion-binding domain (Carvalho *et al*., 2003; Sanchez-Navarro *et al*., 2006). In the case of the MP of the *Cauliflower mosaic virus* (CaMV), the C-terminus interacts indirectly with the cognate CP via the virion-

associated protein (Stavolone *et al*., 2005). The C-terminal region of the corresponding MPs of the *Cucumber mosaic virus* (CMV) and the *Brome mosaic virus* (BMV) controls the requirement of the CP for intercellular movement (Nagano *et al*., 2001; Sanchez-Navarro and Bol, 2001; Takeda *et al*., 2004). Different C-terminal deletion (12, 38 or 42 aa) mutants of the *Prunus necrotic ringspot virus* (PNRSV) (Frederic Aparicio *et al*., 2010) revealed that MP genes lacking the C-terminal 12 or 38 aa did not block the virus transport. However, deletion of the C-terminal 42 residues restricted to single cells (Frederic Aparicio *et al*., 2010). Recently, Singh *et al*. (2014) reported that deletion of the C-terminal coiled coil domain of NSm abolish the vesicle formation and targeting of vesicle to plasmodesmata

The mutation in the region of C-terminal of AMV MP did not affect cell-to-cell transport but completely blocked systemic movement of the virus (Vander *et al*., 1994). The mutations in the MP and CP genes both affected cell-to-cell movement of AMV (Sanchez-Navarro and Bol, 2001; Vander *et al*., 1994). Transient expression of AMV MP in tobacco protoplasts resulted in the formation of tubular structures on the protoplast surface (Zheng *et. al.,* 1997). When protoplasts were infected with AMV, these tubules appeared to be filled with virus particles (Kasteel *et al.,* 1997). Huang *et al.,* 2001 showed that actin or microtubule components of the cytoskeleton are not involved in tubule formation, using Wt and mutant MP gene fused to the GFP. In addition to AMV, tubule formation has been observed in the family *Bromoviridae* for the cucumovirus, CMV; ilarvirus, TSV and the oleavirus, OLV; but the significance of these tubules in cell to cell transport is unclear. In PRNSV, the hydrophobic domain that interacts with membrane interface is needed for virus movement (Martínez-Gil *et al*., 2009).

TSV is considered as a one of the most devasting plant virus, causing severe economic losses (see chapter 2, section 2.2.6, table 2.4). These losses become more intense after movement of the infectious material or virion particle from site of infected cell to healthy cell and subsequently throughout whole plant through phloem/sieve element/companion cell complex (Lucas, 1995). It is remarkable that virtually nothing is known about the structural and cellular distribution facets of movement protein of the TSV. The scanty research in the area of TSV MP is easily recognized in the perspective of huge available literature on different viruses MP reviewed in Harries *et al*., 2010; Niehl and Heinlein, 2011. Some of them for example, TMV (Kragler *et al*., 2003, Curin

et al., 2007, Gillespie *et al*., 2002; Ruggenthaler *et al*., 2009; Pena and Heinlein 2013; Liu and Nelson 2013; Niehl *et al*., 2013a, Niehl *et al*., 2014), CMV (Canto and Palukaitis 2005, Nagano *et al*., 1997), AMV (Sanchez-Navarro and Bol. 2001; Vander, *et al*., 1994, Huang *et al*., 2001), CPMV (Pouwels *et al*., 2002, Carette *et al*., 2002, Carvalho *et al*., 2003; Sanchez-Navarro *et al*., 2006), BMV (Nagano *et al*., 2001; Takeda *et al*., 2004), *Groundnut bud necrosis virus* (Singh *et. al*., 2014), *Oilseed rape mosaic virus* (Niehl *et al*., 2014)

Based on the above literature background we have achieved the main objective of this work by different sub objectives as

- Cloning, overexpression and production of polyclonal antibody.
- Sub cellular distribution of MP using GFP, reporter gene.
- *In silico* analysis of movement protein to get insight into the structure and function.
- Elucidation of MP motif targeting to the PD.

6.2 Materials and methods

6.2.1 Plant material

Nicotiana benthamiana plants were grown in growth chamber that maintained at 27ºC temperature with 70 % humidity and 16/8 hours of light and dark periods.

6.2.2 Oligonucleotide primers

Primers used in this study were synthesised by Integrated DNA technologies (IDT, Coralville, USA). Primers are listed in table 6.1 also refer to chapter 4, table 4.1 for primers described earlier.

6.2.3 Binary vector

In the present study we have used pCB302 binary vector (Gopinath *et al*., 2005) for construction of MP-GFP fusion chimeras. The detail of this vector is mentioned in chapter 5, section 5.2.4.2.

6.2.4 pET28a expression vector

For overexpression of movement protein pET28a vector was used from Novagen, Germany.

Table 6.1: Oligonucleotides used for construction of MP construct

Primer name	Sequences 5'----------3'
MPNcoI+	GCCATGGGCGTTAGTACCAACGATGAAAGC
MPPstI+	CCGCCTGCAGGCGTTAGTACCAACGATGAAAGC
MPN7aa NcoI+	AGGGCCATGGCTTTGACATTCTCAGCA
MPN15aa NcoI+	GGGCCATGGCTGAGACATCTCTGGAG
MPN20aa NcoI+	AGGGCCATGGAGAAGGCTATAACAGAA
MP 15D-A & 16D-ANcoI+	GGATCCATGGCGTTAGTACCAACGATGAAAGCTTTGA CATTCTCAGCAGCTGCTGAGACATCTCTGG
MPD15ANcoI+	TTAACCATGGCGTTAGTACCAACGATGAAAGCTTTGA CATTCTCAGCAGCTGATGAGACATCT
MPD16ANcoI+	TTAACCATGGCGTTAGTACCAACGATGAAAGCTTTGA CATTCTCAGCAGATGCTGAGACATCTCTG
MP XhoI ER1-	GCTC GAG GAA TTC GGC TGA AAG CAG GTT CCT ACC TGC
MPNHisNcoI+	GCCATGG*CACCACCACCACCACCAC*GCGTTAGTACCAA CGATGAAAGC
MPI83A	TTCTCAGCAGCTGCTGAGACATCTCTGG
MPI91A	AGGGCCATGGCTTTGACATTCTCAGCA
MPstopXhoI-	GGG CTCGAG TCAGGC TGA AAG CAG GTT CCT ACC
MPXhoI-	GGG CTCGAG GGC TGA AAG CAG GTT CCT ACC

6.2.5 Overview for construction of the MP Wt, MP-N-His and MP-C-His in pET 28a over expression vector

Primarily , PCR was performed for cloning of three versions of the MP's; MP Wt, MP-N-His and MP-C-His using MP NcoI+ & MP ERI stop XhoI- , MPNHisNcoI+ & MP stop XhoI- and MP NcoI+ and MP XhoI- as a forward and reverse primer respectively. The PCR amplified products were cloned and confirmed in pTZ57R/T cloning vector as described in chapter 3, section 3.2.21. Secondly, three versions of MP genes were sub cloned into pET28a overexpression vector at *Nco*I and *Xho*I restriction site after excising the inserts from the recombinant pTZ57R/T plasmids harboring MP genes with *Nco*I and *Xho*I restriction enzyme. Overview of cloning of the three versions of MP genes in pET28a vector mentioned in fig 6.1.

6.2.6 Quantitative and qualitative analysis of polyclonal antibody

The movement protein antibody was quantified using DAC-ELISA mentioned in chapter 3, section 3.2.13.1.

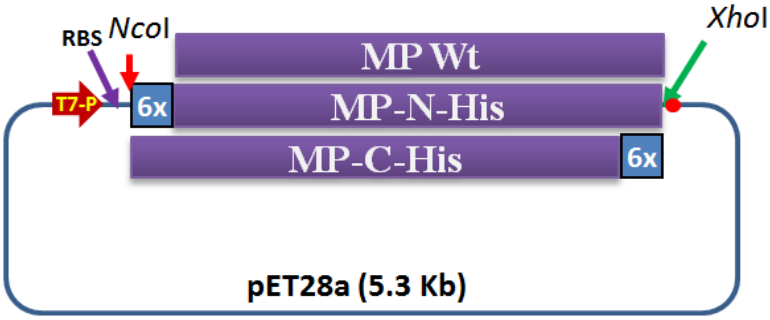

Fig 6.1: Overview for construction of three versions of movement protein, wild type, MP N-terminal his tag, MP with C-terminal his tag in pET28a bacterial expression vector.
Horizontal red color arrow at left side and red color circle at right side of the rectangular box indicate T7 promoter and stop codon respectively. RBS indicate the ribosome binding site and present between promoter and *Nco*I restriction site. 6X indicate the six histidine amino acid i.e. his tag. Violet color box with MP-Wt, MP-N-His and MP-C-His represent wild type MP, MP with N-terminal his tag and MP with C-terminal his tag. *Nco*I and *Xho*I is restriction site where three versions of movement protein were cloned.

6.2.7 Overview for construction of MP-GFP and GFP-MP chimera

To study sub cellular distribution of movement protein *in planta*, we have fused movement protein gene to GFP at N-terminus and C-terminus in pCB302 binary vector under control of 35S double promoter and 35S terminator at *Nco*I and *Xba*I restriction sites (fig 6.2).

The recombinant MP Wild type plasmids (pTZ57R/T vector) were digested with *Nco*I-*Eco*RI; pMP-*Pst*I plasmids with *Pst*I-*Xba*I and pMCSGFP (pTZ57R/T plasmids harboring mGFP5 sequence flanked with *Nco*I, *Eco*RI, *Hin*dIII on 5′-end and *Kpn*I, *Pst*I, *Bam*HI, *Xba*I on the 3′ end respectively) with *Eco*RI-*Xba*I and *Nco*I-*Pst*I standard protocol mentioned in chapter 3 section 3.2.25. The excised MP GFP fragments were gel extracted and ligated into binary vector backbone [In order to get pCB302 backbone, pTSV1a plasmids (recombinant pCB302 plasmid harboring 1a gene at *Nco*I and *Xba*I restriction sites) were digested with *Nco*I and *Xba*I; back bone was gel eluted and used in ligation steps of MP-GFP and GFP-MP at *Nco*I and *Xba*I site]. The ligated products were transformed into DH5α competence cells. The positive colonies were confirmed through double digestion as well as by PCR

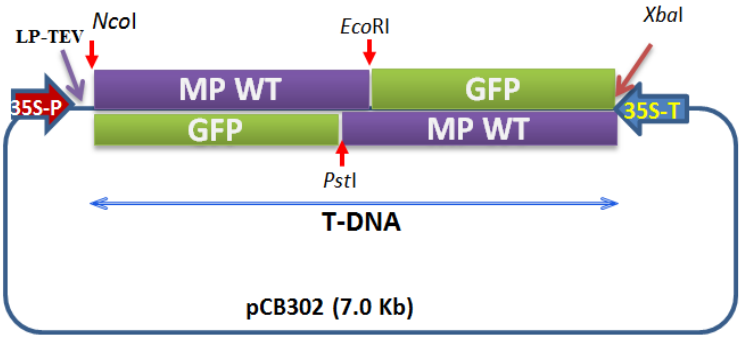

Fig 6.2: Overview for construction of MP-GFP and GFP-MP fusion chimeras in pCB302 binary vector.

The violet color rectangular boxes indicate wild type movement protein at left side and right side of the GFP in upper and lower panel respectively. Big arrow at left side and right side of the rectangular box indicate 35 S double promoter and 35 S terminator respectively. After 35 S double promoter leader peptide sequence showed with solid violet color arrow and it is derived from the *Tobacco etch virus.* Immediately after leader sequence *Nco*I restriction site and before 35S terminator *Xba*I restriction site is present. Fusion chimera was made at *Nco*I and *Xba*I restriction site. *Eco*RI and *Pst*I restriction sites are used for fusion of GFP with MP at N- terminal and C-terminal.

6.2.8 *In silico* analysis of movement protein

In silico analysis, we have used online and off line tools and server for prediction of primary, secondary and tertiary structure of the movement protein.

6.2.8.1 Primary and secondary structure of MP

For prediction of the primary structure and molecular composition of amino acid we utilized amino acid composition option embedded in Bioedit off line software. The secondary structure of the MP predicted by the on line tool MUSTER.

6.2.8.2 Homology modeling of MP

The 3D model of the MP was built by LOMETS (LOcalMEta-Threading-Server). It is a locally installed meta- server method for protein structure prediction. 10 locally installed sever which help in prediction of protein structure based on high resolution crystal structure of homologous proteins present in data base. In present study we have modeled movement protein.

6.2.8.3 Kyte and Doolittle Hydropathy plot

Hydrophobicity of the amino acid contributes to hydrophobicity profile of the protein. Each amino acid has been given a hydrophobicity score between -4.5 to 4.5.

Arginine and Isoleucine contribute the minimum and maximum to the hydrophobicity profile that is -4.5 and 4.5 respectively. A score of 4.5 is the most hydrophobic and a score of -4.5 is the most hydrophilic. A window size is the number of amino acids whose hydrophobicity scores will be averaged and assigned to the middle amino acid in the window. The averages are then plotted on a graph. The y axis represents the hydrophobicity scores and the x axis represents the position in the protein sequence.

6.2.9 Construction of Type I, II and III mutants

Type I mutants include MP-I83A-GFP, MP-I91A-GFP and MP-CΔ12aa-GFP indicate replacement of Isoleucine to Alanine at 83rd, 91st positions of MP, C –terminal deletion of 12 aa amino acids respectively. Type II mutants includes MP-NΔ7aa-GFP, MP-NΔ15aa-GFP, MP-NΔ20aa-GFP indicates N-terminal 7aa, 15aa and 20aa deletion respectively. Type III includes MP-D15A-GFP, MP-D16A-GFP and MP-15DA16DA-GFP indicates that replacement of acidic amino acid, Aspartic acid to Alanine at 15th, 16th position and double mutant respectively. Finally, all sequence confirmed plasmids were mobilized into agrobacterium by freeze thaw method.

6.2.9.1 Overview for construction of Type I mutants

To get MP-I83A-GFP and MP-I92A-GFP construct, Firstly, we designed two sets of mutagenic primer (mentioned in table 6.1) to replace isoleucine to Alanine at 83rd, 91st position of the MP using SDM as mentioned in chapter 5, section 5.2.6. The insertion of mutations was confirmed through sequencing and resultant plasmids designated as pMP-I83A and MPI92A. Secondly, pMP-I83A, MP-I92A plasmids were digested with the *Nco*I-*Eco*RI and pMP-Wt with *Nco*I-*Hin*dIII restriction enzyme. These digested products were used for the fusion of GFP at C-terminal in pCB302 binary vector (fig 6.3, panel A). The positive clones were confirmed through restriction digestion as well as sequencing. The constructed clones were named as pMPI83A-GFP, pMPI92A-GFP and pMP-CΔ12aa-GFP.

6.2.9.2 Overview for construction of Type II mutants

Taking MP wild type plasmid as template, PCR was performed using MPNΔ7aa NcoI+, MPNΔ15aa NcoI+, MPNΔ20aa NcoI+ as a forward primer and MP XbahoI stop ER1- as reverse primer (mentioned in table 6.1). PCR amplified products were extracted

from the gel and used as a template for restriction digestion with *Nco*I and *Eco*RI restriction enzyme. The purified restriction digested products were used as inserts for the construction of the MP-NΔ7aa-GFP, MP-NΔ15aa-GFP, MP-NΔ20aa-GFP chimera after fusing GFP with it. These fusions were carried out using three point ligation in pCB302 binary vector at *Nco*I and *Xba*I restriction sites (fig 6.3, panel B).

6.2.9.3 Overview for construction of Type III mutants

PCR was performed using MPD15ANcoI+, MPD16ANcoI+, MPD15A/D16 NcoI+ as a forward primer and MP XbahoI stop ER1- as reverse primer (mentioned in table 6.1) . The amplified PCR products represent MP-D15A, MP-D16A and MP-15DA16DA with *Nco*I at 5' end and *Eco*RI at 3' end. These products were extracted from the gel and used as a template for restriction digestion with *Nco*I and *Eco*RI restriction enzyme. The purified restriction digested products were used as inserts for the construction of the MP-D15A-GFP, MP-D16A-GFP and MP-15DA16DA-GFP chimera after fusing GFP with it. These fusion was carried out using three point ligation i.e. *Nco*I to *Eco*RI then *Eco*RI to *Xba*I in pCB302 binary vector at *Nco*I and *Xba*I restriction sites (fig 6.3, panel C).

6.2.10 Agroinfiltration and Confocal Laser Scanning Microscopy (CLSM)

Agrobacterium colonies were grown according to method described in chapter 5 section 5.2.13 and infiltration was performed using 0.6 OD of MP-GFP, GFP-MP and mGFP5 plasmid construct cultures. The Agro-infiltrated leaves were collected after 36 h of infiltration. A small section of the infiltrated leaf was cut with sharp razor; placed on the glass slide with forceps then covered with cover slip after adding few drops of water. Mounted sample on glass slide was analyzed through CLSM (Zeiss model: NL700) at wavelength 595 nm.

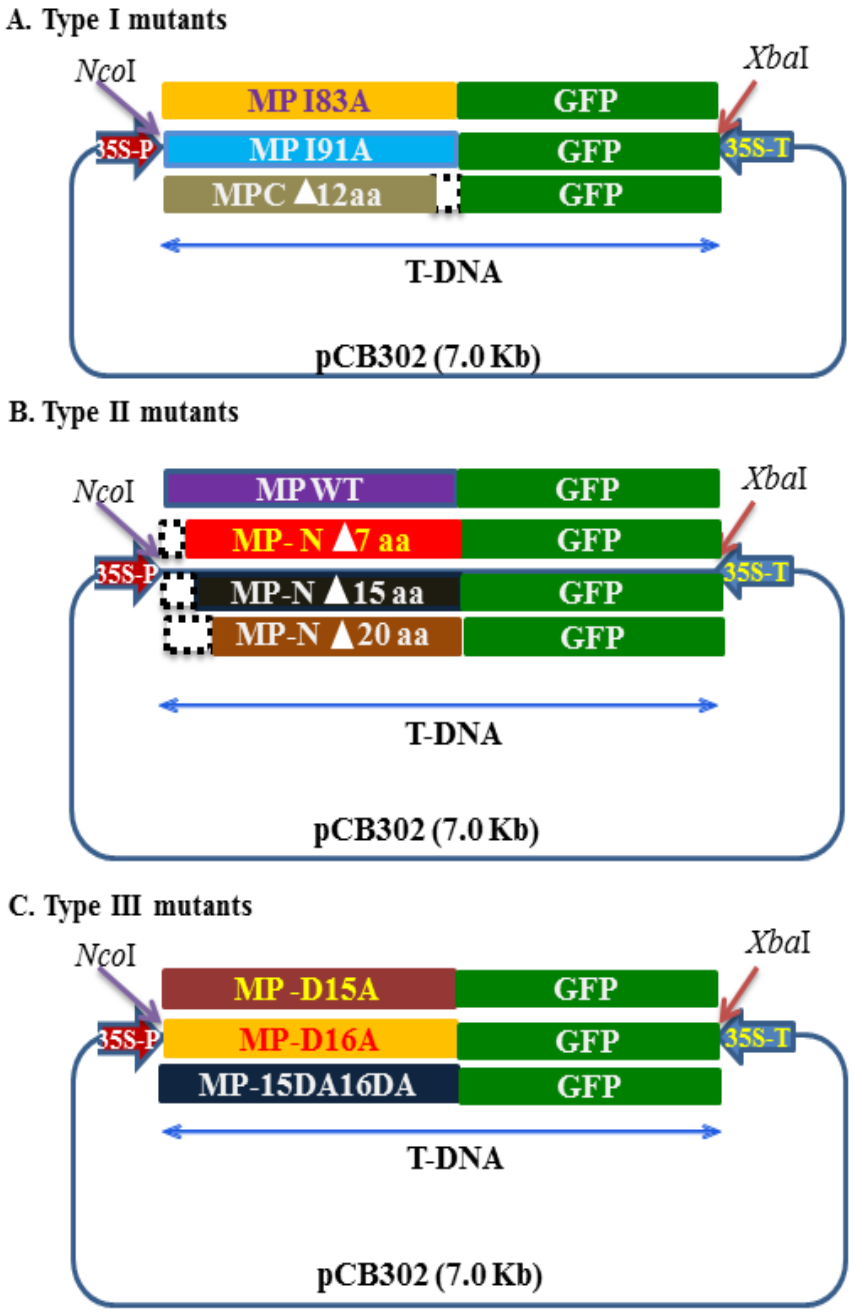

Fig 6.3: Overview for construction of type I, II and III mutants of movement protein GFP fusion chimera in pCB302 binary vector.

In panel A. type I mutants; MP-I83A, MP-I91A indicate replacement of isoleucine to Alanine at 83rd and 91st position of MP and MP-CΔ12aa indicate 12 aa deletion from C-terminal of the MP. In panel B. Type II mutants; MP-NΔ7aa, MP-NΔ15aa, MP-NΔ20aa indicates deletion of 7, 15 and 20 aa deletion from the N-terminal end of MP. In panel C, type III mutants; MP-D15A, MP-D16A and MP-15DA16DA indicating that the replacement of Aspartic acid to Alanine at 15 and 16th position and a double mutant (15th, 16th) respectively. The green color rectangular boxes indicate the GFP. *Eco*RI in all panel indicate the fusion point of MP and its mutants to GFP. 35S-P and 35S-T indicate the 35S double promoter and 35S terminator. MP and its mutant's fusion GFP chimera present between left boarder and right boarder indicated by the T-DNA.

6.3 Results

6.3.1 Cloning, overexpression, purification and production of poly clonal antibody of N-terminal his tagged version of movement protein.

6.3.1.1 PCR amplification, cloning and confirmation of MP gene in pTZ57R vector

Taking RNA3 full length plasmid as a template, PCR was performed for amplification of MP-Wt, MP-N-His and MP-C-His with respective primer as mentioned in table 6.1. The PCR amplified products 853 bp, 891 bp and 853 bp for MP-Wt (fig 6.4, panel A, lane 1), MP-N-His (fig 6.4, panel A, lane 2) and MP-C-His (fig 6.4, panel A, lane 3). The PCR products were cloned into pTZ57R/T cloning vector and clones were confirmed through the restriction digestion. The released inserts showed 853 bp (fig 6.4, panel B, lane 1), 891 bp (fig 6.4, panel B, lane 2) and 853 bp (fig 6.4, panel B, lane 3) after restriction digestion of the recombinant pTZ57R/T plasmid harboring wild type MP, MP-N-His and MP-C-His respectively with *Nco*I and *Xho*I restriction enzyme.

6.3.1.2 Sub cloning and confirmation of MP gene in pET 28a vectors

Wild type MP, C-terminal histag and N-terminus histag MP gene products were excised with *Nco*I and *Xho*I endonucleases from pTZ57R MP Plasmids, gel purified and subsequently cloned into the expression vector pET 28a at *Nco*I and *Xho*I restriction sites. The positive clones were confirmed through restriction digestion with the *Nco*I and *Xho*I restriction enzyme. Restriction digestion products for C-terminal histag and N-terminal histag plasmid of MP showed 853 bp (fig 6.5, panel A, lane 1) and 891 bp (fig 6.5, panel A, lane 2) respectively. The sequence confirmed plasmids were designated as pMP-Wt, pMP-C-His and pMP-N-His.

6.3.1.3 Overexpression and purification of MP with N-terminal histag protein in bacterial cells for raising the polyclonal antibodies

The positive clones were chemically mobilized into bacterial strain (DE3) Rosetta gamy cells and over expressed at 30°C and solubilized with 2 M urea. Supernatant fraction was purified with Ni-NTA Agarose by manufacture protocol (Qiagen) and purity of protein was checked in 12% SDS- PAGE (Fig 6.5, panel B). The purified protein showed 33 kDa (fig 6.5, panel B, lane 2 to 7). The purified protein was injected into the rabbit for polyclonal antibody production.

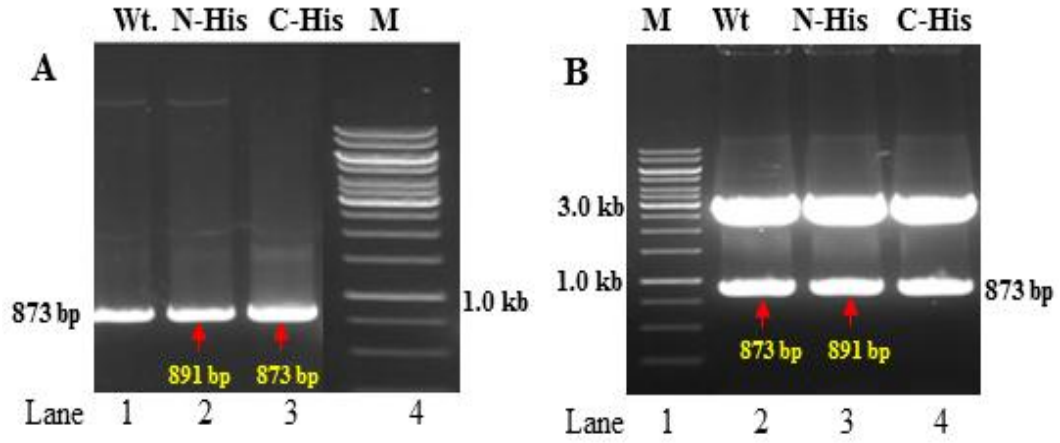

Fig 6.4 PCR amplification and cloning of three versions of MP; wild type, N-terminus histag and C- terminus histag

Panel A. PCR amplification for the three version of movement protein. Lane 1: PCR amplified product with MP NcoI+ forward primer and MP XbahoI stop ER1-reverse primer. Lane 2: PCR amplified product with MP His NcoI+ forward primer and MP stop XhoI- reverse primer. Lane 3: MP NcoI+ forward primer and MP XhoI -reverse primer. Panel B .Restriction digestion confirmation of pTZ57R/T recombinant plasmids harboring three version of the MP gene. Lane 1, 2 and 3 indicates restriction digestion confirmation MP-Wt, MP-N-His and MP-C-His respectively. M: 1.0 kb DNA ladder.

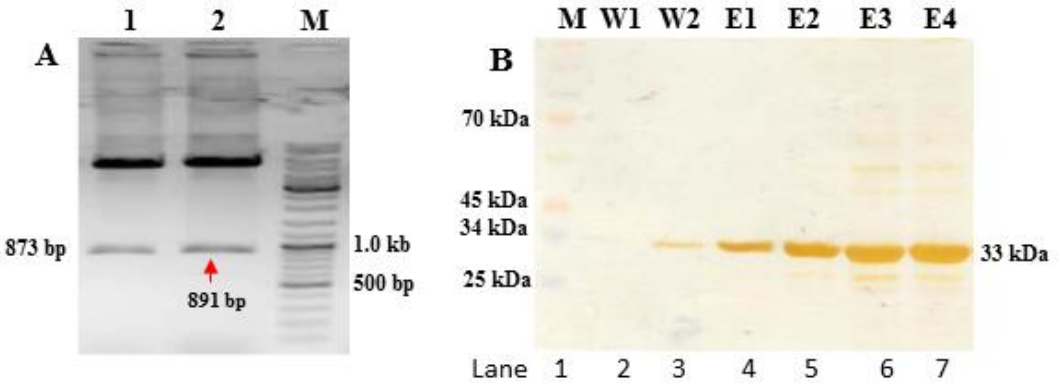

Fig 6.5: Cloning, confirmation, over expression and purification of MP.

Panel A. Cloning and confirmation of C-terminal and N-terminal his tag of MP. Lane 1 and 2: Restriction digestion confirmation of recombinant pET 28 a plasmid harboring MP gene with N-terminal histag and C-terminal histag respectively. M: 1.0 kb DNA ladder. Panel B showed purification profile of over expression MP with N-terminal histag. Supernatant fraction was purified with Ni-NTA Agarose according to manufacturer's protocol. In washing step little amount of protein was visible at 20 mM Imidazole (WI and W2). The proteins were eluted from Ni-NTA Agarose column with 100 mM Imidazole (E1 and E2) and 250 mM Imidazole (E3 and E4). Purity of protein was checked in 12% SDS- PAGE and strained with silver staining. M: Pre stained protein ladder.

6.3.1.4 Quantification of polyclonal antibody

The produced antibody was quantified using DAC-ELISA as mentioned in chapter 3, section 3.2.13.1. After yellow color development in DAC-ELISA, OD has taken at 405 nm. The graph was plotted optical density (OD) verses antibody dilution as 1:1250, 1:2500, 1:5000, 1:10000, 1:20000, 1:40000 and 1:80000 (fig 6.6). The sensitivity of the antibody showed up to 20000 dilutions against 10 ng of the antigen.

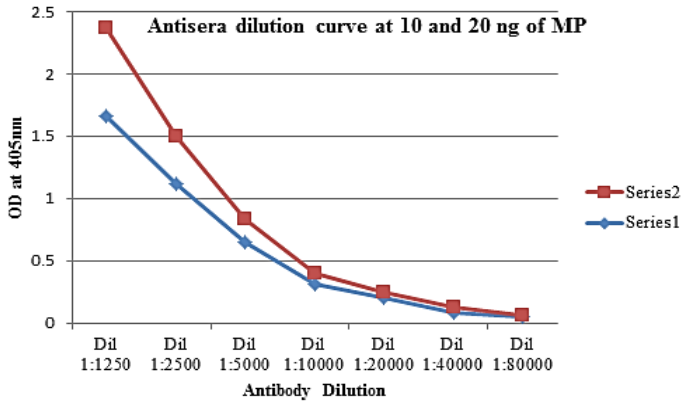

Fig 6.6: Quantification of the produced antibody against MP antigen through DAC-ELISA. X-axis and Y axis of the antibody titer curve represented by optical density at 405 nm and antibody dilution respectively. The antibody dilution was ranges from the 1:1250 to 1:80000. Series 1 and 2, indicates the antigen concentration as 10 ng. and 20 ng

6.3.2 Sub cellular distribution of MP

To elucidate the sub cellular distribution of movement protein, we fused the GFP to the movement protein.

6.3.2.1 Construction and confirmation of MP-GFP and GFP-MP chimera

Movement protein was fused to GFP at N-terminal and C-terminal in pCB302 binary vector at *Nco*I and *Xba*I restriction site as mentioned in section 6.2.6. Restriction digestion of MP-GFP and GFP-MP fusion chimera constructed plasmids showed 1582 bp [MP (853 bp) + GFP (729 bp)] of insert (fig 6.7, lane 1 and 2) in 1% agarose gel after digestion with *Nco*I and *Xba*I restriction enzyme.

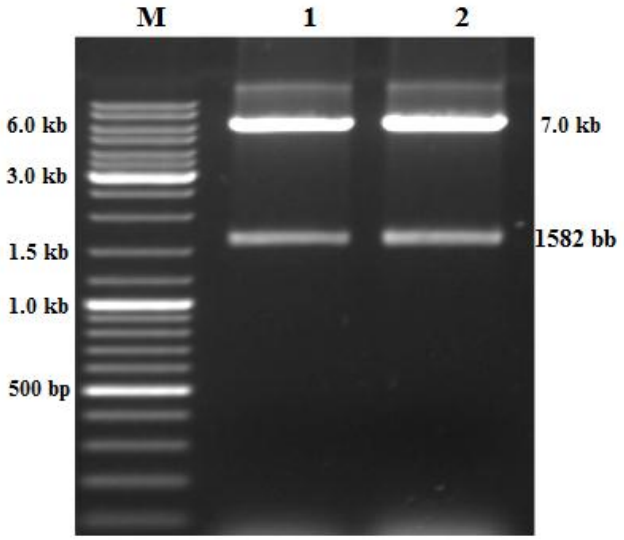

Fig 6.7: Restriction digestion confirmation of MP-GFP and GFP-MP chimera in pCB302 binary vector.
Lane 1: Restriction digestion pattern of pMP-GFP plasmids with *Nco*I and *Xba*I restriction enzyme. Lane 2: Restriction digestion pattern of pGFP-MP plasmids with *Nco*I and *Xba*I restriction enzyme. 1582 bp present at right side of the gel indicates, released insert after restriction digestion. Left side of the gel indicates molecular weight of 1.0 kb ladder.

6.3.2.2 Agroinfiltration and confocal microscopy

The agroinfiltrated *Nicotiana benthamiana* leaf samples were analyzed by confocal laser scanning microscopy. Flurorescence derived from mGFP5 was obsevered in epidermal cells of *Nicotiana benthamiana* leaf localized to all along the cell wall, cytoplasm and nucleus (fig 6.8, panel A, Free GFP). MP-GFP and GFP-MP protein accumulated as a punctate spots in the cell wall, which probably represent clusters of plasmodesmata. To check whether the punctate spot is present in cell wall or not, we co-expressed free RFP (Ds-Red) along with the MP-GFP fusion chimera.

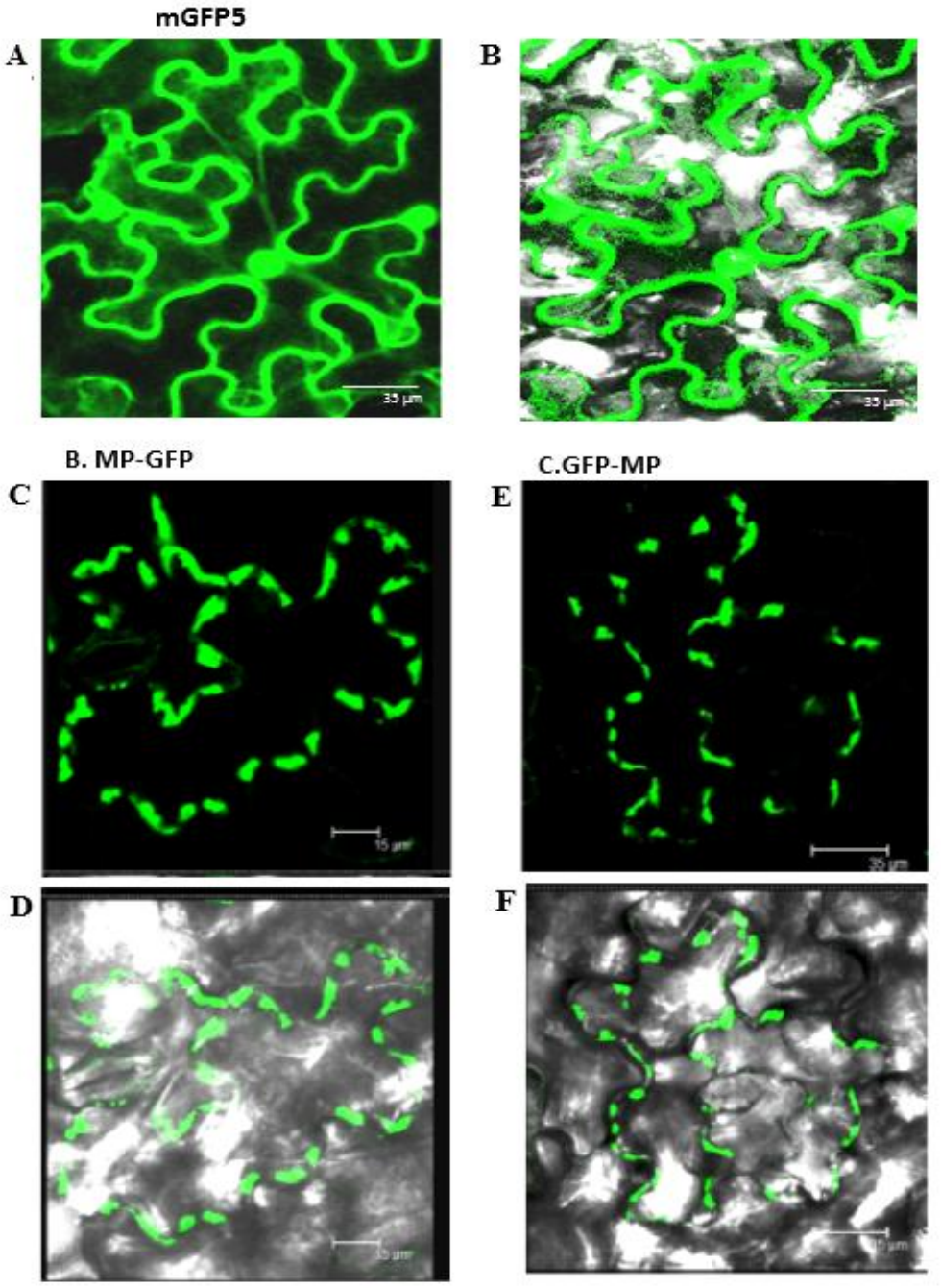

Fig 6.8: Sub cellular distribution of movement protein *in planta.*

MP gene tagged with GFP at N-terminal and C-terminal were expressed transiently in *Nicotiana benthamiana* leaf epidermal cells by agroinfiltration, and fluorescence was analyzed by confocal microscopy. In panel A: Fluorescence derived from mGFP5 in epidermal cells of *Nicotiana benthamiana* leaf seemingly localized all along cell wall as well as nucleus. In panel B: represent the overlay image; derive from the UV scanning and GFP fluorescence. In panel C and D are represented by the MP-GFP fusion chimera. Punctate green fluorescent spots present in the cell wall, which probably represent plasmodesmata. In panel E and F are represented by the GFP-MP fusion chimera. Green color punctate spots present in the cell wall of the host cell represent the plasmodesmata.

6.3.2.3 Co-expression of MP-GFP with free RFP

The agroinfiltration was performed with 0.6 OD of MP-GFP and free RFP of agroconstruct. The green flurorescent punctate spots (fig 6.9, panel A) were observed in confocal microscopy after 48 h of post infiltration. UV scanning of the epidermal cells was shown in fig 6.9, panel B. Red color flurorescence was obsevred all along the cell wall in panel C. This accumulated red color indicate the cell boundary. The red color cell boundary along with the yellow color flurorescent punctate spots was observed in overlay of MP-GFP and free RFP fluorescence. This yellow color spot indicate the clusters of plasmodesmata's.

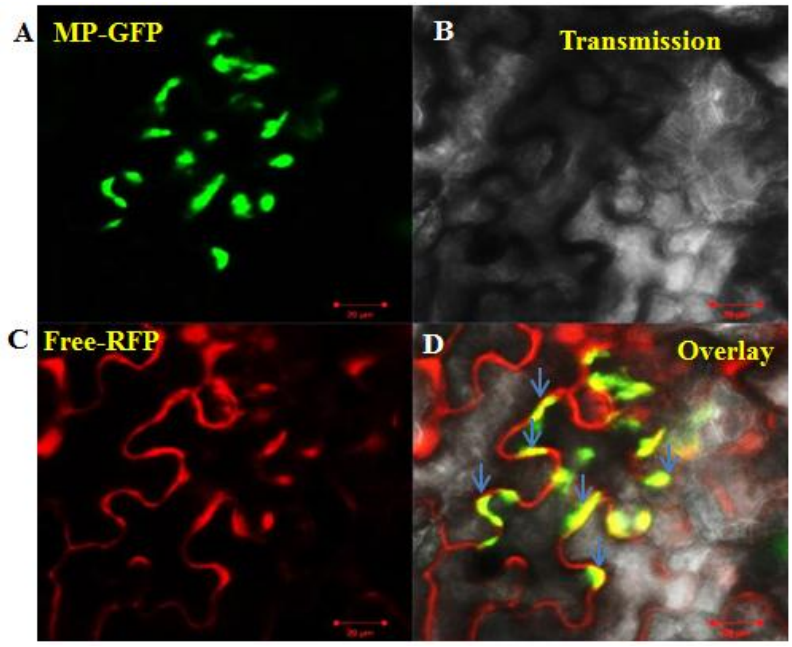

Fig 6.9: Co expression of the MP-GFP fusion chimera with free RFP.
In panel A indicate the Green color punctate fluorescent spot by the MP-GFP fusion chimera in the epidermal cell of *Nicotiana benthamiana* leaf. In panel B indicate UV scanning of the cell. In panel C: the red fluorescent was observed in confocal microscopy after 48 h of the post infiltration. Panel D indicate the overlay image of the UV scanning of the cell, fluorescence derived from the MP-GFP and free RFP. Arrows present in the panel D represents the yellow color punctate spot that indicate the cluster of the plasmodesmata.

6.3.2.4 Western blot confirmation

For immunological detection of GFP, polyclonal antiserum raised against GFP was used. Blotted proteins were detected using commercial ECL Kit (GE-health care) conjugated with HRP antibody. In western blot result of MP-GFP, GFP-MP and free GFP, we have observed signal in lane 3 to 5. No signal was observed in the healthy control (fig 6.10, lane 2) and in soluble fraction of MP-GFP and GFP-MP chimera (data

not shown). The cell wall fraction of MP-GFP and GFP-MP were isolated as mentioned in chapter 5, section 5.2.17. mGFP5 signal was observed at 28 kDa (fig 6.10, lane 5). The fusion chimera of movement protein with GFP; signal was observed at 61 kDa (33 kDa[MP] + 28 kDa[GFP]= 61 kDa) (fig 6.10, lane 2 and 3).

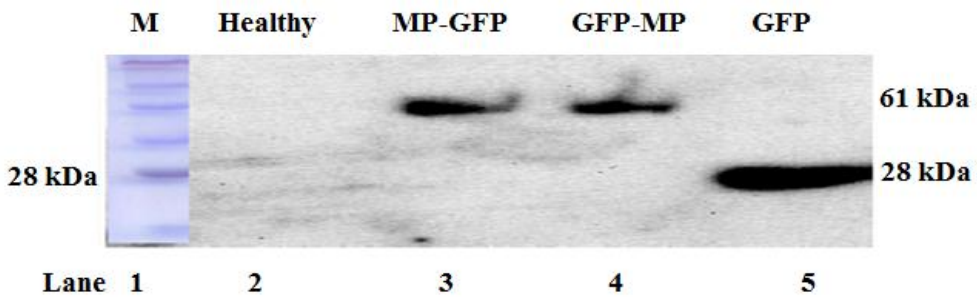

Fig 6.10: Western blot analysis of the GFP fusion chimera of the movement protein.
Western blot analysis for subcellular localized movement protein- green fluorescent protein (MP-GFP and GFP-MP) fusion chimera expressed in epidermal cell of *Nicotiana benthamiana.* Lane 1: protein ladder. Lane 2: healthy control, lane 3; membrane fraction of the MP-GFP; lane 4; membrane fraction of GFP-MP fusion chimera and lane 5; soluble fraction of the free GFP. Right side of the blot indicate the molecular weight of the free GFP i.e. 28 kDa and molecular weight of the GFP fusion chimera of the MP i.e. 61 kDa.

Based on the above results and literature we are sure that TSV movement protein targeting to the plasmodesmata. So, we want to elucidate the motif targeting to plasmodesmata. Towards this, we have performed extensive *in silico* study of the MP.

6.3.4 Insilco study of Movement protein

6.3.4.1 Primary structure of Movement protein

Primary structure of protein is linear arrangement of the amino acid in protein. Total 292 amino acids are present in movement protein of the TSV. Its calculated molecular mass is 31786.67 Daltons. The molecular composition of the amino acids present in movement protein showed in table 6.2. Leucine (L) is the amino acid that contributed maximum percentage i.e. 10.27% to movement protein followed by serine (9.59%), Alanine (8.90%). Tryptophan contributed lowest percentage of amino acid i.e. 1.03 % followed by cysteine (1.37%) and glutamine (1.71%).

Table 6.2: Amino acid composition for movement protein of TSV

Amino acid	Number	Percentage (%)
Ala A	26	8.90
Cys C	4	1.37
Asp D	15	5.14
Glu E	17	5.82
Phe F	10	3.42
Gly G	16	5.48
His H	6	2.05
Ile I	14	4.79
Lys K	20	6.85
Leu L	30	10.27
Met M	9	3.08
Asn N	9	3.08
Pro P	12	4.11
Gln Q	5	1.71
Arg R	13	4.45
Ser S	28	9.59
Thr T	25	8.59
Val V	22	7.53
Trp W	3	1.03
Try Y	6	2.05

6.3.4.2 Secondary structure analysis

Secondary structure was generated by the MUSTER on line server using amino acid sequence of movement protein. In secondary structure of MP, we observed eleven different lengths of α-helix (fig 6.11, panel B). Eleven variable lengths of arrows were showed the β-sheets (fig 6.11, panel B), 16 loops and 4 turn. Maximum amino acid residues were present in loop and it accounts for 135 aa and subsequently by the α-helix with 83 aa, β-sheet with 39 aa and turn with 32 aa. The percentage of the amino acid residues were observed in secondary structures of MP is 28.71%, 13.41%, 46.71% and 11.01% for α-helix, β-sheet, loops and turn respectively.

MALVPTMKAMTFSADDETSLEKAITEALSGSVELNMGLRRCAAFPAVNTGAFLCELTTKETKSFIGKFS
DKVRGRTFVDHAVIHLLYLPVILKTTYAISELKLKNLATGDELYGGTKVDLSKAaFILTMTWPRSLFAEAV
HAHRGLYLGGTVSCASSVPSNAKIGMWYPVWSEKVSNKQLYQNTVNIHSTEALETFTRTMISSDRE
MRSLLRSRASIDIAAKTPEKPVICSERVSLLDQHTQGVDFTVNEIDADKDDDAGTSVLGPKMVPIEQV
PSVKLPSSKAGRNLLSA*X

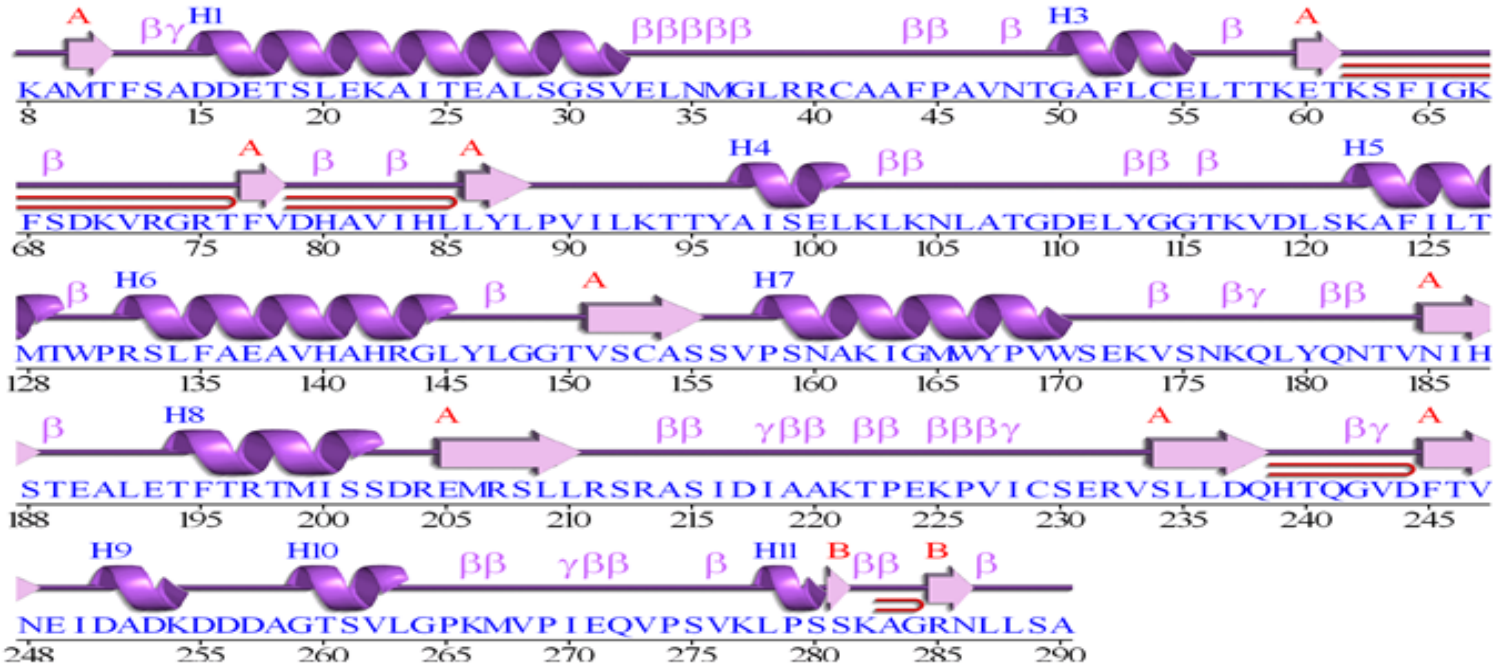

Fig 6.11: Primary and secondary structure of the movement protein.
Upper panel: Indicate the primary structure of the protein, showed linear arrangement of the amino acids
Lower panel: showed secondary structure of the movement protein predicted by the on line MUSTER server

6.3.4.3 3-Dimensional structure analysis

The complete amino acid sequence of the target protein MP was retrieved from NCBI (Accession No. ACT67450) in FASTA format (http://www.ncbi.nlm.nih.gov /Proteins). For a given target, 200 models were generated by 10 component servers where each server generates 20 models as sorted by their Z-scores in each algorithm. The best 10 models are finally selected from the 200 models based on the following scoring function: score(i,j)=Z(i,j)/Z0(i) * conf (i) +seq id(i,j) where Z(i,j) is the Z-score of j-th model of i-th server, Z0(i) is the cutoff of i-th server, conf(i) is the confidence of i-th server which is defined the average template modeling score (TM-score) to native of all predictions in a large-scale benchmark test. Seq id (i,j) is the sequence identity to query of j-th model of i-th server. The final model showed in fig 6.12 after energy minimization.

6.3.4.3.1 Model quality evaluation

In order to check the correctness of the geometrical parameter and quality of the homology model structure different parameters were analyzed such as Ramachandran plot, main chain parameter and side chain parameter of the protein. Here, we have emphasized on Ramachandran plot and main chain parameter of the movement protein which are the most important parameter to assess the quality and structural geometry of the protein (Ramachandran *et al*., 1963).

6.3.4.3.1.1 Ramachandran plot analysis of MP

The model has 95.7% of the residues in allowed region and 1.9% of the residues were found in the disallowed region of the Ramachandran plot (fig 6.13). The residues that were present in generously allowed and disallowed region of the Ramachandran plot are close to the regions of insertions that were looped out during model building. These residues are away from the active site and hence do not affect the structure function correlation studies of the protein.

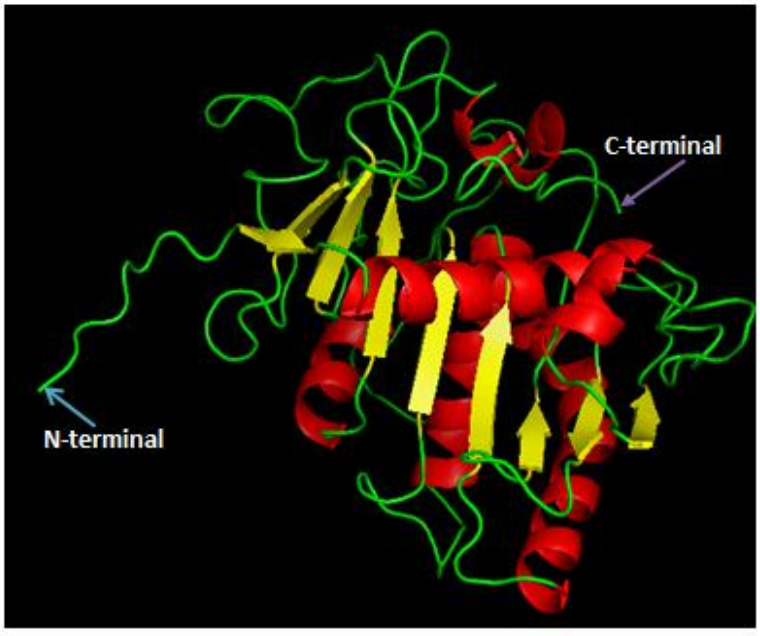

Fig 6.12: 3-Dimensional homology model of TSV movement protein.
Helix indicated by the red color, beta sheet represented by the yellow color. Green color thread indicates the loop of the MP. Arrow indicates the N-terminal and C-terminal end of the MP.

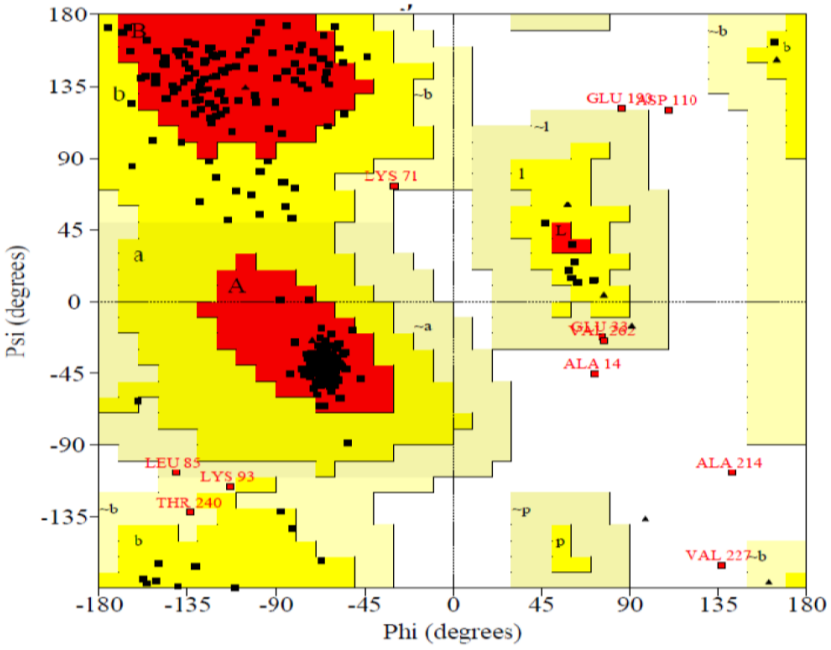

Fig 6.13: Ramachandran plot for TSV MP.
X-axis represented by the Phi (in degree) and y-axis represented by the Psi (degree). Red color A, B and L indicates the most favored region of the amino acids residues. Yellow color shaded area represented by a, b, l and p and it indicate the additionally allowed amino acids residues. Area after the yellow shaded symbol represented by the ~ a, ~ b, ~ l and ~ p and it indicate the generously allowed amino acids residues. The white color area indicates the disallowed region of amino acids residues.

6.3.4.3.1.2 Main chain parameters analysis of MP

The model was further analyzed for six different main chain parameters i.e. Ramachandran plot quality assessment, peptide bond planarity, measurement of bad non-bonded interaction, alpha carbon tetrahedral distortion, hydrogen bond energies and overall G- factor. Here, we have highlighted main chain parameters and found that predicted model was within the allowed region for above all six parameter. In the Ramachandran quality plot, the model was in the accepted range because 95.7% of the residues were present in the allowed region (fig 6.14, panel a). Planarity of the peptide bond was represented in fig 6.14, panel b. Omega angle is inversely proportional to the planarity of the peptide bond of the protein. Smaller the value of omega higher the planner of peptide bond of the protein. The planarity of the peptide bond indicates the unfolded nature of the protein and its competence to isomerize in *cis* or *trans* form. The standard deviation of omega torsion angles was 5.2 (fig 6.14, panel b). Bad contacts of the protein were measured for per 100 residues of the protein. Lesser the bad contact good will the model. Here, bad contact of movement protein showed 0.1 (fig 6.14, panel c) that indicate the good model quality. Standard deviation of zeta angle represented in fig 6.14, panel d and its coming acceptable range i.e. 1.7. Standard deviation of the hydrogen bond energy was 0.9 kcal/mol (fig 6.14, panel e). Normality is a stereochemical property of the protein and it is calculated in term of the average value of the overall G- factors of all the residues. G- factor depends on the no of the amino acid residues were present in allowed region of the Ramachandran plot. For highly stable protein, value of G- factor should be zero and it indicate 100% amino acid residues were present in allowed region of the Ramchandran plot. Due to 1.9% of the residues being in the disallowed region, the average G factor was -0.4 at the bond thickness of 2.0 Å (fig 6.14, panel f). The results showed that all the six parameters of model were within the allowed region (Jantana *et al*., 2011). The model which shows approximately 90% of the residues in the most favored region will be accepted by the PROCHECK.

6.3.4.4 Hydropathic index of MP

Hydropathic index of MP was elucidated by Kyte& Doolittle Hydropathy plot software. The range of maximum mean hydrophobicity region was found in between 83-95 aa of MP. The highest peak was observed at 91st position of MP because of isoleucine present at that position and it having maximum hydrophobic index.

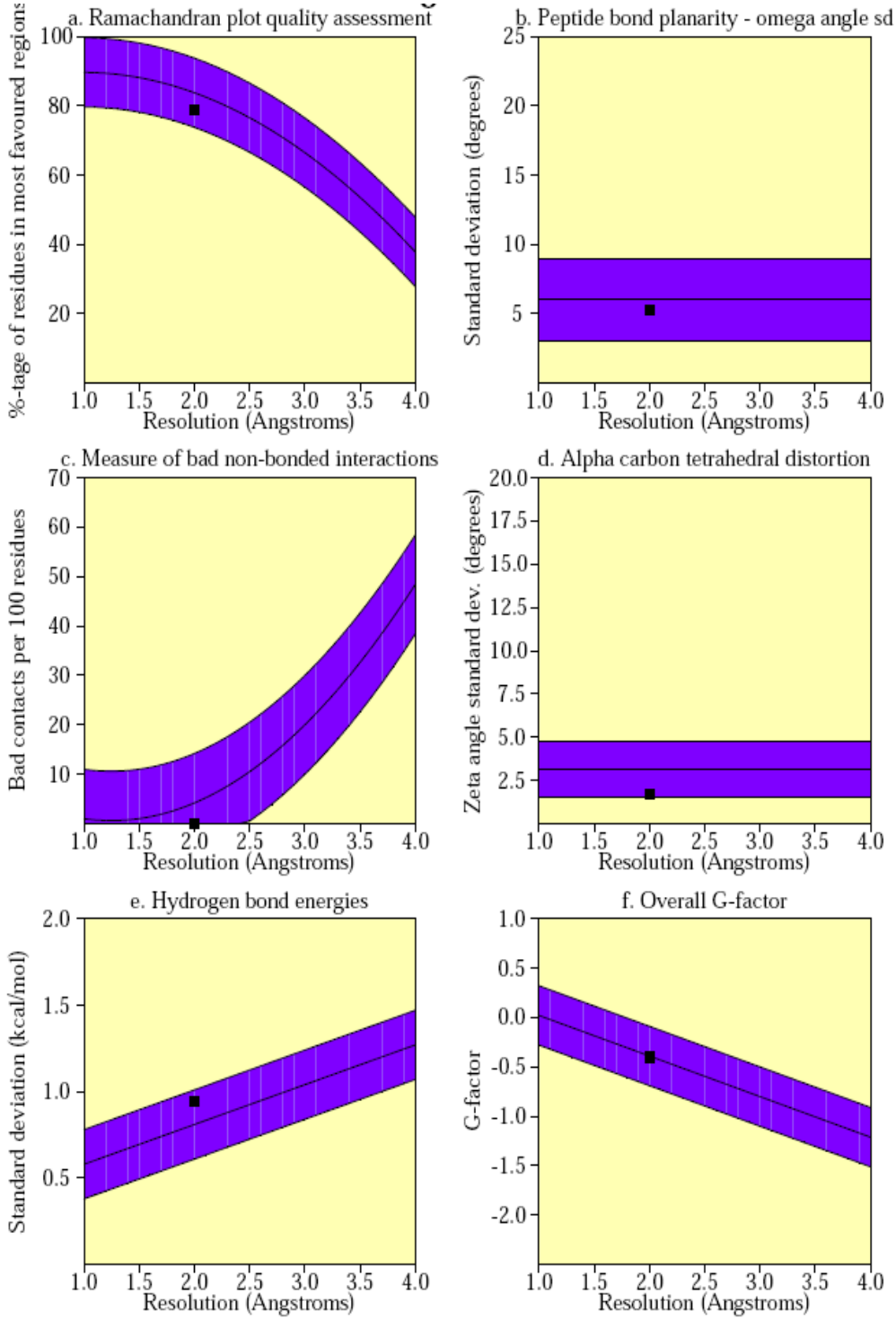

Fig 6.14: Main chain parameters of the model obtained by PROCHECK.

The dark band in each graph represents the result. The central line is a least squares fit to mean trend as a function of resolution and width of the band either side of it corresponds to a variation of one standard deviation about the mean.Panel a, b, c, d, e and f indicate the Ramachandran plot quality assessment, peptide bond planarity, measurement of bad non-bonded interaction, alpha carbon tetrahedral distortion, hydrogen bond energies and overall G- factor respectively. The results of the main chain parameter were explained in text.

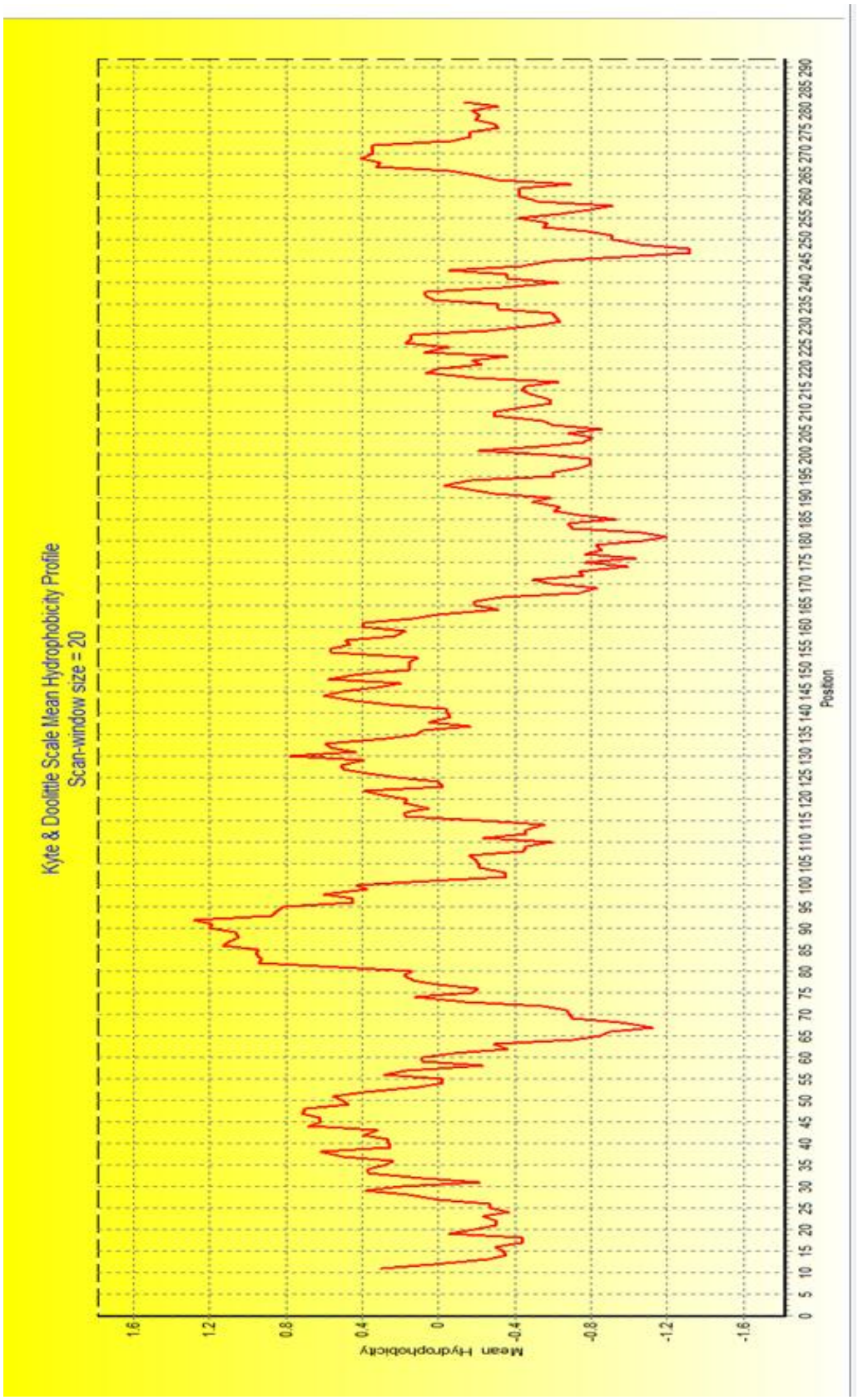

Fig 6.15: Kyte and Doolittle hydrophobicity profile of movement protein.
On the x-axis position of the amino acid and on y-axis mean hydrophobicity of the amino acid.

6.3.5 Elucidation of movement protein motif targeting to the plasmodesmata

Based on the *in silico* studies and literature survey, three types of mutants were generated. Type I mutants based on the hydrophobicity of amino acid viz; MP-I83A, MP-I91A and MP-CΔ12aa indicate replacement of Isoleucine to Alanine at 83rd , 91st position of MP, C-terminal deletion of 12 aa amino acid respectively. Type II mutants includes N-terminal deletion mutants. In this category we generated three mutants i.e. MPNΔ7aa, MPNΔ15aa, MPNΔ20aa indicates N-terminal 7aa, 15aa and 20aa deletion respectively. Type III includes MPD15A, MPD16A and MP15DA16DA indicate that replacement of acidic amino acid as Aspartic acid to Alanine at 15th, 16th and double mutant respectively. Detail of the construction of above constructs mentioned in the section 6.2.8. All mutants of movement protein gene were fused with the GFP at N-terminus in pCB302 binary vector and mobilized into agrobacterium. The resultant GFP chimera of Type I (MP-I83A-GFP, MP-I91A-GFP, MP-CΔ12aa-GFP), type II (MP-NΔ7aa-GFP, MP-NΔ15aa-GFP and MP-NΔ20aa-GFP) and type III (MP-D15A-GFP, MP-D16A-GFP and MP-15DA16DA-GFP) were expressed transiently in *Nicotiana benthamiana*.

6.3.5.1 Role of hydrophobic amino acid targeting to plasmodesmata (Type I)

6.3.5.1.1 Construction and confirmation of Type I mutants

The constructed clone of Type I mutants were confirmed through the restriction digestion. The plasmid pMP-I83A-GFP, pMP-I91A-GFP and pMP-CΔ12aa-GFP restricted digested with the *Nco*I and *Xba*I restriction enzymes. The released insert showed 1582 bp for pMP-I83A-GFP (fig 6.16, lane 2), pMP-I91A-GFP (fig 6.16, lane3) and 1546 bp (fig 6.16, lane 1) for the pMP-CΔ12aa-GFP. The restriction digested constructs were further confirmed through sequencing on both the ends.

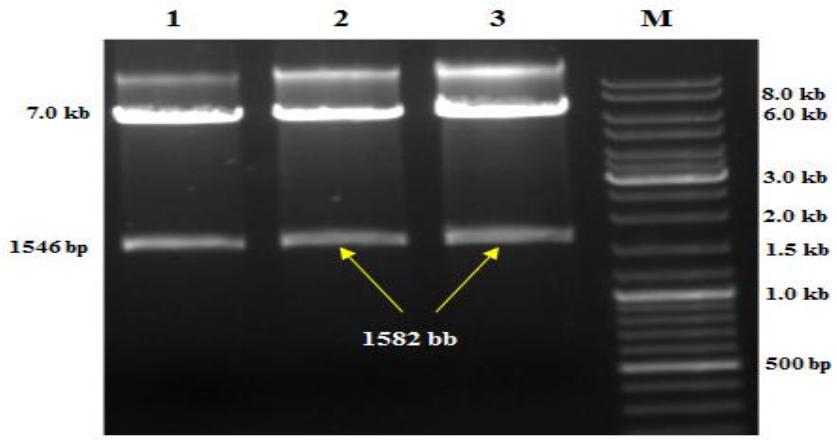

Fig 6.16: Cloning and confirmation of MP-I83A-GFP, MP-I91A-GFP and MP-CΔ12aa-GFP chimera in pCB302 binary vector.
Restriction digestion pattern of the plasmid pMP-I83A-GFP, pMP-I91A-GFP and pMP-CΔ12aa-GFP are in 1% agarose gel. Lane 1: pMP-CΔ12aa-GFP cut with *Nco*I and *Xba*I. Lane 2: pMP-I83A-GFP plasmid restricted digested with *Nco*I and *Xba*I and released 1582 bp. Lane 3: pMP-I91A-GFP plasmid digested with *Nco*I and *Xba*I restriction enzyme and Insert of 1546 bp released. Left side of the gel indicates 1.0 kb ladder.

6.3.5.1.2 Agroinfiltration and confocal microscopy of type I mutants

In type I mutants, MP-I83A-GFP chimera showed more punctate spots and accumulation level (fig 6.17 panel MP-I83A-GFP) compare to the wild type MP-GFP. Fluorescence was derived from the MP-I91A-GFP chimera showed more number of spot all along the cell wall. The nucleus was also observed in case of the MP-I91A-GFP (fig 6.17, panel MP-I91A-GFP). MP-CΔ12aa-GFP mutants located as fluorescent punctuate spots (fig 6.17, panel MP-CΔ12aa-GFP) in the cell wall. Among all the mutants in type I; MP-CΔ12aa-GFP mutants showed more number of spots (visually) compare to wild type and followed by MP-I91A-GFP and MP-I83A-GFP.

6.3.5.1.3 Western blot analysis of type I mutants

Western blot result showed signal in mGFP5 at 28 kDa (fig 6.18, lane 5). The fusion chimera of movement protein with GFP; signal was observed at 61 kDa (33 kDa[MP] + 28 kDa[GFP]= 61 kDa) (fig 6.18, lane 3, 4 and 5). This might indicate that, the fused GFP with movement protein gene is in frame. In case of the empty vector no detectable signal was observed.

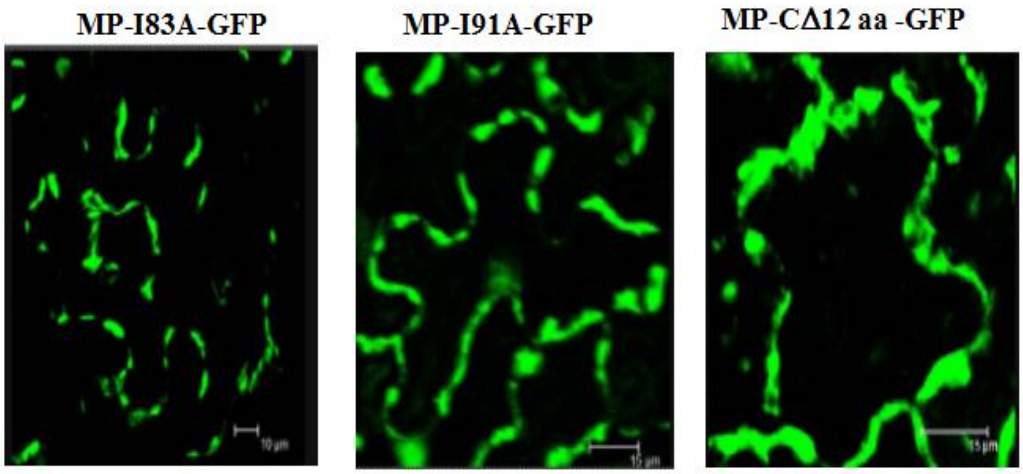

Fig 6.17: Sub cellular distribution of type I mutants *in vivo* in *Nicotiana benthamiana* leaf epidermal cells by agroinfiltration and confocal laser scanning microscopy.
Type I MP mutants gene tagged with GFP at C-teminus (pMP-I91A-GFP, pMP-I83A-GFP and pMPCΔ12aa-GFP). Panel MP-I91A-GFP, MP-I83A-GFP and MPCΔ12aa-GFP showed the flurorescence derived from the epidermal cells *of Nicotiana benthamiana* leaves seemingly localized to plasmodesmata as a punctate spots.

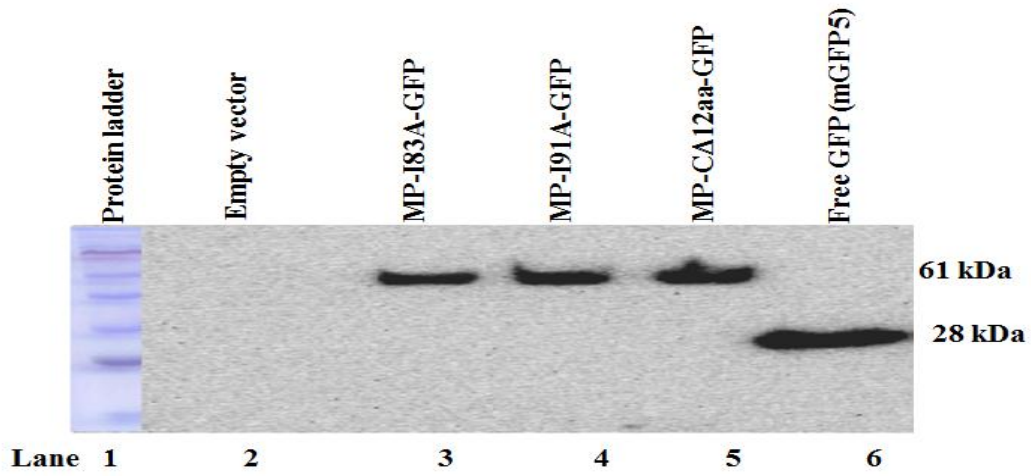

Fig 6.18: Western blot analysis of the type I mutants; MP-I83A-GFP, MP-I91A-GFP and MP-CΔ12aa-GFP.
Western blot for subcellular localized movement protein mutants- green fluorescent protein (MP-I83A-GFP, MP-I91A-GFP and MP-CΔ12aa-GFP) fusion chimera expressed in epidermal cell of *Nicotiana benthamiana.* Lane 1: protein ladder. Lane 2: empty vector control, lane 3: membrane fraction of the MP-I83A-GFP, lane 4: membrane fraction of MP-I91A-GFP, lane 5: membrane fraction of MP-CΔ12aa-GFP and lane 6: soluble fraction of the free GFP. Right side of the blot indicate the molecular weight of the free GFP i.e. 28 kDa and molecular weight of the GFP fusion chimera of the MP i.e. 61 kDa. Here, mGFP5 was used as positive control and empty vector as negative control.

6.3.5.2 Role of N-terminal amino acid targeting to plasmodesmata (Type II)

6.3.5.2.1 Construction and confirmation of Type II mutants

PCR was performed with MP and GFP specific primer for the confirmation of constructed clone. Here, we are showing only representative picture of the one clone from each mutant. Individual clone was confirmed with MPN7aa NcoI+, MPN15aa NcoI+ and MPN20aa NcoI+ as forward primer and reverse primer of MP, GFP specific primer and finally forward primer of respective MP deletion primers MPN7aa NcoI+, MPN15aa NcoI+ and MPN20aa NcoI+ and reverse primer of the GFP. PCR amplified product of the MP-NΔ7aa-GFP, MP-NΔ15aa-GFP and MP-NΔ20aa-GFP construct showed 831 bp (fig 6.19, lane 2), 808 bp (fig 6.19, lane 4) and 793 bp (fig 6.19, lane 7) respectively. The PCR amplified product of GFP for all constructs showed 729 bp (fig 6.19, lane 1, 5 and 8). MP-NΔ7aa-GFP, MP-NΔ15aa-GFP and MP-NΔ20aa-GFP construct showed 1560 bp (fig 6.19, lane 3), 1537 bp (fig 6.19, lane 6) and 1522 bp (fig 6.19, lane 9) amplification products with respective MP deletion forward primer and GFP reverse primer. In case of MP-N20aa-GFP chimera, the amplification of MP came very less intense (fig 6.19, lane 7). PCR confirmed plasmids were sequenced from the both ends. The sequenced confirmed plasmids were mobilized into the agrobacterium and confocal microscopy.

6.3.5.2.2 Agroinfiltration and confocal microscopy of Type II mutants

Type II movement protein gene mutants were infiltrated along with free GFP, free RFP and wild type MP-GFP as a positive control and internal control for each other. Here, MP-NΔ7aa-GFP showed more green fluorescents punctate spots (fig 6.20, panel D) compare to the wild type (fig 6.20, panel C). MP-NΔ15aa-GFP mutant fusion chimera accumulated as more spots (fig 6.20 panel E) (visually) as compare to MP-NΔ7aa-GFP and wild type. In case of MP-NΔ20aa-GFP, fluorescence was observed all along the cell membrane boundary and slightly in cytoplasm (fig 6.20, panel F). The MP-NΔ20aa-GFP mutants behave as the wild type free mGFP5 (fig 6.20, panel A) in all aspect expect the appearance in the nucleus and cytoplasm.

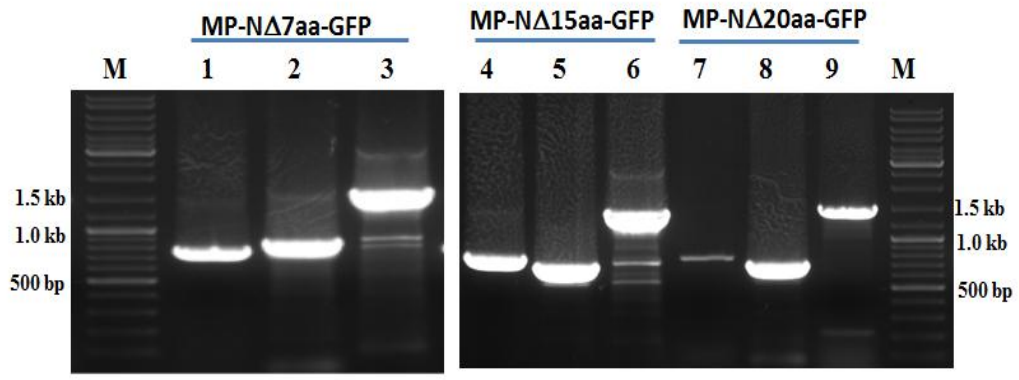

Fig 6.19: PCR confirmation of Type II MP deletion mutants GFP fusion chimera in pCB302 binary vector.

Lane 1 to 3, lane 4 to 6 and lane 7 to 9 indicate PCR confirmation of the MP-NΔ7aa-GFP, MP-NΔ15aa-GFP and MP-NΔ20aa-GFP respectively. Lane 1, 5 and 8 indicate the PCR amplification of the above mentioned constructs with the GFP FP and GFP reverse primer and showed amplification size 729 bp in all cases. Lane 2: PCR amplified product of MP-NΔ7aa-GFP construct with MPN7aa NcoI+ forward primer and MP reverse primer. Lane 3: PCR amplified product of MP-NΔ7aa-GFP construct with MPN7aaNcoI+ forward primer and GFP reverse primer. Lane 4: PCR amplified product of MP-NΔ15aa-GFP construct with MPN15aa NcoI+ forward primer and MP reverse primer. Lane 6: PCR amplified product of MP-NΔ15aa-GFP construct with MPN15aaNcoI+ forward primer and GFP reverse primer. Lane 7: PCR amplified product of MP-NΔ20aa-GFP construct with MPN20aa NcoI+ forward primer and MP reverse primer. Lane 6: PCR amplified product of MP-NΔ20aa-GFP construct with MPN20aaNcoI+ forward primer and GFP reverse primer. M: 1.0 kb DNA ladder.

6.3.5.3 Role of Acidic amino acid of MP targeting to plasmodesmata (Type III)

To understand further which amino acids are responsible for targeting to the plasmodesmata. We have selected acidic amino acid for point mutation, based on the available literature of movement proteins of *Cucumber mosaic virus* (CMV) (Canto and Palukaitis 2005). The selected acidic amino acid (aspartic acid) coming within the deletion mutants of MP-NΔ20aa-GFP. The type III movement protein includes three fusion chimeras; MP-D15A-GFP, MP-D16A-GFP and MP-15DA16DA-GFP. Detail of these mutants construction and confirmation were explained in the section 6.2.9.3.

6.3.5.3.1 Agroinfiltration and confocal microscopy of Type III mutants

MP-D15A-GFP showed more fluorescent punctate spots (fig 6.20, panel G) in epidermal cell of infiltrated *Nicotiana benthamiana* leaf compare to the wild type MP-GFP fusion chimera. In case of MP-D16A-GFP; the fluorescence was observed all along the cell wall and diffuse near cell membrane (fig 6.20, panel H). In the double mutants (MP-15DA16DA-GFP), sharp and intense green fluorescence were observed all along the cell wall.

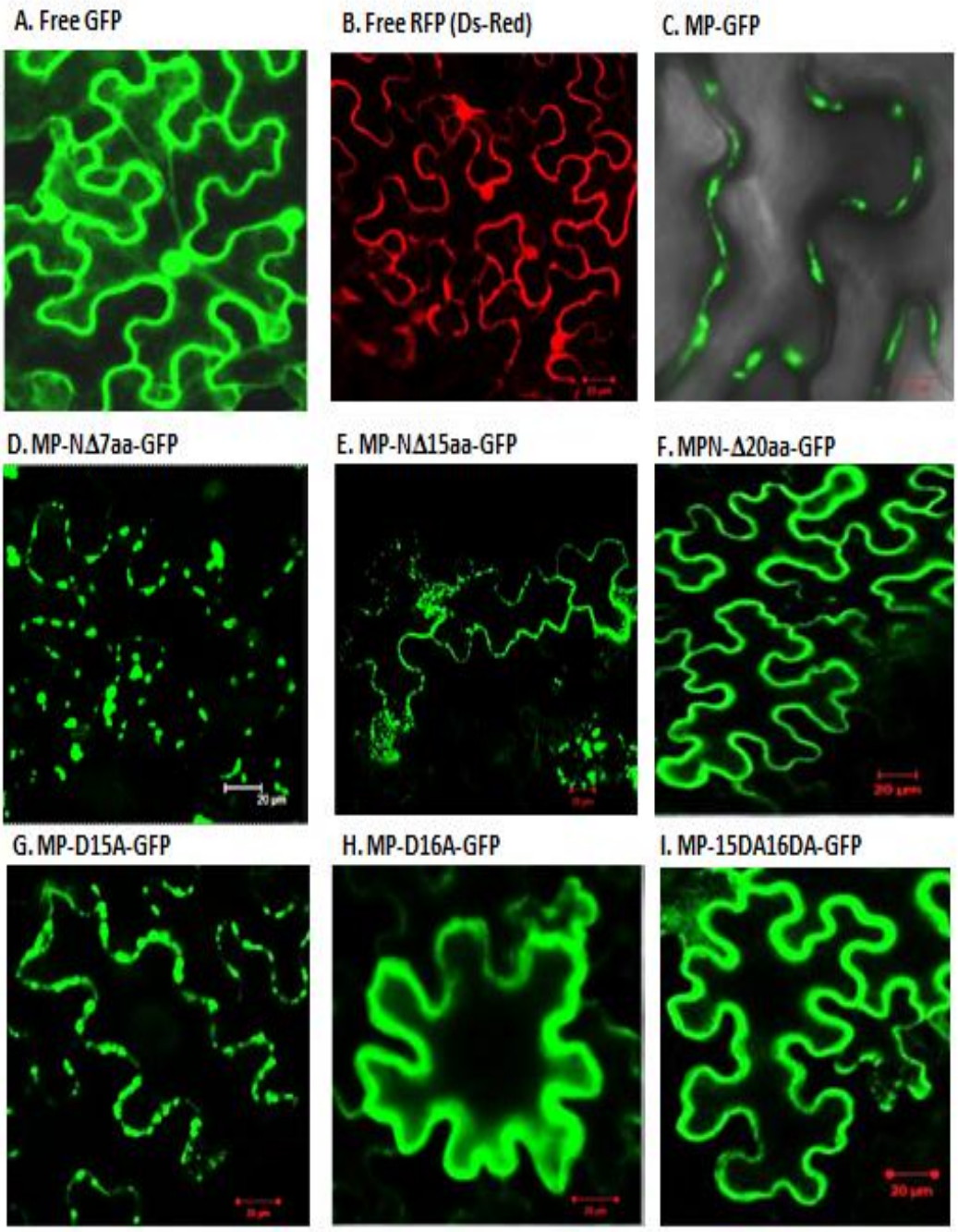

Fig 6.20: Sub cellular distribution analysis of the Type II and III MP mutants GFP fusion chimera through agroinfiltration and confocal laser scanning microscopy.
Panel A, B and C represent the free GFP, free RFP (Ds-Red) and MP-GFP respectively as positive and internal control for this experiment. Panel D, E and F indicate the type II mutants and panel G, H and I indicate the type III mutants. Green fluorescent was observed all along the cell wall, cytoplasm and nucleus (panel A). Red colour fluorescence was observed all along the cell wall, cytoplasm and nucleus (panel B). Punctate green fluorescence was observed in cell wall indicate the cluster of the plasmodesmata (panel C, D, E and G). In panel F, and I showed green fluorescence all along the cell wall. In panel H showed green colour fluorescence all along the cell wall and slightly in cytoplasm. Images were collected at 2 days after post infiltration and viewed by confocal microscopy.

6.4 Discussion

The work has been carried on MP of *Tobacco streak virus* at the molecular level is very less even though this virus has huge impact on the economy of the world. It is known to infect more than 20 field crops mainly in India (chapter 2, section 2.2.6.2, table 2.4). These losses become more severe once the movement of virion particle starts moving from infected cell to neighboring healthy cell and this process most of the time mediated by the MP by enlarging the size exclusion limit of the plasmodesmata. In the present study, we have tried to find the movement protein motif targeting to the plasmodesmata using *in silico* and mutation analysis approaches.

Initially, we have cloned three versions of movement protein gene to over express in bacterial system. Moment protein with N-terminal his tag version of MP gene was overexpressed and solubilized fraction was purified with Ni-NTA agarose bead. The produced polyclonal antibody against MP showed sensitivity 1:20,000 toward 10 ng of antigen. The produced antibody will be using, western blot analysis, Tissue imprinting and screening of the TSV infected sample.

Cellular distribution of movement protein was observed after fusing GFP tag at N-and C-terminus. Confocal laser scanning microscopy elucidated that; agroinfiltrated construct of MP-GFP and GFP-MP fusion chimera showed green color punctate spots in cell wall of the epidermal cell of *N. benthamiana*. These punctate spots might be cluster of plasmodesmata based on the available report of other plant virus movement proteins such as AMV (Huang *et al*., 2001), CMV(Canto and Palukaitis, 2005), *Red clover necrotic mosaic virus* (Tremblay *et al*., 2005) MNSV (Genovés *et al*., 2012) and *Oilseed rape mosaic virus* (Niehl *et al*., 2014). To validate further we have co-expressed MP-GFP fusion chimera construct along with the free RFP (Ds-Red) and found that yellow color punctate spot with red color cell boundary (fig.6.9). Yellow color punctate spots in the overlay image indicate the cluster of the plasmodemata.

In western blot, signal of the fused protein was observed at 61 kDa (33 kDa [MP] + 28 kDa [GFP]= 61 kDa) (fig 6.10, lane 3 and 4). This result might indicate that, the fused GFP with movement protein at N-terminal and C-terminal is in frame as it is showing 61 kDa. Soluble fraction of the GFP chimera of MP signal was not observe in western blot, however, in membrane fraction signal was at 61 kDa. As MP is associated with the membrane, it might target to the plasmodesmata. The intensity of signal indicate, level of protein accumulation. Level of accumulation of proteins was more in

case of GFP alone as compare to the fusion protein even though the membrane fraction of the fusion proteins were concentrated 20 time before loading in SDS-PAGE. Based on the confocal microscopy and western blot result we presume that movement protein of TSV targeting to the plasmodesmata.

Further, we have performed extensive *in silico* study to known the structural and functional relationship of MP. Towards this; the 3-D model of MP was generated and quality of the model was confirmed by different parameters such as Ramachandran plot quality assessment, peptide bond planarity, measurement of bad non-bonded interaction, alpha carbon tetrahedral distortion, hydrogen bond energies and overall G- factor respectively. All the parameters were obtained in allowed region. Hydrophobicity profile of MP showed that Isoleucine present at 83 nt and 91 nt position of the MP contributing maximum hydrophobicity.

Based on the *in silico* analysis and literature survey, three types of mutants were generated to elucidate the motif targeting to the plasmodesmata. Type I mutant mainly, based on the replacement of hydrophobic amino acid to the Alanine. We did not observe much difference in MP-I83A-GFP and MP-I91A-GFP chimera compare to the wild type. However, the accumulations of these mutants were targeting more compare to wild type. Martínez-Gil *et al*., (2009) reported in case of PRNSV, the hydrophobic domain that interacts with membrane interface is needed for virus movement. An another mutant of type I i.e MP-CΔ12aa-GFP, we have observed more accumulation in the cell wall compared to the wild type, MP-I83A-GFP and MP-I91A-GFP. This results agreeing with available literature on the other virus MP; PRNSV (Martínez-Gil *et al*., 2009) and [AMV (Vander *et al*.,1994), Huang *et al*., 2001]. However, in case of PNRSV, deletion of 42 amino acid residues of C-terminal MP resulted to single cells (Frederic Aparicio *et al*., 2010), in case of BMV, deletion of C-terminal region MP effect the intercellular movement (Nagano *et al*., 2001; Sanchez-Navarro and Bol, 2001; Takeda *et al*., 2004). Based on the above results we presumed that, selected hydrophobic amino acids and C-terminal 12 aa present in the type I mutants were not completely abolished targeting of MP to PD. However, these mutants increase the number of spots as well accumulation level of the mutants MP toward the cell wall (visually).

Once the C-terminal deletion and hydrophobic amino acids mutants did not abolished the targeting of MP to PD, then we have selected N-terminal region of the MP

for generation of deletion and point mutation. Here, we have generated three deletion mutants and three point mutations for our study. Out of the three deletion mutants; only one MP-NΔ20aa-GFP mutant was behaved as free GFP and indicating that the 20 amino acid residues of N-terminal MP might have a role for targeting to the plasmodesmata. Further, we have explored role of single or double amino acid residues present in the N-terminal of MP targeting to PD. Three point mutants were generated; MP-D15A-GFP, MP-D16A-GFP and MP-15DA16DA-GFP. Out of the three mutants; MP-D16A-GFP showed fluorescence all along the cell wall and diffuse near cell membrane. But, in case of double mutants (MP-15DA16DA-GFP), sharp and intense green fluorescence were observed all along the cell wall. Based on above results, we presume that aspartic amino acids present at 15^{th} and 16^{th} position of the MP having a role in targeting to the PD. However, Canto and Palukaitis 2005 reported; CMV MP loses its function targeting to the PD after replacement of Asp-20 and Asp 21 with Ala residues. In case of *Tomato spotted wilt virus*, Li *et al*., (2009) reported that replacement of charged amino acid acids [(Lysine (K), Arginine (R), Aspartic acid (D), Glutamic acid (E) and Histidine (H)] in conserved domain of NSm (KGK54-56, HH93-94, DSRK122-125, D154, DKDK230-233, and KKQLKE269-274) to Alanine abolished cell-to-cell movement.

Chapter–7

Summary

Summary

Virus-host interactions is an exciting topic in the field of molecular plant virology; how viruses on their way hijack most sophisticated plant defense systems and cause undesirable pathological disorders and crop losses. These pathological disorder are caused after successful completion of virus life cycle in host plant. The life cycles of plant viruses include phases of genome replication, virion assembly, cell-to-cell movement, systemic movement and plant to plant transmission. The annual estimated crop losses due to plant viral diseases range from $ 60-70 billion globally. Crop losses in peanut crops in the Anantapur district of Andhra Pradesh, India, alone are estimated to exceed 42 million pounds (Reddy *et al*., 2002). *Tobacco streak ilarvirus* (TSV) was also shown to cause sunflower (*Helianthus annuus*) necrosis disease (SND) (Prasada Rao *et al*., 2000). The combined losses in these two crops exceed US$ 90 million per year. Due to the economic importance of *Tobacco streak ilarvirus* (TSV), we have chosen as a model system in the laboratory to study the virus-host interaction.

TSV is a fast emerging and devastating plant virus transmitted by the Arthropod vector thrips, belongs to the family Bromoviridae and genus *Ilarvirus.* The genome of the virus is segmented and multipartite in nature; segregated in to three RNA molecules RNA1, RNA2, and RNA3

In present study we have set following objectives

1. Field surveys and partial characterization of *Tobacco streak ilarvirus* infecting different vegetable crops.

2. Complete nucleotide sequence and diversity analysis of three RNAs (RNA1, RNA2 and RNA3) of TSV-Okra strain.

3. Construction and characterization of full-length infectious clones for TSV-Okra strain.

4. *In planta* analysis of TSV movement protein (MP) as a GFP chimera and functional analysis of MP-GFP chimeric mutants through confocal laser scanning microscopy (CLSM).

In the first phase, we have identified four strains of TSV from the 500 virus infected field samples through serodiagnosis.

In serodiagnosis, majority of infected leaf material was observed TMV infections which accounted up to 29%. The disease incidence due to TSV, PBNV, CMV, and potyvirus are 20%, 28%, 14% and 8% respectively. We have observed mixed infections as well and selected four strains of TSV one each from okra, sunflower, peanut and tomato and single lesion assayed. Of the four; only okra strain of TSV replicated systemically in *Nicotiana benthamiana*.

In the host range studies, we have observed characteristics symptom for TSV and it established red bordered local lesions in *Gompherena globosa*, systemic symptom in *Datura stramonium*, chlorotic local lesions in *Chenopodium quinoa*, necrotic local lesions in *Phaseolus vulgaris* and chlorotic spots/vein clearing with dropping of inoculated leaves in *Vigna unguiculata* cv. C-152 respectively. We have identified *Nicotiana plumbigifolia* as a new experimental host for the TSV strain of okra with the characteristic symptom (chlorotic spots) within 4 days of the post inoculation.

TSV was purified from the *Phaseolus vulgaris* and purity was confirmed through SDS-PAGE and western blot analysis. The purified virus from sunflower source showed 28 kDa CP monomer as well as dimmer (56 kDa). Peanut and okra strain of TSV showed multiple bands in the higher order in SDS-PAGE analysis as well as western blots analysis with CP antibodies.

Polyclonal antiserum was produced against native and denatured virion particles. Polyclonal antibodies produced are highly specific which could detect up to 10 ng of purified virus and could detect up to 1:40,000 dilution in ELISA.

Transmission electron microscopy of purified virion particles with 1% uranyl acetate as negative stain revealed icosahedral (28 nm in diameter) morphology.

Coat protein gene of identified four strains of TSV were cloned into pGEM-T easy vectors and sequenced on both strands. NCBI blast search result of the sunflower strain of the TSV showed maximum homology (99.98 %) with the cotton strain of TSV and 99.58 % homology to sunflower strain. Peanut strain of TSV showed 99.78 % homology to the Kurnool peanut strain of TSV. Okra strain of TSV showed 99.98% homology with okra strain of Tamil Nadu. Tomato strain of the TSV was found closer to the reported peanut strain of the TSV with homology 99.68 % and 100 % at nucleotide and protein level respectively. To our knowledge, this is the first report of TSV infecting tomato from Indian subcontinent

Upon completion of the first phase we are successful in obtaining a TSV (Okra) strain which infects *Nicotiana benthamiana* model plant. Since, we would like to use this strain in the laboratory as a model virus we set the objective of achieving the complete genome sequence of the three RNA molecules using reverse transcribing (RT-PCR) approaches as the second objective.

Using NCBI data base TSV-okra strain as a template (FJ561302.1 for RNA1; FJ561303.1 for RNA2 and FJ561304.1 for RNA3 respectively), specific/degenerate primers were designed and several cDNA reactions were performed using *pfu* polymerase. The resultant DNA fragments from RT-PCR were gel purified, polyadenylated using *Taq* DNA polymerase and cloned into pGEMT-easy cloning vectors (Promega) and sequenced in both the directions. The 5' and 3' authentic ends of all viral RNAs were confirmed through 5'-RACE and 3'-polyadenylation.

Complete nucleotide sequence of RNA1, RNA2 and RNA3 were deduced by BioEdit software using different overlapping clone sequences. Overall, RNA1 has a very short 5' UTR (37 nt), 3279 nt of 1a ORF and 207 nt of 3' UTR. RNA2 also has short 5' UTR (42 nt), 2379 nt of 2a ORF, 600 nt of 2b ORF and 140 nt of 3' UTR. RNA3 had 211 nt of 5' UTR, 873 nt of MP ORF, 123 nt of inter cistronic region (ICR), 717 nt of coat protein ORF and 289 nt of 3' UTR respectively.

NCBI blast result of 1a gene of TSV okra strain showed homology of 99.7-99.8% with Indian strain, 79-80% with Australian strain and 85-86% with USA strain of TSV at nucleotide level. At amino acid level it showed homology of 98-99% to Indian strain, 86-93% with Australian strain and 89-93% with USA strain. Phylogenetic trees were constructed for nucleotide and amino acid sequence of genes using MEGA 6 software; showed two clusters; all Indian strains are clustering together and USA strains are forming another cluster, Australian strain 1973 showed maximum variation and separated as an out group member. Phylogenetic and BLAST analysis result showed that RNA3 was more conserved and less susceptible to the evolutionary pressure. However, RNA2 was showed maximum variation at amino acid as well as nucleotide level. 2b gene showed more diverse in nature among the TSV encoded gene.

After achieving the complete genomic sequences in the form of cDNAs of RNA1, 2, 3 and 4, we have converted these RNAs molecules into infectious cDNA clones by fusing 35S promoter at 5' end and ribozyme at 3' end and cloned into

pCB301 binary vector at *Bgl*II and *Xma*I restriction sites (Gopinath *et al*., 2005). In similar way TSV genome encoded genes (1a, 2a, MP and CP) were cloned under control of 35S double promoter at 5' end and 35S terminator at 3' end at *Nco*I and *Xba*I restriction sites in pCB302 binary vector (Gopinath *et al*., 2005). The positive clones are mobilized into *Agrobacterium* strain EHA105 by freeze thaw method.

Primarily, we have check the biological activity and infectious nature of the constructed clones after infiltrating different combination of agroconstructs with proper internal controls. None of the combinations were resulted visual expression of the symptom.

Further, we have analyzed the *in planta* transcription of the cDNA constructs by performing to the total RNA of infiltrated leaves. The expected PCR amplicon (400 bp) at the 3' end of the viral genome was amplied with specific primer sets. This indicates that the transcription is efficiently starting from the 5' end reaching to the 3' end.

We have checked translation products from these transcripts by western blot analysis using the polyclonal antibodies raised against encoded protein 1a, (truncated version), 2a, MP and CP genes.

Even though all the constructed clones were able transcribe and translate efficiently not able to produce the visible symptom on the *N. benthamiana* and *Phaselous vulgaris.* So, in the present study, constructed clone showed not biological active.

In the final chapter, we have set the objective of analyzing sub cellular localization/distribution characteristics of the MP and functional analysis of movement protein of TSV *in planta.* Towards this, we have fused movement protein gene to GFP at N- and C-terminus and cloned in to pCB302 binary vector under the control of 35S double promoter and 35S terminator. Resultant fusion clones MP-GFP and GFP-MP chimeras were mobilized into *Agrobacterium* EHA 105 strain; expressed transiently in *Nicotiana benthamiana* as described in the above section and analyzed by CLSM.

Flurorescence derived from the positive control mGFP5 construct, GFP fluorescence in the epidermal cells of *Nicotiana benthamiana* leaf apparently localized all along the cell wall as well in the nucleus. MP-GFP and GFP-MP fusion proteins accumulated as fluorescent punctate spots in the cell wall, which in all

probability represent clusters of plasmodesmata (PD). These fusions were confirmed through the western blot analysis.

To elucidate the MP motif targeting to PD; *in silico* analysis of MP was performed using secondary structure prediction by MUSTER, 3D structure by homology modeling and hydropathic index by Kyte & Doolittle hydropathy plot software. Based on *in silico* analysis, three types of MP-GFP

Type I chimeric MP mutant located as fluorescent punctuate spots in the cell wall as that of wild type MP, indicating that the selected hydrophobic amino acids and C-terminal 12 amino acids are not responsible for targeting of MP to plasmodesmata.

Type II MP-N-terminal deletion mutant; MP-NΔ7aa-GFP showed fluorescent punctuate spot pattern as that of wild type; however, MP-NΔ15aa-GFP showed more fluorescent punctuate spots (visually) in the cell wall than the wild type. Surprisingly, MP-NΔ20aa-GFP showed accumulation all along the cell wall similar to that of the positive control mGFP5, indicating that the N-terminal 20 amino acids might have a role in targeting the MP to plasmodesmata.

Type III MP mutant chimeras; MP-D15A-GFP showed more fluorescent punctuate spots compared to the wild type but in case MP-D16A-GFP fluorescence was observed all along the cell wall and slightly diffuse near the cell boundary. The green fluorescent was observed more intense and sharp all along the cell wall from MP-15DA16DA-GFP double mutant. The mutation at Aspartic acids at position 15 and 16 might have a role in the MP targeting to the PD.

References

and

Appendix

References

Adetuyi, F.O., Osagie, A.U. and Adekunle, A.T. 2008. Effect of Postharvest Storage Techniques on the Nutritional Properties of Benin Indigenous Okra *Abelmoschus esculentus* (L) Moench. Pakistan J. Nutrit. 7: 652-65.

Ahlquist, P., French, R., Janda, M. and Loesch-Fries, L. S. 1984. Multicomponent RNA plant virus infection derived from cloned viral cDNA. Proc. Natl. Acad. Sci. USA 81: 7066-7070.

Akinyele, B. O. and Temikotan, T. 2007. Effect of variation in soil texture on the vegetative and pod characteristics of okra (*Abelmoschus esculentus* (L.) Moench). Intern. J. Agric. Res. 2: 165-169.

Alegbejo, M., Ogunlana, M., and Banwo, O. 2008. Survey for incidence of *okra mosaic virus* in northern Nigeria and evidence for its transmission by beetles. Spanish J. Agric. Res. 6: 408-411.

Ali, M. A., Winter, S. and Dafalla, G. A. 2009. *Tobacco streak virus* infecting faba bean reported from the first time. Plant. pathol. 58: 466.

Almeida, Á. M. R., Sakai, J., Hanada, K., Oliveira, T. G., Belintani, P., Kitajima, E. W., Souto, E. R., Novaes, T. G. and Nora, P. S. 2005. Biological and Molecular Characterization of an Isolate of *Tobacco streak virus* Obtained from Soybeans in Brazil. Fitopatol. Bras. 30(4): 366-373.

Altschul, S. F., Gish, W., Miller, W., Myers, E. W. and Lipman, D. J. 1990. Basic local alignment search tool. J. Mol. Biol. 215: 403-410.

Amari, K., Boutant, K., Hofmann, C., Schmitt-Keichinger, C., Fernandez-Calvino, L., Didier, P., Lerich, A., Mutterer, J., Thomas, C. L., Heinlein, M., Mely, Y., Andrew J. Maule, A. J. and Ritzenthaler, C. 2011. A family of plasmodesmal proteins with receptor-like properties for plant viral movement proteins. PLoS Path. 6 (9): 1-10.

Annamalai, P. and Rao, A. L. N. 2005. Replication-independent expression of genome components and capsid protein of *brome mosaic virus* in planta: a functional role for viral replicase in RNA packaging. Virol. 338: 96-111.

Andret-Link, P. and Fuchs, M. 2005. Transmission specificity of plant viruses by vectors**.** J. Plant. Pathol. 87 (3): 153-165.

Annual progress report of AICRP on oilseeds (sunflower) 1997. Hyderabad, India: Directorate of Oilseeds Research, ICAR. 167 p.

Aparicio, F., Vicente, P. and Sanchez-Navarro, J. 2010. Implication of the C terminus of the *Prunus necrotic ringspot virus* movement protein in cell-to-cell transport and in its interaction with the coat protein. J. Gen. Virol. 91: 1865-1870.

Arslan1, D., Legendre1, M., Seltzer, V., Abergel, C. and Claverie, J. M. 2011. Distant Mimivirus relative with a larger genome highlights the fundamental features of Megaviridae. Proc. Natl. Acad. Sci. USA 108 (42): 17486-1749.

Arun, K. N., Lakhmi, N. M., Zehr, U. B. and Ravi, K. S. 2007. First report of *Tobacco streak virus* infecting *Guizotia abyssinica* from India. Plant Dis. 91: 330.

Arun, K. N., Lakshmi, N. M., Zehr, U. B. and Ravi, K. S. 2008. Molecular characterization of *Tobacco streak virus* causing soybean necrosis in India. Indian J. Bioethanol. 7: 214-217.

Ashby, J., Boutant, E., Seemanpillai, M., Groner, A., Sambade, A., Ritzenthaler, C. and Heinlein, M. 2006. *Tobacco mosaic virus* movement protein functions as a structural microtubule associated protein. J. Virol. 80: 8329-8344.

Asurmendi, S., Berg, R. H., Koo, J. C. and Beachy, R. N. 2004. Coat protein regulates formation of replication complexes during *tobacco mosaic virus* infection. Proc. Natl. Acad. Sci. USA 101:1415-1420.

Atabekov, J. G. and Taliansky, M. E. 1990 Expression of a plant virus-coded transport function by different viral genomes. Adv. Virus. Res. 38: 201-48.

Atkins, D., Hull, R., Wells, B., Roberts, K., Moore, P. and Beachy, R. N. 1991. The *tobacco mosaic virus* 30K movement protein in transgenic tobacco plants is localized to plasmodesmata. J. Gen. Virol. 72: 209-211.

Baltimore, D. 1970. RNA-dependent DNA polymerase in virions of RNA tumour viruses. Nat. 226: 1209-1211.

Barker, H. 1987. Invasion of non phloem tissue in Nicotiana clevelandii by *potato leafroll lutiovirus* is enhanced in plants also infected with potao y potyvirus. J. Gen. Virol. 68: 1223-1227.

Barna, A., Wolf, S., Lucas, W. J., Holt, C. A. and Beachy, R. 1991. The TMV movement protein: role of the C terminus 73 amino acids in sub cellular localization and ffuction. Virol. 182: 695-689.

Bartlett, J. 2003. PCR Protocols. Humana Press. Totowa, NJ.

Benchasri, S. 2012. Screening for yellow vein mosaic virus resistance and yield loss of okra under field conditions in Southern Thailand. J. Animal Plant Sci. 12: 1676-1686.

Benitez-Alfonso, Y., Faulkner, C., Ritzenthaler, C. and Maule, A. J. 2010. Plasmodesmata: gateways to local and systemic virus infection. Mol. Plant-Microbe Interact. 23: 1403-1412.

Berna, A., Gafny, R., Wolf, S., Lucas, W. J., Holt, C. A. and Beachy, R. N. 1991. The TMV movement protein: role of the C-terminal 73 amino acids in subcellular localization and function. Virol. 182: 682-689.

Bhaskara, R. B. V., Sivaprasad, Y., Naresh, K. C. V. M., Sujitha, A., Raja, R. K. and Sai Gopal, D. V. R. 2012. First Report of *Tobacco streak virus* Infecting Kenaf (*Hibiscus cannabinus*) in India, Indian J. Virol. 23 (1): 80-82.

Bhaskara, R. B. V., Prasanthi, L., Sivaprasad, Y., Sujitha, A. and Gridhar, K. T. 2013. First Report of *Tobacco streak virus* Infecting *Lallab purpureus*. New Dis. Reports. 28: 21.

Bhat, A. I., Jain, R. K., Chaudhary, V., Krishna, R. M., Ramaiah, M., Chattannavar, S. N. and Varma, A. 2002. Sequence conservation in the coat protein gene of *Tobacco streak virus* isolates causing necrosis disease in cotton, mungbean, sunflower and sunn-hemp in India. Indian J. Biotechnol.1: 350-356.

Blackman, L. M., Harper, J. D. I. and Overall, R. L. 1999. Localization of a centrin like protein to higher plant plasmodesmata. Eur. J. Cell Biol. 78(5): 297-304.

Bol, J. F. 1999. *Alfalfa mosaic virus* and ilarviruses: Involvement of coat protein in multiple steps of the replication cycle. J. Gen. Virol. 80: 1089-1102.

Bol, J. F. 2003. *Alfalfa mosaic virus*: coat protein-dependent initiation of infection. Mol. Plant Pathol. 4: 1-8

Bol, J. F. 2005. Replication of alfamo-and ilarvirus: Role of the Coat Protein. Ann. Rev. Phytopathol. 43: 39-62.

Bol, J. F., Kraal, B. and Brederode, F. T. 1974. Limited proteolysis of *alfalfa mosaic virus*: influence on the structural and biological function of the coat protein. Virol. 58: 101-110.

Bowers, J. H., Bailey, B. A., Hebbar, P. K., Sanogo. S. and Lumsden. R. D. 2001. The impact of plant diseases on world chocolate production. Online. Plant Health Progress DOI:10.1094/PHP-2001-0709-01-RV.

Boyer, J. C. and Haenni, A. L. 1994. Infectious transcripts and cDNA clones of RNA viruses. Virol. 198: 415-426.

Boyko, V., Ferralli, J. and Heinlein, M., 2000. Cell-to-cell movement of TMV RNA is temperature dependent and corresponds to the association of movement protein with microtubules. Plant. J. 22: 315-325.

Boyko, V., Hu, Q., Seemanpillai, M., Ashby, J. and Heinlein, M. 2007. Validation of microtubule associated *Tobacco mosaic virus* RNA movement and involvement of microtubule aligned particle trafficking. Plant. J. 51: 589-603.

Brandes, J. and Bercks R. 1965. Gross morphology and serology as a basis for classification elongated plant viruses. Adv. Virus. Res. 11: 1-17.

Brigneti, G., Voinnet, O., Li, W. X., Ji, L. H. and Ding, S. W. 1998 Viral pathogenicity determinants are suppressors of transgene silencing in *Nicotiana benthamiana*. EMBO J. 17: 6739-6746.

Braun, A. C. 1943. Studies on tumor inception in crown gall disease. American J. Bot. 30: 674-677.

Briddon, R. W. and Markham, P. G. 2001. *Cotton leaf curl virus* disease. Virus Res. 71: 151-159.

Brill, L. M., Nunn, R. S., Kahn, T. W., Yeager, M. and Beachy, R. N. 2000. Recombinant *Tobacco mosaic virus* movement protein is an RNA binding, α-helical membrane protein. Proc. Natl. Acad. Sci. USA 9: 7112-7117.

Brunt, A. A., Crabtree, K., Dallwitz, M. J., Gibbsand, A. J. and Watson, L. 1996. Viruses of Plant, CAB International, Wellingford, UK, 1484.

Buck, K. W. 1996. Comparison of the replication of positive stranded RNA viruses of plants and animals. Adv. Virus Res. 47: 159-251.

Canto, T. and Palukaitis, P. 1999. Are tubules generated by the 3a protein necessary for cucumber mosaic virus movement. Mol. Plant-Microbe Interact. 12: 985-993.

Canto, T. and Palukaitis, P. 2005. Subcellular distribution of mutant movement proteins of *cucumber mosaic* virus fused to green fluorescent proteins. J. Gen. Virol. 86: 1223-1228.

Cardoso, J. M. S., Felix, M. R., Clara, M. I. E and Oliveira, S. 2012. First characterization of infectious cDNA clones of *Olive mild mosaic virus.* Phytopathologia Mediterranea. 51 (2): 259-265.

Carette, J. E., Verver, J., Martens, J., van Kampen, T., Wellink, J. and Van Kammen, A. B. 2002. Characterization of plant proteins that interact with *Cowpea mosaic virus* '60K' protein in the yeast two hybrid system. J. Gen. Virol. 83: 885-893.

Carrington, J. C., Kasschau, K. D., Mahajan, S. K. and Schaad, M. C. 1996. Cell-to-cell and long distance transport of viruses in plants. Plant Cell 8:1669-1681.

Carvalho, C. M., pouwels, J., Van Lent, J. W., Bisseling, T., Goldbach, R. W. and Wellink, J. 2004. The movement protein of *cowpea mosaic virus* binds GTP and single stranded nucleic acid in vitro. J. Virol. 78 (3): 1591-1594.

Carvalho, C. M., Wellink, J., Ribeiro, S. G., Goldbach, R. W. and van Lent, J. W. M. 2003. The C-terminal region of the movement protein of *Cowpea mosaic virus* is involved in binding to the large but not to the small coat protein. J. Gen. Virol. 84: 2271-2277.

Chander, R. S., Prasada Rao. R. D. V. J., Manoj, K. V., Raman, D. S., Rao, M. A. and Prasad Rao, D. 2003. First report of *Tobacco streak virus* infecting safflower (*Carthamus tinctorius*) in Maharashtra, India. Plant Dis. 87: 1396.

Chao, L. 1997. Evolution of sex and the molecular clock in RNA viruses. Gene. 205**:** 301-308.

Charrier, A. 1984. Genetic resources of *Abelmoschus* (okra). IBPGR Secretarial, Paris, France

Chauhan, D.V. S.1972. Vegetable production in India, Ram Prasad and Sons, India

Clarke, M. F. and Adams, A. N. 1977. Characteristic of the microplate method of enzyme linked immunosorbant assay for the detection of plant viruses. J. Gen. Virol. 34: 475-483.

Cleland, R. E., Fujiwara, T. and Lucas W. J. 1994. Plasmodesmal-mediated cell-to-cell transport in wheat roots is modulated by anaerobic stress. Protoplasma. 178: 81-85.

Citovsky, V., Wong, M. L., Shaw, A. L., Prasad, B. V. V. and Zambryski, P. 1992. Visualization and characterization of *tobacco mosaic virus* movement protein binding to single stranded nucleic acids. Plant Cell. 4: 397-411.

Commandeur, U., Jarausch, W., Koenig, R. L, Y. and Burgermeister, W. 1991. cDNAs of *beet necrotic yellow vein virus* RNAs 3 and 4 are rendered biologically active in a plasmid containing the *cauliflower mosaic virus* 35S promoter. Virol. 185: 493-495.

Converse, R. H. 1972. *Tobacco streak virus* in black rasp berry. Phytopathol. 62: 1001-1004.

Converse, R. H. and Lister, R. M. 1969. The occurrence and some properties of black raspberry latent virus. Phytopathol. 59: 325-333.

Cook, G., Miranda, R. D., Roossinck, M. J. and Pietersen, G. 1999. *Tobacco streak ilarvirus* detected on groundnut in South Africa. Afr. Plant Protect. 5: 13-19.

Cornelissen, B. J. C., Janssen, H., Zuidema, D. and Bol, J. F. 1984. Complete nucleotide sequence of *tobacco streak virus* RNA3. Nucleic. Acids. Res.12: 2427- 2437.

Costa, A. S. and Carvalho, A. M. B. 1961. Studies on Brazilian tobacco streak. Phytopathol. Zeitsch. 42: 113-138.

Costa, A. S., Carvalho, A. M. B., Oliveira, A. R. and Deslandes. J. 1961. Ocorrencia do virus da necrose branca do fumo em tomate. Bragantia. 20: CVII-CXIV.

Costa, A. S. and Lima Neto, V. C. 1976. Transmissão do vírus da necrose branca do fumo por *Frankliniella* sp. In: Resumos, IX Congresso Brasileiro de Fitopatologia. Campinas, SP.

Crawford, K. M. and Zambryski, P. C. 1999. Plasmodesmata signaling: Many roles, sophisticated statutes. Curr. Opin. Plant Biol. 2(5): 382-387.

Cupertino, F. P., Grogan, R. G., Petersen, L. J., Kimble, K. A. 1984. *Tobacco streak virus* infection of tomato and some natural weed hosts in California. Plant Dis. 68: 331-333.

Curin, M., Ojangu, E. L., Trutnyeva, K., Ilau, B., Truve, E. and Waigmann, E. 2007. MPB2C, a microtubule associated plant factor, is required for micro-tubular accumulation of *Tobacco mosaic virus* movement protein in plants. Plant Physiol. 143: 801-811.

Dawson, W., Beck, D. L., Knorr, D. A. and Grantham, G. L. 1986. cDNA cloning of the complete genome of TMV and production of infectious transcripts. Proc. Nat. Acad. Sci. USA. 83: 1832-1836.

De Jong, W. and P. Ahlquist. 1992. A hybrid plant RNA virus made by transferring the noncapsid movement protein from a rod-shaped to an icosahedral virus is competent for systemic infection. Proc. Natl. Acad. Sci. USA 89: 6808-6812.

den Boon, J. A., Chen, J. and Ahlquist, P. 2001. Identification of the sequences in *brome mosaic virus* replicase protein 1a that mediate association with the endoplasmic reticulum membranes. J. Virol. 75: 12370-12381.

Deom, C. M., Lapidot, M. and Beachy, R. N. 1992. Plant virus movement proteins. Cell. 69:221-224.

Deom, C. M., Oliver, M. J. and Beachy, R. N. 1987. The 30-kilodalton gene product of *tobacco mosaic virus* potentiates virus movement. Sci. 237: 2389-2394.

Diaz-Pendon, A., Li, F., Li, W. X. and Ding, S. W. 2007. Suppression of Antiviral Silencing by *Cucumber Mosaic Virus* 2b Protein in Arabidopsis Is Associated with Drastically Reduced Accumulation of Three Classes of Viral Small Interfering RNAs. Plant Cell 19: 2053-2063.

Diaz, J. A., Bernal, J. J., Moriones, E. and Aranda, M. A. 2003. Nucleotide sequence and infectious transcripts from a full-length cDNA clone of the carmovirus *Melon necrotic spot virus*. Arch. Virol. 148: 599-607.

Dilruba, S., Hasanuzzaman, M., Karim, R. and Nahar, K. 2009. Yield response of okra to different sowing time and application of growth hormones. J. Hort. Sci. Orna Plants 1: 10-14.

Ding, B. 1997. Cell-to-cell transport of macromolecules through plasmodesmata: A novel signaling pathway in plants. Trends Cell Biol. 7(1): 5-9.

Ding, S. W., Anderson, B. J., Haase, H. R. and Symons, R. H. 1994. New overlapping gene encoded by the *cucumber mosaic virus* genome. Virol. 198: 593-601.

Ding, S. W., Li, W. X. and Symons, R. H. 1995. A novel naturally occurring hybrid gene encoded by a plant RNA virus facilitates long distance virus movement. EMBO J. 14**:** 5762-5772.

Doijode, S. D. 2001. Seed storage of horticultural crop. Food Product Press, New York, USA.

Domingo, E. and Holland, J. J. **1994.** Mutation rates and rapid evolution of RNA viruses, p. 161-184. *In* S. S. Mores (ed.), The evolutionary biology of viruses. Raven Press, New York.

Donald, R. G. K., petty, I.T.D., Zhou, H. and Jackson, A. O. 1995. Properties of genes influencing *barley stripe mosaic virus* movement phenotype. In Biotechnology and Plant protection; Viral pathogenesis and disease resistance, D. D. Bills and S. D. Lung, eds (Singapore: World scientific Publication Co.): pp 115-150.

Drake, J. W. and Holland, J. J. 1999. Mutation rates among RNA viruses. Proc. Natl. Sci. USA 96: 13910-13913.

Dreher, T.W. 1999. Function of 3' untranslated regions of positive stranded RNA viral genomes. Annu. Rev. Phytopathol. 37: 151-174.

Duckett, C. M., Oparka, K. J., Prior, D. A. M., Dolan, L. and Roberts, K. 1994. Dye coupling in the root epidermis of Arabidopsis is progressively reduced during development. Development, 120(11): 3247-3255.

Dunn, J. J. and Studier, F. W. 1983. Complete nucleotide-sequence of bacteriophage-T7 DNA and the locations of T7 genetic elements. J. Mol. Bio. 166: 477-535.

Ek-Amnuay, P. 2010. Plant diseases and insect pests of economic crops. Amarin Printing and Publishing Public Co. Ltd, Bangkok, Thailand. 379 pp.

Ernst Ruska and Max Knoll 1931. http://en.wikipedia.org/wiki/Transmissionelectron microscopy

Esau, K. 1948. Some anatomical aspects of plant virus disease problems. II. Bot. Rev.1: 413-449.

Fajardo, T. V. M., Ana Peiro., Pallas, V. and Sanchez-Navarro, J. 2013. Syetemic transport of *Alfalfa mosaic virus* can be mediated by the movement proteins of several viruses assigned to five genera of the 30K family. J. Gen.Virol. 94: 677-681.

FAOSTAT., 2011. (http://www.fao.org)

Fauquet, C. and J. C. Thouvenel. 1987. Plant viral diseases in Ivory Coast. ORSTOM, Paris, France. Institut Français de Recherche pour le Développement en Coopération. Collection Initiations Documentations Techniques no. 46.

Ferralli, J., Ashby, J., Fasler, M., Boyko, V. and Heinlein, M. 2006. Disruption of microtubule organization and centrosome function by expression of *Tobacco mosaic virus* movement protein. J. Virol. 80: 5807-5821.

Finlay, J. R. 1974. *Tobacco streak virus* in tobacco. Aus. Plant Pathol. Soc. News Let. 3: 71.

Fujiwara, T., Giesman-Cookmeyer, D., Ding, B., Lommel, S. A. and Lucas, W. J. 1993. Cell-to-cell trafficking of macromolecules through plasmodesmata potentiated by the *red clover necrotic mosaic* virus movement protein. Plant Cell. 5: 1783-1794.

Fulton, R. W. 1985. *Tobacco streak virus*, CMI/AAB descriptions of plant viruses. No. 307. Wellesbourne, UK: Assoc. Appl. Biologists.

Franck, A., Jonard, G., Richards, K., Hirth, L. and Guilley, H. 1980. Nucleotide sequence of *cauliflower mosaic virus* DNA. Cell. 21: 285-294.

Friedberg, J. N. 1998. Overview on the processes, technology, and application of plant transformation. http://www.vivetechnologies.com/jfriedberg/PlantTransformationReview.pdf., accessed on 13th Nov, 2011.

Garcia-Arenal, F., A. Fraile, and J. M. Malpica. 2001. Variability and genetic structure of plant virus populations. Annu. Rev. Phytopathol. 39**:** 157-186.

Genoves, A., Navarro, J. A. and Pallas, V. 2006. Functional analysis of the five *melon necrotic spot virus* genome encoded proteins. J. Gen. Virol. 87: 2371-2380.

Genovés, A., Navarro, A. J. and Pallás, V 2010. The Intra-and Intercellular Movement of *Melon necrotic spot virus* (MNSV) Depends on an Active Secretory Pathway. Mol. Plant-Microbe-Interact. 23 (3): 263-272.

Ghanekar, A. M. and Schwenk, F. W. 1974. Seed transmission of *Tobacco streak virus* in six cultivars of soybeans. Phytopathol. 64: 112-114.

Ghanem, G. A. M. 2003. *Okra leaf curl virus*: a monopartite begomovirus infecting okra crop in Saudi Arabia. Arab J. Biotechnol.6: 139-152.

Giesman-Cookmeyer, D., Silver, S., Vaewhongs, A. A., Lommel, S. A. and Deom, C. M. 1995. Tobamovirus and dianthovirus movement proteins are functionally homologous. Virol. 213: 38-45.

Gilmer, D., Bouzoubaa, S., Hehn, A., Guilley, H., Rlchards, K. and Jonard, G. 1992. Efficient cell-to-cell movement of *beet necrotic yellow vein virus* requires 3' proximal genes located on RNA2. Virol. 189: 40-47.

Gillespie, T., Boevink, P., Haupt, S., Roberts, A. G., Toth, R., Valentine, T., Chapman, S. and Oparka, K. J. 2002. Functional analysis of a DNA shuffled movement protein reveals that microtubules are dispensable for the cell-to-cell movement of *Tobacco mosaic virus*. Plant Cell. 14: 1207-1222.

Givord, L. and Denboer, L. 1980. Insect transmission of *okra mosaic virus* in the Ivory Coast. Annals Appl. Biol. 94: 235-241

Goelet, P., Lomonossoff, G. P., Butler, P. J. G., Akam, M. E., Gait, M. J. and Karn, J. 1982. Nucleotide sequence of *tobacco mosaic virus* RNA. Proc. Natl. Acad. Sci. USA 79**:** 5818-5822.

Gopalan, C., Sastri, S. B. V. and Balasubramanian, S. 2007. Nutritive value of Indian foods, National Institute of Nutrition (NIN), ICMR, India.

Gopinath, K., Dragnea, B. and Kao, C. 2005. Interaction between *Brome mosaic virus* proteins and RNAs: Effects on RNA replication, protein expression, and RNA stability. J. Virol. 79:14222-14234.

Govind, K., Makinen, K. and Savitri, H. S. 2012. *Sesbania mosaic virus* infectious clone: possible mechanism of 3' and 5' end repair and role of poly protein processing in viral replication. PLOS One. 7 (2): 1-13.

Gracia, O. and Feldman, J. M. 1974. *Tobacco streak virus* in pepper. Phytopathol. 80: 313-323.

Greber, R. S., Klose, M. J. and Teakle, D. S. 1991. High incidence of *Tobacco streak virus* in tobacco and its transmission by Microcephalothrips abdominalis and pollen from Ageratum houstonianum. Plant Dis. 75: 450-452.

Grimsley, N., Hohn, T., Davies, J. W. and Hohn, B. 1987. Agrobacterium-mediated delivery of infectious *maize streak virus* into maize plants. Nat. 325:177-179.

Haddidi, A., Khertarpal, R. K. and Koganezawa, H. 1998. Plant Virus Disease Control. APS Press, St. Paul, MN.

Hall, T. 1999. Bio Edit: a user-friendly biological sequence alignment editor and analysis program for Windows 95/98/NT. Nucleic Acids Symp Ser. 41: 95-98.

Harries, P. A., Schoelz, J. E. and Nelson, R. S. 2010. Intracellular transport of viruses and their components: utilizing the cytoskeleton and membrane highways. Mol. Plant-Microbe Interact. 23: 1381-1393.

Hasnoot, P. C., Brederode, F. T., Olsthoorn, R. C. and Bol, J. F. 2000. A conserved hairpin structure in alfamovirus and bromovirus subgenomic promoters is required for efficient RNA synthesis *in vitro*. RNA 6: 708-716.

Haviv, S., Goszczynski, D. E. and Mawassi, M., 2006. The p10 of Grapevine virus A affects pathogenicity on *Nicotiana benthamiana* plants. In 15th Meeting of the International Council for the study of virus and virus-like diseases of the grapevine (ICVG)-Extended abstracts, Stellenbosch, South Africa.

Hayes, R. J. and Buck, K.W. 1990. Infectious *cucumber mosaic virus* RNA transcribed *in vitro* from clones obtained from cDNA amplified using the polymerase chain reaction. J. Gen. Virol. 71: 2503-2508.

Higuchi, R., Krummel, B. and Saiki, R. 1988. A general method of *in vitro* preparation and specific mutagenesis of DNA fragments: study of protein and DNA interactions. Nucleic Acids Res. 16 (15): 7351-7367.

Hobbs, H. A., Reddy, D. V. R., Rajeshwari, R. and Reddy, A. S. 1987. Use of antigen coating method and protein A coating ELISA procedures for detection of three peanut viruses. Plant Dis. 71: 747-749.

Holland, J. J., Spindler, K., Horodyski, F., Grabau, E., Nichol, S. and Vande Pol. S. 1982. Rapid evolution of RNA genomes. Sci. 215**:** 1577-1582.

Hosseini, D., Koohi Habibi, M., Mosahebi, G., Motamedi, M. and Winter, S. 2012. First report on the occurrence of *tobacco streak virus* in sunflower in Iran. J. Plant Pathol. 93(3): 585-589.

Howell, W. E. and Mink, G. I. 1976a. Host range, purification and properties of a flexuous rod-shaped virus isolated from carrot. Phytopathol. 66: 949-953.

Hu, X., Meacham, T., Ewing, L., Gray, S. M. and Karasev, A. V. 2009. A novel recombinant strain of Potato virus Y suggests a new viral genetic determinant of vein necrosis in tobacco. Virus Research 143: 68-76.

Huang, M. and Zhang, L. 1999. Association of the movement protein of *alfalfa mosaic virus* with the endoplasmic reticulum and its trafficking in epidermal cells of onion bulb scales. Mol. Plant-Microbe Interact. 12: 680-690.

Huang, M., Jongejan, L., Zheng, H. Q., Zhang, L. and Bol, J. F. 2001. Intracellular localization and movement phenotypes of *Alfalfa mosaic virus* movement protein mutants. Mol. Plant-Microbe Interact. 14: 1063-1074.

Huang, M., Koh, D. C. Y., Weng, L. J., Chang, M. L. and Yap, Y. K. 2000. Complete nucleotide sequence and genome organization of Hibiscus chlorotic ringspot Virus, a new member of the genus Carmovirus: evidence for the presence and expression of two novel 21 open reading frames. J Virol 74: 3149-3155.

Hull, R. 2002. Matthew's Plant virology, 4th Edition, Academic Press, San Diego, CA.

Hull, R. 2014. Plant Virology. 5th Edition. Academic Press, San Diego, CA.

IBPGR 1991. Report of international workshop on okra genetic resources. National Bureau for Plant genetic Resources (NBPGR), New Delhi, India

Ingwell, L. L., Eigenbrode, S. D. and Bosque-Pe´rez, N. A. 2012. Plant viruses alter insect behaviour to enhance their spread. Sci Rep 2: 578.

Itaya, A., Woo, Y. M., Mascuta, C., Bao, Y., Nelson, R. and Ding B. 1998. Developmental regulation of intercellular protein trafficking though plasmodesmata in tobacco leaf epidermis. Plant Physiol. 118: 373-385.

Jain, R. K., Bag, S. and Awasthi, L. P. 2005. First report of natural infection of *Capsicum annuum* by *Tobacco streak virus* in India. Plant Pathol. 54: 257.

Jatana, N., Jangid, S., Khare, G., Tyagi, A. K. and Latha, N. 2011. Molecular modeling studies of Fatty acyl-CoA synthetase (FadD13) from Mycobacterium tuberculosis a potential target for the development of antitubercular drugs. J. Mol. Mod. 17: 301-313.

Jaspars, E. M. J. 1999. Genome activation in alfamo- and ilarviruses. Arch. Virol. 144: 843-63.

Johnson. 1936. Tobacco streak, a virus disease, Phytopathol. 26: 285.

Johnson, H. A. J., Converse, R. H., Amorao, A., Espejo, J. I. and Frazier, N. W. 1984. Seed transmission of *Tobacco streak virus* in strawberry. Plant Dis. 68: 390-392.

Jones, A. T., McGavin, W. J. and Dolan, A. 2001. Detection of *Tobacco streak virus* isolates in North American Cranberry (*Vaccinium macrocarpon*). Online Plant Health Prog. doi:10.1094/PHP-2001-0717-01-RS.

Kahlon, T. S., Chapman, M. H. and Smith, G. E. 2007. In vitro binding of bile acids by okra beets asparagus eggplant turnips green beans carrots and cauliflower. Food Chem. 103: 676-680.

Kaiser, W. J., Wyatt, S. D. and Pesho, G. R. 1982. Natural hosts and vectors of *Tobacco streak virus* in Eastern Washington. Phytopathol. 72: 1508-1512.

Kaiser, W. J., Wyatt, S. D. and Klein, R. E. 1991. Epidemiology and seed transmission of two Tobacco streak virus pathotypes associated with seed increases of legume germplasm in eastern Washington. Plant Dis. 75: 258-264.

Kang, B. C., Yeam, I. and Jahn, M. M. 2005. Genetics of Plant Virus Resistance. Annu. Rev. Phytopathol. 43: 581-612.

Kaplan, I. B., Zhang, L. and Palukaitis, P. 1998. Characterization of *cucumber mosaic virus* cell-to-cell movement requires capsid protein but not virions. Virol. 246: 221-231.

Kasteel, D. T. J., Van der Wel, N. N., Jansen, K. A., Goldbach, R. W., Van Lent, J. W. M. 1997. Tubule forming capacity of the movement proteins of *alfalfa mosaic virus* and *brome mosaic virus*. J. Gen.Virol. 78: 2089-2093.

Kempers, R. and Van Bel A. J. E. 1997. Symplasmic connections between sieve element and companion cell in the stem phloem of Vicia faba have a molecular size exclusion limit of at least 10 kDa. Planta. 201: 195-201.

King, A. M. Q., Adams, M. J., Carstens, E. B. and Lefkowitz, E. J. editors 2012. Virus Taxonomy Ninth Report of the International Committee On Taxonomy of Viruses. San Diego, CA: Elsevier Academic Press. 1327 p

Knorr, D. A. and Dawson, W. O. 1988. A point mutation in the *tobacco mosaic virus* capsid protein gene induces hypersensitivity in *Nicotiana sylvestris*. Proc. Natl. Acad. Sci. USA 85: 170-174.

Koonin, E. V. and Dolja, V. V. 1993. Evolution and taxonomy of positive-stranded RNA viruses: Implication of comparative analysis of amino acid sequences. Crit. Rev. Biochem. Mol. Biol. 28: 375-430.

Kragler, F., Curin, M., Trutnyeva, K., Gansch, A. and Waigmann, E. 2003. MPB2C, a microtubule-associated plant protein binds to and interferes with cell-to-cell transport of *Tobacco mosaic virus* movement protein. Plant Physiol. 132: 1870-1883.

Krab, I. M., Caldwell, C., Gallie, D. R. and Bol, J. F. 2005. Coat protein enhances translational efficiency of *alfalfa mosaic virus* RNAs and interacts with the eIF4G component of initiation factor eIF4F. J. Gen. Virol. 86: 1841-1849.

Krishna Reddy. M., Salil, J. and Samuel, D. K. 2003a. Fruit distortion mosaic diseases of okra in India. Plant Dis. 87: 1395.

Krishna Reddy. M., Devaraj, L. R., Salil, J. and Samuel, D. K. 2003b. Outbreak of *Tobacco streak virus* causing necrosis of cucumber (*Cucumis sativus*) and gherkin (*Cucumis anguria*) in India. Plant Dis. 87: 1264.

Kumar, S., Dagnoko, S., Haougui, A., Ratnadass, A., Pasternak, D. and Kouame, C. 2010. Okra (*Abelmoschus spp*.) in West and Central Africa: potential and progress on its improvement. African J. Agric. Res. 5: 3590-3598.

Ladhalakshmi, D., Ramaiah, M., Ganapathy, T., Krishna, R. M., Khabbaz, S. E., Babu, M. and Kamalakannan, A. 2006. First report of the natural occurrence of *Tobacco streak virus* on blackgram (*Vigna mungo*). Plant Pathol. 12: 55.

Laemmli, U. K. 1970. Cleavage of structural proteins during the assembly of the head of bacteriophage T4. Nat. 227: 680-685.

Laliberté, J. F. and Sanfaçon, H. 2010. Cellular remodelling during plant virus infection. Annu. Rev. Phytopathol. 48: 69-91.

Lamont, W. 1999. Okra a versatile vegetable crop. Hort. Technol. 9: 179-184.

Leiser, R. M., Ziegler-Graff, V., Reutenauer, A., Herrbach, E., Lemaire, O. and Guilley, H. 1992. Agroinfection as an alternative to insects for infecting plants with *beet western yellows luteovirus*. Proc. Nat. Acad. Sci. USA 89: 9136-9140.

Lengsfeld, C., Titgemeyer, F., Faller, G. and Hensel, A. 2004. Glycosylated compounds from okra inhibit adhesion of Helicobacter pylori to human gastric mucosa. J. Agric. Food Chem. 52: 1495-1503.

Levy, A., Zheng, J. Y. and Lazarowitz, S. G. 2013. The tobamovirus *Turnip vein clearing virus* 30 kilodalton movement protein localizes to novel nuclear filaments to enhance virus infection. J. Virol. 87: 6428-6440.

Lewsey M., Surette, M., Robertson, F. C., Ziebell, H. and Choi, S. H. 2009. The role of the *cucumber mosaic virus* 2b protein in viral movement and symptom induction. Mol. Plant-Microbe. Interact 22: 642-54.

Li, W., Lewandowski, D. J., Hilf, M. E. and Adkins, S. 2009. Identification of domains of the *Tomato spotted wilt virus* NSm protein involved in tubule formation, movement and symptomatology. Virol. 390: 110-121.

Lister, R. M. 1966. Possible relationships of virus-specific products of tobacco rattle virus infections. Virol. 28: 350-53.

Lister, R. M. and Bancroft, J. B. 1970. Alteration of *tobacco streak virus* component ratio is altered by host and extraction procedure. Phytopathol. 60: 689-694.

Liu, C. and Nelson, R. S. 2013. The cell biology of *Tobacco mosaic virus* replication and movement. Front. Plant. Sci. 4: 12.

Liu, L. and Lomonossoff, G. 2002. Agroinfection as a rapid method for propagating *Cowpea mosaic virus* based constructs. J. Virol. Methods 105: 343-348.

Liu, I. M., Liou, S. S., Lan, T. W., Hsu, F. L. and Cheng, J. T. 2005. Myricetin as the active principle of *Abelmoschus moschatus* to lower plasma glucosein streptozotocin-induced diabetic rats. Planta Medica 71: 617-621.

Leisner, S. M. and Howell, S. H. 1993. Long distance movement of viruses in plants. Trends Microbiol. 1:314-317.

Li, Q. and Palukaitis, P. 1996. Comparison of the nucleic acid and NTP-binding properties of the movement protein of *cucumber mosaic cucumovirus* and *tobacco mosaic tobamovirus*. Virol. 216: 71-79.

Liu, J. Z., Blancaflor, E. B. and Nelson, R. S. 2005. The tobacco mosaic virus 126-kilodalton protein, a constituent of the virus replication complex, alone or within the complex aligns with and traffics along microfilaments. Plant Physiol. 138: 1853-1865.

Lucas, W. J. 1995. Plasmodesmata-intercellular channels for macromolecular transport in plants. Curr. Opin. Cell Biol. 7: 673-680.

Lucas, W. J., Ding, B. and Van der Schoot C. 1993. Plasmodesmata and the supracellular nature of plants. New Phytology 125: 435-476.

Lucas, W. J. and Gilbertson, R.L. 1994. Plasmodesmata in relation to viral movement within leaf tissues. Annul Reviews in Phytopathology 32: 387-411.

Maiss, E., Tmpe, U., Brisske R. D. E. A., Lesemann, D. E. and Casper, R. 1992. Infectious *in vivo* transcripts of a plum pox potyvirus fulllength cDNA clone containing the *cauliflower mosaic virus* 35S RNA promoter. J. Gen. Virol. 73: 709-713.

Mandahar, C. L .2006. Multiplication of RNA plant viruses. First edition, Springer, Printed in the Netherlands.Chapter 1; page 1.

Markose, B. L. and Peter, K. V. 1990. Okra review of research on vegetable and tuber crops. Kerala Agricultural University Press, Kerala, India

Martınez-Gil, L., Sanchez-Navarro, J. A., Cruz, A., Pallas, V., Perez-Gil, J. and Mingarro, I. 2009. Plant virus cell-to-cell movement is not dependent on the transmembrane disposition of its movement protein. J. Virol. 83: 5535-5543.

Mathur, C., Mohan, K., Usha Rani, T. R., Krishna Reddy, M. and Savithri, H. S. 2014. The N-terminal region containing the zinc finger domain of *tobacco streak virus* coat protein is essential for the formation of virus-like particles. Arch. Virol. 159: 413-423.

Matthieu, L., Bartoli. J., Shmakova, L., Sandra, J., Labadie, K., Adrait. A., Magali, L., Olivier, P., Lionel, B., Bruley, C., Yohann, C., Elizaveta, R., Chantal, A. and J. Michel, J. C. 2014. Thirty-thousand-year-old distant relative of giant icosahedral DNA viruses with a pandoravirus morphology Proc. Natl. Acad. Sci. USA 111(11): 4274-4279.

McLean, B. G., Zupan, J. and Zambryski, P. C. 1995. *Tobacco mosaic virus* movement protein associates with the cytoskeleton in tobacco cells. Plant Cell. 7: 2101-2114.

Melton, D. A., Krieg, P. A., Rebagliati, M. R., Maniatis, T. and Green, M. R. 1984. Efficient In vitro synthesis of biologically active RNA and RNA hybridization probes from plasmids containing a bacteriophage SP6 promoter. Nucleic. Acids Res. 12: 7035-7056.

Meshi, T., Ishakawa, M., Motoyoshi, F., Semba, K. K. and Okada, Y. 1986. In transcription of infectious RNAs from full-length cDNAs of *tobacco mosaic virus.* Proc. Nat. Acad. Sci. USA 83: 5043-5047.

Miller, W. A. and Koev, G. 2000. Synthesis of subgenomic RNAs by positive strand RNA viruses. Virol. 273: 1-8.

Moekchantuk, T. and Kumar, P. 2004. Export okra production in Thailand. Inter-country programme for vegetable IPM in South & SE Asia phase II Food & Agriculture Organization of the United Nations, Bangkok, Thailand.

Mowat, W. P. and Dawson, S. 1987. Detection and identification of plant viruses by ELISA using crudesap extracts and unfractionated antisera. J. Virol. Methods. 15: 233-347.

Mullis, K., Faloona, F., Scharf, S., Saiki, R., Horn, G. and Erlich, H. 1986. Specific enzymatic amplification of DNA in vitro the polymerase chain reaction . Cold spring Harbour symposium in Quantitative Biology. 51: 263-273.

Murant, A. F. 1972. Parsnip mosaic virus. CMI/ AAB Description of plant viruses. Set5, No.91.

Nadège, P., Matthieu, L., Gabriel, D., Yohann, C., Olivier, P., Magali, L., Arslan, D., Virginie, S., Lionel, B., Christophe, B., Garin, J., Claverie, J. M. Chantal, A. 2013. Pandoraviruses: Amoeba Viruses with Genomes Up to 2.5 Mb Reaching That of Parasitic Eukaryotes. Sci. 341: 281-286.

Nagano, H., Okuno, T., Mise, K. and Furusawa, I. 1997. Deletion of the C-terminal 33 amino acids of *cucumber mosaic virus* movement protein enables a chimeric brome mosaic virus to move from cell-to-cell. J. Virol. 71: 2270-2276.

Nagyova, A and Subr, Z. 2007. Infectious full length clones of plant viruses and their use for construction of viral vectors. Acta Virol. 51: 223-237.

Nagano, H., Mise, K., Furusawa, I. and Okuno, T. 2001. Conversion in the requirement of coat protein in cell-to-cell movement mediated by the cucumber mosaic virus movement protein. J. Virol. 75: 8045-8053.

Ndunguru, J., Rajabu, A.C. 2004. Effect of okra mosaic virus disease on the above-ground morphological yield components of okra in Tanzania. Scientia Horticulturae 99: 225-235.

Neeleman, L., Linthorst, H. J. M. and Bol, J. F. 2004. Efficient translation of alfamovirus RNAs requires the binding of coat protein dimers to the 3'termini of the viral RNAs. J. Gen. Virol. 85: 231-240.

Neeleman, L., Olsthoorn, R. C. L., Linthorst, H. J. M. and Bol, J. F. 2001. Translation of a non polyadenylated viral RNA is enhanced by binding of viral coat protein or polyadenylation of the RNA. Proc. Natl. Acad. Sci. USA 98: 14286-14291.

Niehl, A. and Heinlein, M. 2011. Cellular pathways for viral transport through plasmodesmata. Protoplasma. 248: 75-99.

Niehl, A., Amari, K., Gereige, D., Brandner, K., Mély, Y. and Heinlein, M. 2012. Control of *Tobacco mosaic virus* movement protein fate by CELL-DIVISION-CYCLE protein 48 (CDC48).Plant. Physiol. 160: 2093-2108.

Niehl, A., Amari, K. and Heinlein, M. 2013a. CDC48 function during TMV infection: regulation of virus movement and replication by degradation. Plant. Signal. Behav.8: e22865.

Niehl, A., Peña, E. J., Amari, K. and Heinlein, M. 2013b. Microtubules in viral replication and transport. Plant. J. 75: 290-308.

Niehl, A., Pasquier, A., ferriol, I., Mely, Y. and Heinlein, M. 2014. Comprision of the Oilseed rape mosaic virus and Tobacco mosaic virus movement protein (MP) reveals common and dissimilar MP functions for tobamovirus spread. Virol. 456-457: 43-54.

Nishiuchi, M., Motoyoshi, F. and Oshima, N. 1978. Behaviour of a temperature-sensitive strain of tobacco mosaic virus in tomato leaves and protoplasts. J. Gen. Virol. 39: 53-61.

Nishiuchi, M., Motoyoshi, F. and Oshima, N. 1980. Further investigation of a temperature-sensitive strain of tobacco mosaic virus: its behaviour in tomato leaf epidermis. J. Gen. Virol. 46: 497-500.

Nouri, S., Arevalo, R., Falk, B. W. and Groves, R. L. 2014. Genetic Structure and Molecular Variability of *Cucumber mosaic virus* Isolates in the United States. PLoS ONE 9(5): e96582. doi:10.1371/journal.pone.0096582.

o'Donell, I. J., Shukla, D. D. and Gough, D. H. 1982. Electro blot immunoassay of virus infected plant sap A powerful technique for detecting plant viruses. J. Virol. Methods. 4: 19-26.

Ohki, S.T., Doi, Y., Yora, K. 1978. *Carrot latent virus* a new rhabdovirus of carrot. Annals Phytopathol. Soc. Jap. 44: 202-204.

Oparka, K. J., Roberts, A. G., Boevink, P., Santa Cruz, S., Roberts, I., Pradel, K. S., Imlau, A., Kotlizky, G., Sauer, N. M. and Epel, B. 1999. Simple, but not branched, plasmodesmata allow the nonspecific trafficking of proteins in developing tobacco leaves. Cell. 97: 743-754.

Olsthoorn, R. C. L., Mertens, S., Brederode, F. T. and Bol, J. F. 1999. A conformational switch at the 3'end of a plant virus RNA regulates viral replication. EMBO J. 18: 4856-64.

Owolarafe, O. K. and Shotonde, H. O. 2004. Some physical properties of fresh okra fruit. J. Food Engin. 63: 299-302.

Pappu, H. R., Hammett, K. R. W. and Draffel, K. I. 2008. Dahlia mosaic virus and Tobacco streak virus in dahlia (Dahlia variabilis). Plant Dis. 92: 1138.

Peña, E. and Heinlein, M. 2013. Cortical microtubule associated ER sites : organization centers of cell polarity and communication. Curr. Opin. Plant. Biol.16: 764-773.

Petty, I. T. D., French, R., Jones, R. W. and Jackson, A. O. 1990. ldentification of barley stripe mosaic virus genes involved in viral RNA replication and systemic movement. EMBO J. 9: 3453-3457.

Pouwels, J., Van Der Krogt, G. N. M., Van Lent, J., Bisseling, T. and Wellink, J. 2002. The cytoskeleton and the secretory pathway are not involved in targeting the *cowpea mosaic virus* movement protein to the cell periphery. Virol. 297: 48-56.

Prasada Rao, R. D.V. J., Reddy, A. S., Chander Rao, A. S., Varaprasad, K. S., Thirumala-Devi, K., Nagaraju., Muniyappa, V. and Reddy, D. V. R. 2000. *Tobacco streak ilarvirus* as causal agent of sunflower necrosis disease in India. J. Oilseeds Res. 17: 400-401.

Radford, J. E. and White R.G. 1998. Localization of a myosin like protein to plasmodesmata. Plant J. 14: 743-750.

Rafiq, A., Ali, S., Jahan, T. and Naqvi, Q. A. 2008. Virus causing yellow net disease on carrot (*Daucus carota* L.) identified as Alfalfa mosaic virus. Nat Acad. Sci. Lets, 31: 39-43.

Ramachandran, G.N., Ramakrishan, C. and Sasisekhran, V.1963. Stereochemistry of polypeptide chain configuration. J. Mol. Biol. 7: 95-99.

Ramaiah, M., Bhat, A. I., Jain, R. K., Pant, R. P., Ahlawat, Y. S., Prabhakar, K. and Varma, A. 2001. Isolation of an isometric virus causing sunflower necrosis disease in India. Plant Dis. 85: 443.

Rashid, M. H., Yasmin, L., Kibria, M. G., Mollik, A. K. M. S. R. and Hossain, S. M. M. 2002. Screening of okra germplasm for resistance to yellow vein mosaic virus under field conditions. Pakistan J. Plant Pathol. 1: 61-62.

Reddy, A. S., Prasada Rao, R. D. V. J., Thirumala-Devi, K., Reddy, S. V., Mayo, M. A., Roberts, I., Satyanarayana, T., Subramaniam, K. and Reddy, D. V. R. 2002. Occurrence of *Tobacco streak virus* on peanut (*Arachis hypogaea* L.) in India. Plant Dis. 86: 173-178.

Reichelt, S., knight, A. E., Hodge, T. P., Baluska, F., Samaj, J., Vokmann, D. and Kendrick-Jones J. 1999. Characterization of the unconventional myosin VIII in plant cells and its localization at the post-cytokinetic cell wall. Plant Journal, 19: 555-567.

Rico, P. and Hernandez, C. 2009. Characterization of the subgenomic RNAs produced by *Pelargonium flower break virus*: Identification of two novel RNAs species. Virus Res. 142: 100-107.

Roossinck, M. J. 2002. Evolutionary history of *Cucumber mosaic virus* deduced by phylogenetic analyses. J. Virol. 76: 3382-3387.

Roossinck, M. J. 2003. Plant RNA virus evolution. Curr. Opin. Microbio. 6: 406-409.

Roossinck, M. J. 2013. Plant Virus Ecology. PLoS Pathog 9(5): e1003304. doi:10.1371/journal.ppat. 1003304.

Ruggenthaler, P., Fichtenbauer, D., Krasensky, J., Jonak, C. and Waigmann, E. 2009. Microtubule-associated protein AtMPB2C plays a role in organization of cortical microtubules, stomata patterning, and tobamovirus infectivity. Plant Physiol. 149: 1354-1365.

Saifullah, M. and Rabbani, M. G. 2009. Evaluation and characterization of okra (*Abelmoschus esculentus* L. Moench.) genotypes. SAARC J. Agric. 7: 92-99.

Saito, T., Meshi, N., Takamatsu, N. and Okada. Y. 1987. Coat protein gene sequences of *tobacco mosaic virus* encode a host response determinant. Proc. Natl. Acad. Sci. USA 84: 6074- 6077.

Salazar, L. E., Abad, J. A. and Hooker, W. J. 1982. Host range and properties of a strain of *Tobacco streak* virus from potatoes. Phytopathol.72: 1550-1554.

Sambade, A., Brandner, K., Hofmann, C., Seemanpillai, M., Mutterer, J. and Heinlein, M. 2008. Transport of TMV movement protein particles associated with the targeting of RNA to plasmodesmata. Traffic. 9: 2073-2088.

Sambrook, J., Fritsch, E. F. and Maniatis, T. 1989. Molecular cloning: A laboratory Manual (2).Cold Spring Harbor Laboratory, Cold Spring Harbor, New York.

Sa´nchez-Navarro, J. A. and Bol, J. F. 2001. Role of the *Alfalfa mosaic virus* movement protein and coat protein in virus transport. Mol. Plant. Microbe-Interact. 14: 1051-1062.

Sanchez-Navarro, J. A. and Herranz, C. 2006. Cell to cell movement of *Alfalfa mosaic virus* can be mediated by the movement protein of Ilar-, bromo- cucumo-, tobamo- and comoviruses and does not require virion formation. Virol. 346: 66-73.

Sastry, K. S. M. and Singh, S. J. 1974. Effect of *yellow-vein mosaic virus* infection on growth and yield of okra crop. Indian Phytopathol. 27: 294-297.

Schneider, W. L. and Roossinck, M. J. 2001. Genetic diversity in RNA viral quasispecies is controlled by host-virus interaction. J. Virol. 7: 6566-6571.

Scholthof, H. B. 2005. Plant virus transport: motions of functional equivalence. Trends Plant Sci. 10: 376-382.

Scholthof, H. B., Morris, T. J. and Jackson, A. O. 1993. The Capsid protein gene of *tomato bushy stunt virus* is dispensable for systemic movement and can be replaced to localized expression of foreign genes. Mol. Plant. Microbe-Interact. 6: 309-322.

Schulz, A. 1995. Plasmodesmal widening accompanies the short term increase in symplasmic phloem unloading in pea roots under osmotic stress. Protoplasma. 188: 22-37.

Sdoodee, R. and Teakle, D. S. 1987. Transmission of *Tobacco streak virus* by *Thrips tabaci*: A new method of plant virus transmission. Plant Path. 36: 377-380.

Sdoodee, R. and Teakle, D. S. 1993. Studies on the mechanism of transmission of pollen associated *Tobacco streak virus* by *Thrips tabaci*. Plant Path. 42: 88-92.

Seshadri, G. T. E., Vemana, K., Reddy, D. L., Mahammed, K. C. S., Padma, J. G., Shabbir, S., Venkateswarlu, N. C., Naik, K. S. S., Sampath, K. D., Anthony, J. A. M. and Subramanyam, K. 2013. First report of *Tobacco streak ilarvirus* infecting jasmine and horsegram, New Dis. Reports. 28: 7.

Serra P, Gago S and Duran-Vila N, 2008. A single nucleotide change in Hop stunt viroid modulates citrus cachexia symptoms. Virus Res. 138: 130-134.

Sharman, M., Thomas, J. E. and Persley, D. M. 2008. First report of *Tobacco streak virus* in sunflower (*Helianthus annuus*), cotton (*Gossypium hirsutum*), chickpea (*Cicer arietinum*) and mung bean (*Vigna radiata*) in Australia. Austr. Plant Dis. Notes 3: 27-29.

Sharman, M. and Thomas, J. E. 2013. Genetic diversity of subgroup 1 ilarviruses from eastern Australia. Arch Virol 158: 1637-1647.

Shepherd, D. N., Martin, D. P., van der Walt, E., Dent, K. and Varsani, A. 2010. *Maize streak virus*: an old and complex "emerging" pathogen. Molec. Plant Pathol. 11: 1-12.

Sherwood, J. L., German, T. L., Moyer, J. W. and Ullman, D. E. 2003. Tomato spotted wilt. The Plant Health Instructor. DOI:10.1094/PHI-I-2003-0613-02.

Sivaprasad, Y., Bhaskara, B. V. R., Rekha, K. R., Raja, K. R. and Sai Gopal , D. V. R. 2010. First report of *Tobacco streak ilarvirus* infecting onion (*Allium cepa*). New Dis. Reports. 22: 17.

Singh, P., Indi, S. S. and Savithri, H. S. 2014. *Groundnut bud necrosis virus* encoded NSm associates with membranes via Its C-terminal domain. PLoS ONE. 9(6): e99370.doi:10.1371/journal. pone. 0099370.

Sivaprasad, Y., Bhaskara, R. B. V., Sujitha, A. and Sai Gopal, D. V. R. 2012. First report of Tobacco streak virus infecting Cyamopsis tetragonoloba, Journal of Plant Pathol. 94(4).

Stanley, W. 1935. Isolation of a Crystalline Protein Possessing the Properties of *Tobacco Mosaic Virus*. Sci. 81: 644-645.

Stavolone, L., Villani, M. E., Leclerc, D. and Hohn, T. 2005. A coiled coil interaction mediates *cauliflower mosaic virus* cell-to-cell movement. Proc. Nat. Acad. Sci. USA 102: 6219-6224.

Stenger, D. C., Ruth, H. and Morris, T. J. 1987. Characterization and detection of the Strawberry necrotic shock isolate of *Tobacco streak virus*. Mol. Plant.Pathol. 77: 1330-1337

Stewart, C. N. 2008. Plant biotechnology and genetics: principles, techniques and applications. John Wiley & Sons, Inc., Hoboken, New Jersey. Pp 1-365.

Stewart, F. C. 1910. New york Ag EXP Stat, Geneva Bulletin 329: 305-404.

Su, S., Liu, Z., Chen, C., Zhang, Y., Wang, X., Zhu, L., Miao, L., Wang, X. C. and Yuan, M. 2010. *Cucumber mosaic virus* movement protein severs actin filaments to increase the plasmodesmal size exclusion limit in tobacco. Plant Cell. 22: 1373-1387.

Sudhir, K., Tamura, K. and Nei M. 1994. MEGA: molecular evolutionary genetics analysis software for microcomputers. Comput Appl Biosci. 10: 189-191.

Suzuki, M., Kuwata, S., Masuta, C. and Takanami, Y. 1995. Point mutations in the coat protein of *Cucumber mosaic virus* affect symptom expression and virion accumulation in tobacco. J. Virol. 76: 1791-1799.

Taniguchi, T., Palmieri, M. and Weissmann, C. 1978. Q1 DNA containing hybrid plasmids giving rise to QB phage formation in the bacterial host. Nat. 274: 2293-2298.

Takeda, A., Masanori, K., Okuno, T. and Mise, K. 2004. The C-terminus of the movement protein of *Brome mosaic virus* controls the requirement for coat protein in cell-to-cell movement and plays a role in long-distance movement. J. Gen. Virol. 85: 1751-1761.

Temin, H. M. and Mizutani, S. 1970. RNA dependent DNA polymerase in virions of *Rous sarcoma virus.* Nat. 226: 5252.

Tilsner, J., Amari, K. and Torrance, L. 2011. Plasmodesmata viewed as specialized membrane adhesion sites. Protoplasma. 248: 39-60.

Tremblay, D., Vaewhongs, A. A., Turner, K. A., Tim, L. S. and Lommel, S. A. 2005. Cell wall localization of *Red clover necrotic mosaic virus* movement protein is required for cell-to-cell movement. Virol. 333: 10-21.

Tyulkina, L. G., Karger, E. M., Sheveleva, A. A. and Atabekov, J. G. 2010. Binding of monoclonal antibodies to the movement protein (MP) of Tobacco mosaic virus: influence of subcellular MP localization and phosphorylation. J. Gen. Virol. 91: 1621-1628.

Tzfira, T. and Citovsky, V. 2006. *Agrobacterium*-mediated genetic transformation of plants: biology and biotechnology. Curr. Opin. in Biotechnol. 17: 147-154.

Tzfira, T. and Citovsky, V. 2008. *Agrobacterium: From Biology to Biotechnology*. Springer, New York. Pp 1-734.

Ueki, S and Citovsky, V 2011. To gate, or not to gate: regulatory mechanisms for intercellular protein transport and virus movement in plants. Mol. Plant. 4: 782-793.

Valleau, W. D. 1932. Ky Agr Exp Sta Bulletin. 327: 89-103.

Varmudy, V. 2011. Marking survey need to boost okra exports. Department of economics, Vivekananda College, Puttur, Karnataka, India

Van Bakoven, H., Verver, J., Wellinck, J. and Van Kammen, A. 1993. Protoplasts transiently expressing the 200K coding sequence of cowpea mosaic virus B-RNA support replication of M-RNA. J. Gen. Virol. 74: 2233-2241.

Van der Schoot C. and Rinne P. 1999. Networks for shoot design. Trends Plant Sci. 4: 31-37.

Vander, V. E.A., Neeleman, L. and Bol, J. F. 1994. Early and late functions of *alfalfa mosaic virus* coat protein can be mutated separately. Virol. 202: 891- 903.

Vemana, K. and Jain, R. K. 2010. New Experimental Hosts of *Tobacco streak virus* and Absence of True Seed Transmission in Leguminous Hosts. Indian J. Virol. 21 (2): 117-127.

Vemana, K., Seshadri, G. T. E., Reddy, D. L., Venkateswarlu, N. C., Naik, K. S. S., Sampath, K. D., Padma, L. Y. and Desai, S. 2014. First Report of *Tobacco streak virus* infecting Pigeon pea (*Cajanus cajan*) in India, Plant Dis. 98 (2): 287.

Vives, M. C., Martín, S., Ambrós, S., Renovell, A., Navarro, L., Pina, J. A., Moreno, P. and Guerri. J. 2008. Development of a full-genome cDNA clone of *Citrus leaf blotch virus* and infection of citrus plants. Mol. Plant Pathol. 9: 787-797.

Vlot, C. A. Sebastiaan, M. L. and Bol, J. F. 2003. Coordinate Replication of *Alfalfa Mosaic Virus* RNAs 1 and 2 Involves *cis*- and *trans*-Acting Functions of the Encoded Helicase-Like and Polymerase-Like Domains. J. Virol. 77(20): 10790-10798.

Waigmann, E. and Zambryski, P. 1995. TMV-MP mediated protein transport through trichome plasmodesmata. Plant Cell. 7: 2069-2079.

Walkey, D. 1991. Applied Plant Virology. 2nd edition. Chapman and Hall, London.

Waqar, A., Butt, T. B., Insan, J. and Rehman, A. 2003. Natural occurrence of *Tobacco streak virus* in cotton in Pakistan and screening for its resistance sources. Pak J Bot. 35: 401-408.

Weber, H., Haeckel, P. and Pfitzner, A. J. P. 1992. A cDNA clone of *tomato mosaic virus* is infectious in plants. J. Virol. 66: 3909-3912.

Weng, Z. and Xiong. Z. 1997. Genome organization and gene expression of *saguaro cactus carmovirus*. J. Gen. Virol. 78: 525-534.

White, R. G., Badelt, K., Overall, R. L. and Vesk, M. 1994. Actin associated with plasmodesmata. Protoplasma. 80: 169-184.

Wolf, S., Deom, C. M., Beachy, R. N. and Lucas, W. J. 1989. Movement protein of *tobacco mosaic virus* modifies plasmodesmatal size exclusion limit. Science. 246: 376 -379.

Xin, H. W and Ding, S. W. 2003. Identification and molecular characterization of a naturally ccurring RNA virus mutant defective in the initiation of host recovery.Virol. 317: 253-262.

Xin, H. W., Ji, L. H., Scott, S. W., Symons, R. H. and Ding, S. W. 1998. Ilarviruses encode a Cucumovirus-like 2b gene that is absent in other genera within the Bromoviridae. J. Virol. 72: 6956-6959.

Yamashita, S., Ohki, S., Doi, Y. and Yora, K. 1976. Identification of two viruses associated with the carrot yellow leaf syndrome. Annals Phytopathol. Soc. Jap. 42: 382-383.

Zheng, H., Wang, G. and Zhang, L. 1997. *Alfalfa mosaic virus* movement protein induces tubules in plant protoplasts. Mol. Plant-Microbe Interact. 10:1010-1014.

Appendix-1

Complete sequence of TSV RNA3 after sequencing (Fragmented into 5′UTR, MP, ICR, CP and 3′UTR)

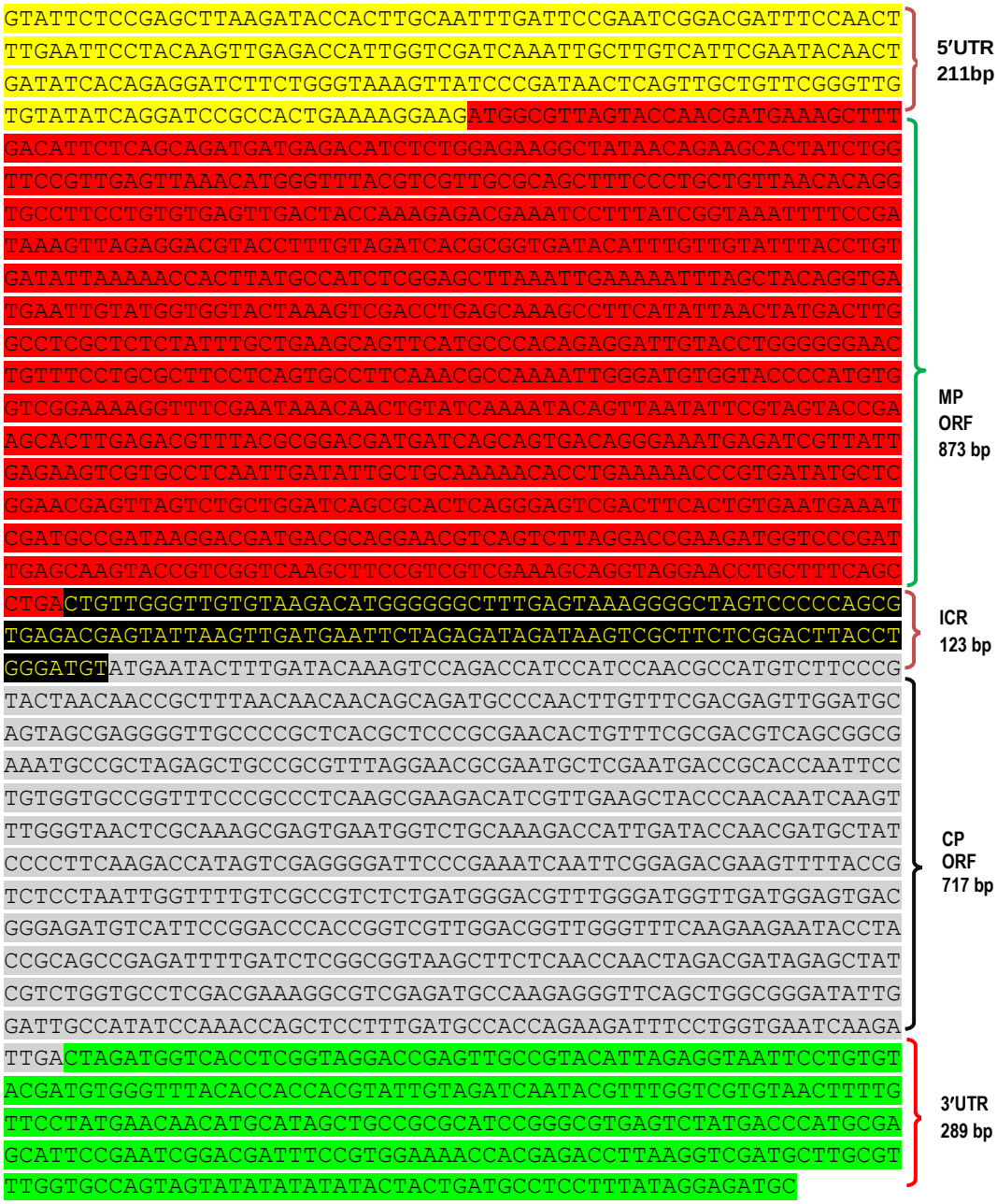

Appendix- 2

Complete sequence of TSV RNA2 after sequencing (Fragmented into 5′UTR, 2a, 2b and 3′UTR)

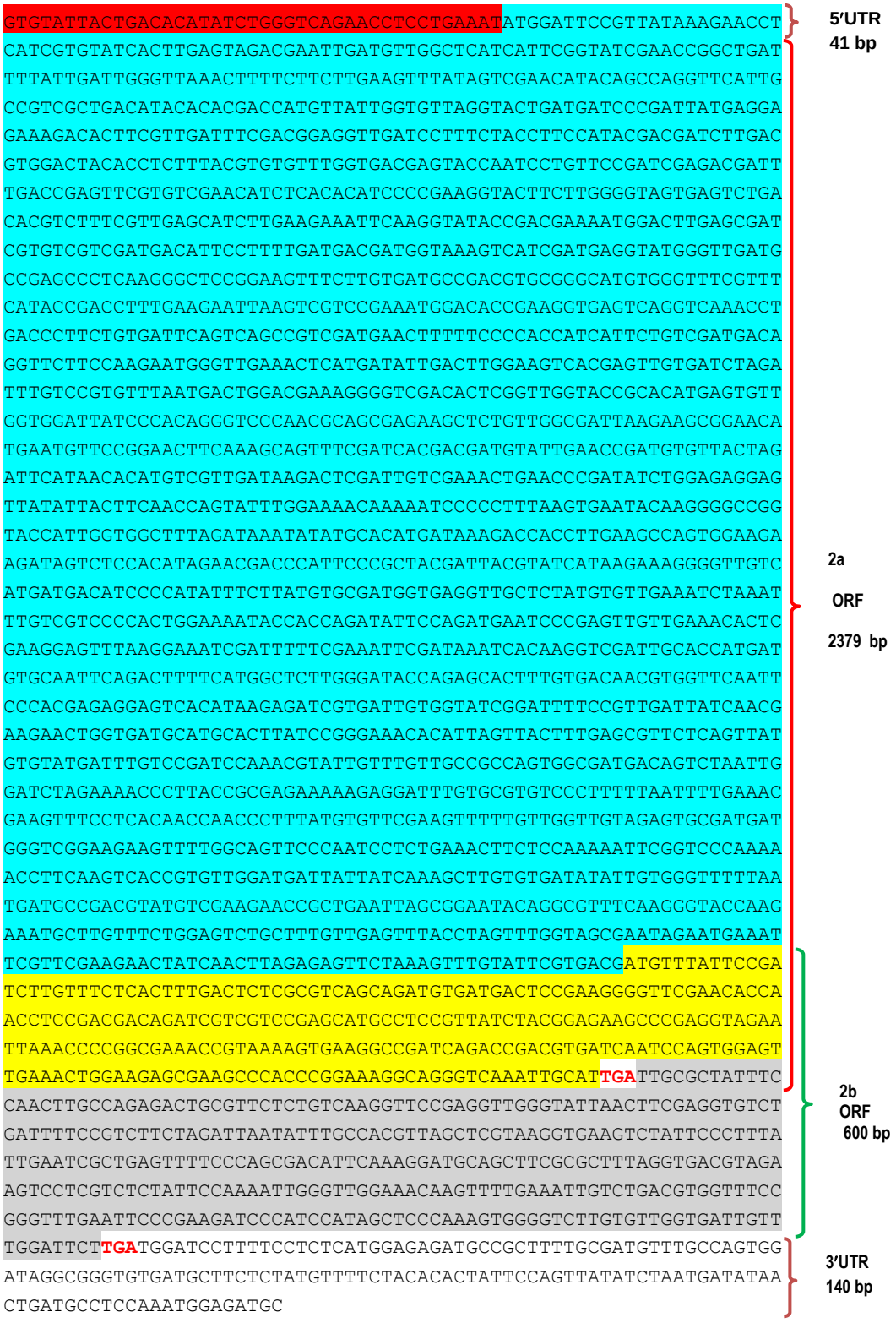

Appendix-3

Complete sequence of TSV RNA1 after sequencing (Fragmented into 5′UTR, 1a and 3′UTR)

GTATTACTGTTTTGTATCCGAAACAGAACCTCCAGAAATGGATTCTCGTTCATTACCCACCGTGAGT
GACGTTACTGTTCCGGCTTTGAACGTTGACAGTCTCGTGCGAGACTATGTCAGCAATGTGAGAGCCG
ATGATAGCAATAACGTCAGTAGATTCCTCGGTGAAGTAGCCTTGAGAGAAATTAAATCTCAAGTTGA
CACCAGCAATGGTGATTTCCAGAAGTTAAACGTCGGTTTTCGTTTGACTCCTGATGAGAAGAACGCT
TTGAAGGCGAATTTTCCTGGTCTTGAAATTGCGTTTAAAGACTCGTGTCATTCGTCTCATAGTTTTG
CCGCAGCACATAGAGTCTGCGAGACCCTAGAGATATACAATCGGTTTAAAACAAAAACCGAGCGCAT
TATCGACCTTGGTGGCAATTATGTCACCCATGCGAAACAAGGTCGATCCAATGTGCATTCCTGCTGT
CCCATCCTTGATGTGCGAGACGGTGCCAGGCATACCGATCGTTATATATCTCTAGCTGCCTCTGTTG
AGAATCGTCACAGAGAGTTACCAGTAGATTTCTGTTGCCATAAGTTCGAAGAATGTGATGTCAAAGC
ACCGTTTGCTATGGCAGTGCATTCCATCAGTGACATTCCTATTTCAACGGTTGCAACACACTGCGTT
AGGCGCGGTGTGCGAAAGTTGATAGCTTCTGTCATGATGGATCCGCTTATGATGCTTTATGACAAAG
GTCATATACCCTTACTCAACGTTGATTGGGAAAAGGAAGACATTGAAGAGGGGAAAACCCTGATTCA
TTTCCATTTTGTTGACGCCCCCGGATTAAGCTATTCACACGATTTTAATGTACTGTCCCAATACATG
ATCACGAATCACGTTATTGTTAATAATACCTACTCTTTTAGGGTAGAGAGGACAGCCTGTTTATCAG
GTGTATATATCGTGGAGATGACTCTGTCTATGACAGATGGTTGTTCTTTAGCTTATCTGAAGCCCAT
GCGTGATGTATCTTGCGCGTGGTTGTCAAGCCTGAGGAAGAAAGTTTTCGTCAAATTAGCCGTACCC
GTAAGTGCCGAATGGTATACTGAACAATTCGAGGTTAGGTACGCGTTGATGGACGAATCTTTAGTTC
GCTATGTTTCCGAAGCTGCATTTCGACAGTTTTCGAAGACTAAAGACCCTGAAACACTGGTTCAGTA
CATAGCAACTATGTTATCTTCCTCTTCGAATCATGTGGTCATAAACGGGATAACAATGCGAAGTGGT
AGTCCCATCAATTTCGATGAGTACGTTCCGCTTGCTGTCACGTTTTATGTTATGGCCGCATGGCGTT
ACAAAATGATTGCCCCTGGTATCGATGCCGTAAAAACTCGTACCGAGAAAAACATTGACGCTCTCGA
TGAGAAAGGTCTTATCAAGGAAGACTTCAATCTCGTCAATGAATTTCTCGAAGAAGCTGGGTTGGTT
GGACCCAATTTGCCCCGTCTCACGGATGTCATTAAAAGCGCGGGACTCCGAAGTTTCGGGAAGAAAA
CGATCGAGAAAACCAGGGATGATGTTTCTTTAATAAAACCGAGAAACTTGTTGCGTGAAGTGATTTA
CACGGTCCGAAGTATCTTCGGGTTAACGATCCTAGACTCAGACTACAATTTAGTGTCAGGTATTCCC
TCCCACATGAAGGCAACCCATGTGTGGAATGTCTTTGTCGGGAATCTCGCTTTCCCATCCAGTCTCA
ACGTCAATGAATGTGTTAACGAGTTGCTTGCTAATCACATAGAAATGATGGAAGAGACTGTGAAGGA
AGAAACACGTCAACAAGCTTTCAAAGATGCCAGAGATCGAGCTCTGATGACGATAGCGAAAGCTATC
GAAAAGGATCAGACCGTTAAGGATGGTCTGTTACCAATTCTCGACTTATGTAAAATAACGGAAGAAT
TGAATGCAGCTTCGAATTCCTTGAACTTGACTCCAGAAGCTATAGAAAGAACAGACTCGCGATTGGC
GAGAGCATCGGGAAGTGACGTTAATCCCTACGCCGATTCCATAAAGGAAGCCATACACTACTTCAAT
GAAGTTGAGGTGGCTAACACACGGAATTTGCGCAGTTTAGGAACTTATCTTGGATGGTCCATTCCCA
AGAGTAGGCAAACCTACGATGCTTTGAAAGGCAGAAATGATTCTGTCAGGGTGTACGTACCTTATGA
AAATAAGTGGTACCCCTCTGCACCCTCCGGTCAGTACGAAAGAGCTATGACCGTTGATGGGTATGTG
TCGCTTCAATGGAATTCTGAGGCGATTACCGACAAATGCAGGAAAGATTTGGTGAAATATCATGTCC
TCGTTGTCGATGATTCTTGCATTTTCTGTTCAGGTCAGAGAATGATTCCAGCTTTAGAAGCCGCCTT
AAAACTGGTCCCAACCTTTAAGATCACGATTGTTGATGGTGTCGCAGGTTGTGGTAAGACTACACAT
CTGAAGAAGATCGCGCGTATTGATTCAAACGCTGCGGGTAGTCCAGATTTGGTGCTGACGAGTAATC
GCAGTTCATCCGATGAGTTGAAAGAAGTTATAGATTGTCCAGATGTGATGAAGTACCGCATCAGGAC
TGTCGATAGCTATCTAATGCTCAAATCCTGGTTTTCGGCTGAGCGACTTTTGTTTGATGAATGCTTC
TTGACACATGCGGGTTGTGTTTATGCCGCAGCCACTCTGGCTCAAGTGAAGGAAGTAATTGCTTTCG
GTGACACCGAGCAAATCCCTTTCATATCTAGATTACCAGAGTTTCGCATGGAACACCATAGAATCGT
TGGAAAGATTGATGTCCAGACAACGACCTACAGGTGTCCGAGAGATGCCACAGCTTGTTTGAAAAAT
TTCTTCTACAAAAACAAGACTGTGAAGTCGGCGAGCGTCATCGAGCGTTCGCTTGAGTTAAACCCAA
TACAGAGTGTGATTCAAATTCAACCAGAGCGTGATGTTTTGTACATGACACACACGCGAGCAGATAA
AGAAGCCCTCCTGAGAATACCGGGGATGCCGAAGGATAGGATTAAAACTACCCATGAAGCCCAAGGT
GAAACCTGGGATCATGTGGTGATGTTCAGACTTTCGAAGACTACTAATCTGCTTCATTCTGGGAAAG
GATCCGAGGGTCCTTGTCACAATTTGGTTGCCATATCTAGACATCGTAAATCGTTCAGGTACTGTAC
GGTAGCTCCTCATGATAACGATGATCAGATAGTGAAGTGTATCAATTTCGCCAAATCTCTGAGTTCG
GGAGATTTGGATGGGGTCCGAATTTTAACTTGATACATTAGTGTACATAATTCCATTATTATGTTGC
CGCAGGGAACCTGCGATGTTTTGGATTCTTGATGGATCCTTTTCCTCTCATAGAGAGATGCCGCTTT
TGCGAAGATTGCCAGTGGATAGGCGGGTGTGATGCTTCTCTAACACACTTCCACTGATGCTGTTTAT
GTCTAATGACATAAACAATGCCTCCTTTAAAGGAGATGC

5′UTR
37 bp

1a
ORF
3279 bp

3′UTR
207 bp